

Table of Contents

Chapter 1	Introduction	1
1.1	Motivation & Purpose of this Thesis	3
1.2	Thesis Outline	4
Chapter 2	Introduction to the Related Techniques.....	6
2.1	Cognitive Radio.....	7
2.1.1	Cognitive Radio Interpretation and Definition	8
2.1.2	Regulatory Issues	10
2.1.3	The Cognitive Cycle	11
2.2	UWB Techniques and UWB Propagation.....	13
2.2.1	UWB Regulations	14
2.2.2	UWB Transmission Techniques	15
2.2.3	UWB Path Loss Model	18
2.2.4	UWB Frequency Selective Fading Channel Modelling Techniques	25
2.2.5	Cognitive UWB	30
2.3	Game Theory in Wireless Communications	31
2.3.1	Definition of Game Theory.....	32
2.3.2	Important Concepts of Game Theory	33
2.3.3	Game Strategy.....	35
2.3.4	Mathematical Expressions of a Game.....	38
2.3.5	Applying Game Theory to Wireless Communications	41
2.4	Reinforcement Learning in Wireless Communications	42
2.4.1	Reinforcement Learning and Q-Learning	43
2.4.2	Multi-agent Q-Learning	44
2.4.3	Applying Reinforcement Learning to Wireless Communications.....	46
2.5	Power Allocation by Traditional Optimization Process.....	47
2.5.1	Introduction to the Optimization Problem and Lagrange Multiplication.....	48
2.5.2	Application of the Water Filling Technique in Wireless Communications	50
2.6	Chapter Conclusion	51

Chapter 3 Performance Modelling and Verification Techniques	53
3.1 Simulation Tools	54
3.2 Simulation Techniques and Methods	55
3.3 Performance Measures and Verifications	58
3.3.1 Channel Interference Model and Signal to Interference Plus Noise Radio.....	58
3.3.2 Shannon Channel Capacity and Truncated Shannon Capacity.....	59
3.3.3 Power Efficiency.....	60
3.4 Chapter Conclusion	61
Chapter 4 Game Based Approach in UWB Power Allocation	63
4.1 Gradient Power Allocation.....	64
4.1.1 The Purpose of the Gradient Power Allocation and the Analysis of Its Performance	64
4.1.2 Analysis of the Possible Performance.....	67
4.1.3 Simulation Setup and Results	71
4.2 Game Model and Utility Function	82
4.2.1 Game Model and Utility Function that describes the UWB Power Allocation Problem	82
4.2.2 Existence of a Nash Equilibrium	90
4.3 Chapter Conclusion	101
Chapter 5 Performance of Game Approach in UWB Multichannel Power Allocation Problem.....	102
5.1 A Game Strategy for Radio Resource Sharing Game	103
5.1.1 Classification of the Actions.....	103
5.1.2 The Proposed Game Strategy.....	104
5.2 Simulation Setup	105
5.3 Snapshot Analysis	109
5.3.1 Snapshot Analysis under a Flat Fading Channel	109
5.3.2 Snapshot Analysis under a Frequency Selective Fading Channel	115
5.4 General Performance under a Flat Fading Channel	122
5.5 General Performance under a Frequency Selective Fading Channel	125
5.6 Performance Comparison between Proposed Scheme and Iterative Water Filling Scheme	128

5.6.1	Iterative Water Filling Technique	129
5.6.2	Simulation Setup	131
5.6.3	Simulation Results	133
5.7	Chapter Conclusion	139
Chapter 6 Performance of Game Approach in Extended Range Scenario		140
6.1	Design of the Power Allocation Scheme for Longer Ranges.....	141
6.1.1	Link Budget Analysis and Power Threshold Design.....	141
6.1.2	Power Impact Factor	146
6.1.3	Estimation of Maximum Mutual Target Data Rate	147
6.2	Power Allocation Design and Simulation Setup.....	148
6.3	Snapshot Performance Analysis.....	154
6.3.1	Snapshot Analysis under a Frequency Selective Fading Channel in Four User Coexistence Scenario.....	159
6.3.2	Snapshot Analysis in a Six User Coexistence Scenario.....	165
6.4	General Performance of Four Users Coexistence Scenario	170
6.5	General Performance of Various Number of Users Scenario	175
6.6	Chapter Conclusion	180
Chapter 7 Future Work		182
7.1	Future Improvement based on Current Work	182
7.1.1	Dynamic Target Requirement with a Dynamic User Number.....	183
7.1.2	Primary User Recognition.....	183
7.2	Cognitive Power Allocation in Sensor Network and Cellular Network	186
7.3	Multi-agent Q-learning.....	186
7.4	Chapter Conclusion	187
Chapter 8 Conclusions		188
8.1	Summary of the Original Contributions.....	191
	Reference	193

List of Figures

Figure 1-1 Spectrum utilization measurement (0–6GHz). (Taken from [1]).....	1
Figure 1-2 Spectrum of UWB and existing narrow band systems (Taken from [10]) ..	3
Figure 2-1 RF flexibility versus intelligence [7].....	10
Figure 2-2 Cognitive circle (taken from [9])	12
Figure 2-3 UWB emission limits for indoor handheld devices released by FCC in May 2002 (Taken from [10])	14
Figure 2-4 UWB emission limits for outdoor handheld devices released by FCC in May 2002 (Taken from [10])	15
Figure 2-5 UWB transmission approaches: (a) single- and (b) multiband approaches [10].....	16
Figure 2-6 Band division in the multiband OFDM standard proposal.	17
Figure 2-7 Time–frequency representation of the multiband OFDM signal with time–frequency code {1 3 2 1 3 2} [10]	17
Figure 2-8 Channel model match in the LOS scenario.....	21
Figure 2-9 Channel model match in the NLOS scenario.....	21
Figure 2-10 Required transmit power analysis	24
Figure 2-11 Relationships between the channel frequency-transfer function and a signal with bandwidth W (taken from [48]).....	26
Figure 2-12 100 impulse response based on a NLOS UWB channel model (taken from [40]).....	27
Figure 2-13 Illustration of a Single Stage	37
Figure 2-14 Illustration of a <i>TitforTat</i> Strategy	38
Figure 2-15 Example of a game in the matrix form.....	40
Figure 2-16 Reinforcement Learning (adapted from [72])	46
Figure 2-17 Geometric interpretation of the optimization problem (taken from [80])	48
Figure 2-18 Water-filling in a frequency selective fading channel (taken from [46]).	51
Figure 3-1 Flow chart of a snapshot of the simulation	56
Figure 3-2 Flow chart of a Monte-Carlo simulation.....	57
Figure 3-3 An example of the channel interference model (taken from [12]).....	58
Figure 4-1 Flow chart of the gradient power allocation process	66
Figure 4-2 Illustration of the gradient power allocation	67
Figure 4-3 System layout.....	73
Figure 4-4 Transmit power and SINR at receivers in the initial stage.....	75
Figure 4-5 Transmit Power and SINR at receivers at the final stage.....	76
Figure 4-6 Transmitted power and SINR at receivers in the initial stage.....	78
Figure 4-7 Transmit power and SINR at receivers at the final stage.....	79
Figure 4-8 Number of channels versus transmit power of user 1	80
Figure 4-9 Number of channels versus transmit power of user 2	81
Figure 4-10 Example of a utility function(taken from [61]).....	85
Figure 4-11 Graph of equation 4.14	87
Figure 4-12 Illustration of the utility function	88
Figure 4-13 Relationship between the utility and the target data rate	89
Figure 4-14 Transmit power of user 1 versus its utility.....	89
Figure 5-1 Illustration of the proposed game strategy	105
Figure 5-2 Geographical layouts of the competing systems	107

Figure 5-3 Acquired data rate analysis under a flat fading channel in direct link longest (upper) user direct link shortest (lower) scenarios	110
Figure 5-4 Power allocation pattern under a flat fading channel at the first iteration (Direct link longest)	112
Figure 5-5 Power allocation pattern under a flat fading channel at the final iteration (Direct link longest)	112
Figure 5-6 Power allocation pattern under a flat fading channel at the first iteration (Direct link shortest)	114
Figure 5-7 Power allocation pattern under a flat fading channel at the final iteration (Direct link shortest)	114
Figure 5-8 Utility analysis under a flat fading channel in direct link longest (upper) user direct link shortest (lower) scenarios	115
Figure 5-9 Acquired data rate analysis under a frequency selective fading channel in direct link longest (upper) user direct link shortest (lower) scenarios	116
Figure 5-10 Power allocation pattern under a frequency selective fading channel at the first iteration (direct link longest)	118
Figure 5-11 Power allocation pattern under a frequency selective fading channel at the final iteration (direct link longest)	118
Figure 5-12 Power allocation pattern under a frequency selective fading channel at the first iteration (direct link shortest)	120
Figure 5-13 Power allocation pattern under a frequency selective fading channel at the final iteration (direct link shortest)	121
Figure 5-14 Utility analysis under a frequency selective fading channel in direct link longest (upper) user direct link shortest (lower) scenarios	122
Figure 5-15 Mean degree of convergence under a flat fading channel.....	123
Figure 5-16 Convergence speed analysis under a flat fading channel.....	123
Figure 5-17 Mean degree of convergence under a flat fading channel (direct link longest).....	124
Figure 5-18 Mean degree of convergence under a flat fading channel (direct link shortest).....	125
Figure 5-19 Mean degree of convergence under a frequency selective fading channel (direct link longest).....	126
Figure 5-20 Mean degree of convergence under a frequency selective fading channel (direct link shortest).....	126
Figure 5-21 Mean convergence speed under a frequency selective fading channel (direct link longest).....	127
Figure 5-22 Mean convergence speed under a frequency selective fading channel (direct link shortest).....	128
Figure 5-23 Flow chart of the iterative water filling technique	130
Figure 5-24 Mean number of iterations versus target data rate under a frequency selective fading channel.....	135
Figure 5-25 Mean SINR of 4 users under a frequency selective fading channel (direct link longest)	136
Figure 5-26 Mean SINR of 4 users under a frequency selective fading channel (direct link shortest).....	137
Figure 5-27 Mean power efficiency over the target data rate under a frequency selective fading channel.....	139
Figure 6-1 Required transmit power for a closed link margin in the outdoor environment	142

Figure 6-2 Illustration of a gradient power profile that used to determine the highest transmit power	143
Figure 6-3 Illustration of a relationship between the total transmit power, estimated power floor, adjustment factor and the upper bound of transmit power.....	145
Figure 6-4 Flow chart of the new gradient power allocation process.....	148
Figure 6-5 Geographical layouts of competing systems.....	152
Figure 6-6 Example of channel path gains	153
Figure 6-7 Acquired data rate analysis in direct link longest (upper) and direct link shortest (lower) scenarios	155
Figure 6-8 Power allocation pattern at the first iteration (Direct link longest).....	156
Figure 6-9 Power allocation pattern at the final iteration (Direct link longest).....	156
Figure 6-10 Power allocation pattern at the first iteration (Direct link shortest).....	157
Figure 6-11 Power allocation pattern at the last iteration (Direct link shortest).....	157
Figure 6-12 Utility analysis under a flat fading channel in direct link longest (upper) user direct link shortest (lower) scenarios	158
Figure 6-13 Acquired data rate analysis under a frequency selective fading channel in direct link longest (upper) user direct link shortest (lower) scenarios.....	160
Figure 6-14 Power allocation pattern under a frequency selective fading channel at the first iteration (Direct link longest)	162
Figure 6-15 Power allocation pattern under a frequency selective fading channel at the final iteration (Direct link longest)	162
Figure 6-16 Power allocation pattern under a frequency selective fading channel at the first iteration (Direct link shortest)	163
Figure 6-17 Power allocation pattern under a frequency selective fading channel at the final iteration (Direct link shortest).....	163
Figure 6-18 Utility analysis under a frequency selective fading channel in direct link longest (upper) user direct link shortest (lower) scenarios	164
Figure 6-19 Acquired data rate analysis under flat fading (upper) frequency selective fading channel (lower) channels	166
Figure 6-20 Power allocation pattern at the first iteration (flat fading channel)	167
Figure 6-21 Power allocation pattern at last iteration (flat fading channel)	167
Figure 6-22 Power allocation pattern at first iteration (frequency selective fading channel).....	168
Figure 6-23 Power allocation pattern at the final iteration (frequency selective fading channel).....	168
Figure 6-24 Total utility analysis under flat fading (upper) frequency selective fading (lower) channels.....	169
Figure 6-25 Degree of convergence under a flat fading channel.....	172
Figure 6-26 Degree of convergence under a frequency selective fading channel	173
Figure 6-27 Convergence speed under a flat fading channel.....	174
Figure 6-28 Convergence speed under a frequency selective fading channel	174
Figure 6-29 Power Impact Factor under flat fading (left) frequency selective fading (right) channels	175
Figure 6-30 Degree of convergence under a flat fading channel.....	176
Figure 6-31 Degree of convergence under a frequency selective fading channel	177
Figure 6-32 Convergence speed under a flat fading channel.....	179
Figure 6-33 Convergence speed under a frequency selective fading channel	179
Figure 6-34 Power Impact factor under flat fading (left) frequency selective fading (right) channels	180

Figure 7-1 System model	184
Figure 7-2 Alternative system model.....	185

List of Tables

Table 2-1 Timing parameters	17
Table 2-2 IEEE 802.15.4a path loss model for the outdoor LOS	22
Table 2-3 IEEE 802.15.4a path loss model for the indoor office NLOS	22
Table 2-4 Walfish-Ikegami path loss model for the outdoor LOS	22
Table 2-5 COST231 Hata path loss model for the indoor office NLOS	22
Table 2-6 Parameters of the link budget analysis	23
Table 4-1 Parameters of the indoor office path loss model	72
Table 4-2 Geographical locations of 4 systems	73
Table 4-3 Simulation parameters	74
Table 4-4 Channel assignment pattern at the final stage	77
Table 4-5 Total transmit power of 4 systems	78
Table 4-6 Change of the channel assignment pattern	79
Table 5-1 Parameter of the indoor office path loss model	106
Table 5-2 Parameters used in the simulations	108
Table 5-3 Parameters used in the simulations	133
Table 6-1 Parameters of the outdoor path loss model from 802.15.4a	149
Table 6-2 Walfish-Ikegami path loss model for the outdoor LOS	150
Table 6-3 Parameters used in the simulations	152
Table 6-4 Power impact factors analysis under a flat fading channel	159
Table 6-5 Power impact factors analysis under a frequency selective fading channel	165
Table 6-6 Power impact factor analysis under flat fading and frequency selective fading channels	170
Table 6-7 Target data rates analysis under a flat fading channel	177
Table 6-8 Target data rates under a frequency selective fading channel	178

List of Abbreviations and Acronyms

CDMA	Code Division Multiple Access
CR	Cognitive Radio
DCPA	Distributed Cognitive Power Allocation
DSL	Digital Subscriber Line
DSP	Digital Signal Processing
FCC	Federal Communications Commission
ISM	Industry Science and Medicine Band
ISP	Intelligent Signal Processing
ITU	International Telecommunication Union
IW	Iterative Water Filling
LOS	Line of Sight
MAC	Media Access Control
NLOS	None Line of Sight
NE	Nash Equilibrium
OFDM	Orthogonal Frequency-Division Multiplexing
PIF	Power Impact Factor
RF	Reinforcement Learning
SINR	Signal to Interference plus Noise Ratio
SIR	Signal to Interference Ratio
SDR	Software-Defined Radio
SNR	Signal to Noise Ratio
UWB	Ultra Wide Band
VOIP	Voice Over Internet Protocol

Acknowledgements

I would express my sincere gratitude my first supervisor, Dr. David Grace, for his continued encouragement and technical support as my mentor during my PhD study.

I am also grateful to my second supervisor, Dr. Paul Mitchell, who gives me helpful comments and useful suggestions on this project.

Further I would like to thank my colleagues in the Communications Research Group for providing a pleasant atmosphere to work and make my life much easier in York.

Finally, I would like to express my deepest gratitude to my parents for their unconditional love and selfless support.

Declaration

Some of the research presented in this thesis results in some publications, which are listed at the end of this thesis.

All contributions presented in this thesis as original are as such to the best knowledge of the author. References and acknowledgements to other researchers have been given as appropriate.

Chapter 1 Introduction

Contents

1.1	Motivation & Purpose of this Thesis	3
1.2	Thesis Outline	4

The radio spectrum is the most precious resource for wireless communications due to the increasing proliferation of wireless devices which exacerbate the congestion of the spectrum. However, it is currently used in an inefficient and uneven way [1-6]. Such observation can be found in figure 1.1 [1], in which spectrum utilization in downtown Berkeley has been measured revealing the actual utilizations in the 3-4 GHz and 4-5 GHz frequency bands are only 0.5% and 0.3% respectively, while the intensive spectrum usage concentrates below 2.4 GHz.

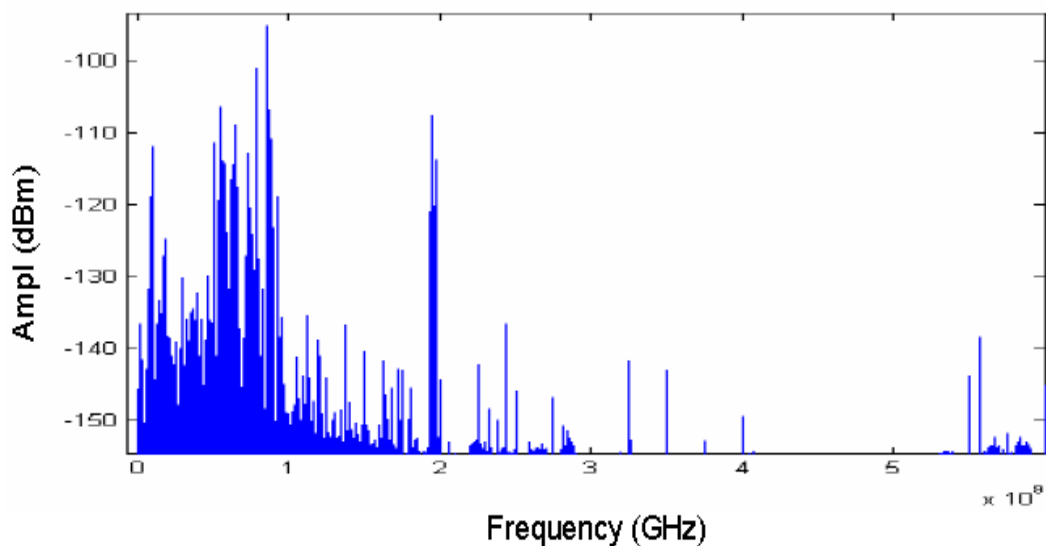


Figure 1-1 Spectrum utilization measurement (0–6GHz). (Taken from [1])

To address the low utilization of conventional wireless communication techniques, the Cognitive Radio (CR) concept has been developed to exploit the better utilization of radio spectrum. Instead of a fixed spectrum allocation, the spectrum utilization can be greatly improved by allowing the secondary users opportunistically to access the

spectrum holes that are not currently occupied by the primary users in a particular geographical location. The term primary user means an entity which owns the frequency band and has primary access rights to it [7-9]. A secondary user represents the cognitive devices that can share unused frequency bands without severely interfering with the licensed user [9]. A spectrum hole is a band of frequencies, which is legally assigned to the primary users, but is currently not being occupied by any of the primary users. Given the observation from the current spectrum utilization in figure 1.1, the spectrum holes at lower frequencies can be spectrum with a narrow bandwidth that can be opportunistically accessed by CR with a high transmit power emission level in order to maintain a specific performance such as the data rate requirement, while spectrum holes at higher frequencies can be spectrum with much wider bandwidth where a lower transmit power emission level can grant the cognitive radio devices the same level of data rate requirement.

An ultra wide bandwidth (UWB) system addresses the spectrum utilization problem in a very different way; it grants the radio system the ability to access a much wider bandwidth at a higher frequency band that crosses several licensed and unlicensed bands. In order to avoid severe interference to the primary users, an extremely low transmission power mask has to be imposed. The UWB system however does not require spectrum sensing as a result of the low power emission level. A UWB spectrum is illustrated in Figure 1.2 as well as some typical wireless services. The large spectrum pool provides UWB systems with a very large raw channel capacity. However, this also introduces difficulties and limitations. The extreme low transmit power density and the absence of spectrum sensing poses two challenges to UWB systems: one has been the difficulty of coordination in a multi-user coexistence scenario, while the other is the increased path loss and fading at extended range. A cognitive radio based UWB system may well be the solution to these problems. Such systems could make use of the ultra wide spectrum capable that is able to satisfy high data rate demanding scenarios while avoiding the interference either from other homogenous systems, or to existing agile services by means of allocating a dynamically sculptured power profile.

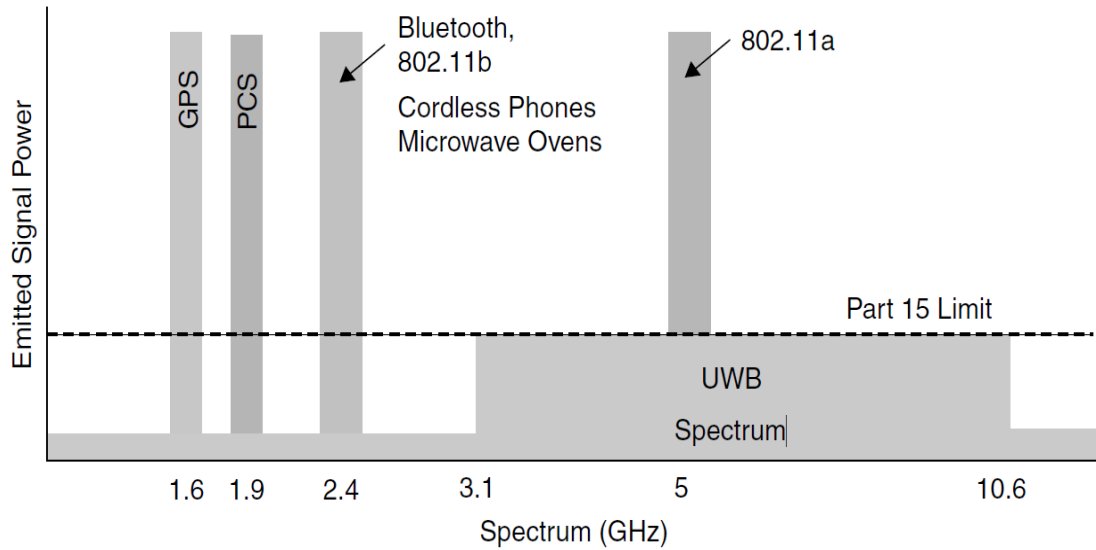


Figure 1-2 Spectrum of UWB and existing narrow band systems (Taken from [10])

1.1 Motivation & Purpose of this Thesis

Cognitive Radio has been widely regarded as one of the most important technique for future wireless communications after its advent in 1999 [11]. Many research projects have been so far carried out that are related to cognitive radio [12-18], and many organisations have been involved in establishment of regulation and concept development [4, 7, 19]. On the UWB side, there are also many organizations that are catering for standardising UWB systems. Two of the major transmission techniques (I R-UWB, MB-OFDM) have been established. Despite these efforts, some critical issues prevent UWB from further blossoming in the market. The FCC established the first UWB regulation in USA, but this was not accepted worldwide, and the worries about the possible heavy interference to primary users in a future dense deployment scenario keep increasing. We perceive that the Cognitive Radio technique can bring great benefit to the UWB. By combining these two wireless techniques, we thereby are able to address the challenges faced by UWB systems.

The purpose of this thesis is to design a Distributed Cognitive Power Allocation (DCPA) scheme that can be used to solve the distributed power allocation problem in scenarios where several UWB systems coexist. Further, we want to demonstrate that the methodology we developed can be applied in a range extension scenario, in which

a UWB system is modelled as a secondary user with a large spectrum pool that can be accessed opportunistically. By either sensing the channel usage pattern of the primary user or resorting to the local database from the regulators, the cognitive system can transmit a power profile that is higher than the current FCC spectrum mask without causing excessive amounts of interference to the primary users. Our hypothesis for this thesis is that a DCPA scheme can bring great benefit in to a multicarrier based radio system in terms of interference reduction, energy efficiency and range extension, and it can be applied to solve a OFDM based UWB power allocation problem in order to explore its potential application at extended ranges.

1.2 Thesis Outline

This thesis investigates an applicable DCPA scheme for a UWB wireless system in a point-to-point configuration.

Chapter 2 introduces the background knowledge of Cognitive Radio including a discussion of its regulatory issues. The UWB transmission techniques and the corresponding regulations are also introduced in this chapter. The possible methods of combining Cognitive Radio and UWB are also discussed. Three theoretical approaches of solving cognitive power allocation are introduced in this chapter. We also provide a concise review of game theory and its application to wireless communications. This is followed by an introduction to Reinforcement Learning and its application in wireless communications. Lastly, we wrap everything up with an introduction to a traditional optimisation process and its application to wireless communications.

In chapter 3, we provide a detailed introduction to the method we used in generating random geographical layout of multiple wireless agents. Regarding the performance measurement, the interference model of a multi-system coexistence scenario is introduced as well as the measure of the Signal to Interference plus Noise Ratio and power efficiency. In addition, the verification techniques are introduced.

In chapter 4, we investigate a game based DCPA scheme. A novel gradient power allocation scheme is studied, and the associated game model is used to describe the distributed UWB power allocation problem as a game competition for spectrum resources among homogeneous UWB competitors. We firstly introduce our proposed gradient power allocation scheme, and we demonstrate how the proposed scheme is an efficient channel partitioning scheme, which paves the way for a game based strategy acquiring a data rate associated with a specific transmit power. We then develop a mathematical proof of the existence of a Nash Equilibrium as a theoretical demonstration of the convergence of our proposed scheme.

Chapter 5 examines the performance of our proposed DCPA scheme by studying a four user coexistence power allocation problem. We examine the performance under both flat fading and frequency selective fading channels. We also investigate the general performance by means of Monte Carlo simulation. Lastly we present a comparison between our proposed DCPA scheme and a Iterative Water Filling based approach.

In chapter 6, we adapt our DCPA scheme so that it can work with radio links that have longer ranges than the conventional UWB systems. We lift the power density limitation by means of a new dynamic maximum power threshold design in order to cope with channel path loss at longer ranges while maintaining an overall low power emission. The increased interference impact towards the primary user due to the higher transmitter power emission density is discussed and a measure of such impact is measured by a Power Impact Factor.

Future work is presented in chapter 7 with the final overall conclusion presented in chapter 8.

Chapter 2 Introduction to the Related Techniques

Contents

2.1	Cognitive Radio.....	7
2.1.1	Cognitive Radio Interpretation and Definition	8
2.1.2	Regulatory Issues	10
2.1.3	The Cognitive Cycle	11
2.2	UWB Techniques and UWB Propagation.....	13
2.2.1	UWB Regulations	14
2.2.2	UWB Transmission Techniques	15
2.2.3	UWB Path Loss Model	18
2.2.4	UWB Frequency Selective Fading Channel Modelling Techniques	25
2.2.5	Cognitive UWB	30
2.3	Game Theory in Wireless Communications	31
2.3.1	Definition of Game Theory.....	32
2.3.2	Important Concepts of Game Theory	33
2.3.3	Game Strategy.....	35
2.3.4	Mathematical Expressions of a Game.....	38
2.3.5	Applying Game Theory to Wireless Communications.....	41
2.4	Reinforcement Learning in Wireless Communications	42
2.4.1	Reinforcement Learning and Q-Learning.....	43
2.4.2	Multi-agent Q-Learning	44
2.4.3	Applying Reinforcement Learning to Wireless Communications.....	46
2.5	Power Allocation by Traditional Optimization Process.....	47
2.5.1	Introduction to the Optimization Problem and Lagrange Multiplication.....	48
2.5.2	Application of the Water Filling Technique in Wireles Communications	50
2.6	Chapter Conclusion	51

The main purpose of the thesis is to develop an efficient Distributed Cognitive Power Allocation (DCPA) scheme that explores and takes advantage of Ultra Wide Band (UWB), and further extend the range over the current limits of UWB systems. There is no doubt that, Cognitive Radio (CR) and the relevant DCPA and Spectrum Assignment schemes have attracted a great deal of research interest in recent years, and many theoretical tools have been applied to DCPA problems. In this research, we apply a game theoretical approach to the UWB power allocation problem. We need however to give a detailed introduction to the relevant techniques that we will encounter later in this thesis.

This chapter is organised as follows. Sections 2.1 and 2.2 introduce the general idea of CR, UWB techniques and propagation. Game theory in wireless communications will be covered in section 2.3. The literature reviews of the alternative approaches such as reinforcement learning and traditional power allocation optimising techniques will be covered in sections 2.4 and 2.5.

2.1 Cognitive Radio

Currently, most radio systems are fixed to their specified frequency bands with fixed spectrum access techniques framed by their network operators. Such spectrum utilization can render low spectrum efficiency overall and will soon become a limitation for future wireless communication [19]. Several estimations have been made and it is forecast that the demand for spectrum will soon exceed what can be offered according to past statistical data [7]. With the promise of efficient radio spectrum utilization, Cognitive Radio (CR) has sparked new research areas in wireless communication such as assisting in green radio concepts. Cognitive radio, a term firstly introduced by Mitola [11, 20], is proposed to be an intelligent wireless communication system that will be endowed with high re-configurability and the ability to be aware of the surrounding environment, and user requirements. Then wireless communication links can be established in a dynamic manner and can share spectrum autonomously according to a cognitive learning cycle [9] [3]. CR and related research keep flourishing along with advancements in radio techniques and

emergence of the new industry requirements – as an example CR has been proposed for use in TV White Space [21].

2.1.1 Cognitive Radio Interpretation and Definition

Emphasising different aspects of cognitive radio research, researchers tend to have the following interpretations of CR.

1) Full cognitive radio: With full flexibility of configuration and full cognitive function in all of the Open Systems Interconnection (OSI) layers, a full cognitive radio can cognitively adapt itself to both the needs of the user and its local environment [7].

2) Spectrum sensing cognitive radio: As its name suggests, only the spectrum status is observed for CR devices to make a decision (The higher OSI layers are not involved) [7, 22, 23].

3) Licensed band cognitive radio: A cognitive radio that operates in the licensed bands, senses the presence of licensed users and vacates a short period after the licensed user reclaims the frequency bands [7, 24].

4) Unlicensed band cognitive radio: Cognitive radio that operates in the unlicensed bands and improves multisystem coexistence [7, 24].

5) Regulatory data based cognitive radio: The cognitive radio operates in both licensed and unlicensed bands, and the spectrum access behaviour of the CR devices is guided by a local regulatory database. [4, 24]

For both unlicensed and licensed bands, the interest in adopting CR is that it permits the coexistence of different wireless networks to improve bandwidth efficiency. For example, the coexistence of IEEE 802.11b WiFi and 802.16a WiMax is analyzed in [25] by a system model based on reactive CR algorithms, and the results indicate significant improvements in both 802.11b and 802.16a throughputs. In [8], CR is

proposed to be used in the newly allocated 5.470-5.725 GHz band and the 3.650-3.700 GHz band; the potential approaches of implementation are given with the analysis of the challenge. With the rapid increase in the deployment of wireless terminals, there emerges a new dimension of CR. The idea of green radio has recently become popular, a concept aimed at making wireless systems more environmentally friendly by more tightly and dynamically controlling energy usage.

Given the interpretations and the research trends of CR, CR, in a broader sense, can be defined as a fully flexible wireless system of cross layer intelligence in the OSI model, which produces best use of spectrum [5, 8, 19]. However the scope of flexibility and the degree of intelligence can vary dramatically depending on either specific design requirements or the technique availability. A preferable definition of CR has been given by the Office of Communications (OFCOM) in [7], which ignores the introduction of intelligence to higher OSI layers and hence becomes more realizable. It defines a CR as a radio system that has a certain degree of intelligence to reconfigure its own RF front end. RF front end flexibility is provided by means of software defined radio (SDR) and the intelligence is provided by means of intelligent signal processing (ISP). The potential levels of RF front end flexibility and intelligence are illustrated in Figure 2.1. The SDR as the precursor of CR has been developed for many years. Compared with the conventional radio system, a software defined radio system can implement modulation, demodulation, amplifiers and detectors without special purpose hardware. (Usually an SDR uses a number of special purpose digital signal processors (DSPs)). In theory, all of the radio functions can be implemented by means of analog-to-digital converter (ADC) digital-to-analog conversion (DAC), a general purpose signal processor and a reconfigurable RF front end [26, 27]. The dimensions of the CR however are limited by the hardware development and advance of intelligent signal processing algorithms [7].

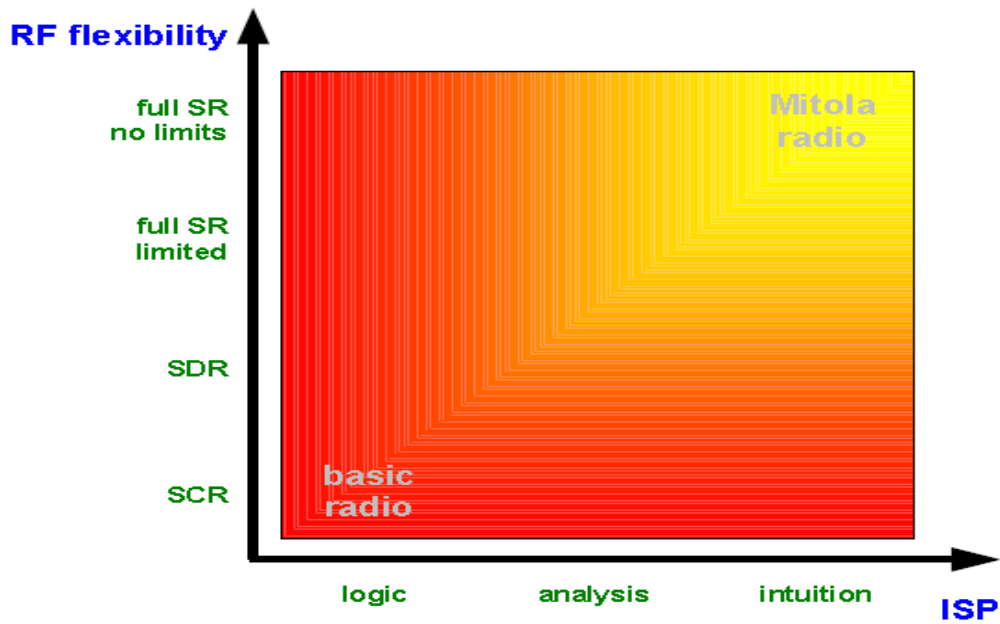


Figure 2-1 RF flexibility versus intelligence [7]

2.1.2 Regulatory Issues

Although CR holds the promise and great potential of much more efficient use of spectrum, it faces many challenges in both technical and policy aspects.

Technically, CR faces the hidden terminal problem [28-30]. This manifests itself as failure to detect primary users, which is caused by many reasons, either from the weak transmissions of primary users, or from shadowing. Therefore, the unwanted interference transmitted by a CR in the licensed bands may severely hamper the reception of licensed users. The successful and efficient solution to this problem is still one of the topics of CR research.

From a policy point of view, the advantage of CR being able to access the spectrum of licensed primary users could also be a disadvantage to primary users. Currently, many radio technologies are bounded to their fixed frequency bands. The licensees are firmly holding their licensed spectrum which is protected by law. As mentioned in [24], one possible solution is spectrum leasing so that the CR users can access the spectrum of licensed primary user bands on condition of leasing the spectrum from the licensees. This solution, however, will bring extra costs imposed on licensed users

to adapt their terminals to cognitive users, and the difficulty of enforcement of interference protocols [24]. Despite these challenges, the regulatory environment is becoming more CR friendly. As mentioned in the report of the International Telecommunication Union – Radio communication Sector (ITU-R) [31], many communications administrators around the globe have begun to investigate the use of CR and SDR based technology. Many standards bodies are participating in the area and examining possible data protocols required for deploying heterogeneous CR networks, such as IEEE-1900 and Defence Advanced Research Project Agency (DARPA) [19]. The latest breakthrough in UK and the US has made a significant step towards enabling CR, where the OFCOM and FCC have approved of accessing TV white spaces (television broadcast frequencies) for data transmission [21].

In addition to its applications in licensed bands, CR techniques have great potential to be implemented on unlicensed frequency bands like the 2.4GHz and 5.1GHz ISM bands, which are largely dominated by existing wireless services such as Wifi and Bluetooth, and faced with spectrum congestion. Implementing CR and its dynamic spectrum sharing behaviour will greatly improve the spectrum efficiency and reduce the aggregate interference on those unlicensed bands.

The problems faced with CR have been faced by many other radio technologies, and require combined study by both regulators and researchers because dynamic spectrum access techniques might also minimise the burden of spectrum management in the future.

2.1.3 The Cognitive Cycle

To endow a radio system with certain degree of cognition, a basic cognitive cycle is proposed to dynamically establish spectrum access according to requirement and environment. As can be seen from Figure 2.2, a cognitive cycle comprises three main procedures [9, 32].

1. Spectrum sensing: The CR systems begin by detecting the surrounding radio environment, collecting information about interference levels and the presence of primary users.
2. Spectrum analysis: The detected spectrum information is analysed to estimate the channel-state information (CSI) and spectrum opportunity.
3. Power allocation and spectrum management: The best spectrum access decision available for the current radio environment is made according to a reasoning process.

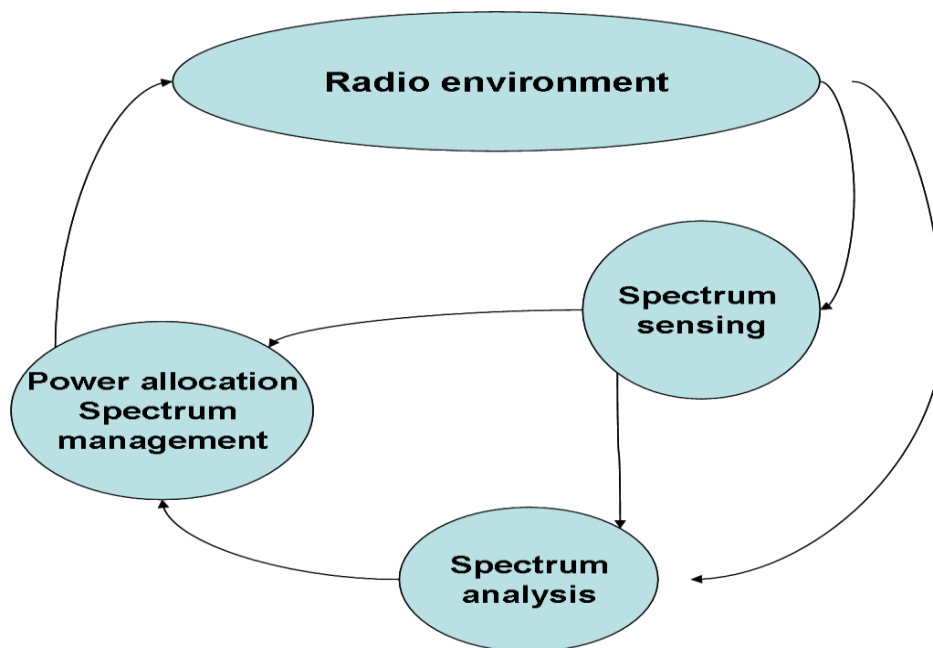


Figure 2-2 Cognitive circle (taken from [9])

Obviously the design of the whole cognitive cycle is a cross-layer optimisation problem. Our research is focussed on the spectrum management and power allocation problems at the physical layer. Perfect spectrum sensing and channel state information are assumed.

2.2 UWB Techniques and UWB Propagation

Ultra Wide Band (UWB) communications offer a totally different approach to address the spectrum shortage by allowing UWB communications to coexist with the existing licensed users with minimal or no interference [33].

Compared with other conventional wireless communications, UWB communications technology has almost the same long history or even longer! The first transmission of ultra wide bandwidth signals can be dated back to 1901 when Guglielmo Marconi transmitted Morse code sequences across the Atlantic Ocean using spark gap radio transmitters [34]. Modern UWB research gained momentum from the 1960's, when the U.S military considered using pulse transmission (impulse radio) for covert imaging, radar and 'stealth' communications. However, the recent advancements in semiconductor technology have made UWB ready for commercial applications, and a brand new market for UWB devices has already opened up since the 1990's [34].

Compared to conventional narrow-band communication techniques, the exceptional characteristics of UWB technology which are promising for modern wireless communications can be summarized as follows [10, 34, 35]:

- 1) High fractional bandwidth.
- 2) Multipath resolution.
- 3) Low fading power loss.
- 4) Very high capacity.
- 5) Resistance to jamming.
- 6) Low probability of intercept and detection.
- 7) Superior penetration properties.

A variety of communication applications both in military and commercial sectors can be boosted by adopting UWB technology, however, only high datarate applications are considered in this thesis. The following sections include the introduction to UWB regulations, UWB transmission techniques, UWB path loss model, and a brief discussion of Cognitive UWB.

2.2.1 UWB Regulations

On February 14, 2002, the FCC ruled to release an amount of bandwidth for commercial development of UWB technology including 0-960 MHz, 3.1-10.6 GHz, and 22-29 GHz on the condition of an effective isotropic radiation power (EIRP) below -41.3 dBm/MHz with the minimum bandwidth of 500 MHz [10].

Importantly, existing services should be protected from the unacceptable power emission from UWB devices. For this purpose, the FCC has assigned conservative emission masks, which are illustrated in Figure. 2.3 for indoor situations and Figure. 2.4 for outdoor situations.

Regulations for UWB networking in Europe are still pending, however, it is indicated that the European Commission has chosen to make use of only part of the spectrum that was approved for use in the US in 2002 [33]. Some of the prototypes of UWB device have already been at hand, such as Tzero (Sunnyvale, California) which showed a wireless (UWB) high-definition multimedia interface (HDMI) [36].

It is however believed that the variation of regulations in different areas will hamper the development of the global UWB market [37].

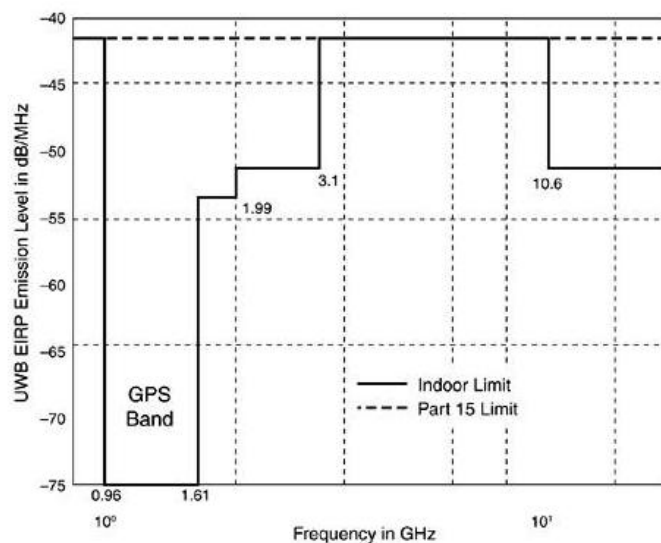


Figure 2-3 UWB emission limits for indoor handheld devices released by FCC in May 2002 (Taken from [10])

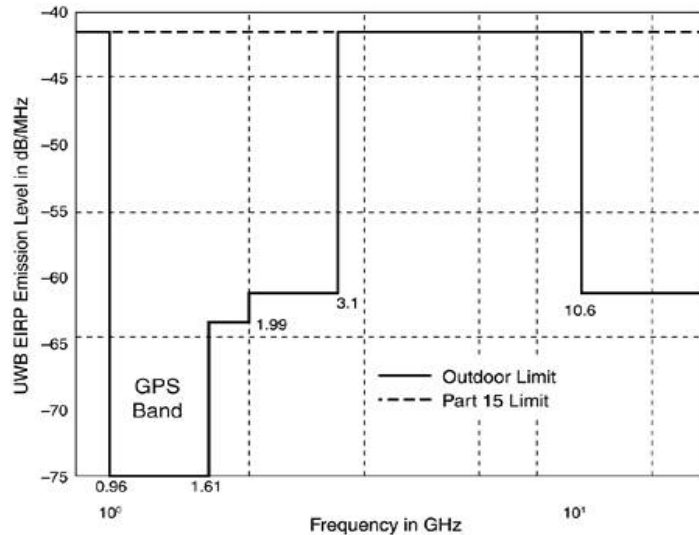


Figure 2-4 UWB emission limits for outdoor handheld devices released by FCC in May 2002 (Taken from [10])

2.2.2 UWB Transmission Techniques

Although the FCC regulation defined the UWB spectrum mask, it did not impose any restriction on UWB signal generation techniques. There are so far many UWB transmission schemes which can be categorized into two radically different approaches. Our current research deals with the UWB multiband approach. Figure 2.5 illustrates a UWB signal in the time and frequency domains for UWB single band approach and UWB multiband approach respectively.

1. UWB single band approach: Information is modulated on a sequence of impulse like waveforms which in the frequency domain each occupy the entire available bandwidth of 7.5GHz[38].
2. UWB multiband approach: Unlike impulse waveforms that dominate the whole 7.5GHz, the multiband approach divides the UWB frequency band into several sub-bands, where each subband occupies 528MHz bandwidth. Orthogonal frequency division multiplexing (OFDM) is used to modulate information in each subband with a subcarrier of 4.125MHz [39].

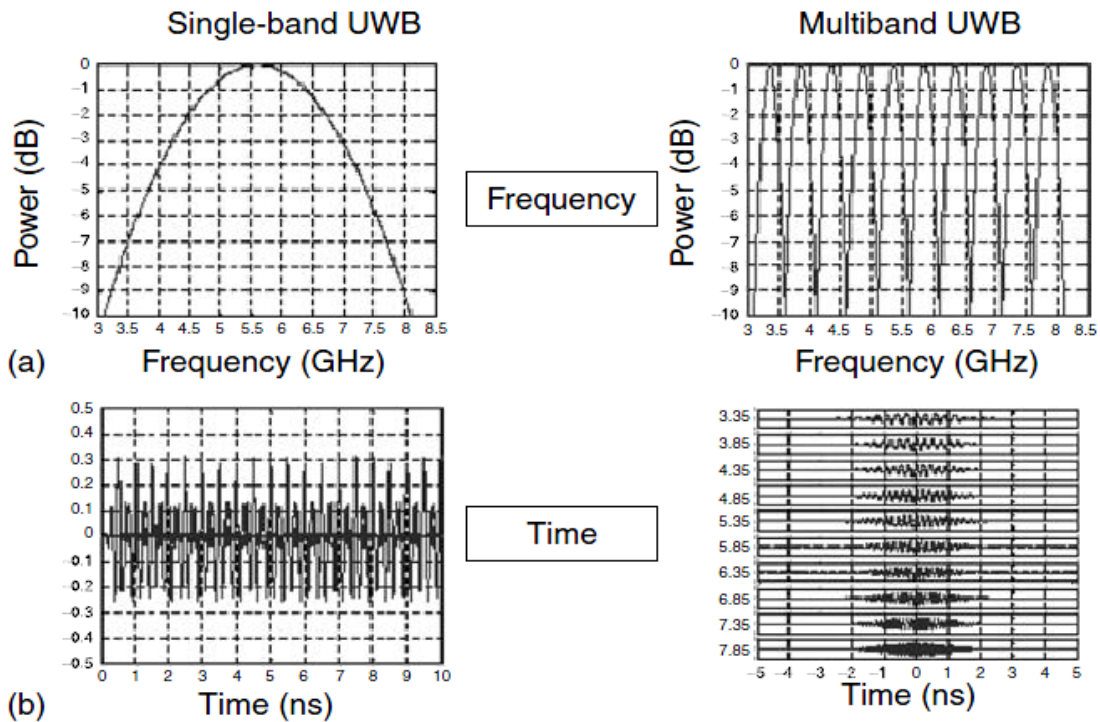


Figure 2-5 UWB transmission approaches: (a) single- and (b) multiband approaches [10]

The current UWB-multiband approach also known as Multiband-OFDM (MB-OFDM) was proposed by the IEEE802.15.3a in 2002 and has been proved a successful wireless personal area networking (WPAN) standard. It is now supported by The WiMedia Alliance, a consortium of over 350 member companies or nonprofit-organizations globally [10].

According to the IEEE802.15.3a standard, there are 14 frequency bands that cover the entire 7.5GHz UWB band, and as can be seen from Figure 2.6, each band occupies 528MHz. The subband of 528MHz is further divided into 128 subcarriers using OFDM. Unlike a traditional OFDM system with higher symbol counts in the modulation schemes, MB-OFDM used quadrature phase shift keying (QPSK) to modulate the transmit signal because of the limited UWB transmit power. Parameters of MB-OFDM are listed in Table 2.1. With regard to the MB-OFDM multiplexing technique, time-frequency codes were invented which are a set of fixed hopping sequences allowing a four user piconet to transmit simultaneously with an average collisions rate as low as 1/3 [16]. Figure 2.7 shows the example of TF code operation for MB-OFDM.

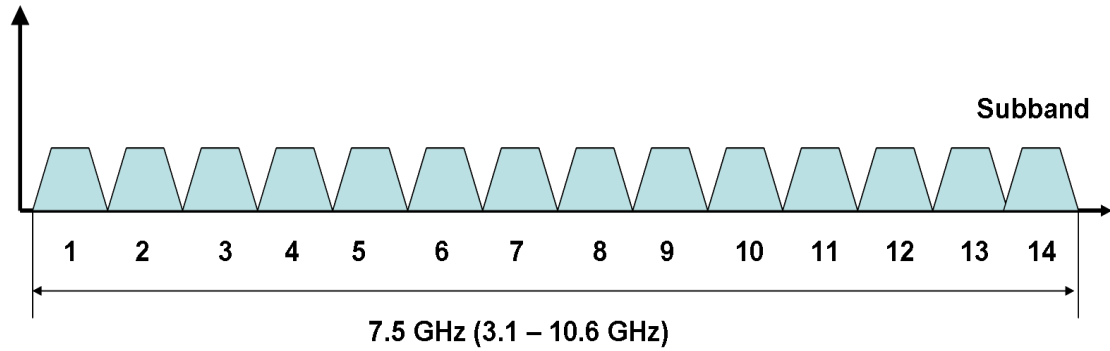


Figure 2-6 Band division in the multiband OFDM standard proposal.

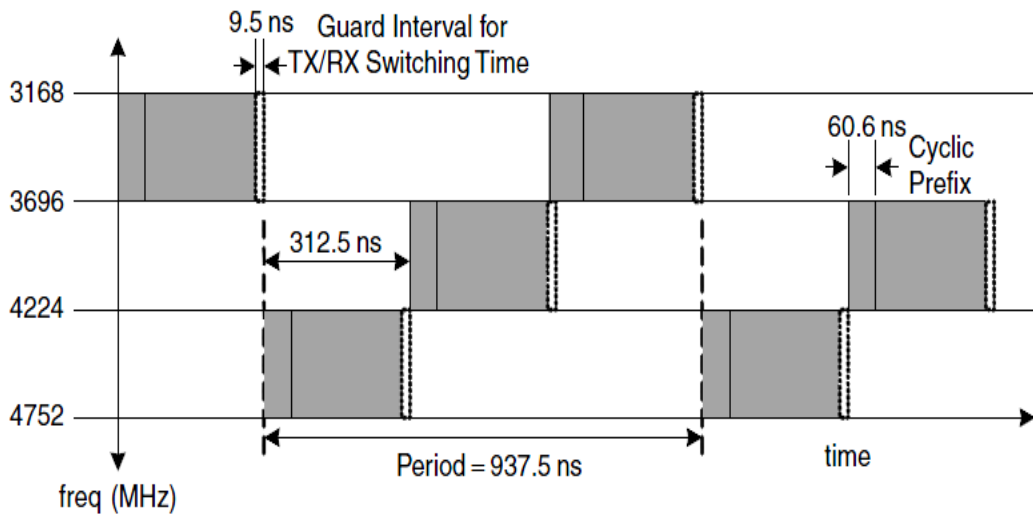


Figure 2-7 Time-frequency representation of the multiband OFDM signal with time-frequency code {1 3 2 1 3 2} [10]

Parameter	Value
Number of OFDM subcarriers	128
Number of data subcarriers	100
Number of defined pilot subcarriers	12
Number of guard subcarriers	10
Subcarrier frequency spacing (MHz)	4.125
IFFT/FFT period (ns)	242.42
Cyclic prefix duration (ns)	60.61
Guard interval duration (ns)	9.47
Symbol duration (ns)	312.5

Table 2-1 Timing parameters

2.2.3 UWB Path Loss Model

Before the introduction to the UWB Path loss Model, it is worth mentioning that two UWB channel models exist for UWB Personal Area Networks (PANs). One is developed by IEEE802.15.3a and the other is developed by IEEE802.15.4a.

2.2.3.1 802.15.3a and 802.15.4a UWB Channel Model

The UWB channel model for IEEE 802.15.3a standard has firstly been established and documented in Channel Models for UWB Personal Area Networks [40]. Later, the channel modelling subgroup of IEEE 802.15.4a developed and published the IEEE 802.15.4a channel model-final report [41], which took into account several effects that were neglected by the IEEE802.15.3a channel model, such as frequency dependent path loss for high frequency bands is studied in [42, 43] and has a form of $\sqrt{PL(f)} \propto f^{-\kappa}$, where in [43] it was found that κ ranges between 0.8 to 1.4. Considering the measurement of channel state at the subcarrier level, we decided to use the IEEE802.15.4a channel model because path loss can be assumed constant across the narrow band subcarriers.

The recommended path loss model in [41] can be expressed as the following equation

$$PL(d, f) = \frac{1}{2} PL_0 \eta_{TX-ant}(f) \eta_{RX-ant}(f) \frac{(f / f_c)^{-2(\kappa+1)}}{(d / d_0)^n} \quad 2.1$$

Where d is the distance between transmitter and receiver, f is the operating frequency or the central frequency of subcarrier; η_{TX-ant} and η_{RX-ant} , are the antenna efficiency factors.

Large-scale fading, also called the shadowing effect, is the variation in signal attenuation around the mean path loss value. Empirical channel studies have revealed that the UWB channel has shadowing behaviour similar to that in narrowband

systems, which is lognormally distributed with zero mean and standard deviation σ_S [41, 43].

Small-scale fading is also referred to as multipath delays in the signal received over a short period of time. Small-scale fading in a UWB channel shows distinctive phenomena, which differ from that of narrowband channels in two main aspects:

1. The effect of channel fading is not as severe as that in narrowband channels, because the number of multipath components that arrive at the receiver within the short UWB waveform becomes much smaller than that in the waveforms of narrowband signals [10]. Consequently, the UWB signal bandwidth is much larger than the coherence bandwidth of the propagation channel, and the multipath fading for UWB signal will not be as severe as for narrow band signals.
2. It shows that the multipath components arrive in clusters rather than in a continuous way as is showed in narrowband channels [43] due to the discontinuity of the arrived multipath components.

2.2.3.2 Path Loss Model for Extended Range

The current UWB channel models, (both 802.15.3a and 802.15.4a), are developed for the purpose of short range Personal Area Networks (PANs) at ranges up to 20 metres. It is necessary to find a suitable channel model if we want to study the UWB power allocation problem with an extended range over 30 metres, and their range extension will be considered in detail in chapter 7. There is however no such channel model to date for UWB, and most of the channel models of the range beyond 1km are only suitable for frequencies below 2.4 GHz [44]. In [45], the author examines two most popular propagation models (COST 231 Hata Model and COST 231 Walfish-Ikegami Model) at high frequency bands 5.725 – 5.825 GHz, and the conclusions are the following:

1. The modified Hata model for urban environment offers the best prediction for the None-Line-of-Sight (NLOS) case at high frequency bands.

2. The Walfish-Ikegami model fits the Line-of-Sight case at high frequency bands.

These conclusions inspired us to examine the usability of these models for UWB. We tested in our simulations and found that these two channel models can be used as UWB channel model in LOS scenario and NLOS scenario respectively.

The path loss of the modified Hata Model can be expressed as the following equations.

$$L(d) = 45.5 + 35.46 * \text{Log}_{10}(f_c) - 13.82 * \text{Log}_{10}(h_b) - \alpha(h_m) + (44.9 - 6.55\text{Log}_{10}(h_b))\text{Log}_{10}(d) + C_m$$

$$\alpha(h_m) = (1.1\text{Log}_{10}(f_c) - 0.7)h_m - (1.56\text{Log}_{10}(f_c) - 0.8)$$

$$C_m = 0 \tag{2.2}$$

Where $L(d)$ is the pathloss between transmitter and receiver at a distance of d , h_b is the height of the base station h_m is the height of the mobile devices, f_c is the operating frequency and d is the distance between base station and mobile receivers

The Walfish-Ikegami model can be expressed as

$$L(d) = 42.6 + 26\text{Log}_{10}(d) + 20\text{Log}_{10}\text{Log}_{10}(f_c) \tag{2.3}$$

Figure 2.8 shows the match between the IEEE 802.15.4a channel model with Walfish-Ikegami in the LOS scenario, and Figure 2.9 shows the match between the IEEE 802.15.4a channel model and the Modified Hata model in the NLOS scenario.

It shows a good match with less than 1 dB difference at range 18 metres in LOS case and 1km in NLOS case. The reason for considering the difference at 18 metres is because the IEEE 802.15.4a model is only available up to 17 metres, whereas the

Walfish-Ikegami model is available for the range from 0.02 km to 5km. Similarly testing point at 1km was chosen for the NLOS scenario, but we extended the range of the IEEE 802.15.4a model to 1km because it offers better match between two channel models. Some of the important parameters can be found in Table 2.2, Table 2.3, Table 2.4 and Table 2.5

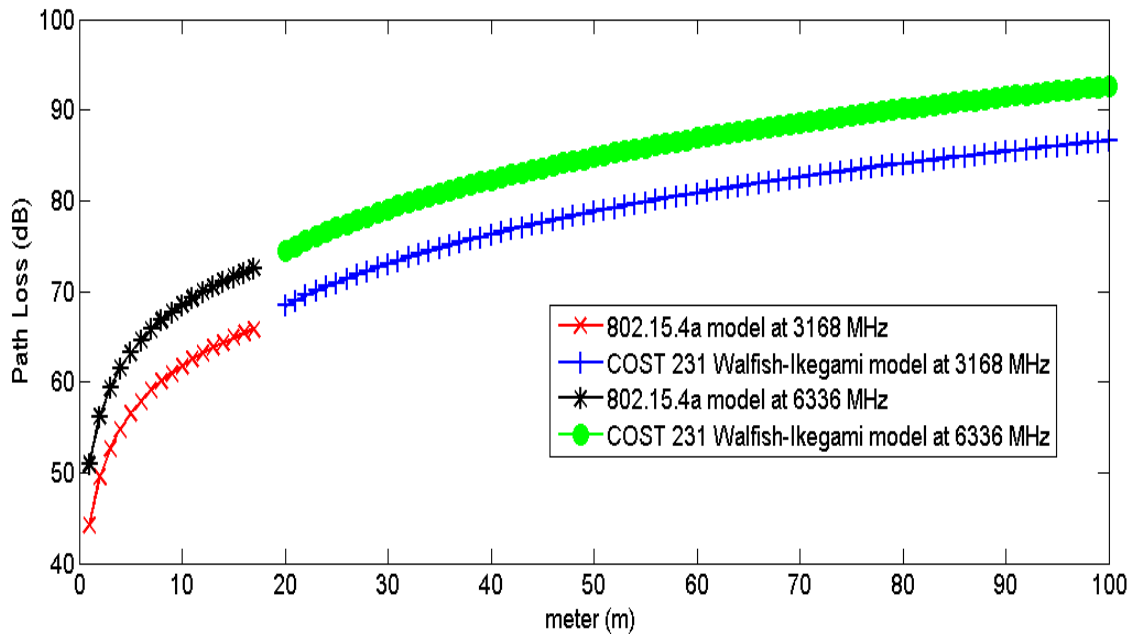


Figure 2-8 Channel model match in the LOS scenario

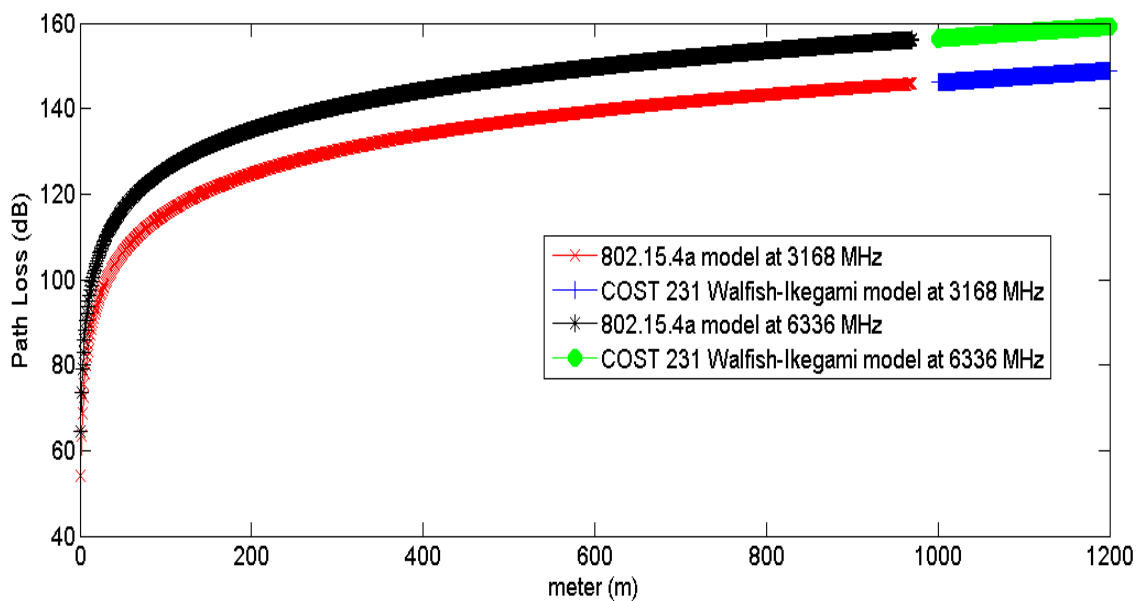


Figure 2-9 Channel model match in the NLOS scenario

LOS (802.15.4a)	
Parameters	Value
n	1.76
PL_0	45.6
κ	0.12

Table 2-2 IEEE 802.15.4a path loss model for the outdoor LOS

NLOS (802.15.4a)	
Parameters	Value
n	3.07
PL_0	3.9
κ	0.71

Table 2-3 IEEE 802.15.4a path loss model for the indoor office NLOS

LOS (Walfish-Ikegami)	
Parameters	Value
Mobile Height (m)	1 - 3
Distance (km)	0.02 - 5
Base Station Height (m)	4 - 50

Table 2-4 Walfish-Ikegami path loss model for the outdoor LOS

NLOS (Hata)	
Parameters	Value
Mobile Height (m)	1 - 10
Distance (km)	1 - 20
Base Station Height (m)	30 - 200

Table 2-5 COST231 Hata path loss model for the indoor office NLOS

2.2.3.3 UWB Link Budget and Link Margin Analysis

It is useful and necessary to clarify the UWB link budget before delving into the UWB power allocation problem. It enables us to estimate whether or not the received power is sufficiently large or a particular channel is useful for sending data. The amount by which the received power exceeds receiver sensitivity is called the link margin. A link budget for a radio communication system is the received power from the transmitter accounting for all the gain and loss through radio media [46], and it can be expressed as

$$\text{Received Power} = \text{Transmitted Power} + \text{Gains (dB)} - \text{Losses (dB)} \quad 2.4$$

Table 2.6 shows an example of UWB link budget for a single subcarrier

Parameters	Value
Path Loss (dB)	61.7
Antenna Gain (dB)	0
Antenna Efficiency	100%
Bandwidth (MHz)	4.125
Transmit Power Density (dBm/Hz)	-41.3
Transmit Power (dBm)	-35.1

Table 2-6 Parameters of the link budget analysis

On the other hand, the link margin measures the difference between received power and the receiver sensitivity. It indicates how much extra attenuation a particular radio link can tolerate subject to a minimal required signal to noise ratio (SNR). In the UWB scenario, due to the limited maximum power emission specified by the FCC mask, the system may not be able to utilize the wide bandwidth because of the overall lower link margin, hence restricting the range of the UWB applications. However, in the future Cognitive UWB may extend its transmission range by assigning transmit power over the spectrum mask in a cognitive way, meanwhile maintaining the minimum impact on other devices required by the existing FCC spectrum mask.

$$\text{Receiver Sensitivity} = \text{SNR}_{\text{required}} + \text{Noise Power} \quad 2.5$$

Where $\text{SNR}_{\text{required}}$ is the required minimum signal to noise ratio for a given modulation scheme, and we choose 4.6dB in our simulation for QPSK modulation [36, 47]. The required transmit power for the certain sensitivity is calculated by equation 2.6, which assumes 0 dB link margin.

$$\text{Required Transmit Power} = \text{Receiver Sensitivity} + \text{Path Loss} \quad 2.6$$

Figure 2.10 shows the required transmit power versus distance, and the certain transmit power corresponding to the FCC spectrum mask is illustrated as a horizontal line. It should be noted that we use a bandwidth of 4.125 MHz which is the bandwidth of the subcarrier as mentioned in section 2.2.2.

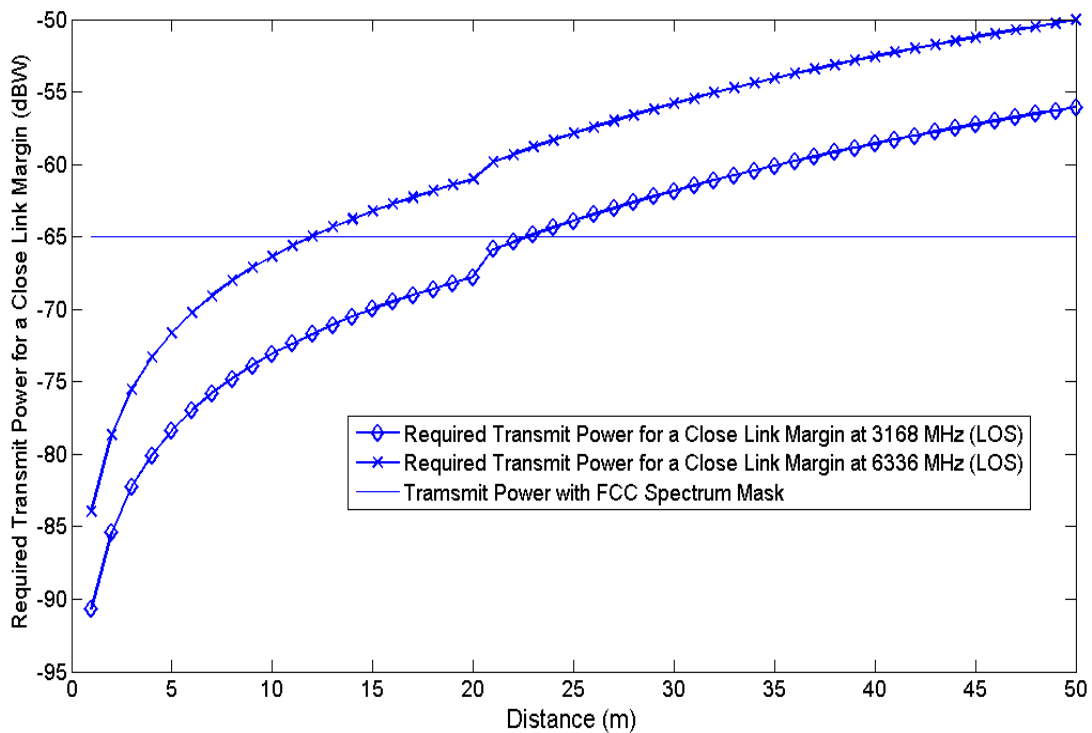


Figure 2-10 Required transmit power analysis

It can be interpreted from Figure 2.10 that the system can work with the transmit power limits given by the FCC spectrum mask up until 25 metres for 3168 MHz and

13 metres for 6336 MHz. The sudden change at 18 metres is due to the change of channel model from 802.15.4a to Walfish-Ikegami.

2.2.4 UWB Frequency Selective Fading Channel Modelling Techniques

We have introduced UWB channel path loss and discussed the channel path loss at extended ranges. We now discuss the frequency selective behaviour of the UWB channel. It is however, important to introduce the topic of multipath propagation first. In practice, the beam of radio energy that is sent by the transmitter is not received at the receiver with only one beam, but instead from many beams. These multiple radio beams (after reflection and diffraction on the surface of objects) will arrive at the receiver at a slightly different time and phase. The received rays at the receiver will add up or cancel out which gives rise to multipath fading (rays that have opposite phase will add up destructively).

Multipath fading is also referred to as frequency selective fading. This frequency selective fading distorts the received signal when the frequency components of the signal are not all affected equally [48]. More specifically, frequency selective fading happens when the signal's spectrum is wider than the channel coherence bandwidth, and hence the spectrum components that are outside the coherence bandwidth will be affected differently than those within the coherence bandwidth. An illustration is shown where in Figure 2.11, where f_0 is the coherence bandwidth.

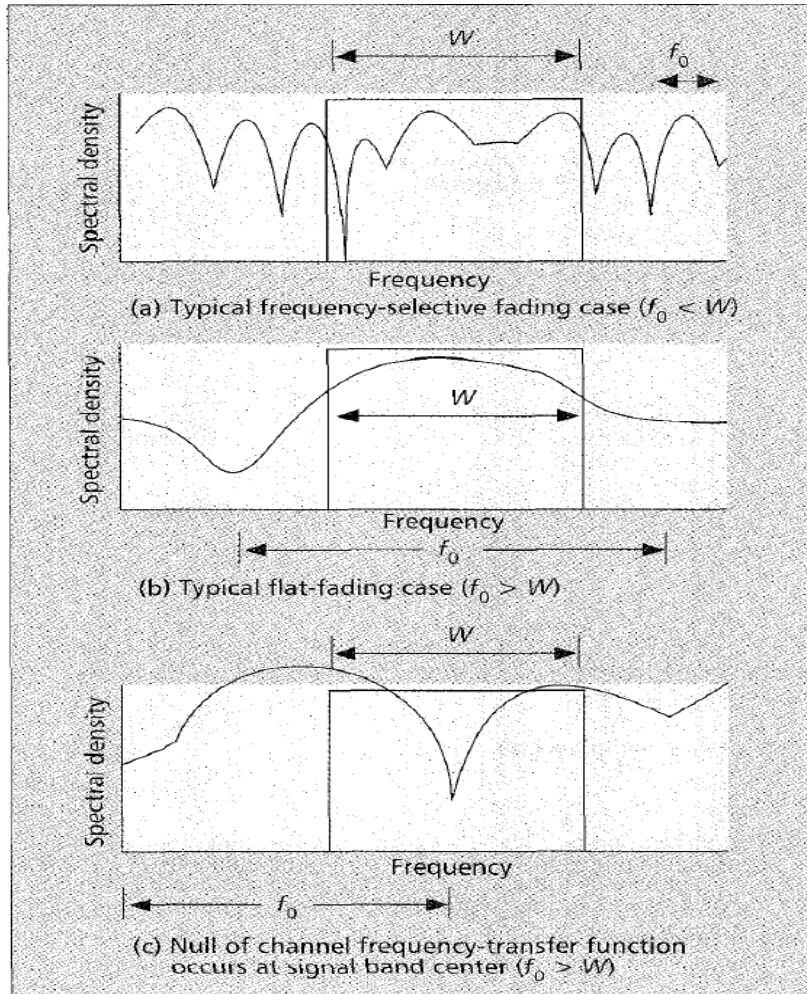


Figure 2-11 Relationships between the channel frequency-transfer function and a signal with bandwidth W (taken from [48])

As can be seen from Figure 2.11, subFigure (a) shows that the signal is distorted by frequency selective fading, and some of the frequency components experience deeper fading than other frequency components. SubFigure (b) and subFigure (c) show the signal after undergoing a flat fading channel. The signal in subFigure (b) is distorted very little while that in subFigure (c) suffers deep fading.

2.2.4.1 UWB Channel Coherence Bandwidth

The channel coherence bandwidth can be expressed in the following equation, which shows that the coherence bandwidth is inversely proportional to the factor Δ , where Δ is the delay spread.

$$f_0 \propto \frac{1}{\Delta} \quad 2.7$$

$$\Delta = \sqrt{\frac{\sum_i (\tau_i - d)^2 |h_i|^2}{\sum_i |h_i|^2}} \quad 2.8$$

Equation 2.8 is the root mean square of the channel power delay profile from its impulse response [49], where d is the mean delay of the channel power profile.

$$d = \frac{\sum_i \tau_i^2 |h_i|^2}{\sum_i |h_i|^2} \quad 2.9$$

Lastly, the received signal that undergoes a multipath fading channel can be expressed by the following equation in the time domain.

$$y(t) = \int_{-\infty}^{\infty} h(t, \tau) x(t - \tau) d\tau \quad 2.10$$

Figure 2.12 illustrates 100 impulse responses based on a NLOS UWB channel model.

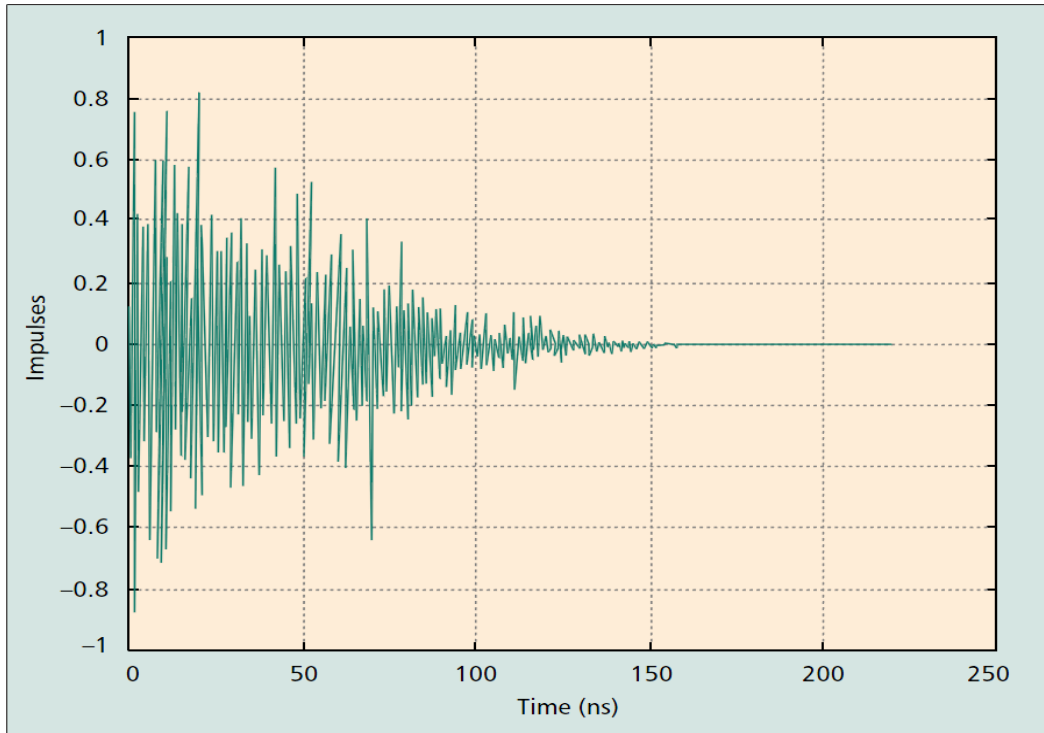


Figure 2-12 100 impulse response based on a NLOS UWB channel model (taken from [40])

In this particular channel impulse response, the root mean square delay spread is 15ns [40], which in turn provides us with an indirect measure of a UWB channel coherence bandwidth. The relationship between coherence bandwidth and the channel delay spread has been specified in [48]. A coherence bandwidth that is equal to the inverse of the RMS delay spread means that frequencies that are located close to each other within the coherence bandwidth can be considered as experiencing the same fading. In [41], the author claims that a higher delay spread of 25 ns can cover worst case situations. In this case the inverse of the delay spread is 40MHz. Hence, the spectrum components that lie within 40MHz will experience the same fading. It is now obvious that frequency selective fading is unavoidable as the UWB transmission uses a minimum of 512MHz bandwidth. On the other hand, the assumption that we made later in our simulation that subcarriers of 4.125MHz will have the same amount of fading within that bandwidth is reasonable.

2.2.4.2 UWB Channel Time Variance

According to [48] a moving receiver will give rise to a Doppler spectrum, and the received signal will undergo a different fading in the time domain. There are two terms used to describe the fading speed: *fast fading* and *slow fading*. The fast fading is used to describe the channels with a coherence time shorter than the time duration of the transmission symbol. Slow fading on the contrary, describes channels with a coherence time longer than the time duration of the transmission symbol. The slow fading channel can be thought of as static over the symbol period.

In [40], the 802.15 standard model assumes that the channel stays completely static or changes completely in about 100 μ s in the worst case scenario. It is because the transmitter and receiver in the short range application are considered to be stationary. A person moving between transmitter and receiver, however, will inevitably introduce fading and the channel may shift from LOS to NLOS. This is not considered in this thesis.

Based on the worst case scenario from [40], we can approximately estimate the target performance for our proposed DCPA scheme. The worst case scenario has a period of

100 μ s over which a specific channel will be completely static, and hence we expect our proposed DCPA scheme can converge within this time period. We assume that it takes two symbol periods and a round trip time for each iteration of our proposed DCPA scheme.

$$T_{iteration} = 2 \times \frac{d}{c} + 2 \times T_{symbol} + 2 \times T_{process} \quad 2.11$$

The processing time however is ignored. Now, take the parameters from MB-OFDM specification in Table 2.1. The UWB symbol period is of 312.5ns. A round trip time for a link length of 50 metres is 333.3 ns, which is derived from the round trip distance $2d$ divided by light speed c . The duration of each iteration is 958.3ns. Therefore, there can only be a maximum of 104 iterations in order to guarantee convergence under the worst case scenario.

2.2.4.3 Expression of the UWB Fading Channel

We have so far analysed the UWB frequency selectivity behaviour, and show that it is necessary to explore frequency selective fading in our channel model. We can now explore a suitable expression for the UWB fading channel.

It is suggested that in case of mobile radio, the received signal can be expressed by the multiplication between the large scale fading component and the small scale fading component as can be seen in equation 2.12 [48]

$$r(t) = m(t)r_0(t) \quad 2.12$$

Where $m(t)$ is the large scale fading component, and $r_0(t)$ is small scale fading component. It is suggested that the small scale fading is superimposed on large scale fading [48]. For a UWB channel the received signal can be expressed as equation 2.13

$$r(f, t) = p(f, t)PL(f, d, t)r_0(f, t) \quad 2.13$$

Where $r(f, t)$ is the received power of the subcarrier with central frequency f at time instance t . $p(f, t)$ is the transmit power of subcarrier with central frequency f at time

instance t . $PL(f, d, t)$ is the frequency dependent path loss. $r_0(f, t)$ is the multipath fading factor on the channel with central frequency f , at time instance t .

In the frequency domain, frequency dependent fading can be written as $H(f)$ and we derive this frequency selective fading from the normalized channel impulse response by means of Fourier transform. Assuming that the radio environment remains static for a short range link, the fading path loss and the frequency selective fading are not a function of time.

$$r(f, t) = p(f, t)PL(f, d)H(f) \quad 2.14$$

2.2.5 Cognitive UWB

We have so far introduced the concepts of CR and UWB. The following questions are yet unanswered, what is the possible way to combine CR and UWB and why it is so promising? With the spectrum mask in mind, we should firstly introduce the terms underlay and overlay. The definitions of underlay and overlay given here might be slight different from some definitions in the other articles [50-52]. The term underlay means that UWB devices will have power emissions under the FCC power spectrum mask; the term overlay means the CR devices transmit power at a similar level to licensed users by opportunistically sharing the frequency bands.

Cognitive Radio as discussed in section 2.1 offers wireless communications some degree of intelligence, sensing and adapting dynamic spectrum conditions to meet specific user requirements. It is assumed that CR works on a relative narrow band in an overlay scenario, provided with precise awareness of the spectral environment and techniques for the effective avoidance of licensed users. UWB communications, however, utilizes a vast spectrum and works on a highly restricted underlay scenario, and normally does not consider the detection and avoidance of the existing wireless services because of the so called vanishingly low emission power density. Nevertheless, it may become troublesome in a future dense deployment environment [23, 53], where the collective interference from densely deployed UWB devices may

jeopardize some crucial wireless services such as aircraft guidance systems [54]. Reducing the collective interference by spectrum sensing, intelligent spectrum sharing and power allocation offered by CR techniques can be substantial.

On the other hand, an overlay cognitive UWB that can opportunistically reach a higher emission power density over the current spectrum mask will extend the range of UWB devices by allocating a dynamically sculptured power profile to overcome the high attenuation meanwhile avoiding the interference to the existing agile services of primary users.

The term Cognitive UWB, was suggested in [55, 56], where the idea of a CR empowered UWB system was put forward as a research objective. A number of research issues have been raised including interaction strategies for efficient cooperation and cooperative coding strategies for spectrum sharing. The possible analytical tool given in [55] is game theory, which we also think of as a feasible tool to realize a cognitive engine. There are, however, more tools that we could use to enable a DCPA for cognitive UWB such as reinforcement learning and Water Filling.

2.3 Game Theory in Wireless Communications

It has been recognised that the study of game theory has a long history and can be dated back to the ancient time of the Talmud (0-500 AD) which contains some results that are consistent with the modern game theory [57]. It is however not until the 1940s that the general theory of strategic situations was called game theory. The goal of formulating optimal strategies has puzzled mathematicians for hundreds of years, and a powerful and influential tool of modern social science is finally established though the efforts of both modern mathematicians and economists [57]. Although game theory has mostly been used in economics, it is becoming increasingly important and a vital methodology that is applicable to various fields, such as political science, biology and law, and it has lately been introduced to communications. In this section we will introduce the technical definition of a game, the most important concepts of games, and then introduce the mathematic representation of a game. Finally we will

give a general methodology of applying game theory to communications followed by an introduction to the game strategy

2.3.1 Definition of Game Theory

Games in real life, according to [58], are a result of conflict and cooperation which can be described as strategic settings. Game theory, according to [57], is therefore defined as a methodology of formally studying situations of interdependence in a mathematically precise and logically consistent structure.

The definition of a game implies that it should involve multiple decision makers with conflicting interests, and the actions within a certain game context which can be either competition or cooperation. Also it means that a game model is appropriate only when the problem involves several autonomous agents that make decisions on their own, and the outcome is a result of the actions and counter actions of all agents. In real life, a game can be as common as a poker game or a chess game, which involve several interdependent players and an autonomous decision making process. A game model is also appropriate in scenarios where it is difficult to optimise using a conventional optimisation process, such as commercial events in which sellers and buyers made their decision on goods and selling price. The buyer prefers a lower price with good quality, and the seller wants to set the price to the goods as high as the market will support to maximize their income. In this scenario, the buyers may have conflicts between price and the quality of the goods while the seller may have conflicts between sale price and the amount of selling. The buyer and the seller alone can be viewed as performing an optimisation process, however interactions between seller and buyer add an additional dimension to the problem so that it can hardly be solved by an optimisation process which maximizes both buyers and sellers satisfaction. On the other hand, real life engineering problems can be modelled as game, such as a car navigation problem, which involves multiple cars navigating and optimising their routes to their final destinations, however, restricted by sharing the roadway.

Game Theory by definition researches the interactive decision making process in a solid mathematical and analytical way. By understanding the actions and strategy that

players play in a certain game scenario, we can even predict the outcome of the game, and hence optimise the game play. Therefore, game theory can be viewed a collection of modelling tools that assist us with analysing and solving some of the most complex optimisation problems that involve interaction and conflicts between multiple autonomous agents. It is however necessary that a game model can be expressed in a mathematically precise form.

The fundamental structure of the game in game theory is made up of three components: firstly, a set of players, who are interdependent and seek to maximize their own interests through a game competition. Secondly, a set of actions, the players may take in the competition. Thirdly, a preference relationship, which maps the actions to some real values and can be compared numerically. The preference relationship is also called a utility function. Through the utility function, a player will prefer an action that leads to a higher outcome (utility) than a lower one.

2.3.2 Important Concepts of Game Theory

There are some most important game concepts that we need to understand in order to apply the Game Theory properly in modelling and analysing wireless communications.

1) *Non-cooperative Game and Cooperative Game*

There are two major frameworks of modern Game theory: Non-cooperative Games and Cooperative Games.

- a) Non-cooperative Games as the name suggest, treat all of the agents' actions as individual actions, where individual actions refer to the decisions that the player decides on his own. Therefore there is no direct negotiation between agents. In [58], a Non-cooperative game is thought to be the most realistic way of modelling the players' options. It is because the individual player is most likely to make their decisions based only on their own interests. However, the drawback of such a framework is that it is usually difficult to analyse a non-cooperative game [58], because of the incomplete information of the game

from the perspective of a single agent. Therefore, agents may behave unpredictably due to the lack of information exchange.

- b) Cooperative Games by contrast describe any outcome of the game as a result of a joint action, which means agents negotiate with all the others in order to decide their action. In most cases it can simplify the analysis of the game, and is preferred for the study of contractual relations in economics [57, 58]. Nevertheless, a real game in the everyday sense is usually not a cooperative game, as the players in most of the cases choose their actions independently.

2) Utility Theory

As we introduced before, the essential of the Game Theory is to study the interactive decision making process in a solid mathematical and analytical way. To study the decision making process, we need to firstly define decision in a mathematical solid way.

It is clear that agents make decisions based on their preferences. In decision theory, we use \succ or \succcurlyeq , a binary relation to express a preference. Such as $x \succ y, x, y \in X$ means x is preferred to y . However, it requires *completeness* and *transitivity* to have a binary relation to be a preference relation. *Completeness* means that preference can be made on completely different objects, such as a person prefers having a laptop than a tablet. They are two different types of things that can satisfy different needs. *Transitivity* means absolute distinction between objects, such as if a person prefers more sugar in her tea, then 3 spoons of sugar should be more preferable than 1 spoon of sugar for her.

In order to quantify the satisfaction, we need utility functions to express a preference relation in an analytical way. In [58], the utility function is defined, $u: X \rightarrow \mathbb{R}$, when

$$x \succ y \Leftrightarrow u(x) > u(y), x, y \in X \quad 2.15$$

Equation 4.1 means that a utility function is a mapping from objects to certain values. Say if x is strictly preferred over y , then there must be numerical relationship $u(x)$ bigger than $u(y)$.

3) Game Strategy

A strategy is a complete contingent plan for a player in the game, and the complete contingent is referred to the full specification of a player's behaviour, which describes the actions that the player would take at each of his possible decision points [57]. However there are two distinct strategies.

- a) A mixed strategy for a player is the act of selecting a strategy according to a probability distribution, which reflects the uncertainty that players choose their strategy when they doubt the behaviour of their counterparts.
- b) The strategy of the player that does not follow a probability distribution is called a pure strategy, which is reasonable for program based computer agents.

4) Solution Concept

Importantly, Game Theory helps us predict the result of the interaction of the players in a game, which leads to the solution concepts that a game may finally achieve some stable operation points [57]. The most common solution concept of a game is called *Nash equilibrium* defined by John Nash [59]. A *Nash equilibrium* can be viewed as stable operating point, where no player can achieve any higher outcome by changing actions. Another important solution concept is called a *Pareto efficient*, and we can view a *Pareto efficient* as an improved *Nash equilibrium* where it is not only a stable operation point but also an optimum operation point.

2.3.3 Game Strategy

We have introduced the definition of strategy and the distinction between mixed strategy and pure strategy. Next, we present a further introduction to the concepts of

game strategy. A strategy in a game is a complete plan for a player countering other player's actions. Similar to the importance of the choice of the utility function which is used to express preference, the strategies employed by players decide a Game's outcome or alternatively speaking, a good plan yields a better outcome [60]. A proper strategy will enforce a distributed power allocation game reaching an efficient Nash Equilibrium collectively.

2.3.3.1 Behaviour of Game Competition

In a game competition, players interact repeatedly and select their actions to counter their counterparts' actions. The possible actions that a player may behave in a game can be categorized into two categories: Cooperation and Defection.

The cooperation action is defined as behaviour in a game that is intended to produce a fair share of the radio resources between agents. Such behaviour in a radio resource competition game can be a certain amount of deduction of transmit power [61] or a reduced offered traffic or a reduced quality of service requirement [62].

The defection action on the other hand can be defined as behaviour that aims at a better share of the radio resources. Such behaviour for a radio system can be an intended transmit power increase, or even cheating behaviour such as informing a wrong channel gain message to the other systems [58]. However, the defection action in a game can also be defined as a punishment in response to the defection action of the opponents. Consequently, a player that performs defection may have two motivations. On one hand, the player may simply intend to increase its utility. On the other hand, the player may intend to counter the defection action of the other players.

2.3.3.2 A Dynamic Strategy of a Game

We have introduced the possible actions that a player can take in a game. Then it is important to understand under which circumstances should a player use certain

behaviours? We now introduce a stage based dynamic multistage game strategy that is used to decide the behaviour of players in the game competition.

A Stage of the Strategy

Systems autonomously make decisions on cooperation or defection in a game. We define that the decision is made at the end of each stage, and we define a stage as a single action such as cooperation action or defection action.

B Dynamic Strategy

A stage based dynamic strategy can be viewed as an event-driven decision making model, which decide the stage transition [63]. We can use state machines to model the dynamic strategy. Figure 2.13 illustrates the definition of the state machine for a single cooperation stage, where $n=1$ represents the initial stage.

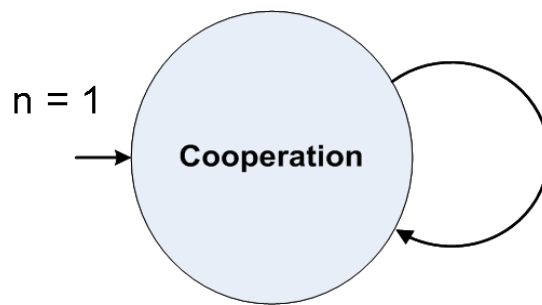


Figure 2-13 Illustration of a Single Stage

In [63], six different strategies have been investigated both in single stage and multiple stage games. We are particularly interested in the *TitforTat* (TFT) strategy which is shown in Figure 2.13. The TFT strategy works in such a way that player cooperates as long as the opponents cooperate and punishes the opponent immediately if a defect action is identified, but the player is willing to return to cooperate if the opponents cooperate again.

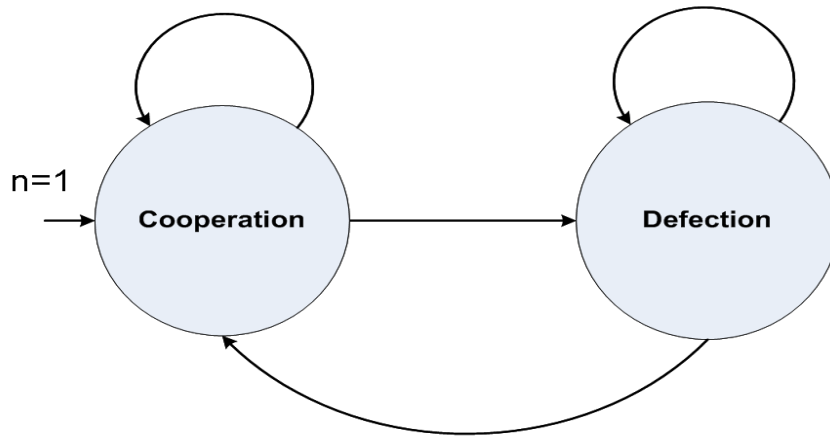


Figure 2-14 Illustration of a *TitforTat* Strategy

The TFT strategy is effective for the iterative prisoner's dilemma problem [63], and this simple strategy has already been used in real applications such as peer to peer file sharing, where BitTorrent peers use this strategy to boost the overall download speed [58]. The peer to peer sharing program works in such a way that a higher download speed can only be acquired by sharing the already downloaded resources with other users who willing to download it, therefore. The overall download speed can be boosted by users sharing the resources or alternatively speaking acting cooperatively.

2.3.4 Mathematical Expressions of a Game

We have introduced the definition of Game Theory and reviewed some of its most important concepts. We now look into the mathematical representation of a game, and the important solution concept.

As we introduced before, a game is made up of three main components:

- 1) The players or agents: The set of players can be expressed as I , and $i \in \{1, 2, \dots, I\}$.
- 2) Strategy profile: The strategy profile is the complete contingent actions for each player. The strategy profile can be expressed as $A = A_1 \times A_2 \times \dots \times A_I$, where A_i is the set of possible actions of player I .

3) The utility function: The utility function also called a payoff function maps the action profile of player into real numbers [58], which can be expressed as $u_i : A \rightarrow U$ where u_i is the utility of the player i .

4) Solution Concepts

Recall the definitions of solution concepts we introduced before. In a real game, a player often takes the simple form of an agreement to play a specific strategy profile. The *Nash equilibrium* is such a strategy profile that no player may gain benefit by deviating from the current strategy. A strategy profile is said to be *Pareto efficient* if it is impossible to improve the utility of any player without reducing the utility of the other.

a) Nash Equilibrium: The Nash Equilibrium of a game can be expressed by the following inequality:

$$U_i(a_i, a_{-i}) \geq U_i(\tilde{a}_i, a_{-i}) \quad 2.16$$

Where $\tilde{a}_i \in A_i$ expresses a stable operating point where no player has any incentive to change strategy [57]. a_{-i} denotes the actions taken by the other $N-i$ players.

b) Pareto efficiency: Pareto efficiency can be defined as an inequality

$$U_i(\tilde{a}_i) \geq U_i(a) \quad 2.17$$

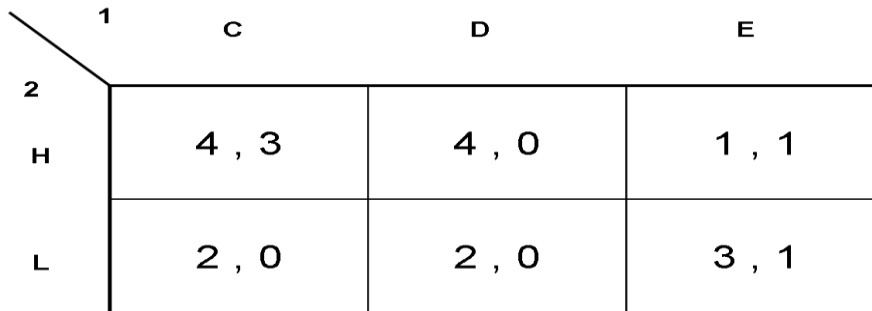
Where there is no action that results in higher utility then the operating point is at Pareto efficiency.

However many stable operating points for a game competition may exist. The reason that a game may have many different stable operation points is due to the lack of coordination, or selfish behaviour of the players. Imagine a CDMA cellular network, if we let the mobile phone itself decide the uplink transmit power, the result may be an overall worst Signal to Interference plus Noise Ratio (SINR), when either an

increased or reduced transmit power will not result in a better SINR. Alternatively an optimum stable operation point could be obtained if the players are rational and choose their action according to some fine strategy.

5) Strategy Space

A matrix is one of the most convenient ways of describing the strategy spaces of the players and their utility functions for two-player games. Each player has a finite number of strategies. As can be seen from Figure 4.1, letter C, D, and E represent actions of player 1, and the letters H and L represent actions of player 2. The entries of the matrix are the utility values corresponding to the actions played by player 1 and player 2.



		1		
		C	D	E
2	H	4 , 3	4 , 0	1 , 1
	L	2 , 0	2 , 0	3 , 1

Figure 2-15 Example of a game in the matrix form

We can find two Nash Equilibriums from the game shown in Figure 4.1: one is (C, H) which means player 1 plays strategy C and player 2 plays strategy H. The other is (L, E). Only strategy (C, H) is Pareto efficient. As we explained before, there may be a few Nash Equilibriums in a game competition. However the optimal operating point can be obtained by means of a well designed game strategy.

The agents can have certain preferences over their actions, which give rise to a pure strategy space as in the matrix we showed above. On the other hand, the agents can be uncertain regarding their actions, which give rise to probabilities associated with actions. We call a strategy space with uncertain actions, a *mixed strategy*. A game with a mixed strategy will have an expected utility, which is the average payoff of all possible utilities.

$$u_i(a_i, \rho_{-i}) = \sum_{a_{-i} \in A_{-i}} \rho_{-i}(s_{-i}) u_i(a_i, a_{-i}) \quad 2.18$$

Where ρ_i is the probability distribution over the strategy of the user i , and $\rho_i \in \Delta A_{-i}$ where ΔA_{-i} represents the probability distributions over the strategies of all the other players. Note that we will not discuss mixed strategy game as our system model is designed as a pure strategy game.

2.3.5 Applying Game Theory to Wireless Communications

Game theory was firstly introduced to economics to analyse and simulate the behaviour of multiple conflicting agents in a particular market context. Recently, game theory was expanded and has become a proper and feasible tool that can be applied in the telecommunication field [64-66]. On one hand, many of the wireless communication optimization problems are proven to be NP-hard problems, and many once solvable optimisation problems can become computationally infeasible as the size of networks increase. Game theory, since it studies the individual decision making process, has a high scalability, and will be less restricted by the increased size of the network. The distributed nature of many emerging wireless networks such as ad-hoc networks or mesh networks are better designed using a game-theoretic approach rather than an optimisation algorithm, because the distributed network power energy or routing optimisation problems, are restricted by the distributed nature of the network. A single distributed node may not have the full knowledge of the network and the parameters of all the other nodes in the same network. A *non-cooperative game* is used to study such distributed decision making process and is proven to be capable of solving such problem [65]. Lastly, in game theory, it is normally assumed that the players are perfectly rational but selfish in order to maximize their utility in the game. This may not be true in human society, but can be achieved in a program controlled wireless network.

Related work in wireless communications can be divided into two categories: one research area deals with unlicensed band spectrum sharing. In [67], a comprehensive analysis of the efficiency of the Nash Equilibrium is given, and it is numerically proven that distributed global efficiency can be achieved though enforced punishment

strategies. In [63], multiple strategies are analysed in a radio resource sharing game, and decentralized cooperation between different systems is proven to improve the overall spectrum efficiency. The other research area focuses on applying game theory to licensed bands. In this case, researchers tend to formulate a communication problem in terms of existing game models in economics. In [62], the author introduces a refereed game into the CDMA power control problem to achieve a global optimum Nash Equilibrium point which is also referred to as Pareto efficiency. The following work of applying game theory to the CDMA power control problem can be found in [61, 62]. In [68], the concept of a Cournot game [69] is used to model coexistence between primary and secondary users, where the primary user is modelled as oligopolist (a term in economics describing an organisation with higher authority) which prices the secondary user based on spectrum usability. The stability and efficiency of the Nash Equilibrium is analysed, and the relative work in mathematical economy can be found in [69].

We have so far introduced the expression of a game, and the major components of a game model in Game theory, so that we can model a wireless network using Game theory. A set of wireless systems (which includes transmitter and receiver) can be modelled as players who need to compete for radio resources subject to some limitations in a resource allocation game; a set of possible actions for each wireless node to react the strategies of its counterparts, and a common utility function that maps all the possible actions to real numbers [65]. Lastly, the strategies that are adopted by communication systems are designed to ensure that the game reaches global optimization or a global stable Nash Equilibrium. In the next chapter we will introduce our game model, and utility function to solve a distributed UWB power allocation problem.

2.4 Reinforcement Learning in Wireless Communications

According to [70, 71], research on multi-agent learning technique has been mostly concentrated on a unique type of learning: Reinforcement Learning (RL). It is because of certain strength and merits that Reinforcement Learning has impressed the

researchers. These merits can be summarized into one significant advantage: The capability of shaping the environment from which the agents learn their optimistic actions.

To date, Reinforcement Learning has been applied to a wide variety of domains including auto pilots, Adaptive Load Balancing (distributed resource management), and wireless power allocation. This section reviews the literature upon RL, and its applications for wireless communications. We will introduce the well defined single agent Q-learning technique and explain the difficulties faced by the multi-agent RL. Then we will introduce the applications of RL in wireless communication.

2.4.1 Reinforcement Learning and Q-Learning

Reinforcement Learning (RL) is initially applied by an agent in a trial and error fashion, it is this repeated iteration between the agent and its acting environment that potentially leads the learning process to converge on an optimal solution which yields the best reward [70, 72]. The agent evaluates and quantifies its actions on every trial it makes in order to choose its further actions. We can express such learning process in the following equation.

$$V^\pi(S) = r + \gamma r_1 + \gamma^2 r_2 + \dots + \gamma^n r_n \quad 2.19$$

Where r is the *immediate reward*, which is the reward or response of the environment to a certain action. $V^\pi(S)$ is the so called *cumulative reward* acquired by following an arbitrary action sets π . We can also call π a strategy or policy of the agent that determines the action that agent will take in each state. γ is a constant $0 \leq \gamma < 1$, which is the discount factor that controls the relative reward value. Setting $\gamma = 0$ means that the agent takes no account of the rewards from following actions; while γ approaching 1 means that the agent emphasises the future actions. n is the state number and r is the immediate reward from taking a specific action on state n . The task of the agent can be expressed by equation 2.20

$$\pi^* = \operatorname{argmax} V^\pi(S), (\forall S) \quad 2.20$$

Equation 2.20 means the learning task for an agent is to learn a strategy π that will maximize the *cumulative reward* $V^\pi(S)$.

Given that only a sequence of immediate rewards of an action is assessable to the agent, it is difficult to learn an optimal policy that will maximize the cumulative reward [72]. However, the optimal policy can still be learned though an iterative approximation, by calculating the *action-value function* (Q-function) [72].

$$Q(s, a) = r + \gamma \cdot \max V^\pi(S) \quad 2.21$$

Equation 2.21 means that the Q value is obtained by current reward r on stage s plus a discounted maximum cumulative reward. The optimal Q value can not be acquired directly but can be acquired by an iterative estimation 2.22, which satisfies the *Bellman optimality equation* [72].

$$Q^*(s, a) = r + \gamma \max_{a'} Q^*(s', a') \quad 2.22$$

Where $Q^*(s, a)$ is the estimate of the actual Q value at stage s . The estimation is conducted by an exhaustive search of the maximum immediate rewards over all possible actions in a new state s' , defined by $\max_{a'} Q^*(s', a')$. The Q value Table for the current state is then updated accordingly given the equation 2.22. It should be noted that we simply assign $Q^*(s, a) = V^\pi(S)$, in order to initiate the iterative estimation.

2.4.2 Multi-agent Q-Learning

We have introduced machine learning and Q-learning on a single agent basis, and it has been proven to obtain an optimal policy that maximizes cumulative rewards [71]. However, when it comes to multi-agent Q-learning, it soon becomes challenging and analytically difficult to apply Q-learning in a multi-agent context [70, 71]. It is because the theoretical guarantees of single agent Q-learning are no longer available for multi-agent Q-learning (it is possible to apply single agent Q-learning immediately

to agents in a multi-agent context but the performance is not guaranteed [70]). On the other hand, the interference from the actions of the other agents will heavily influence the learning process and the immediate reward. It is suggested in [18, 71, 73] that the agents learning from joint actions outperform a corresponding agent who learns only in terms of its own actions.

Multi-agent Q-learning can be formulated in the equation below:

$$Q^*(s, a^1, a^2, \dots, a^n) = r(s, a^1, a^2, \dots, a^n) + \gamma \max_{a'} Q^*(s', a'^1, a'^2, \dots, a'^n)$$

2.23

Where $Q^*(s, a^1, a^2, \dots, a^n)$ is the estimate of the actual Q value in a multi-agent learning context. a^2, \dots, a^n are the actions of the homogeneous agents at stage s . In a similar way to single agent Q learning, multi-agent Q learning has to conduct an exhaustive search of the maximum immediate rewards over all possible actions in a new state s' where the not only the direct response from the environment, the possible actions of homogeneous agents have to be learned as well. This is written as: $\max_{a'} Q^*(s', a'^1, a'^2, \dots, a'^n)$. $r(s, a^1, a^2, \dots, a^n)$ is the immediate reward to the action of an agent given the actions of all the other agents.

This equation shows that an agent has to keep records of both the immediate reward of all other competitive agents and the entire searching Table of the estimated Q of its opponents in order to obtain optimistic cumulative rewards.

It is possible to replicate and update the Q-Table of all the agents. In [71] the authors develop an Optimal Adaptive Learning (OLA) that coordinates the joint actions of the multi-agent by biasing the recently selected optimal actions, and the author proved that the OLA algorithm can achieve a joint optimal policy. However, the need for coordination brings in extra complexity.

2.4.3 Applying Reinforcement Learning to Wireless Communications

While the game theoretical approach is considered as a proper tool for DCPA technique, reinforcement learning in wireless power allocation has gained significant research interest in recent years. In wireless communications, reinforcement learning can be used to learn the channel usage pattern. The past sensing knowledge multiplied by a discount value, and summed up so that the heavily used channel or severe fading or interference will be identified and marked in the spectrum pool as less preferable channels. Successful transmissions can also be weighted and learned by the radio agent and the sum of the weighted successful transmissions could be used as a channel preference index to decide future channel assignment [18, 74].

Reinforcement learning for a radio agent can be modelled in Figure 2.16.

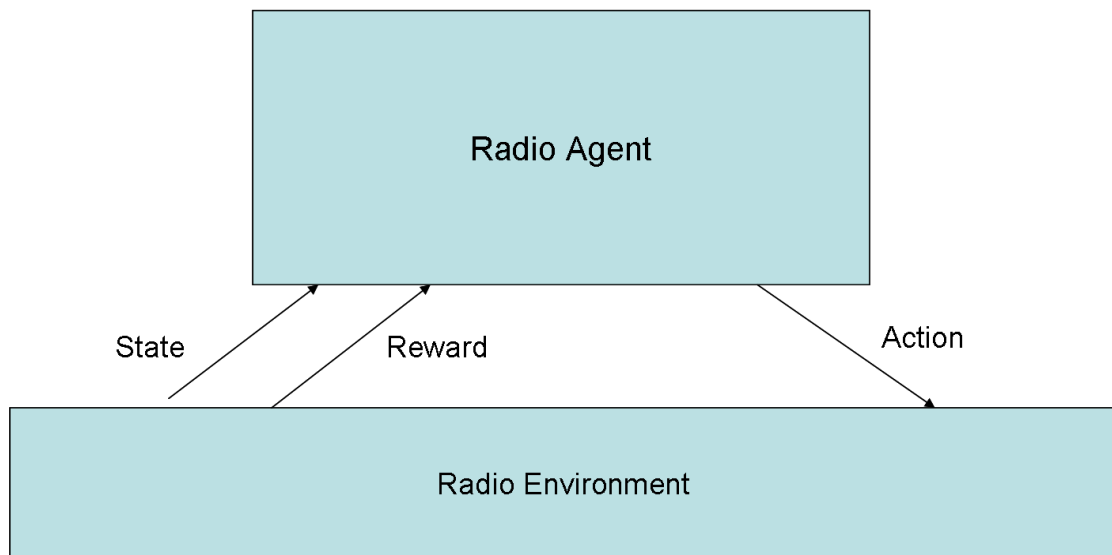


Figure 2-16 Reinforcement Learning (adapted from [72])

As can be seen from Figure 2.16, the radio environment is the channel pattern that a radio agent would like to learn and recognise as knowledge for its future channel assignment. The state is the current sensing information of the radio environment and the reward is the result of a cumulative reward function which can be a mathematical representation of the weighted channel pattern of the past sensing history. The action can be a channel assignment according to cumulative reward function or simply another sensing action. In case of the multiple wireless agents spectrum sharing

problem where the actions of actions of the competing agents have to be learned in order to guarantee the convergence, some form of information sharing can be formulated to help the learning algorithm converge. In [18] a *Docitive Paradigm* is invented, where the radio systems periodically share their policies by exchanging Q-tables with the competitive radio systems.

In [74], a Q-learning based Dynamic Channel Assignment Technique is developed for a mobile cellular network. It shows that Q-learning based Dynamic Channel Assignment clearly outperforms a Fixed Channel Assignment scheme in terms of blocking probability. It also demonstrates the same level of performance in comparison with a maximum availability-based dynamic channel assignment, MAXAVAIL.

Despite being popular in recent spectrum sharing research [75-77], some of the drawbacks of applying RL to wireless communication also need to be tackled in the future: Firstly, delayed reward is the delay introduced by learning algorithms in which agent has to conduct an exhaustive search of the maximum immediate rewards over all possible actions, which means the channel pattern may not be recognised within a short period of time. Secondly, either the channel pattern or the primary users may only partially be observed due to strong interferences or deep channel fading (hidden terminal). This may cause false recognition given a certain learning period, unless we assume life time observation and learning, and the learning algorithm may never converge. Finally, the requirement for coordination under a multi-agent learning context currently reduces its suitability for a DCPA scheme (It is possible to learn locally without coordination, however the optimal Q estimation is not guaranteed [70]).

2.5 Power Allocation by Traditional Optimization Process

We have outlined the idea of the game theoretical approach and reinforcement learning in channel assignment, It is clear that these methods can deliver exceptionally good performance in certain scenarios such as applying game

theoretical approach to distributed multi-agent channel assignment, or applying reinforcement learning to centralized channel assignment in a cellular network. Traditionally, research on power allocation and channel assignment centred on the so-called optimization process [78, 79], which is targeted at finding the maximum channel capacity subject to the total transmission power. In this section, we will review the optimization process and its application in wireless communication.

2.5.1 Introduction to the Optimization Problem and Lagrange Multiplication

An optimization problem and its solution can be interpreted geometrically along with mathematic expressions.

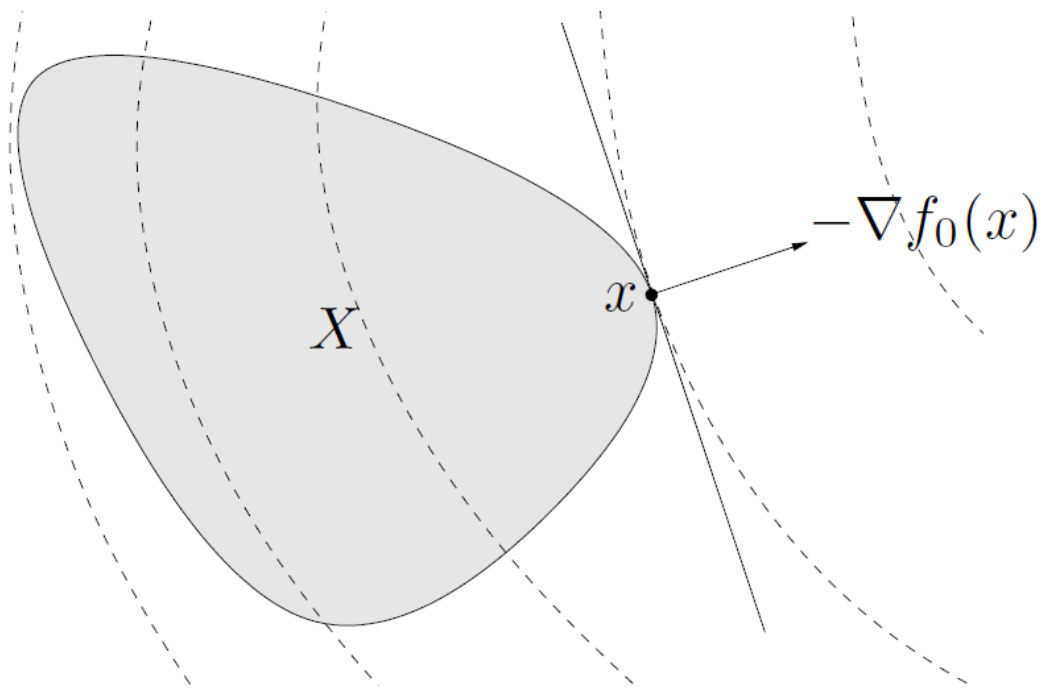


Figure 2-17 Geometric interpretation of the optimization problem (taken from [80])

Figure 2.17 shows a geometric interpretation of the optimization problem. The curves with dashed lines are the target function f_0 . The shaded shape X is the feasible set. The optimization problem can be interpreted as finding the maximum (or minimum)

point of function $f_0(x)$ on condition that $x \in X$. The maximum point can be found when the derivative of $f_0(x)$ with respect to x is equal to zero $\nabla f_0(x) = 0$.

The typical optimization problem often takes the form of the following equation

$$\begin{aligned} &\text{Minimize } f_0(x) \\ &\text{Subject to } h_i(x) \leq 0 \quad i = 1, \dots, m \end{aligned} \tag{2.24}$$

Equation 2.24 describes the problem of finding an optimal x that minimizes the function $f_0(x)$, while simultaneously meeting the conditions $h_i(x) \leq 0 \quad i = 1, \dots, m$. The variable $x \in R^n$ is the optimization variable and the function $f_0: R^n \rightarrow R$ is the object function. The inequalities $h_i(x) \leq 0$ are the constraint functions [80].

To solve such an optimization problem, we often resort to Lagrange multiplication (Lagrange Dual Function), which reforms equation 2.24 into equation 2.25

$$L(x, \lambda) = f_0(x) + \sum_{i=1}^m \lambda_i h_i(x) \tag{2.25}$$

The L is referred to as the *Lagrangian* $L: R^n \times R^m \rightarrow R$, and λ_i is called the *Lagrange multiplier* which is associated with the i th constraint function $h_i(x) \leq 0$.

Importantly, the existence of optimal variables in the problem we described in equation 2.25 relies on the Karush-Kuha-Tucker(KKT) condition [80] given in equation 2.26. Assuming that the function $f_0(x)$ and $h_i(x)$ are differentiable

$$\begin{aligned} \nabla f_0(x^*) + \sum_{i=1}^m \lambda_i^* \nabla h_i(x^*) &= 0 \\ h_i(x) &\leq 0 \\ \lambda_i^* &\geq 0, \\ \lambda_i^* h_i(x^*) &= 0 \end{aligned} \tag{2.26}$$

Where x^* and λ_i^* are the optimal points. Lagrange multiplication offers us a solution concept for a constraint optimization problem.

2.5.2 Application of the Water Filling Technique in Wireless Communications

The *water filling* technique gains its name by resembling the process of filling a limited amount of water in a container, where the water is an analogue of total transmission power and the container is analogous to the wireless channel. The volume of water that can be placed into the container is decided by both the amount of water that is available and the size of the container [81].

Mathematically, finding the maximum channel capacity given certain power constraint and the radio channel condition can be formed as a constraint optimization problem.

We firstly express the *Shannon Capacity* equation for a time invariant frequency selective fading channel.

$$C = \sum_{\max P_i: \sum_i P_i \leq P} B_w \log_2 \left(1 + \frac{|H_i|^2 P_i}{N_0 B_w} \right) \quad 2.27$$

Where $|H_i|^2$ is the channel path gain on sub-channel i , P_i is the power allocated to the i th sub-channel which is subject to the inequality $\sum_i P_i \leq P$, P is the total transmit power constraint. B_w is the bandwidth of each sub-channel and N_0 is the additive Gaussian white noise density.

We then reform it into *Lagrangian L*, which gives equation 2.28

$$L(P_i) = \sum_{\max P_i: \sum_i P_i \leq P} B_w \log_2 \left(1 + \frac{|H_i|^2 P_i}{N_0 B_w} \right) - \lambda \sum_i P_i \quad 2.28$$

Now we differentiate 2.28 in terms of P_i and set the derivative equal to zero. Solving P_i with the constraint that $\sum_i P_i \leq P$, gives us the optimal power allocation that maximizes the channel capacity.

$$\frac{P_i}{P} = \begin{cases} \frac{1}{\gamma_0} - \frac{1}{\gamma_i} & \gamma_i \geq \gamma_0 \\ 0 & \gamma_i < \gamma_0 \end{cases} \quad 2.29$$

Where γ_i is Signal to Noise Ratio (SNR) of channel i and γ_0 is a constant chosen so that the power constraint is met. It can be interpreted as a ‘‘cutoff’’ value so that a channel with the SNR value below than it would carry no data transmission, or alternatively speaking, no power is allocated to the sub-channels with SNR lower than γ_0 . Such a power allocation resembles filling ‘‘water’’ into a spectrum pool, as can be seen from Figure 2.17. We call it water filling power allocation.

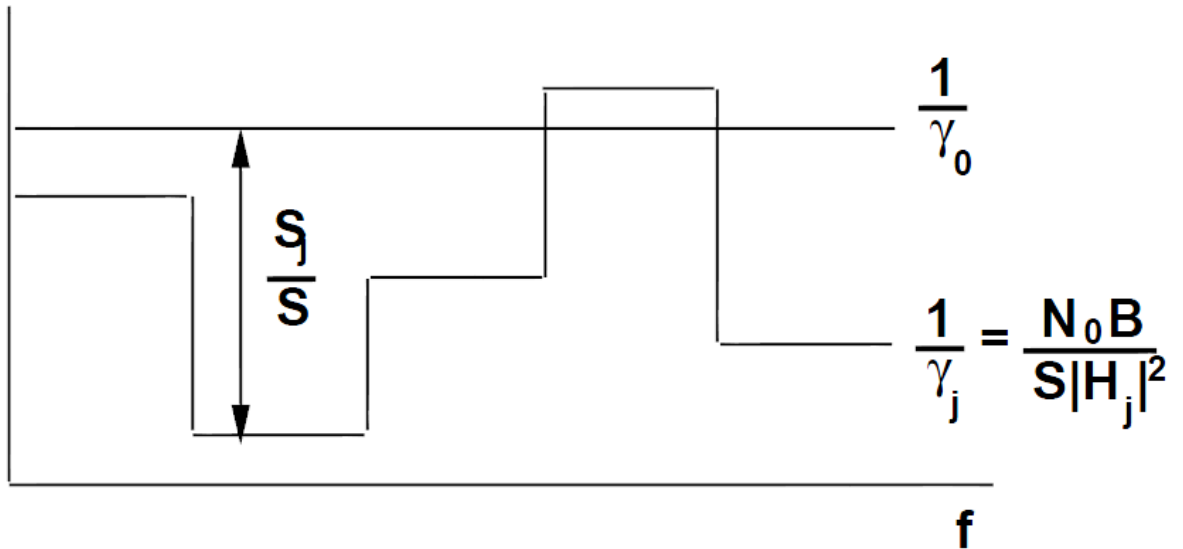


Figure 2-18 Water-filling in a frequency selective fading channel (taken from [46])

2.6 Chapter Conclusion

In this chapter we have presented a detailed introduction to some of the key areas used in this thesis. First and foremost we introduced the Cognitive Radio concept

which is the basis of our proposed DCPA scheme. Next, the UWB transmission technique and UWB propagation were introduced in detail, which will be used as our propagation models throughout our simulations. In particular, UWB channel frequency selective fading and time variance are investigated. An introduction to game theory provides the framework of our research. In addition, literature reviews of some alternative approaches are provided, such as popular reinforcement learning, the traditional optimization process, and the water filling technique in wireless communications.

Chapter 3 Performance Modelling and Verification Techniques

Contents

3.1	Simulation Tools	54
3.2	Simulation Techniques and Methods	55
3.3	Performance Measures	58
3.3.1	Channel Interference Model and Signal to Interference Plus Noise Ratio	58
3.3.2	Shannon Channel Capacity and Truncated Shannon Capacity	59
3.3.3	Power Efficiency	60
3.4	Validation and Verification Techniques	61
3.5	Chapter Conclusion	61

Mathematical analysis plays a crucial role in our work. A game theoretic tool is used to build the game model that imitates the radio resource competition between distributed wireless agents. A mathematically precise and logically consistent analysis helps us predict the possible outcome of the proposed power allocation scheme. In particular, set theory and convex optimisation are used to prove the existence of Nash Equilibrium (the mathematical analysis will be introduced when required in each chapter). On the other hand, computer simulation is used to build the connection between analytical research and the real life scenario. We use computer simulation to imitate wireless environment, to generate wireless agents and program their behaviour. In this thesis mathematical analysis provides us with a theoretical basis, while computer simulation helps us predict and evaluate the performance of our proposed Distributed Cognitive Power Allocation (DCPA) scheme. It is however important to avoid the pitfalls of simulation as a single wrong parameter can lead to completely wrong conclusion in a sensitive simulation environment. It is then important to justify the proper simulation tools and methods. In this chapter we will

introduce the simulation tool and methods that we used in the simulation and specify the channel interference model as well as the performance measures. The performance of the proposed scheme is then verified through a comparison between analysis and the simulation results.

3.1 Simulation Tools

There are many well developed tools at hand that have long been used for simulation and modelling, such as C++, OPNET, NS2, NS3 and Matlab, and each of them have their own strength and weakness. C++ is one of the most popular and versatile programming languages and it has been widely used as the core programming language of many simulations. OPNET is a software tool that is cater for performance analysis of computer networks and applications. NS2 and its updated version NS3 are open network simulators primarily used in network research, while Matlab is one of the most popular and powerful computing systems that is capable of handling complex mathematical calculations in scientific research. Among these powerful tools, we chose Matlab as our simulation tool as Matlab is a very capable simulation tool that meets our simulation requirement and helps us develop simulation models efficiently. The shortcomings of the Matlab, however, is its slow code executing speed.

Our work is benefited from Matlab in three major aspects. Firstly, Matlab is designed for matrix computation, and our simulation requires computing signal power at the receivers which involves matrix multiplication and addition between multiple channel path gains of subcarriers and transmit power array. Matlab makes this type of computation particular easy. Secondly, programming Matlab script is simple and straightforward, and the Matlab prompt can be executed interactively, which means the results of the Matlab prompt can be shown immediately with only Matlab prompt on the working space so that we do not have to program a proper Matlab script and compile it in order to get the answer of some simply calculations. Lastly, the plotting function is versatile and ease of use, which helps us in presenting simulation results and illustrating performance analysis. Although the general ease of use nature of

Matlab is somehow at the cost of code execute speed, however, we can resort to Matlab profiler to find which lines in our script slow down the entire process in cases of the especially long processing time.

3.2 Simulation Techniques and Methods

Regarding the simulation technique itself, we use the Monte Carlo method to predict a statistical performance of our proposed DCPA scheme. The Monte Carlo method is used in the following fashion [82]:

- 1 Define the *sample space* which is a set of measurement defined by simulation scenario.
- 2 Generate a sample randomly from the sample space and carry out the simulation process according to this random sample.
- 3 Repeat the process 2 for a large number of iterations.
- 4 Observe the record of simulation results.

By repeatedly sampling the value from a probability distribution, the Monte Carlo method can be very useful predicting the performance of simulations with significant uncertainty in inputs. Take wireless spectrum assignment as an example, the performance of the spectrum assignment scheme is strongly affected by geographical locations of the nodes and surrounding environment (interference level) of the radio system. It needs a large amount of test samples to determine the overall performance as the different geographical location setups can lead to significant different outcomes on a case-by-case basis.

Discrete event driven simulation method is used in our work. This is different from the time continues simulation, the discrete event driven simulation observes the system changes only in response to the arrival of the discrete events, while time continuous simulation observes the change of the system continuously over the time [82]. Despite being less detailed than a time continuous simulation, a discrete event driven simulation is much simpler to implement [82] and less time consuming. We describe our simulation as a short burst of events that simulates a process of a series

of changes of the power allocation and the corresponding changes of radio environment. The discrete events are the iterations of changing power allocations. The simulation ceases when there is no change in the environment. The following flowchart Figure 3.1 shows the entire simulation process.

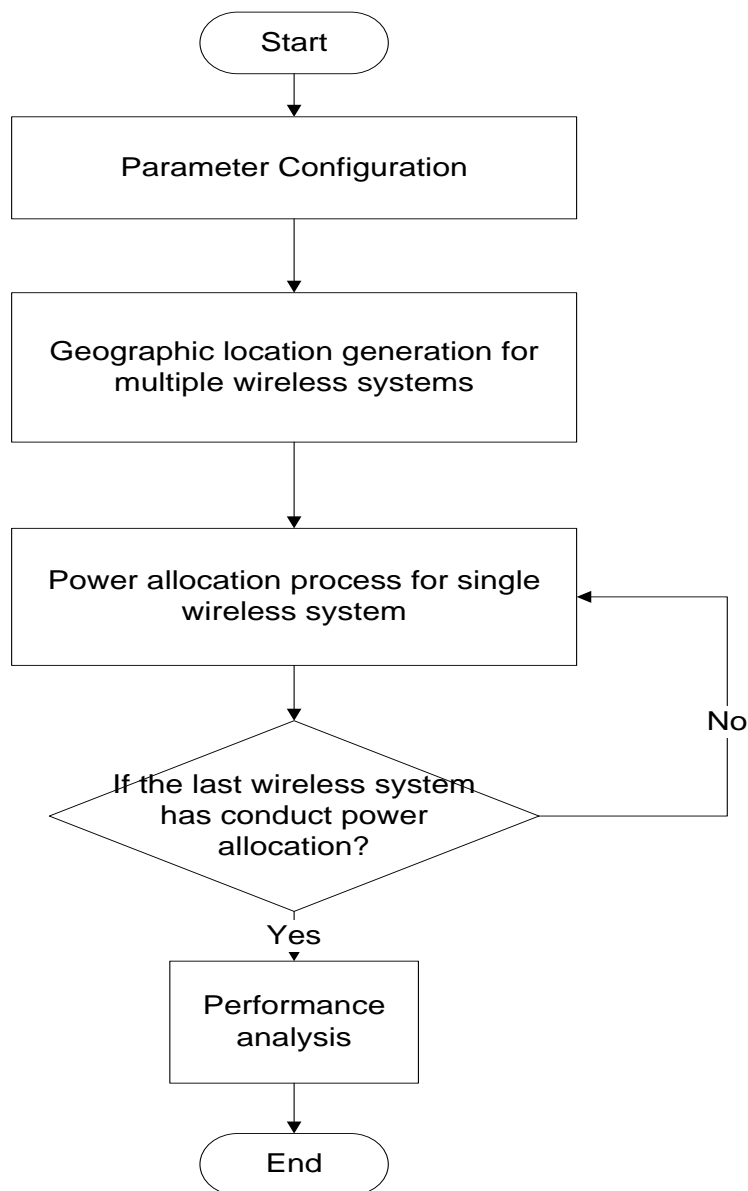


Figure 3-1 Flow chart of a snapshot of the simulation

The flow chart in Figure 3.1 only demonstrates a single simulation event that is related to a specific geographical location setup. We call it a snapshot of the simulation. A Monte-Carlo simulation flowchart is illustrated in Figure 3.2.

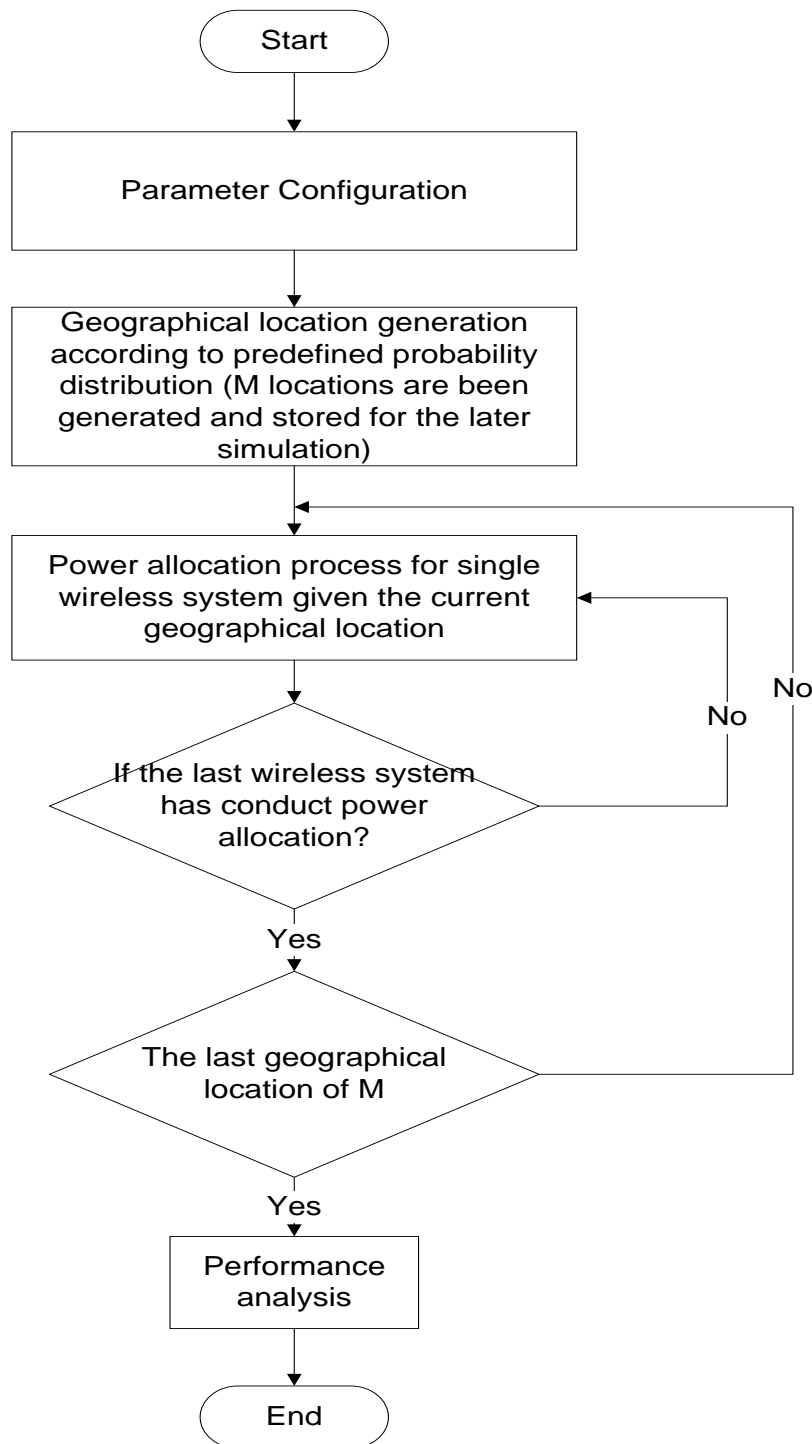


Figure 3-2 Flow chart of a Monte-Carlo simulation

We run the snapshot simulation many times with a different geographical location setup each times. The geographical location of the radio system is generated randomly

according to a random distribution M in Figure 3.2 in order to observe a general performance of our proposed DCPA scheme.

3.3 Performance Measures

Performance of the proposed DCPA scheme is assessed according to the performance measure we specified in our simulation. It is important to give the proper performance measure so that the results of simulations can be interpreted and illustrated graphically. Moreover, different performance measure may be required depended on the specific system design. In the following chapter, a number of important performance measures that we used to evaluate our simulation results are introduced.

3.3.1 Channel Interference Model and Signal to Interference Plus Noise Radio

It is important to specify the channel interference model in a distributed wireless channel assignment scenario so that the signal to interference plus noise ratio (SINR) of each channel can be expressed. Figure 3.3 is used to illustrate a multichannel wireless interference model. The interference sources are the transmitters of homogenous wireless systems.

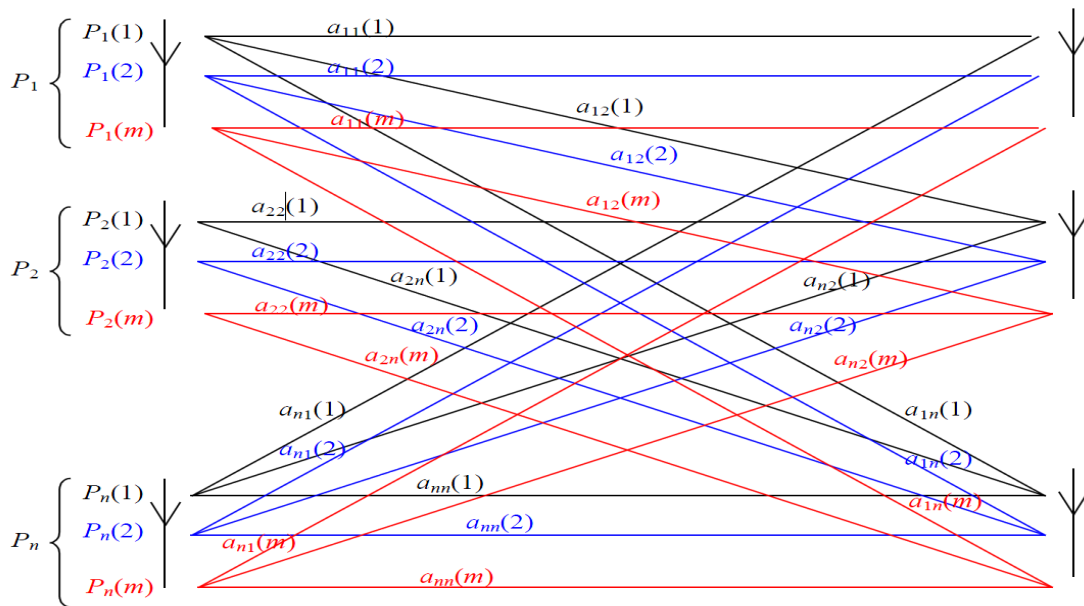


Figure 3-3 An example of the channel interference model (taken from [12])

$a_{nn}(m)$ is used to describe the channel path gain between transmitter n and receiver n on subcarrier m . $P_n(m)$ is used to describe the power allocate pattern of system n on subcarrier m

Signal to interference plus noise ratio (SINR) is an important measure in order to determine the channel quality. In information theory, the SINR is used to calculate the channel capacity, and it is also used as a threshold to determine if the radio system can meet a minimal SINR requirement given a certain error probability. The SINR can be expressed by the following equation

$$SINR(m) = \frac{P_i(m)|a_{ii}|_m^2}{\sum_{j \neq i}^L P_j(m)|a_{ji}|_m^2 + noise} \quad 3.1$$

Expression 5.20 calculates the SINR value of a single channel m at the receiver of user i . Where $|a_{ii}|_m^2$ represents the channel path gain of user i on channel m . $m \in M$. M is the total number of channels that a user can allocate power on. Where $noise$ is the Gaussian white noise.

3.3.2 Shannon Channel Capacity and Truncated Shannon Capacity

The Shannon Channel Capacity is one of the most important performance measures that calculate the maximum achievable data rate of a given power allocation pattern on the channels with certain channel condition [83]. Given the SINR expression in 3.1, the Shannon channel capacity can be expressed as the following equation 3.2

$$C = Bw \cdot \sum_{m=1}^M \log_2(1 + SINR(m)) \quad 3.2$$

Where Bw represents the bandwidth of each channel, and M is the total amount of channels. $SINR(m)$ is the signal to interference plus noise ratio of channel m at the receiver end.

Despite being able to calculate the maximum throughput, the real achievable throughput is also dependent on the modulation scheme and specific error control coding scheme of wireless system. A truncated Shannon Capacity is thereafter been used to evaluate a near realistic performance of our proposed DCPA scheme.

$$C(m) = \begin{cases} 0, & \text{if } \text{SINR} \leq \text{SINR}_{\min} \\ \alpha \cdot Bw \cdot \log_2(1 + \text{SINR}(m)), & \text{if } \text{SINR}_{\min} \leq \text{SINR} \leq \text{SINR}_{\max} \\ Bw \cdot C_{max}, & \text{if } \text{SINR}_{\max} \geq \text{SINR} \end{cases} \quad 3.3$$

Taken from [84] the idea of the Truncated Shannon Capacity is to calculate the throughput of the received signal to interference plus noise ratio between SINR_{\min} and SINR_{\max} . Where SINR_{\min} is the minimum decoding threshold that the channel with the SINR level lower than SINR_{\min} will consider as conveying no data given a specific modulation scheme [84]. Where SINR_{\max} indicate an upper threshold that the maximum throughput can be achieved, while the channel with a SINR value higher than SINR_{\max} will remain the same throughput C_{max} . It should be noted that SINR_{\min} and SINR_{\max} are based on the performance of the practical modulation and coding scheme.

3.3.3 Power Efficiency

The performance of the distributed power allocation scheme can be evaluated in terms of the power efficiency. High power efficiency for a distributed power allocation scheme is crucial and it means longer battery life for a mobile system and an overall lower power emission of the wireless system.

The power efficiency can be expressed in terms of transmit power and the received throughput.

$$eff = C/P \quad 3.4$$

$$\sum_{m=1}^M C = C(m) \quad 3.5$$

Where P is total transmit power, C is the total received throughput and it is calculated by equation 3.5, where $C(m)$ is the throughput on a specific channel m .

3.4 Validation and Verification Techniques

According to [82], validation is a necessary process that a specific simulation model can be justified as a suitable and accurate representation of the real system. In this work, we validate our simulation model by investigating into the existing systems and their parameters. The assumptions are carefully made according to either the existing systems, or an educated guess. The specific parameters and assumptions are introduced when required in each chapter. On the other hand, by restricting the scale of our model, (we do not model the specific modulation and channel estimation process, parameters taken from the existing documents will reflect an achievable performance such as achievable data rate at a specific SINR level), we can largely get avoid of inaccurate parameters or extravagated assumptions.

However, a logical conclusion can only be deduced when the simulation is correctly been implemented. Verification, on the other hand, checks if the specific simulation performs as intended. In this work, we verify our simulation from two aspects: firstly, simulation results are compared with mathematical analysis in order to check if the simulations meet our theoretical prediction. Secondly, the simulation results are carefully compared with the established techniques such as the performance comparison between the existing water filling technique and the proposed DCPA scheme.

3.5 Chapter Conclusion

In this chapter, we introduce the simulation techniques and methods as well as the important verification technique. Simulation flow chat is given in order to better understand the process of our simulation. In the end we introduce a number important performance measures which are used to evaluate the results of the simulation. SINR

of the multicarrier system model is expressed as well as a measure of a near realistic throughput. Power efficiency is also discussed as an important performance measure for wireless power allocation scheme.

Chapter 4 Game Based Approach in UWB Power Allocation

Contents

4.1	Gradient Power Allocation.....	64
4.1.1	The Purpose of the Gradient Power Allocation and the Analysis of Its Performance	64
4.1.2	Analysis of the Possible Performance.....	67
4.1.3	Simulation Setup and Results	71
4.2	Game Model and Utility Function	82
4.3	Chapter Conclusion	101

As introduced in chapter 2, distributed wireless networks designed and modelled using game theoretical methods are capable of greatly improving performance in terms of power or bandwidth efficiency, while conventional optimization algorithms may be computational infeasible [15, 61, 85]. However, it is important to avoid the potential pitfalls of a game inspired method. It has been pointed out in [58], that the majority of mistakes come from the lack of understanding of the distinctions between game theoretical approaches and conventional optimisation algorithms. In particular, a game model is appropriate only when the players involved in the model make decisions on their own. On the other hand, many problems are proven to be better solved by optimisation techniques and employing game theory may not necessarily lead to better results, such as centralised power allocation problems with a limited number of nodes and full information exchange [58]. In this chapter, we will discuss our design of a game-inspired UWB power allocation scheme. Firstly, we will demonstrate our gradient power allocation scheme and explain the purpose and benefits of applying it to the UWB power allocation problem. Then, we will discuss our utility function design. Furthermore, we will prove that there exists a Nash Equilibrium under our Utility function. Lastly, we will introduce a Game strategy

which ensures that our UWB power allocation game converges to the Nash Equilibrium point in a flat fading channel.

4.1 Gradient Power Allocation

A typical orthogonal frequency division multiplexing (OFDM) system conveys signals over multiple channels, and some channel frequencies may suffer severe interference or fading, while others may not. The transmitter can transmit with adaptive modulation levels on different channels according to the signal to noise ratios (SNR). The water filling technique [46] can be used to explore the maximum data rates of an OFDM system. However it is restricted by the distributed nature of UWB systems. Next, we will explore the OFDM system in a radically different way and specify the reasoning and advantages of our method in this chapter.

4.1.1 The Purpose of the Gradient Power Allocation and the Analysis of Its Performance

In this section, we present the concept of our proposed gradient power allocation scheme, and analyse the convergence of such a scheme in a simplified scenario with two user, two channels sharing scenario. It should be noted that the user we used here include both transmitter and its receiver.

The UWB Multiband-OFDM system as introduced in chapter 2 occupies a minimum bandwidth of 528MHz that is able to deliver the data rate of transferring HDTV program. However, it is limited by an extremely low power emission profile as we introduced in chapter 2. The challenge of an efficient cognitive power allocation scheme for such a UWB system is that it can suffer either from the high attenuation of the UWB channel at higher frequency bands, or most likely strong interference from the homogeneous UWB systems operating in the vicinity. Narrow band interference from other wireless devices is not a major problem, as it can be simply notched by not allocating power on the specific channels that present heavy interference [56]. However the homogeneous UWB systems in the vicinity occupying the same

frequency bands, without proper information exchange scheme, will impose strong interference upon each other.

It is safe to say that the UWB power allocation problem is not subject to limited capacity because of ultra wide spectrum provides the radio system with huge raw channel capacity, but it is instead subject to interference from homogeneous UWB systems operating in the same frequency bands, and path loss attenuation due to the highly restricted UWB power emission regulations. Therefore orthogonal power allocation is needed in order to maintain the required signal to interference plus noise ratio (SINR), which means that different systems allocate power to different channels.

In order to better partition the channel, we designed a gradient power allocation scheme, consisting of a transmitter gradient power allocation, and a receiver SINR ranking. The idea is to allocate a unique power to each channel with gradient factor α according to the interference level present at receiver. The incentive behind this power allocation is that we assume wireless agents prefer a higher signal to interference ratio than a lower signal to interference ratio. On the other hand, gradient power allocation provides a simple and efficient way to help partition the channels. The whole process is shown in Figure 4.1.

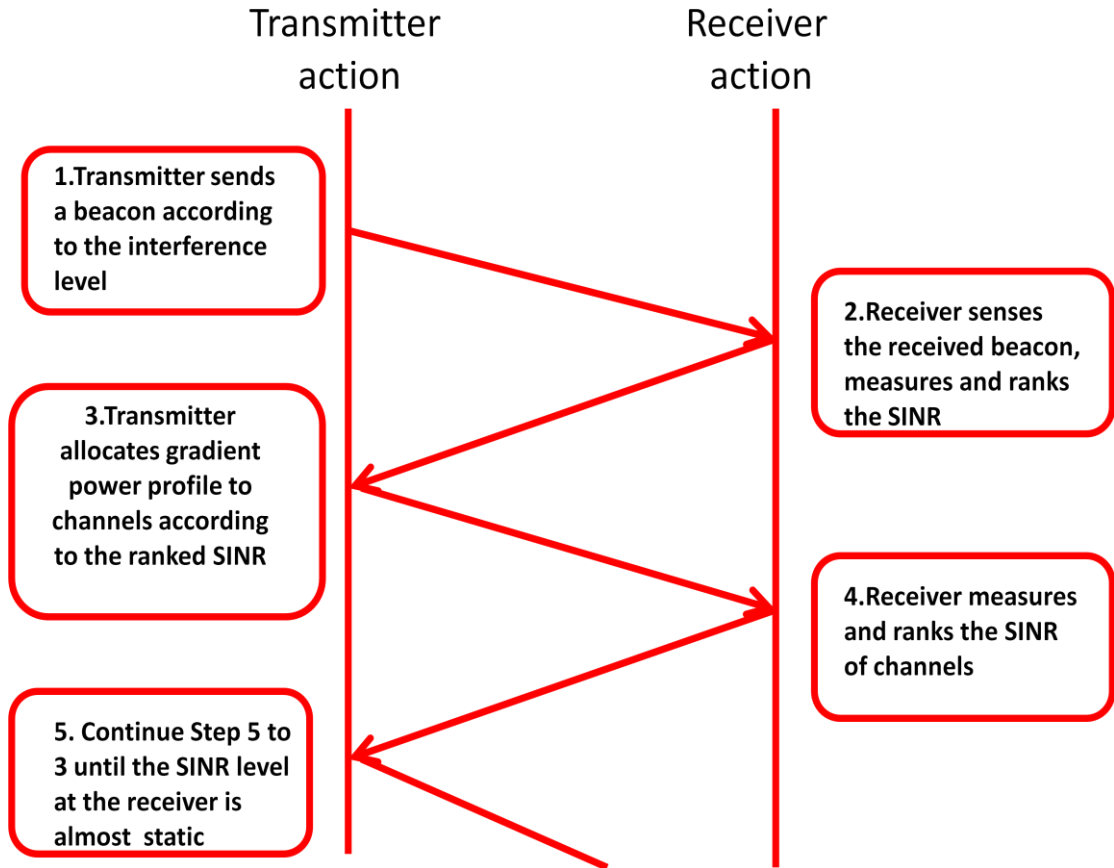


Figure 4-1 Flow chart of the gradient power allocation process

A value α is used to differentiate the power allocated to different channels whereby the receiver will observe a differentiated signal to noise ratio for all channels. The iteration begins with transmitter beaconing. At the receiver, the signal to interference plus noise (SINR) ratio on each channel is ranked, and this ranked SINR information is sent to the transmitter. However channels where the SINR is lower than a predetermined threshold corresponding to a specific modulation scheme as determined by the bit error rate (BER), will be ruled out from the ranking sequence. A transmitter in stage three will allocate a gradient power profile according to the ranked information. The power allocation algorithm can be seen in equation 4.1. Stages 2 and 3 (of Figure 4.1) will continue until convergence.

$$P_{total} = P_{int} + P_{int}\alpha^{-1} + P_{int}\alpha^{-2} + \dots + P_{int}\alpha^{-(n-1)} + P_{int}\alpha^{-n} \quad 4.1$$

Where P_{int} is the power allocated to the channel with highest SINR at the receiver (which is limited by the UWB spectrum mask). P_{total} is the total power, and n is the number of channels in the ranked sequence.

Figure 4.2 illustrates the possible behaviour of the proposed power allocation algorithm. The upper graph is the possible received SINR versus the channels on the horizontal axis. Note that the threshold is the required SINR. The lower graph shows the gradient power allocation, according to rank information in the replies from the receiver. It should also be noted that the upper threshold is set by the FCC spectrum mask, which specifies the UWB transmitter emission power limit.

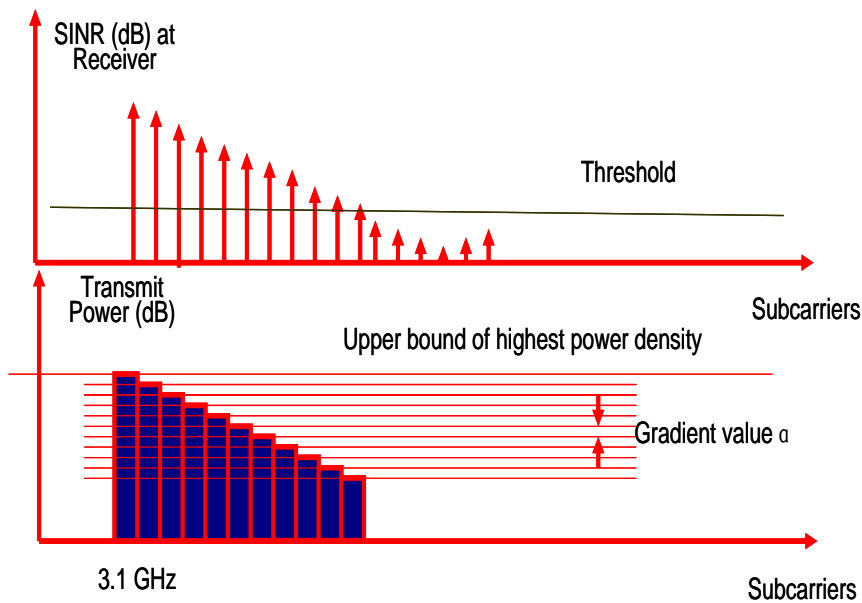


Figure 4-2 Illustration of the gradient power allocation

4.1.2 Analysis of the Possible Performance

Let us start by analysing the possible performance for a simple scenario where there are two channels shared by two homogenous systems. It should be noted that the signal to interference ratio (SIR) is used instead of SINR, because it is easier to compare SIR than SINR, and a higher SIR can suggest a higher SINR given the noise is *Gaussian White Noise*.

Analysis 1: Depending on the value α , the systems applying our proposed power allocation scheme will converge into a state where the ratio between highest SIR and lowest SIR among channels will be separated by a sufficiently large amount, on condition of 4.2.

$$p_{max} > \frac{SNR_{req} \cdot N_0[f]}{\beta[f]} \quad 4.2$$

Where SNR_{req} is the required signal to noise ratio for a specific modulation scheme. f is the arbitrary carrier centre frequency in a multichannel OFDM system. $N_0[f]$ is the white Gaussian noise power present in a given channel. $\beta = |h[f]|^2$, and h is the channel transfer function. p_{max} is the maximum possible power allowed to be transmitted in a channel, which is limited by spectrum mask in the UWB case. Condition 4.2 is necessary to guarantee that the receiver can hear the transmitter. It means that the transmitted signal after channel attenuation should be above the power required by a specific signal to noise ratio at the receiver when there is no interference present on that channel.

Let us consider the following simplified model:

$$y_1[f] = h_{11}x_1[f] + h_{21}x_2[f] + n_1[f] \quad 4.3$$

$$y_2[f] = h_{22}x_2[f] + h_{12}x_1[f] + n_2[f] \quad 4.4$$

Where x , y , n are the input of a specific user, the output and Gaussian noise respectively. Some assumptions are required:

1. We assume a flat fading channel.
2. Interference from the other users is treated as additive noise.
3. The systems are turned on sequentially, which is highly possible in reality, given that wireless devices turned on and off asynchronously.

The signal to interference ratio can be expressed by following equation.

$$SIR[f] = \frac{p_i[f]\beta_{ii}[f]}{p_j[f]\beta_{ji}[f]} \quad 4.5$$

Where SIR is the signal to interference ratio, and p the user transmit power. The total transmit power can be denoted as $p_{total}=p[f_1]+p[f_2]$. We can furthermore express our gradient power profile in this way.

$$p_{total} = p[f_1] + \frac{p[f_2]}{\alpha'} \quad 4.6$$

Where α' is the linear transform of α since we express α in dB form. For now, we will assume that the two users transmit the same amount of total power across the carriers, and apply the same gradient power profile with the same gradient value α . We can therefore derive the expressions of all SIR values. We need only to show the full set of first user's SIR expressions, because the SIR expressions for both users are symmetrical.

All possible signal to interference ratio combinations that a specific receiver can acquire in a two systems two channel scenario can be listed as follows:

$$\begin{aligned} SIR_1 &= \alpha' \frac{\beta_{ii}}{\beta_{ji}} \\ SIR_2 &= \frac{\beta_{ii}}{\alpha' \beta_{ji}} \\ SIR_3 &= \frac{\beta_{ii}}{\beta_{ji}} \end{aligned} \quad 4.7$$

Where SIR_1 , SIR_2 , and SIR_3 are the three possible SIR values that a user can acquire on either of the two channels. However only SIR_1 , SIR_2 , are logical results of channel 1 and channel 2 respectively when our proposed power allocation is applied. These are derived by allocating a higher power to the channel with a higher signal to interference plus noise ratio (SINR), while SIR_3 is derived by allocating a higher

power to the channel with lower SINR, which is against the logic of our power allocation scheme. Therefore, SIR_3 will never be the result of our proposed power allocation scheme. The SIR difference between two channels under the proposed scheme is α'^2 , and it can be infinitely large if we cut off the power transmitted on the second channel.

Analysis 2: It is reasonable and necessary to prune the channels which have insufficient signal to interference plus noise ratio.

The worst condition, when the receiver and transmitter are separated by a distance is that the receiver only acquires the minimum required signal to noise ratio (SNR). This can be expressed as $p = T_h \cdot N_0[f] / \beta[f]$. By applying our power allocation scheme, the SNR values on two channels are $T_h / \beta[f1]$ and $T_h / (\beta[f2] \cdot \alpha')$ respectively. The SNR value at channel 2 cannot support the given modulation level. Therefore, the transmitter will not transmit power on channel 2 and the SIR for channel 2 will be 0. Therefore the SIR ratio between two channels becomes arbitrary large, and channel 2 is now free of interference to the other systems. The merit of such a scheme is that it is an efficient channel partitioning scheme if all conditions are met.

On the other hand, as can be seen from equation 4.7, the factor β_{ii} / β_{ji} can profoundly influence the value of the SIR. If $\beta_{ii} < \beta_{ji}$, the wireless system will not be able to receive data successfully, because the interference will be higher than the received signal, and hence a channel partition is the only feasible solution. If $\beta_{ii} / \beta_{ji} \gg \alpha'$ then, SIR_1 , SIR_2 and SIR_3 will be infinitely close and channel partitioning is seemingly not the best solution because the wireless system may acquire a higher data rate by water filling all channels [46]. The water filling technique is a well known optimisation technique, which is normally used in solving constraint optimization problem. As its name suggests, the water filling technique is an optimal power allocation scheme, which allocates power to each channel according to the exact signal to interference plus noise ratio presented at the receiver. The relevant introduction can be seen in chapter 2. To date, a significant amount of research [86-88] on efficient power allocation has concentrated on maximizing the overall channel capacity, while we think maintaining a specific target data rate and a fair spectrum sharing among wireless systems should

be a more reasonable goal. Therefore, channel partitioning will become more beneficial when the fairness is required. In order to achieve such fairness in a distributed manner, however, we need to introduce a game theory inspired strategy. We will further specify our game strategy in this chapter.

4.1.3 Simulation Setup and Results

To better understand the gradient power allocation technique and its performance, we proposed a simulation which models a UWB four user coexistence scenario, all of which use the gradient power allocation scheme.

A. Simulation Setup

MB-OFDM defines a 528MHz spectrum region as a single band, which comprises 128 OFDM channels. We currently use only the first frequency band, which is located between 3168 MHz and 3696 MHz in our proposed scenario. We use a single band for multi-users sharing the spectrum. The IEEE 802.15.4a path loss model can be expressed as the following equation, and the reason we use IEEE802.15.4a path loss model has been specified in chapter 2.

$$PL(d, f) = \frac{1}{2} PL_0 \eta_{TX-ant}(f) \eta_{RX-ant}(f) \frac{(f / f_c)^{-2(\kappa+1)}}{(d / d_0)^n} \quad 4.8$$

Table 4.1. shows the parameters of the path loss model that are used for an indoor office environment [41].

Office		
Parameters	Value	Value
PATHLOSS	LOS	NLOS
n	1.63	3.07
PL_0 [dB]	35.4	57.9
A_{ant}	3 dB	3 dB
K	0.03	0.71

Table 4-1 Parameters of the indoor office path loss model

We generate random locations of the UWB systems in a $30 \times 30 \times 30$ square metre volume according to a uniform distribution. An example layout of the systems can be viewed from Figure 4.3. The reason we use a 3 dimensional model in our simulation can be summarized by the following points:

1. UWB is a short range radio technique, and a 3D model can better represent the indoor multi-system coexistence pattern, while the 2D model is better suited to for modelling long range radio systems.
2. We can have the situation where all radio systems are parallel to each other for both transmitters and receivers (such as people having devices in different floors within the same house), which cannot be demonstrated by using a 2D model.

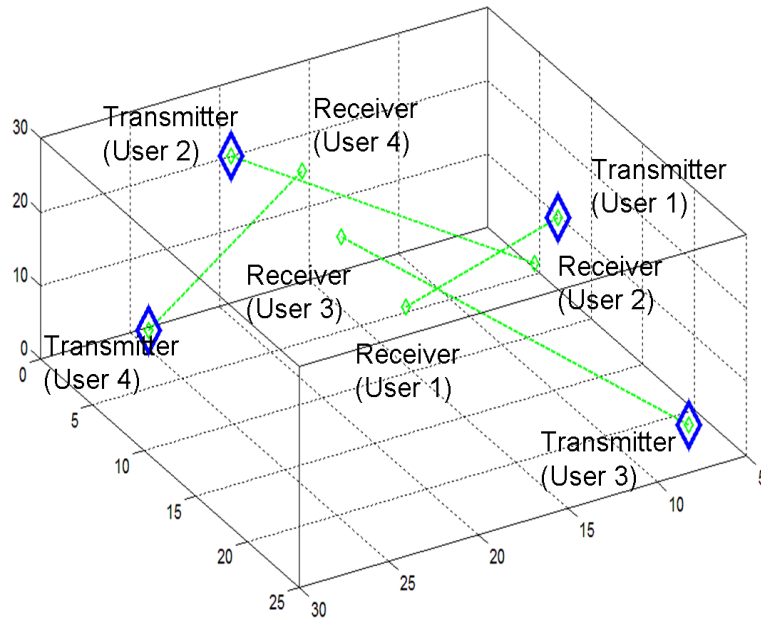


Figure 4-3 System layout

The distance between transmitter and receiver in this example can be found in Table 4.2

	Distance (metres)
System 1	18.0
System 2	18.3
System 3	22.4
System 4	12.4

Table 4-2 Geographical locations of 4 systems

The assumptions we made here are the same with the ones we made in previous SIR analysis:

1. We assume a flat fading channel.
2. Interference from the other users is treated as additive noise.
3. The systems are turned on sequentially, which is highly possible in reality, given that wireless devices are normally turned on and off asynchronously by users.

The important parameters can be viewed in the following Table 4.3

Parameters	Value
P_{total} (dBW)	-44
α (dB)	3

Table 4-3 Simulation parameters

The total transmit power of a single system is -44 dBW, which is derived by summing transmission power on all channels. The selection of gradient value α will be examined in the following chapter 5.

B. Performance Analysis

Figure 4.4 shows the first stage of our proposed power allocation during which the transmitter will send a beacon with the gradient power allocation.

It is notable that the transmit power we used in all of our following simulations is not the real transmit power but an advertised value used to calculate the power transmission on each channel. This is because the maximum transmit power on channel is subject to the FCC spectrum mask. The following equation can help better understand the purpose of advertised transmit power:

$$P_{advertised} = P_{int} + P_{int}\alpha^{-1} + P_{int}\alpha^{-2} + \dots + P_{int}\alpha^{-(n-1)} + P_{int} \quad 4.1$$

$$P_{real} = \min(P_{int}, P_{T_h}) + \min(P_{int}\alpha^{-1}, P_{T_h}) + \min(P_{int}\alpha^{-2}, P_{T_h}) + \dots + \min(P_{int}\alpha^{-(n-1)}, P_{T_h}) + \min(P_{int}\alpha^{-n}, P_{T_h}) \quad 4.9$$

Where P_{T_h} is derived by multiplying the FCC spectrum density mask with the bandwidth of the channel:

$$P_{T_h} = Mask \cdot Bw \quad 4.10$$

We use equation 4.1 to calculate P_{int} and hence the power allocation pattern can be calculated given a gradient value α . However, the real total transmit power is expressed by equation 4.9 because the peak transmit power is restricted by the FCC spectrum mask. According to document [33], the mask we used in 4.10 is set to -40.3 dBm and B_w in 4.10 is the bandwidth of the channel which is 4.125 MHz. Therefore P_{T_h} is equal to -65.15 dBW. This setup will not affect the overall performance as it only constrains the highest transmit power, while not affecting the behaviour of the gradient power allocation on channels with a transmit power less than the threshold. On the other hand, advertised transmit power will be equal to the real transmit power if there is no limitation on the maximum power density. For simplicity, from now on in the thesis we will just use the term total transmit power instead of advertised total transmit power.

In Figure 4.4, we can observe the effect of the spectrum mask. The peak transmit power on a single channel is equal to -65.15 dBW, which is limited by P_{T_h} .

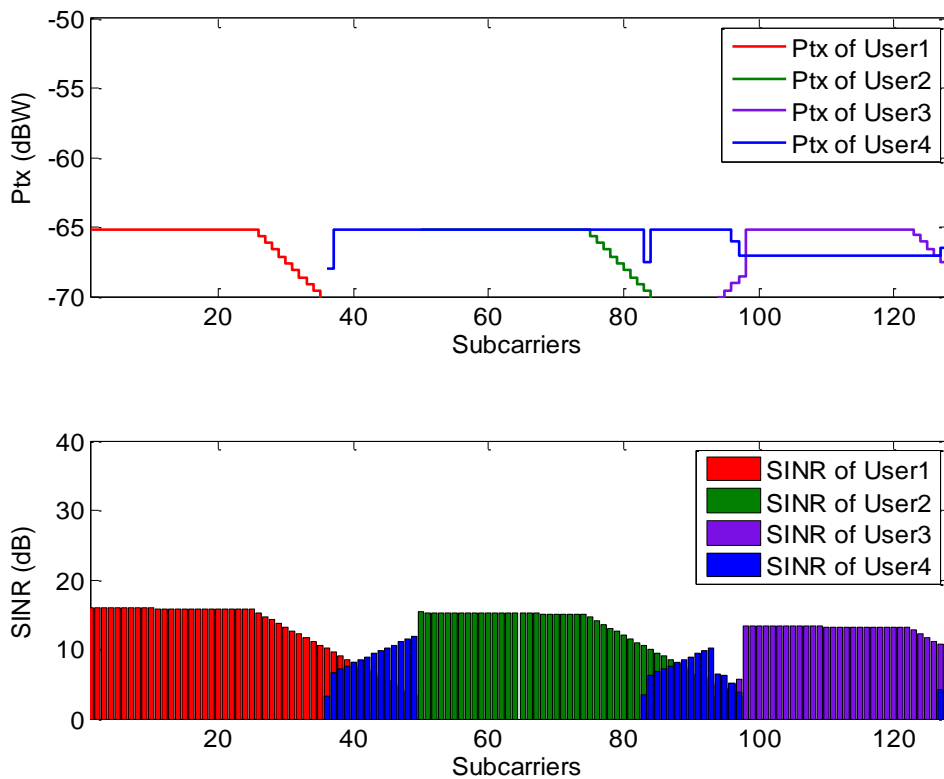


Figure 4-4 Transmit power and SINR at receivers in the initial stage

It also shows that system finds its best spectrum by means of sensing the beacon sent by the transmitter.

Figure 4.5 shows the convergence stage when there is no significant change of SINR. In the convergence stage, the channels that do not achieve the specific SINR threshold are cut off and the total transmit power will be redistributed to the remaining channels. Note that the highest possible power density of the channels is strictly restricted to the FCC spectrum mask, but we will later relax the constraint in chapter 6.

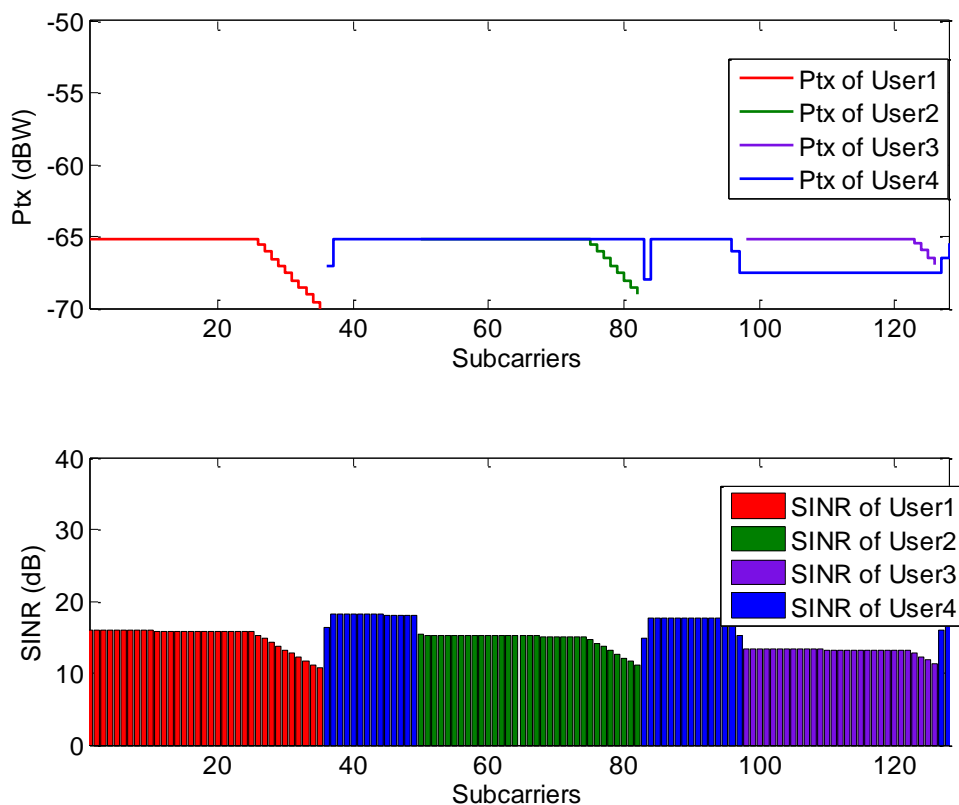


Figure 4-5 Transmit Power and SINR at receivers at the final stage

Table 4.3 shows the channel assignment pattern at the final stage, the number showed below is the channel number that has been assigned to the specific system.

	System 1	System 2	System 3	System 4
Channel assignment pattern	1 - 49	50-97	94-128	36-49 83-97 127-128

Table 4-4 Channel assignment pattern at the final stage

The channel partitioning can be seen clearly from the power allocation pattern at the final stage. It should be noted that the power allocation pattern is subject to the specific geographical layout of the UWB systems, and will change as their geographical layout of the systems changes. We will examine effect of different geographical layouts on the power allocation pattern in chapter 5. It should also be noted that channel reuse exists for system 2, system 3, and system 4. This is because the channel with a lower signal to interference plus noise ratio (SINR) will have a lower power allocated to that channel while creating less interference to other systems. Hence lower collective interference can be expected on the channel, and such channels can be shared by multiple systems.

Furthermore, the spectrum assignment will change as a result of changes in the total transmitted power. We will demonstrate one most important property of our gradient power allocation: the amount of channels acquired by a specific user in the coexistence context can increase or decrease, as a result of increases or decreases in the total transmit power.

Next, we try a new example set of total transmit powers, which can be seen in Table 4.4. We keep the previous geographical locations of systems, and increase or decrease the total transmit power of each system. The results show in Figure 4.6 and Figure 4.7.

	System 1 (dBW)	System 2 (dBW)	System 3 (dBW)	System 4 (dBW)
Total transmit power	-44	-50	-30	-40

Table 4-5 Total transmit power of 4 systems

It is shown in Figure 4.7 that the channel assignment changes as a result of the change of transmitted power, and consequently in this specific simulation user 2 decreases its number of channels, while user 3 increases its channels.

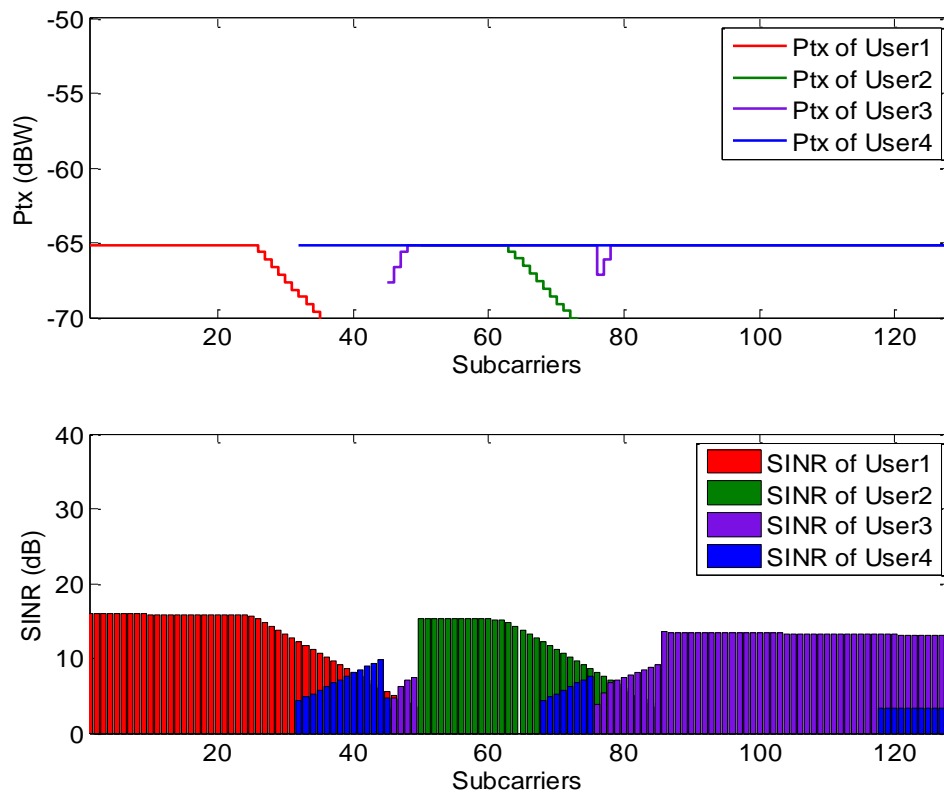


Figure 4-6 Transmitted power and SINR at receivers in the initial stage

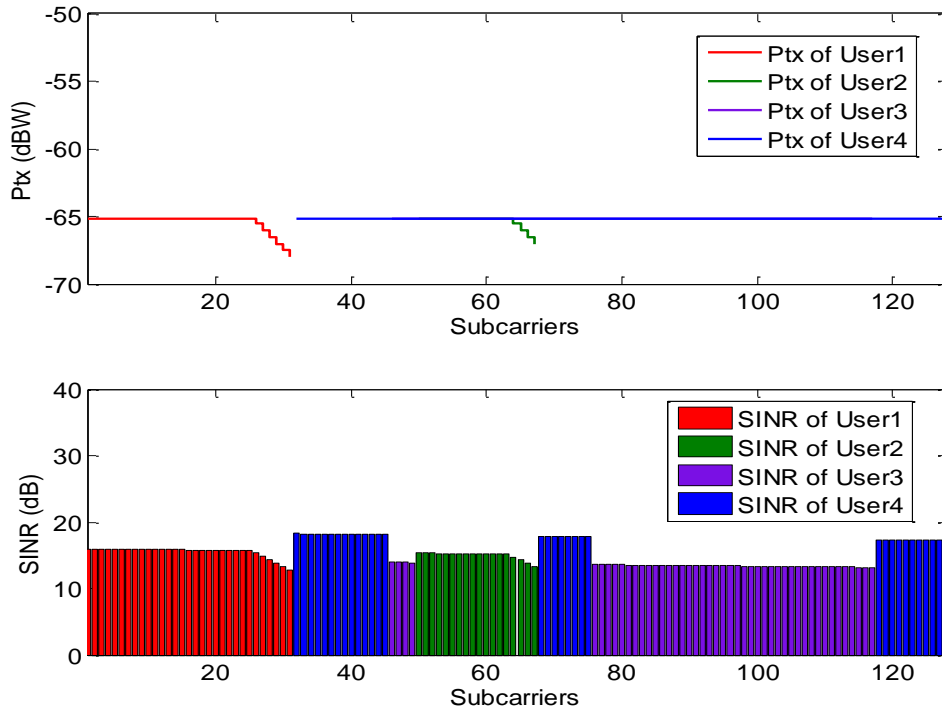


Figure 4-7 Transmit power and SINR at receivers at the final stage

Table 4.5 demonstrates that the number of channels that each user acquires can be changed by adjusting the total transmit power of that user.

	System 1	System 2	System 3	System 4
Total transmit power 1 (dBW)	-44	-44	-44	-44
Channel assignment pattern 1	1 – 49 (50)	50-97 (48)	94-128(35)	36-49 83-97 127-128 (31)
Total transmit power 2 (dBW)	-44	-50	-30	-40
Channel assignment pattern 2	1-31 (31)	50-67 (18)	46-49 76-117 (46)	32-45 68-75 118-128 (33)

Table 4-6 Change of the channel assignment pattern

As can be seen from the Table 4.5, system 2 decreases its transmit power and has its acquired number of channels decreased by 30. System 3 and system 4 increase their transmit power and have their number of channels acquired increased by 11 and 2 respectively. Although the system 1 remains with its transmit power unchanged, it suffers from the increased transmit power of other systems, and the number of acquired channel drops from 50 to 31.

To better understand the behaviour of such power allocation, we keep systems 2, 3 and 4 transmitting at a fixed -44dBW, and investigate the change in channel assignments by varying the transmit power of system 1 from -54dBW to -34dBW with a step of 1dBW. The simulation results are shown in Figure 4.8.

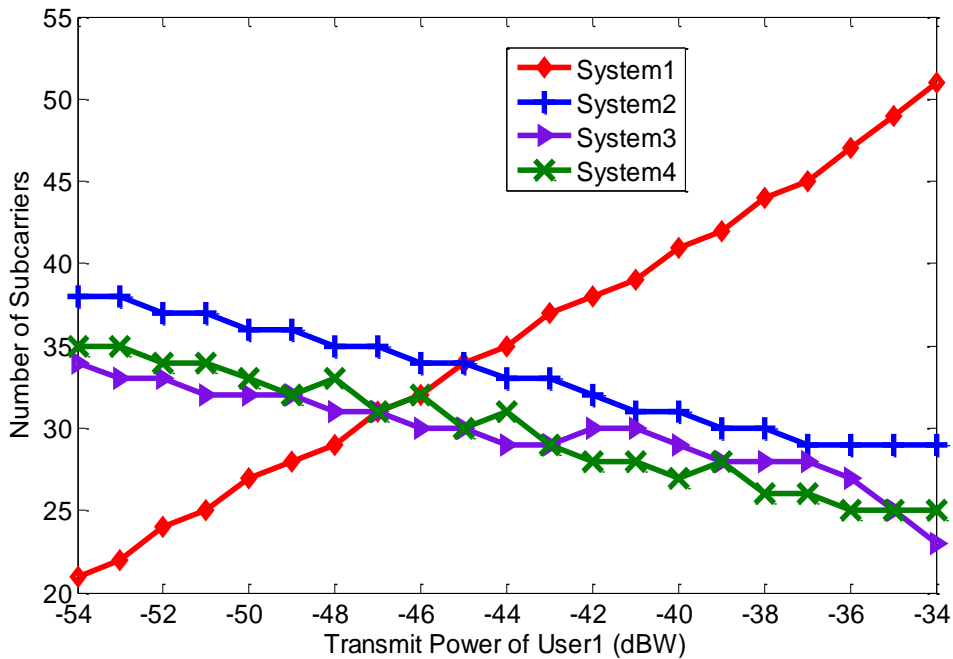


Figure 4-8 Number of channels versus transmit power of user 1

From the simulation results, we can observe that the number of channels that are allocated to the other systems decrease as the system 1 increases its transmit power from -54dBW to -34dBW, during which system 1 increases its channels by 30. Similarly, we increase the transmit power of system 2, and keep the transmit power of the other system. The result in Figure 4.9 shows similar behaviour. In this sequel, we

can conclude that the system can acquire more channels at the cost of decreasing the number of channels of the other systems.

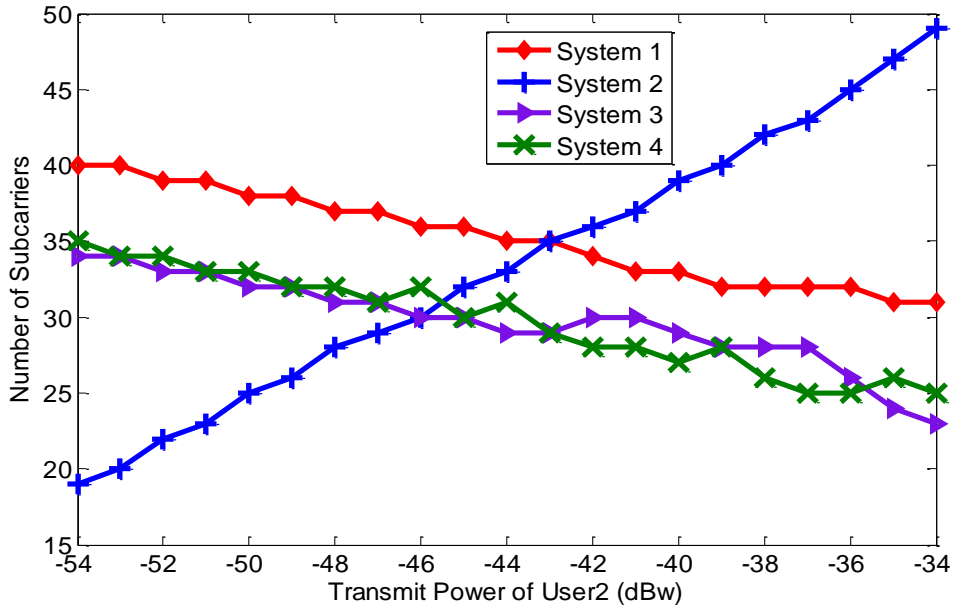


Figure 4-9 Number of channels versus transmit power of user 2

Also, we can observe that systems 3 and 4 decrease their amount of channels in slightly different manners in two simulations which may result from the geographical differences between systems. Therefore the increase of the transmit power in system 1 has a different interference impact on systems 3 and 4 than increasing the transmit power of system 2. It should be noted that the line in Figures 4.8 and 4.9 are not straight which is due to the fact that the systems change their power allocation alternatively and hence the same transmit power of all systems appear on different time instance.

Thus, there are two facts we observe from the simulations:

1. The gradient power allocation partitions the channels according to the relative geographical locations of users.
2. Users can acquire more channels by increasing their transmit power at the cost of decreasing the number of channels available for other coexisting users.

It is clear that gradient power allocation alone is not capable of maintaining a specific performance in a multiuser coexistence environment if every user is targeted on achieving maximum channel capacity. Next we will introduce a game inspired model and strategies, which take advantage of gradient power allocation while maintaining a specific performance target for every user.

4.2 Game Model and Utility Function

We have demonstrated the gradient power allocation scheme in last section, and we show that, the gradient power allocation can be used as a channel partitioning scheme. Further, we learned from the simulation that gradient power allocation alone behaves in a selfish way. We now introduce a game model that is intended to guarantee that homogeneous UWB systems achieve a target data rate by means of gradient power allocation in a fully distributed manner. In this section, we will formulate a utility function which is an abstract representation of the outcome of the radio resource competition. Then we will prove the existence of a Nash Equilibrium for our game model.

4.2.1 Game Model and Utility Function that describes the UWB Power Allocation Problem

We have so far introduced some important background knowledge of game theory and the possible applications of games to telecommunications. We now consider how to solve the Cognitive UWB power allocation problem by means of a game inspired approach.

To map a real wireless communication problem into a game competition, as introduced before, requires

- 1) a set of communication systems which need to compete for radio resources subject to some limitations
- 2) a set of possible actions for each communication node to react the strategies of its counterparts.

- 3) a common utility function mapping all the possible actions to real numbers [58].

First, we define our power allocation game model as a non-cooperative game assuming there is no information exchange between systems [57]. We consider our game to only have pure strategy points, which means systems do not take randomized actions, and each action gives a specific value of utility. As a non-cooperative game, the system can only affect the outcomes of its competitors through the consequences of its behaviour. Therefore, the system will observe a varying outcome once its competitors change their behaviour.

Next, it is assumed that each of the systems prefers to acquire a data rate that is as close to its target data rate as possible, and the degree of the satisfaction is defined as the gap between target data rate and the acquired data rate. Therefore, an acquired data rate that is much higher or much lower than the target data rate should be regarded as undesirable.

Next, we will have to select an action space from which each system takes an action to counter the actions of other systems. Since the outcome is measured by the gap between the acquired data rate and the target data rate, the action should be the transmit power which is associated with acquired data rate, and the transmit power of the other systems. Recall that with the gradient power allocation scheme introduced in section 4.1, we concluded that the proposed scheme can have an acquired data rate increase or decrease as the transmit power increases or decreases provided that the transmit power meets the condition of the equation 4.2.

We can use the proposed gradient power allocation to acquire a unique data rate (we will prove this uniqueness property of gradient power allocation in section 4.2.2) in a multisystem coexistence scenario corresponding to a specific transmit power. Hence the action space of our power allocation game is the combination of all possible transmit powers.

The utility function should link the defined action space to the outcome of the competition, and the utility should be a numerical representation of the outcome. Before we move on to our utility function, we need refer to some typical utility functions in wireless communications and the methodology that is used to design utility functions. One of the most common utilities in wireless communication is directly the transmission efficiency with the unit of bits per Joule. In [61], the utility of a CDMA system is expressed as

$$u_j(p_j, \gamma_j) = \frac{R}{p_j} (1 - 2\text{BER}(\gamma_j))^L \quad 4.11$$

Where R is the transmit information rate with the unit bits/second in L bit packets of a Spread-spectrum bandwidth of $W(\text{Hz})$. P_j is the transmit power of user j . γ_j is the SINR of user j , and $\text{BER}(\gamma_j)$ is the bit error rate achieved by a given transmission scheme. The SINR is defined as the following equation.

$$\text{SINR} = \gamma_j = \frac{W}{R} \frac{h_j p_j}{\sum_{\forall i \neq j} h_i p_i + \sigma^2} \quad 4.12$$

Where h_j is the path gain of user j to the base station and σ^2 is the power of the background noise at the receiver.

The graph of the utility function shown in equation 4.11 can be shown as Figure 4.10

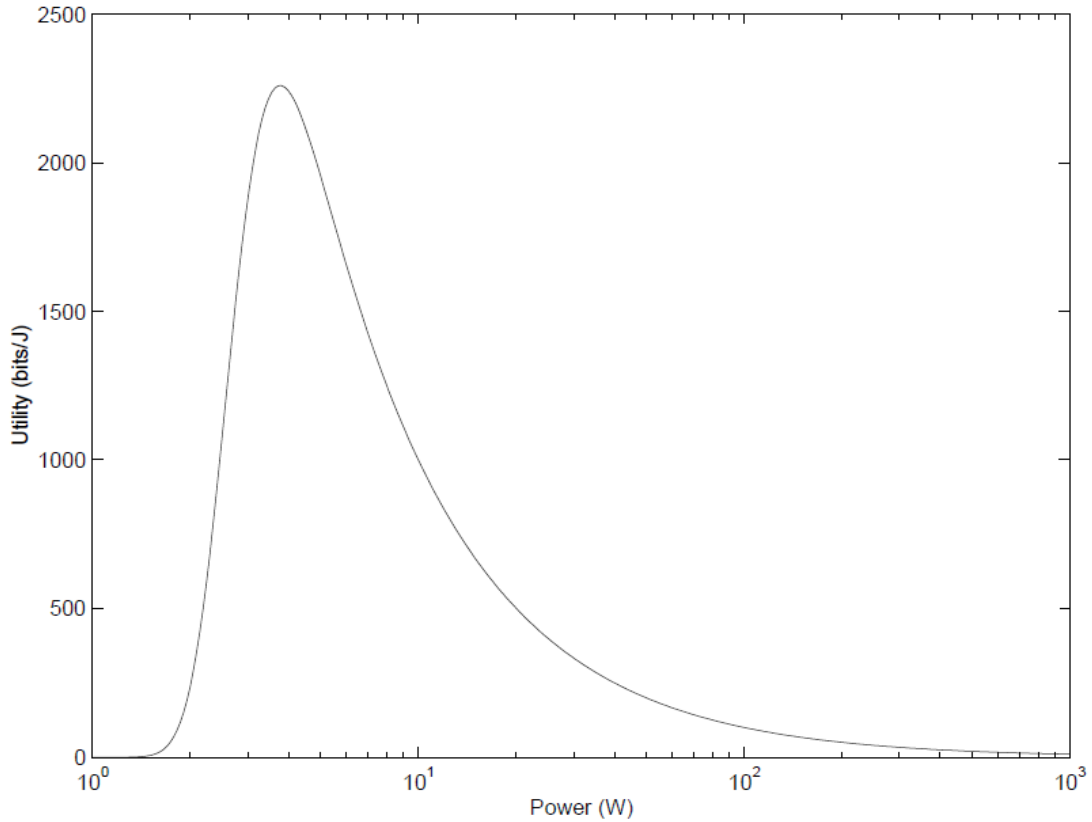


Figure 4-10 Example of a utility function (taken from [61])

As can be seen from Figure 4.10, the utility function for a user is a convex function. The x axis shows the transmit power of a user and the y axis shows the utility of the user assuming that all other users' transmit power are fixed. From the graph, the user's utility increases as the system increases transmit power until the maximum utility, and the utility decreases if the user keep increasing its transmit power over this maximum point. This characteristic of the utility function is necessary for having a Nash Equilibrium point in an N-person game [89].

It is proven that the Nash Equilibrium exists if the utility function of a specific N-person game is a quasi-concave function or a concave function, because a concave function is also a quasi-concave function [89]. Hence the utility function of our proposed power allocation game should be designed as a quasi-concave function.

We denote systems competing within the spectrum as player i , and $i \in \{1, 2, \dots, N\}$, where N is the total number of players. We define A_i as the set of strategy profiles for player i , and $A_i = \{a_i^1, a_i^2, \dots, a_i^M\}$ denotes all possible combination of strategies, a_i^M is

the possible combination of two parameters: total transmit power P_{total} and gradient factor α . The utility function in our game measures the degree of closeness between acquired theoretical data rate and the target data rate. The logic of such a utility function can be summarised below:

- 1.) The utility function should measure the gap between the acquired data rate and target data rate.

$$gap = |R_i(a_i, a_{-i}) - target| \quad 4.13$$

Where $target$ is the target data rate. $\alpha^i \in A_i$ denotes player i 's action and a_{-i} denotes the actions taken by the other $-i$ player. Hence, $R_i(a_i, a_{-i})$ is the outcome of our proposed gradient power allocation for player i and the other players $-i$.

$$R_i(a_i, a_{-i}) = Bw \cdot \sum_{n=1}^N \log_2 \left(1 + \frac{P_{in}|H_{in}|^2}{N_0 + \sum_{j \neq i}^M P_{jn}|H_{jn}|^2} \right) \quad 4.14$$

Equation 4.14 measures the data rate of user i , where Bw is the bandwidth of the channel which is 4.125 MHz according to [90]. N is the total number of channels. P_{in} is the power that user i transmitted on channel n . P_{jn} is the power that other users transmitted on channel n .

- 2.) The utility should be maximized when the acquired data rate is equal to target data rate. Then the gap function in 4.13 should be written as the inverse of the gap function $-|(a_i, a_{-i}) - target|$.
- 3.) It is reasonable to have positive utility values. Then a constant should be introduced.

$$Utility = C_1 - |R_i(a_i, a_{-i}) - target| \quad 4.15$$

Currently, we use a large enough value to have the $C_1 - |R_i(a_i, a_{-i}) - target|$ over 0 in order to guarantee the utility be positive.

$$C_1 = Bw \cdot N \tag{4.16}$$

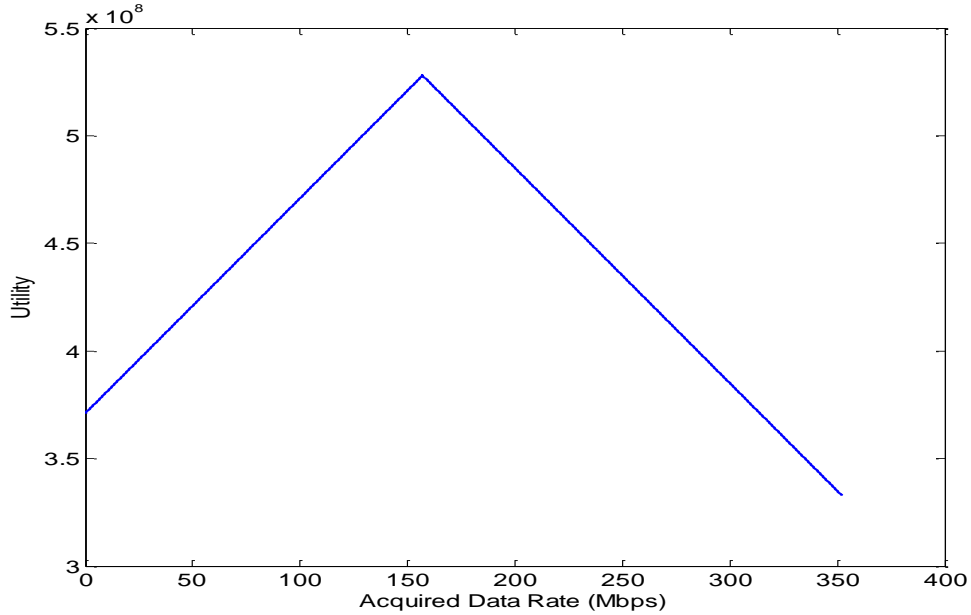


Figure 4-11 Graph of equation 4. 14

Figure 4.11 illustrates the graph of the utility function 4.15. It should be noted that the utility peaks at the target data rate. The x axis shows the acquired data rate of a user, and the y axis shows the utility of the user assuming that all other users' transmit power are fixed. The peak utility occurs when the acquired data rate perfectly matches the target data rate, then the utility decreases as the acquired data rate exceeds the target data rate. Therefore, it is a concave function and maximized at target data rate. However, the utility that is derived by equation 4.15 has a very large value, and we need to introduce another constant to reduce its value in order to better compare the actions (strategies) in terms of utility. On the other hand, the utility in equation 4.15 has a fixed rate of changing due to its gradient that is equal to 1 and -1. In practice, we may want to have the utility changing dramatically when it is close to the maximum utility if the initial utility is close to the maximum. Or we could have the utility changing faster when it is further away from maximum value, when the initial utility is further away from maximum value. Therefore, we introduce a logarithmic constant to equation 4.15.

$$U_i(a_i, a_{-i}) = \left(\frac{C_1 - |R_i(a_i, a_{-i}) - tg|}{C_2} \right)^{C_3} \tag{4.17}$$

The constant $C_2 > 0$ in equation 4.17 is used to reduce the size of the utility. The constant value $C_3 > 0$ is used to introduce a varying gradient to the utility function. The utility function will change faster when it is close to the maximum value as shown in Figure 4.10. C_2 is 10^8 and C_3 is set as 4. Note that the utility function in Figure 4.12 is not a strict concave function but rather a quasi-concave function.

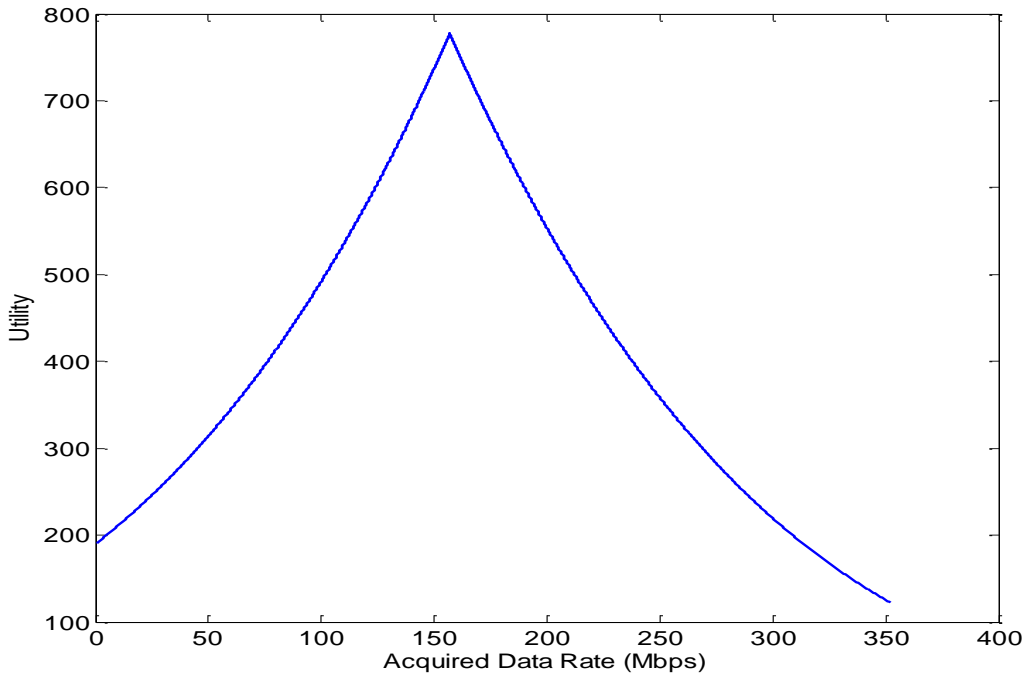


Figure 4-12 Illustration of the utility function

On the other hand, the peak utility will move when the target data rate changes. Figure 4.13 illustrates the fact that different target data rates will have different peak utility values.

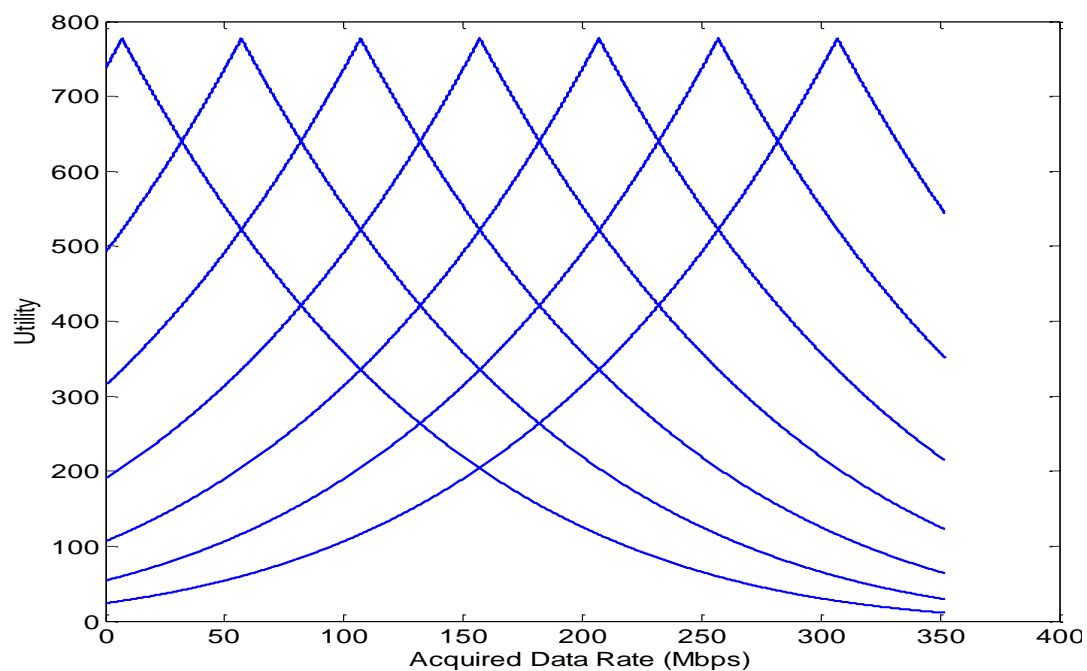


Figure 4-13 Relationship between the utility and the target data rate

Furthermore, we illustrate the relationship between the total transmit power and the utility in Figure 4.14. Assuming the total transmit powers of the other systems are fixed; only system 1 changes transmit power and the target data rate is 88Mbps.

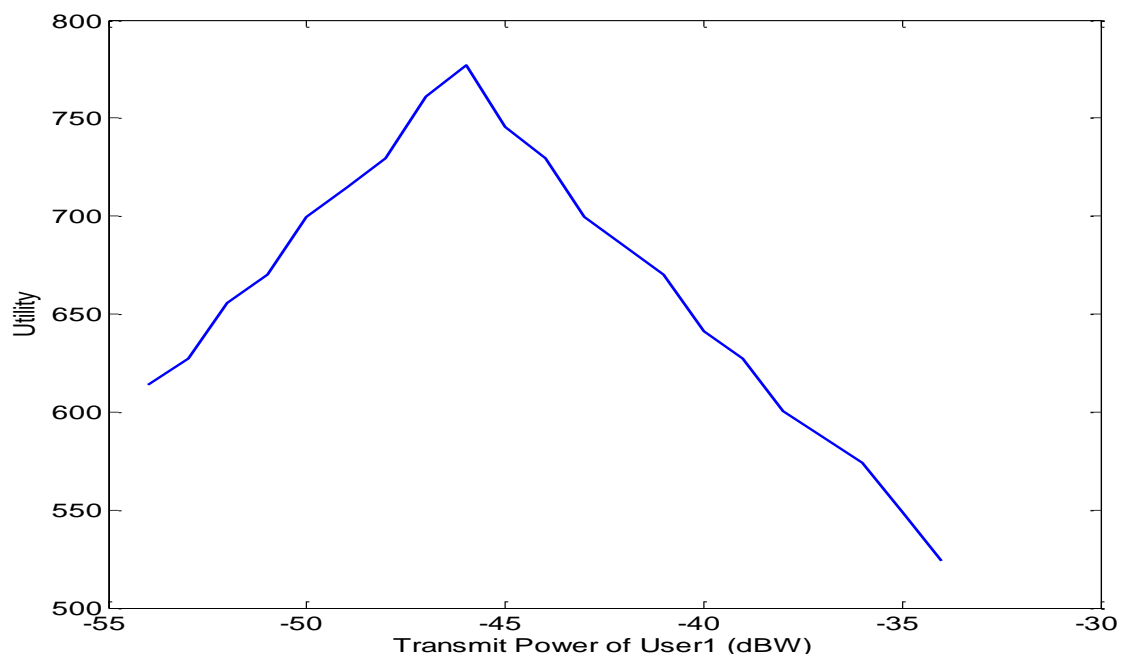


Figure 4-14 Transmit power of user 1 versus its utility

It is noted that the utility is not smooth, which is because the utility function 4.17 is a composition function between $R_i(a_i, a_{-i})$ and $U_i(a_i, a_{-i})$. $R_i(a_i, a_{-i})$ is subject to the power allocation pattern and hence subject to the total transmit power limitation. Later in this chapter, we will prove that the utility function preserves its quasiconcave nature.

The Nash Equilibrium of this game can be expressed by the following inequality.

$$U_i(a_i, a_{-i}) \geq U_i(\tilde{a}_i, a_{-i}) \quad 4.18$$

Where $\tilde{a}_i \in A_i$. It expresses a stable operating point where no player has an incentive to change strategy at the equilibrium [58].

The action space for our game model can be expressed as

$$P \in [P_{min}, P_{max}] \quad 4.19$$

Where P_{min} and P_{max} represent the max and minimum transmit power respectively.

1.1.2 Existence of a Nash Equilibrium

We associate the UWB power allocation problem with a non-cooperative game. It is now important to prove that there exists an operating point at which all UWB users in a resource sharing game competition can acquire a data rate that meet a designated target. Alternatively speaking, we will prove the existence of a Nash Equilibrium in our proposed game model. We will firstly establish the existence of a Nash Equilibrium under a flat fading channel. Later, we will prove that the Nash Equilibrium also exists under frequency selective fading channels.

As can be seen from equation 4.14, the acquired data rate $R_i(a_i, a_{-i})$ is obtained after the convergence of gradient power allocation. We begin by proving that users under a

specific total transmit power will apply a fixed power profile, and acquire a fixed data rate by means of gradient power allocation.

Theorem 1: Under flat fading channel condition, upon the convergence of gradient power allocation, users with fixed total power budget will acquire a unique data rate.

Proof: We prove the theorem by showing that any other data rate derived from applying a different power allocation to channels is contradictory to the gradient power allocation scheme.

The proof requires two basic assumptions about the channel and interference level at each stage of gradient power allocation.

Assumption 1: The users change their power profile alternately, and interference from the homogeneous UWB system remains unchanged when one of the users changes its power profile.

Assumption 2: The UWB channel remains unchanged during the entire gradient power allocation process.

Assumption 3: The UWB channel gain does not vary much across the entire bandwidth and hence it is assumed that the channel path gain for all channels is equal.

Assumption 1 is reasonable, because on one hand the users are programmed to perform the gradient power allocation and hence all users will obey the rule of gradient power allocation. On the other hand, it is reasonable to assume that user change their power profile alternatively, therefore the interference level will remain unchanged of each stage of gradient power allocation.

Assumption 2 is reasonable if we assume a slow fading channel (see our analysis of UWB channel in chapter 2) which is plausible if the power allocation converges in a small number of iterations. We will later demonstrate in our simulation that our proposed power allocation scheme converges very fast in general within 30 iterations.

Assumption 3 is reasonable if the channel is a flat fading channel. Under a flat fading channel, we simulate the path gain of a 512 MHz wide bandwidth at 3.1 GHz. The ratio of the path gain between the last channel and the first channel is 0.7297 in our simulation, and hence it is assumed to be equal across the entire bandwidth. This assumption will be lifted when we assume the channels exhibit frequency selectivity.

The gradient power allocation can be expressed as equation 4.1 at the end of each iteration. Further, we can express it in terms of the rank of *SINR*

$$P_{total} = \sum_{rank=1:N} P_{int} \alpha^{1-rank} \quad 4.20$$

Where N is the number of total available channels at any stage of gradient power allocation, $rank \in [1:N]$ is the ranked *SINR* values on the available channels.

We can then deduce a general *SINR* expression of channels in terms of their ranks.

$$SINR(ni) = \frac{P_{int} |h_{ii}|_n^2 \alpha^{-ni}}{\sum_{j \neq i}^L P_{int} |h_{ji}|_n^2 \alpha^{-nj} + noise} \quad 4.21$$

Expression 4.21 calculates the *SINR* value of a single channel n at the receiver of user i . Where $|h_{ii}|_n^2$ represents the channel path gain of user i on channel n . $n \in N$. N is the total number of channels that a user can allocate power on. Where ni is the rank of *SINR* on channel n of user i . and *noise* is the Gaussian white noise. For simplicity, the aggregated interference can be expressed by the following equation

$$intf_{stage} = \sum_{j \neq i}^L P_{int} |h_{ji}|_n^2 \alpha^{-nj} \quad 4.22$$

Where $j \in L$ denotes the interfering users that coexist in a L user game model. $|h_{ji}|_n^2$ is the channel cross gain and n_j is the rank value corresponding to the interference level of user j on channel n .

Given our assumption 1 that the interference level remains unchanged when one of the users changes its own power profile at each stage, we can deduce the $SINR_{ni}$ in a simplified form

$$SINR(ni, intf_{stage}) = \frac{P_{int}|h_{ii}|_n^2 \alpha^{-ni}}{intf_{stage}^n + noise} \quad 4.23$$

Now, it is easy for us to express the ranking value at each stage. we assume during a stage that the highest power will be allocated to the channel with highest $SINR$, and lowest power will be allocated to the channel with lowest $SINR$. The specific power level on each channel is derived from channel $SINR$ ranking and the total transmit power.

Define

$$s = \{y | SINR(y, intf_{stage}^n) = \max_{z \in N, z > s} SINR(z, intf_{stage}^n)\} \quad 4.24$$

Equation 4.24 means the channel with rank s will give rise to the higher $SINR$ value on channel n than all the other channels with ranked value higher than s .

Lemma 1: the interference presented at a specific channel n with a ranking value s is smaller than that of the channel q with ranking value z if $s < z$.

We will prove this by looking back to our gradient power allocation in Figure 4.1. The first stage is the transmitter sending a beacon with a gradient power profile according to the immediate interference level presented at receiver. At the receiver, the received signal on a channel n with a ranking s can be described as $P_{int}|h_{ii}|_n^2 \alpha^{-s}$, and we assume there is a ranking value z on channel q that $s < z$, then at the receiver the following inequality must be true at stage one

$$\frac{P_{int}|h_{ii}|_n^2 \alpha^{-s}}{intf_{stage1}^n + noise} > \frac{P_{int}|h_{ii}|_q^2 \alpha^{-z}}{intf_{stage1}^q + noise} \quad 4.25$$

Inequality 4.25 means the $SINR$ value on channel n with a ranking value s is bigger than the channel q with a ranking value z . Assuming that $|h_{ii}|_n \approx |h_{ii}|_q$, also we have $intf_{stage1}^n < intf_{stage1}^q$ and hence $intf_{stage1}^n + noise \leq intf_{stage1}^q + noise$, given $\alpha^{-s} > \alpha^{-z}$. On the next stage (iteration), we will have the ranking value s_l which is bounded smaller than z due to $SINR_s > SINR_z$ at first stage. Therefore, the power allocated on channel n will always be bigger than $P_{int}\alpha^{-z}$.

The consequence is that the other users will receive a increased interference on channel n . Then the ranking value will be higher for channel n than that of channel q for all the other users, and hence a smaller collective interference can be expected on channel n . $intf_{stage_m}^n < intf_{stage_m}^q$.

Next, make s the ranking of the channel n , and assume that there could be ranking value m bigger than s . $m > s$, $m \in N$ on channel n that can lead to an even higher $SINR$. Then we can express $SINR_m$ as a possible outcome.

$$SINR(m, intf_{stage}^n) = \frac{P_{int}|h_{ii}|_n^2 \alpha^{-m}}{intf_{stage}^n + noise} \quad 4.26$$

Assume that the rank m can give rise to a higher $SINR$ value on channel n

$$SINR(m, intf_{stage}^n) > SINR(s, intf_{stage}^n) \quad 4.27$$

Then, according to the gradient power allocation scheme, there must exist a channel q with rank s that

$$\frac{P_{int}|h_{ii}|_n^2 \alpha^{-m}}{intf_{stage}^n + noise} > \frac{P_{int}|h_{ii}|_q^2 \alpha^{-s}}{intf_{stage}^q + noise} \quad 4.28$$

However, according to lemma 1, the interference present on channel q with ranking s should be smaller than the interference present on channel n with ranking m , because $s < m$, therefore $intf_{stage}^n + noise > intf_{stage}^q + noise$. Moreover, $\alpha^{-m} < \alpha^{-s}$.

Therefore, this establishes $\frac{P_{int}|h_{ij}|_n^2 \alpha^{-m}}{intf_{stage}^n + noise} < \frac{P_{int}|h_{ij}|_q^2 \alpha^{-s}}{intf_{stage}^q + noise}$, which is contradictory to inequality 4.28. Hence, there will only be one fixed power allocated to the channel n with rank s . Since this is a general conclusion, we can easily expand it to all the channels. Therefore, there will be only one fixed power allocation upon convergence at a given total power, and hence a fixed data rate from equation 4.14.

Theorem 2: The utility function is a quasi-concave function with a domain of $P \in [P_{min}, P_{max}]$, on condition that $C_1 - |R_i(a_i, a_{-i}) - tg| > 0$, $C_3 > 0$. $C_2 > 0$

The utility function $U_i(a_i, a_{-i}) = \left(\frac{C_1 - |R_i(a_i, a_{-i}) - target|}{C_2} \right)^{C_3}$ is a composition function.

We have to firstly examine function $R_i(a_i, a_{-i})$ and prove that it is a concave and monotonically increasing function with a strategy space of $P \in [P_{min}, P_{max}]$.

Since $R_i(a_i, a_{-i}) = Bw \cdot \sum_{n=1}^N \log_2 \left(1 + \frac{P_{in}|H_{ii}|_n^2}{N_0 + \sum_{j \neq i}^M P_{jn}|H_{ji}|_m^2} \right)$, and according assumption 1 and 2, we can rewrite it as

$$R_i(a_i, a_{-i}) = Bw \cdot \sum_{n=1}^N \log_2 \left(1 + \frac{P_{in}|H_{ii}|_n^2}{N_0 + intf_{stage}} \right) \quad 4.29$$

P_{in} in equation 4.29 is derived from equation $P_{total} = \sum_{Rank=1:N} P_{int} \alpha^{1-rank}$.

$$P_{in} = P_{int} \alpha^{1-rank} \quad 4.30$$

We have demonstrated in the simulation and proved in theorem 1 that the users using gradient power allocation scheme will always obtain a fixed operating point where a fixed total transmit power will give rise to a fixed data rate, as well as a fixed power profile upon convergence. It means the ranking is fixed for a specific P_{total} , and hence α^{1-rank} is regarded as constants.

$$P_{int} = \frac{P_{total}}{\sum_{Rank=1:N} \alpha^{1-rank}} \quad 4.31$$

$$P_{in} = \frac{P_{total}}{\sum_{Rank=1:N} \alpha^{1-rank}} \alpha^{1-L} \quad 4.32$$

Therefore, P_{int} is an affine function with a domain of $P_{total} \in [P_{min}, P_{max}]$, so as P_{in} . Where L in 4.32 is the ranking of a specific channel.

If we define

$$g: p_{total} \rightarrow p_{int} \quad 4.33$$

$$h: p_{int} \rightarrow R_i \quad 4.34$$

Then equation 4.29 can be expressed as a composition function between g and h .

$$f(p_{total}) = h(g(p_{total})), \text{ domain } f = \{p_{total} \in \mathbf{dom}g \mid g(p_{total}) \in \mathbf{dom}h\}$$

Since $g(P_{total})$ is affine and positive on domain $P_{total} \in [P_{min}, P_{max}]$, then $f(p_{total}) = h(g(p_{total}))$ is concave, and monotonically increasing on domain $P_{total} \in [P_{min}, P_{max}]$, because logarithm is strictly concave and mono-increasing on domain R_{++} [80], and the nonnegative weighted sum of a strictly concave function is strictly concave [80].

Axiom 1 A continuous function f is quasiconcave if and only if at least one of the following conditions holds [80].

1. f is nondecreasing
2. f is nonincreasing
3. There is a point $c \in \mathbf{dom}f$ such that for $t \leq c$ (and $t \in \mathbf{dom}f$), f is nondecreasing, and for $t \geq c$ (and $t \in \mathbf{dom}f$), f is nonincreasing. The point c can be chosen as any point which is a global minimizer of f

Now we will prove quasiconcave of our utility function by using condition 3 of Axiom 1.

We expressed equation 4.29 as $f(p_{total})$ and proved that $f(p_{total})$ is concave and mono-increasing on domain $P_{total} \in [P_{min}, P_{max}]$. In a similar way, we express the utility function 4.17 as equation 4.35

$$U(P_{total}) = \left(\frac{C_1 - |f(p_{total}) - target|}{C_2} \right)^{C_3} \quad 4.35$$

We can find a point c that $f(p_{total}) = target$. However, the utility function at c is not differentiable because of the absolute operation. We now differentiate U with respect to P_{total} on condition that $p_{total} > c$.

$$U'(P_{total}) = C_3 \left(\frac{C_1 - (f(p_{total}) - target)}{C_2} \right)^{C_3 - 1} (-1) \frac{f'(P_{total})}{C_2} \quad 4.36$$

Where $C_1 > f(p_{total}) - target$ on condition that $C_1 - |R_i(a_i, a_{-i}) - tg| > 0$ and $C_3 \left(\frac{C_1 - (f(p_{total}) - target)}{C_2} \right)^{C_3 - 1} > 0$ because $C_3 > 0$ $C_2 > 0$. Then $f'(P_{total}) > 0$, because $f(p_{total})$ is concave and monoincreasing on domain $P_{total} \in [P_{min}, P_{max}]$. Therefore $U'(P_{total}) < 0$ for all $p_{total} > c$, and hence $U(P_{total})$ is nonincreasing for $P_{total} > c$.

Next, we differentiate U with respect to P_{total} on condition that $p_{total} < c$.

$$U'(P_{total}) = C_3 \left(\frac{C_1 + f(p_{total}) - target}{C_2} \right)^{C_3 - 1} \frac{f'(P_{total})}{C_2} \quad 4.37$$

Where $C_3 \left(\frac{C_1 + f(p_{total}) - target}{C_2} \right)^{C_3 - 1} > 0$, and $\frac{f'(P_{total})}{C_2} > 0$. Therefore $U'(P_{total}) > 0$, for all $p_{total} < c$.

Here, we see that condition 3 of Axiom 1 is met, and hence the utility function is quasiconcave.

Theorem 3 There exists a Nash Equilibrium for our game model under flat fading channel condition.

According to [89, 91], if a strategic form game with strategy spaces S that are nonempty compact convex subsets of an Euclidean space, also if the utility functions u_i are continuous and quasiconcave in S , there exists a Nash Equilibrium of the game in pure strategy. For our proposed game model, the existence of a Nash Equilibrium relies on two elements:

1. convexity of the strategy domain
2. quasi-concave of a utility function on domain S

We have shown that the strategy space of our game model is $P \in [P_{min}, P_{max}]$, which is a compact and convex set. Then we proved that the utility function on such a domain is quasiconcave. Then it is safe to say there exists a Nash Equilibrium of our game model. Note that our game model only has pure strategies as the strategy domain is a constant sub set of R_{++} .

Theorem 4 The Nash Equilibrium still exists if the power allocated to each channel is limited by a threshold.

Remember we introduced the spectrum mask, which is, according to the FCC, used to limit the maximum emission power on each channel.

$$P_{advertised} = P_{int} + P_{int}\alpha^{-1} + P_{int}\alpha^{-2} + \dots + P_{int}\alpha^{-(n-1)} + P_{int} \quad 4.1$$

$$P_{real} = \min(P_{int}, P_{T_h}) + \min(P_{int}\alpha^{-1}, P_{T_h}) + \min(P_{int}\alpha^{-2}, P_{T_h}) + \dots + \min(P_{int}\alpha^{-(n-1)}, P_{T_h}) + \min(P_{int}\alpha^{-n}, P_{T_h}) \quad 4.9$$

Where P_{T_h} is derived by multiply the FCC spectrum density mask with the bandwidth of a single channel.

$$P_{T_h} = Mask \cdot Bw \quad 4.10$$

We have shown in 4.32 the power transmitted on each channel is calculated from total power, and hence we express it in terms of $P_{advertised}$

$$P_{in} = \min \left(\frac{P_{advertised}}{\sum_{Rank=1:N} \alpha^{1-rank}}, P_{T_h} \right) \quad 4.38$$

Equation 4.38 means the power allocated to channel is bounded by threshold P_{T_h} .

Axiom 2 If f is a concave function then its point wise minimum f is defined by $f(x) = \min \{f(x), C\}$, is also concave [80]. Where C is a constant.

Axiom 3 An affine function is also a concave function [80].

Since $\frac{P_{advertised}}{\sum_{Rank=1:N} \alpha^{1-rank}}$ is an affine function, then P_{in} in equation 4.37 is concave according to Axiom 2 and Axiom 3.

Then similar to the proof we give in Theorem 2, we can prove the Utility function preserves its quasiconcave nature. Therefore according to Theorem 3, we can prove that there exists a Nash Equilibrium if the power allocated to each channel is limited by a upper threshold.

We have proved the existence of the *Nash Equilibrium* under flat fading channel, we will prove the same hold true under frequency selective fading channel.

Theorem 5: Under frequency selective fading channel conditions, upon the convergence of gradient power allocation, users with fixed total power budget will acquire a unique data rate.

Proof:

Looking back to our gradient power allocation in Figure 4.1, the beginning of the power allocation process is the transmitter sending a beacon with a gradient power profile according to the immediate interference level presented at receiver. Under frequency selective fading channel, the proof of lemma 1 will no longer hold. At the receiver, the received signal on a channel n with a ranking s can be described as $P_{int}|h_{ii}|_n^2\alpha^{-s}$, and we assume there is a ranking value $s+1$ on channel q that can lead to two inequalities at the end of the power allocation of iteration 1. It is noted that the equation 4.21 is used to express the SINR at the receiver.

$$\frac{P_{int}|h_{ii}|_n^2\alpha^{-s}}{intf_{stage1}^n+noise} \geq \frac{P_{int}|h_{ii}|_q^2\alpha^{-(s+1)}}{intf_{stage1}^q+noise} \quad 4.39$$

$$\frac{P_{int}|h_{ii}|_n^2\alpha^{-s}}{intf_{stage1}^n+noise} < \frac{P_{int}|h_{ii}|_q^2\alpha^{-(s+1)}}{intf_{stage1}^q+noise} \quad 4.40$$

Inequality 4.39 can be interpreted as $(SINR_n)_1 \geq (SINR_q)_1$, Based on these SINR values, the new ranking value S_1 of channel n must satisfy $S_1 \leq S$, while the new ranking value S_2 of channel q will satisfy $S_1 \leq S_2$. Therefore, on the next iteration, a higher power will be allocated to channel n due to the lower ranking value, and hence a smaller collective interference can be expected on channel n . Consequently, the $SINR$ value of channel n will be higher than that of channel q . $(SINR_n)_2 \geq (SINR_q)_2$ It is safe to say that the ranking value of channel n will always be lower than that of channel q .

Next, consider the channels satisfy inequality 4.40, we can deduce that $|h_{ii}|_n < |h_{ii}|_q$ due to $\alpha^{-s} < \alpha^{-(s+1)}$, $intf_{stage1}^n < intf_{stage1}^q$. On the next stage, the new ranking value S_1 of channel n must satisfy $S_1 > S$, and the new ranking value S_2 of channel q will satisfy $S_1 > S_2$. Therefore, on the next iteration, a lower power will be allocated to channel n due to the lower ranking value, and hence a higher collective interference can be expected on channel n . Consequently, the $SINR$ value of channel n will always be lower than that of channel q .

Since the power profile is controlled by the *SINR* ranking, we can deduce that the channels that satisfy inequality 4.39 or 4.40 will have a fixed power allocation upon convergence of gradient power allocation scheme.

By putting these two conclusions together, theorem 5 is proved.

Theorem 6 There exists a Nash Equilibrium for our game model under frequency selective fading channel conditions.

Theorem 6 can be proved in the same manner of the poof of Theorem 3, as the following proof not affected by the characteristics of the channel.

It should be noted that the Theorem 4 holds true under both flat fading and frequency selective fading channels as the channel condition are irrelevant to the details of the proof.

4.3 Chapter Conclusion

In this chapter, we specified our proposed gradient power allocation and analysed its possible performance in a two user, two channel scenario. The simulation results reveal that the system can acquire a portion of the whole bandwidth according to the transmit power. The amount of channels acquired can be decided by the transmit power. The design of a Utility function is introduced, which is based upon the gradient power allocation. We proved that the acquired data rate is unique on the convergence of the gradient power allocation scheme given a specific total transmit power. Following this we further prove the existence of the Nash Equilibrium of our proposed utility function under both flat fading and frequency selective fading channel conditions.

Chapter 5 Performance of Game Approach in UWB Multichannel Power Allocation Problem

Contents

5.1	A Game Strategy for Radio Resource Sharing Game	103
5.1.1	Classification of the Actions	103
5.1.2	The Proposed Game Strategy	104
5.2	Simulation Setup	105
5.3	Snapshot Analysis	109
5.3.1	Snapshot Analysis under a Flat Fading Channel	109
5.3.2	Snapshot Analysis under a Frequency Selective Fading Channel	115
5.4	General Performance under a Flat Fading Channel	122
5.5	General Performance under a Frequency Selective Fading Channel	125
5.6	Performance Comparison between Proposed Scheme and Iterative Water Filling Scheme	128
5.6.1	Iterative Water Filling Technique	129
5.6.2	Simulation Setup	131
5.6.3	Simulation Results	133
5.7	Chapter Conclusion	139

We study a distributed cognitive power allocation problem (DCPA) for a multicarrier wireless system. The burden of UWB power allocation as we described before is the extremely low transmit power density governed by the spectrum mask. The fully distributed nature of UWB systems also hinders the power allocation problem from finding an optimal solution. However, these disadvantages of the UWB systems are, on the contrary, the most significant advantages over a traditional wireless system. Our idea is to develop a DCPA scheme that can take full advantage of the UWB framework. In this chapter, we will demonstrate that we can achieve a target data rate by partitioning the channel combined with a game strategy; also we will

investigate how efficient of our proposed DCPA scheme, and its performance against the existing power allocation scheme.

5.1 A Game Strategy for Radio Resource Sharing Game

Similar to the importance of the choice of the utility function, the strategies employed by players decide a game's outcome [60]. A proper strategy will enforce a distributed power allocation game reaching an efficient Nash Equilibrium collectively.

We have introduced the possible actions that a player can take in a game. We also introduced the stage based dynamic multistage game strategy that is used to decide the behaviour of players in the game competition. Now, we will introduce our proposed game strategy used in UWB power allocation game.

5.1.1 Classification of the Actions

We have introduced the concepts of Cooperation and Defection in game strategy. Now, we will define cooperation and defection in a context of UWB power allocation spectrum sharing game.

It is always assumed that an opponent's action can be observed and understood by a player, a corresponding action can be taken by the player in turn. Recall that we defined our UWB channel allocation game as a non-cooperative game. It is however very difficult for a system to precisely understand the behaviour of the components under our game model due to the lack of the direct information exchange. The system therefore has to identify the action of the opponents. Similar to the principle we introduced in chapter 2. We define two basic actions for a wireless power allocation game.

A. Cooperation Action

We defined our utility function according to the advertised transmit power of our proposed DCPA scheme. It shows in Figure 5.11 that the utility increases with the increase of the advertised transmit power up to a maximum point and then decreases. Therefore, we define cooperation as a specific amount of decrease of the advertised transmit power, which will

lead to a decrease or increase of utility depended on whether the advertised transmit power is smaller or bigger than the advertised transmit power corresponding to maximum utility.

B. Defection Action

We define the defection action as a specific amount of increase of the advertised transmit power, which will either be a selfish behaviour aimed at increasing the utility or a punishment in response to the defect opponents.

5.1.2 The Proposed Game Strategy

We design a three stage game strategy illustrated in Figure 3, which is made up of three main stages. The Competitive Spectrum Sharing Stage is the gradient power allocation stage during which distributed systems perform the gradient power allocation until there is no significant change of interference. The next stage could be either Cooperation Stage or Defection Stage depending on whether or not the target data rate is achieved. If the data rate acquired by the link is higher data rate by μ more than target rate, the system will act cooperatively, during which the transmitter will reduce total transmit power by δ dB on the next iteration, where δ in our simulation is between 0.5dB and 1dB. If the acquired bit rate is lower than given target bit rate by more than μ , the system will operate in the defection stage, during which the transmitter of defect system will retransmit a beacon with an increased total power of δ dB. Thereby another Competitive Channel Assignment Stage will be triggered that favours the defecting user. The convergence culminates in the static stage where all users acquire the data rate within μ of the target data rate.

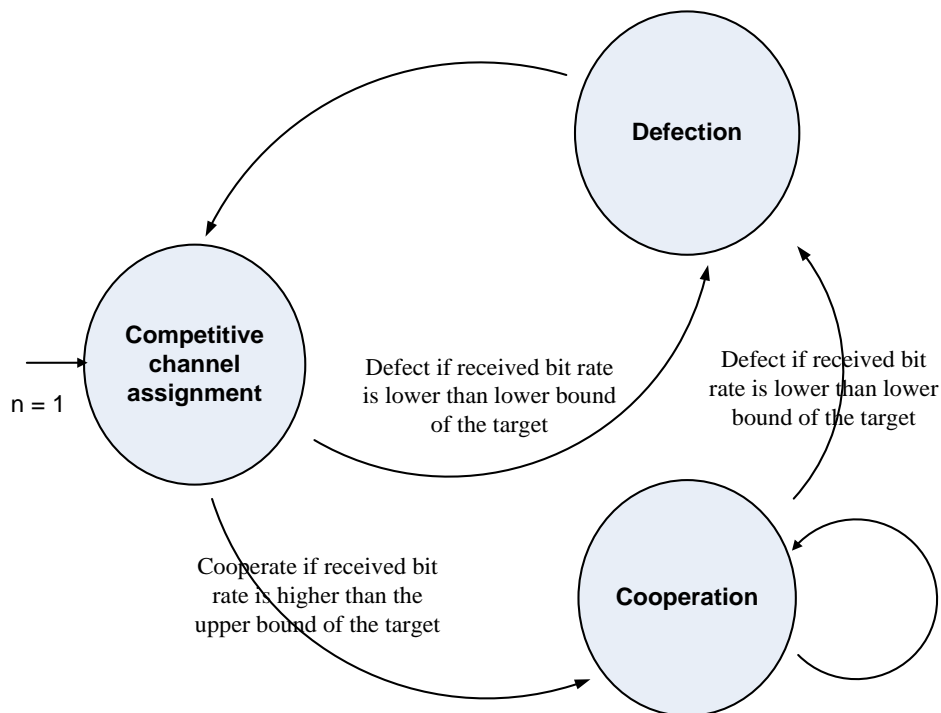


Figure 5-1 Illustration of the proposed game strategy

5.2 Simulation Setup

We examine the performance of our proposed game strategy in a four UWB system coexistence scenario. We now derive the data rate dependent equation since our strategy is based on the comparison between acquired data rate and the target data rate.

The MB-OFDM PHY specification from [47, 92, 93] requires only 4.9dB of SNR for QPSK modulation at the highest speed of 480Mbits/s, and data rate dependent equation can be expressed as

$$\text{Bitrate} = 2 \cdot N \cdot Bw \cdot R \tag{5.1}$$

Where N is the number of available channels with a SNR value higher than minimal 4.9dB assumption, B_w is the bandwidth of a channel, which is 4.125MHz, and R is the code rate.

Chapter 5 Performance of Game Approach in UWB Multichannel Power Allocation Problem

For the path loss channel model, we use the UWB indoor office environment channel model, because it has the widest range of applicability from 3 to 28 metres. The corresponding parameters can be found in the following table. Only LOS channel path gain is tested in our simulation, and the channel path gain for NLOS is too severe that the radio system cannot establish the connection under the current FCC spectrum mask condition.

	Office	
	LOS	NLOS
N	1.63	3.07
PL_0 (dB)	35.4	57.9
K	0.03	0.71

Table 5-1 Parameter of the indoor office path loss model

In addition to a flat fading channel, we will examine the performance of our proposed DCPA scheme under a frequency selective fading channel which we studied in chapter 2. The received signal through a fading channel can be then expressed as the following equation.

$$r(f, t) = p(f, t)PL(f, d, t)r_0(f, t) \quad 5.2$$

Where $r(f, t)$ is the received power of channel with central frequency f at time instance t . $p(f, t)$ is the transmit power of channel with central frequency f at time instance t . $PL(f, d, t)$ is the frequency dependent path loss. $r_0(f, t)$ is the multipath fading factor on the channel with central frequency f at time instance t .

Multipath fading is also referred to as frequency selective fading. In the frequency domain, it can be written as $H(f)$, and we derive this frequency selective fading from the normalized channel impulse response by means of Fourier transform. Assuming the radio environment remains static, then the fading path loss and the frequency selective fading is not a function of time (it is reasonable that we assume a short range system with no motion, which keeps the same path gain and fading factor over time). We can then simplify the equation 5.3

$$r(f, t) = p(f, t)PL(f, d)H(f) \quad 5.3$$

Lastly, UWB devices will be interference sensitive because of the low transmit power density and the co-channel interference which can be significantly increased without coordination. Our simulation takes the relative distance between transmitters and receivers into consideration and generates the geographical locations of the UWB transmission pairs subject to a direct link longest and direct link shortest scenarios in order to better understand the impact of different interference levels on the performance. In the direct link longest scenario, the transmitters are closer to the receivers of the other systems than their own. In the direct link shortest scenario, the transmitter is closer to its receiver but far away from the receivers of the other homogeneous systems. The geographical layout can be seen from Figure 5.2.

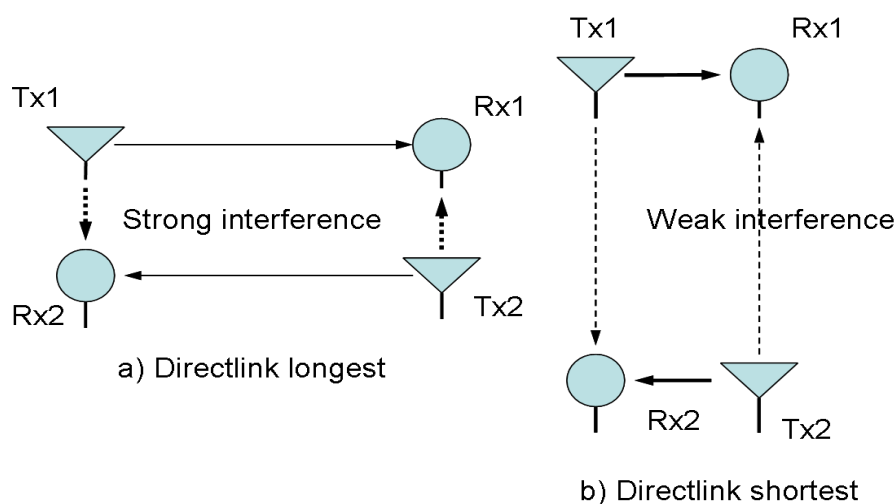


Figure 5-2 Geographical layouts of the competing systems

The bold line in Figure 5.2 indicates the link between transmitter 1 and receiver 1 and the dotted line indicates the link between transmitter 2 and receiver 2. We use T_1R_1 as the distance between transmitter 1 and receiver 1, T_1R_2 as the distance between transmitter 1 and receiver 2, and so on.

It is noted from our analysis in the previous chapter that the channel path gain has a profound influence on the value of Signal to Interference Ratio. If $T_1R_1 < T_2R_1$, the wireless system will not be able to work because the interference will be higher than the received signal, and hence channel partitioning is the only feasible solution. If $T_1R_1/T_2R_1 \gg \alpha'$ where α' is the linear gradient value, then the wireless system may acquire more data rate by filling power to all the

Chapter 5 Performance of Game Approach in UWB Multichannel Power Allocation Problem

channels according to the Signal to Interference plus Noise Ratio at receiver. Similar analysis can be viewed from multiple papers [12, 67, 94], which give rise to geo-location awareness power allocation scheme found in [95]. In [96] it is proved that if $\beta_{i,j} \beta_{j,i} > \beta_{i,i} \beta_{j,j}$, where β is the channel path gain, then the optimal power allocation is orthogonal power allocation which means the different users will use different channels. A simple example is that if there are two systems using half of the bandwidth each when $\beta_{1,2} = \beta_{2,1} = 1/2$, $\beta_{1,1} = \beta_{2,2} = 1$, when bandwidth $BW=1$, $Noise = 1$ for simplicity and $P_1 = P_2 = P$ then the data rate for each system can be expressed by Shannon equation $R_1 = R_2 = 1/2 \log_2(1 + P)$, which tends to infinity when P tends to infinity. If instead users spread the power equally to the two channels, then $R_1 = R_2 = \log_2[1 + \frac{P}{1+\frac{1}{2}}]$ which tends to $\log_2(3)$ when P tends to infinity. However, as we mentioned in last chapter, our scheme caters for achieving a target data rate rather than trying to achieve the highest channel capacity.

Some of the other important parameters that used in our simulations can be found in the following table.

Parameters	Value
C1	352×10^6
C2	10^8
C3	e
BW (MHz)	4.125
R	2/3
$P_{initial}$ (dBW)	-44
δ (dB)	1
α (dB)	0.5
μ (Mbps)	6
channels	128
Target Data Rate (Mbps)	88

Table 5-2 Parameters used in the simulations

Chapter 5 Performance of Game Approach in UWB Multichannel Power Allocation Problem

$C1$, $C2$, and $C3$ are utility related constants. As we analysed in chapter 4, $C1$ is chosen as a large enough value while $C2$ and $C3$ only need to be bigger than 0. The specific values are chosen so that the outcome of power allocation can be better compared in terms of utility. The δ is the total power adjustment factor between state transitions, and it is 1 dB in our simulation because it is test through simulation as the most efficient power adjustment factor that provides both fast convergence speed and reliable convergence. It is also noted that μ is the boundary we applied to determine the state transition of the game strategy, which can also be interpreted as max permitted target data rate variation, it is 6 Mbps in our simulation because it is related to the data rate dependent equation 5.1. According to the equation 5.1, a channel with a received SNR over 4.9dB will acquire a data rate of 5.504 Mbps. Making μ slight bigger than 5.504Mbps will improve the degree of convergence, so that the user can allocate power to one more channel or one less channel than that it is required for a specific target data rate, and the proposed DCPA scheme can still achieve convergence.

5.3 Snapshot Analysis

We begin by analysing the snapshot performance in which we show the performance of the four user coexisting scenario with an arbitrarily generated geographical locations subject to the given distance condition.

5.3.1 Snapshot Analysis under a Flat Fading Channel

Firstly, we examine the performance of our proposed DCPA under a flat fading channel. Although the simulation results are largely subject to the specific geographical layout of the transmitters and receivers, they shed some light on what a general performance might be and help us better understand the mechanism of the power allocation algorithm.

Figure 5.3 shows the unfair channel allocation at iteration 1 on both scenarios, which is due to the sequence of system activation. User 1, 2 and 3 have much more bandwidth at beginning because they join in the game earlier and have less interference at that point, which leaves user 4 with very little spectrum. However, these two games converge at iteration 15 and iteration 6 respectively, when all users acquire data rate within a satisfactory boundary close to the target

Chapter 5 Performance of Game Approach in UWB Multichannel Power Allocation Problem

requirement. The direct link shortest scenario converges faster than the direct link longest scenario; because the interference is lower for all users, and users can easily achieve their target. The ellipses show the state transition points where the competitive stage converges and the users transfer their state by checking the fulfilment of the target requirement. The state transition point can be found when there is a steady period that lasts 2 iterations.

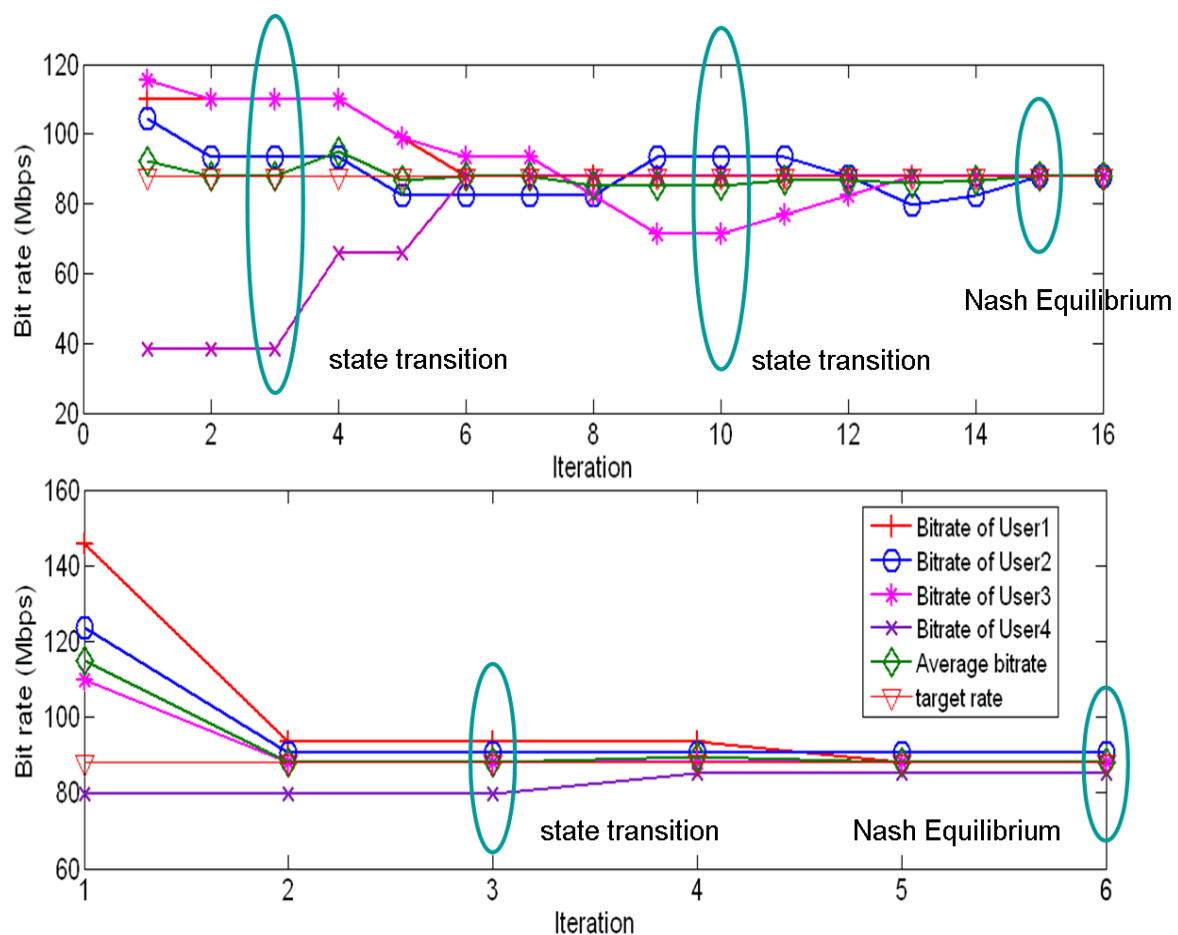


Figure 5-3 Acquired data rate analysis under a flat fading channel in direct link longest (upper) user direct link shortest (lower) scenarios

In order to further understand the behaviour of our Game based power allocation scheme, we should analyse the specific power allocation for each of users in the first iteration and final iteration.

Figure 5.4 shows the power allocation pattern of all four users as well as their SINRs at their receivers. We can observe that the whole bandwidth is divided by 4 users, but not evenly

Chapter 5 Performance of Game Approach in UWB Multichannel Power Allocation Problem

divided among users. The User 4 acquired fewer channels due to the fact that it is the last user joined the competition in the first iteration, and has fewer free channels left for it to share.

In The last iteration, as can be seen from the Figure 5.5, users 1 2 and 3 all give away some of their channels to user 4 while user 4 can finally reach its target data rate by having enough channels.

Chapter 5 Performance of Game Approach in UWB Multichannel Power Allocation Problem

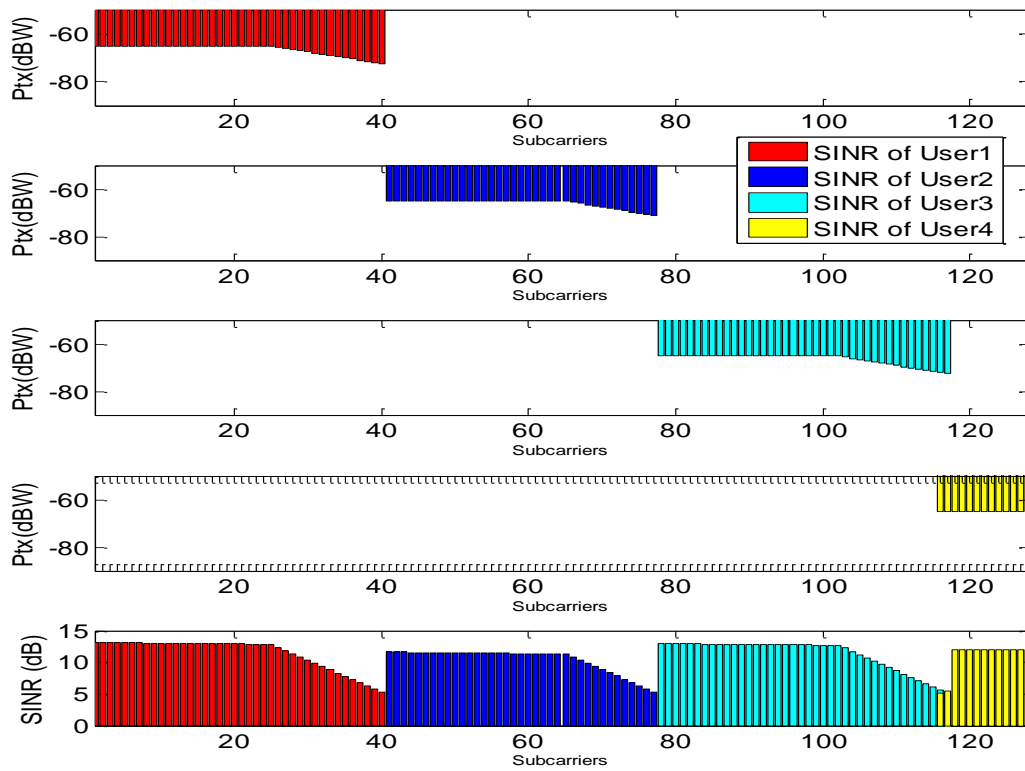


Figure 5-4 Power allocation pattern under a flat fading channel at the first iteration (Direct link longest)

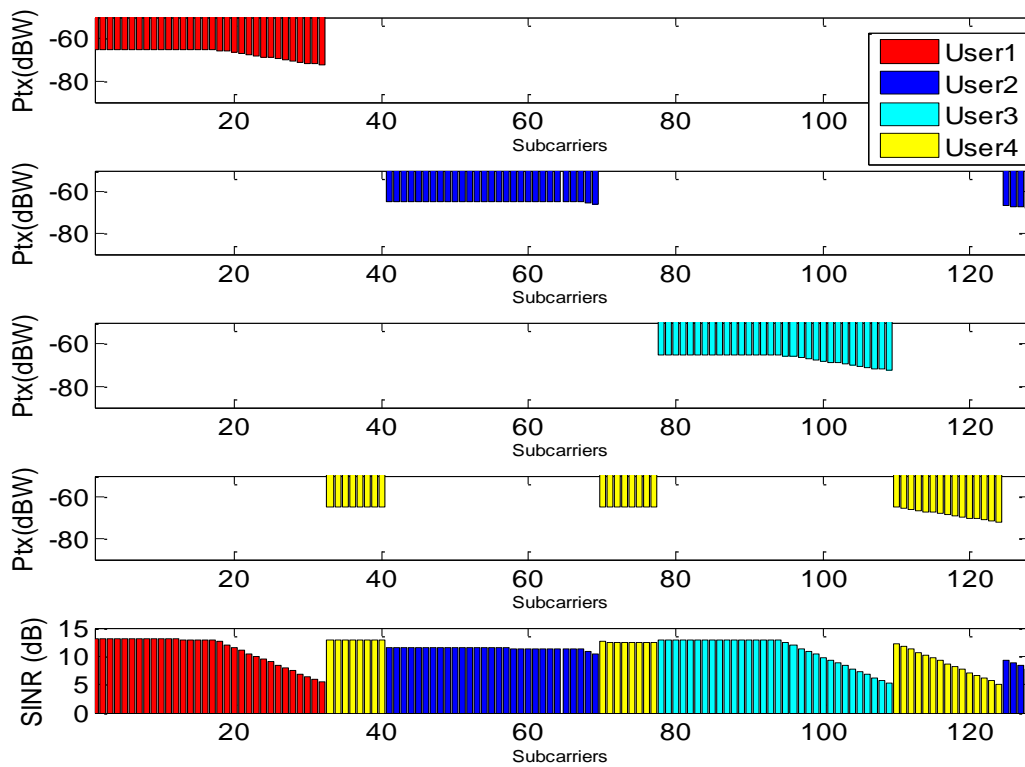


Figure 5-5 Power allocation pattern under a flat fading channel at the final iteration (Direct link longest)

Chapter 5 Performance of Game Approach in UWB Multichannel Power Allocation Problem

Next, we analyse the power allocation pattern in direct link shortest scenario. Figure 5.6 and 5.7 shows the first iteration and final iteration respectively. As opposed to the power allocation pattern shown in Figure 5.4, all users share some of their channels with other users, which is, according to our previous analysis, is due to the reduced interference between users. It also means sharing some of the channels will not pose a significant increase of interference. Also, unlike the final iteration in direct link longest scenario, Figure 5.7 shows that the users will not change their power allocation pattern dramatically. This is because of the reduced inter user interference: each user can easily reach their target data rate without competing for more channels, and hence users in direct link shortest scenario will most likely keep their original power allocation pattern from first iteration. Also, comparing the direct link longest scenario and direct link shortest scenario, it is clear that the Signal to Interference plus Noise Ratio for the direct link shortest is higher than that of the direct link longest, which is also thanks to the closer distance between transmitter and receiver pairs.

Chapter 5 Performance of Game Approach in UWB Multichannel Power Allocation Problem

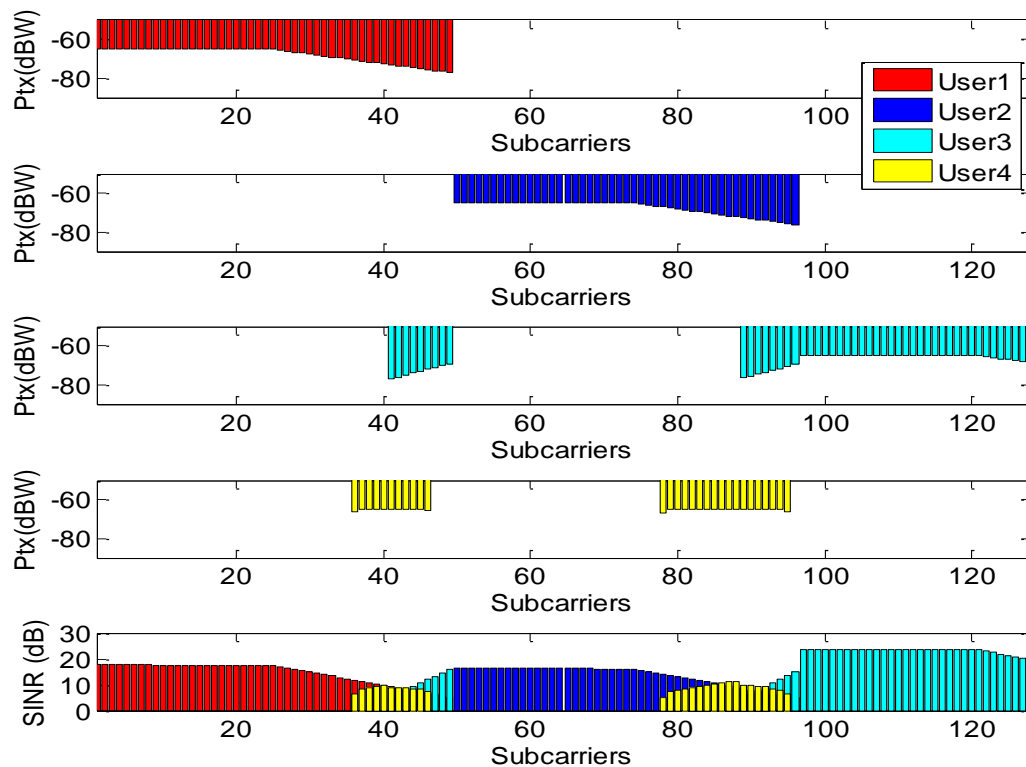


Figure 5-6 Power allocation pattern under a flat fading channel at the first iteration (Direct link shortest)

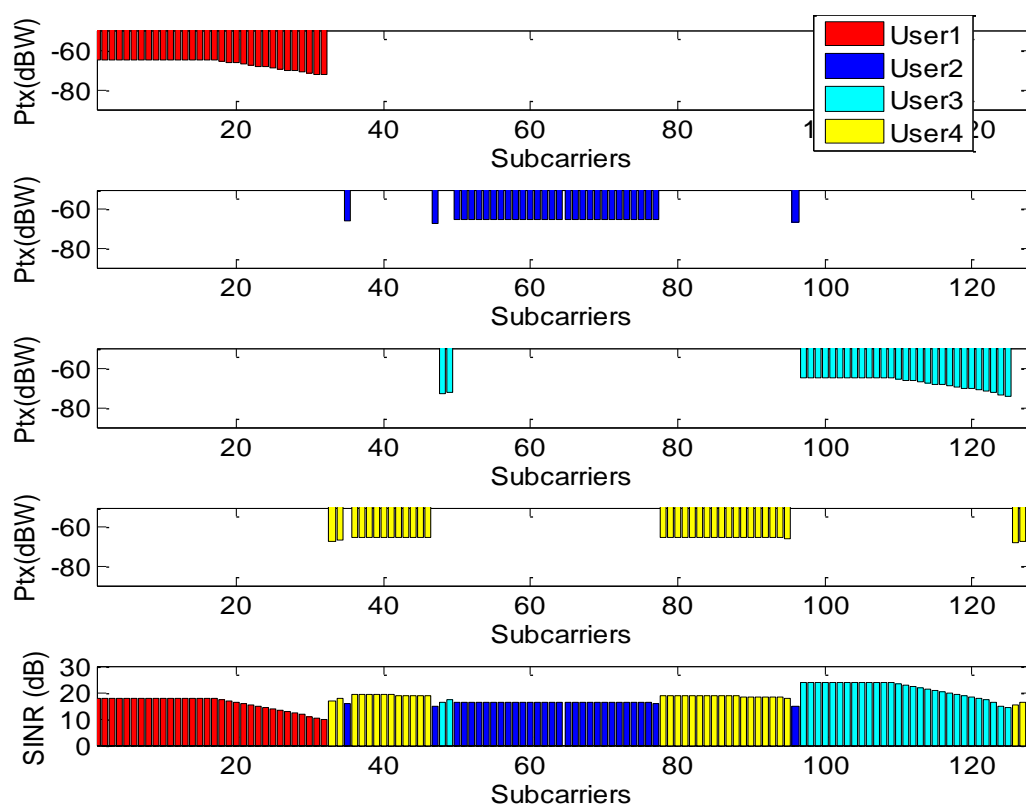


Figure 5-7 Power allocation pattern under a flat fading channel at the final iteration (Direct link shortest)

Chapter 5 Performance of Game Approach in UWB Multichannel Power Allocation Problem

The graph of utility shows that the global utility increases to a maximum, and the game reaches the Nash Equilibrium. It is also noted that the global utility reduced at iteration 8 in the direct link longest scenario. It is because we apply a boundary close to the target data rate, within which the user will not leave its current cooperative state even when the acquired data rate diverts from target which decreases its utility.

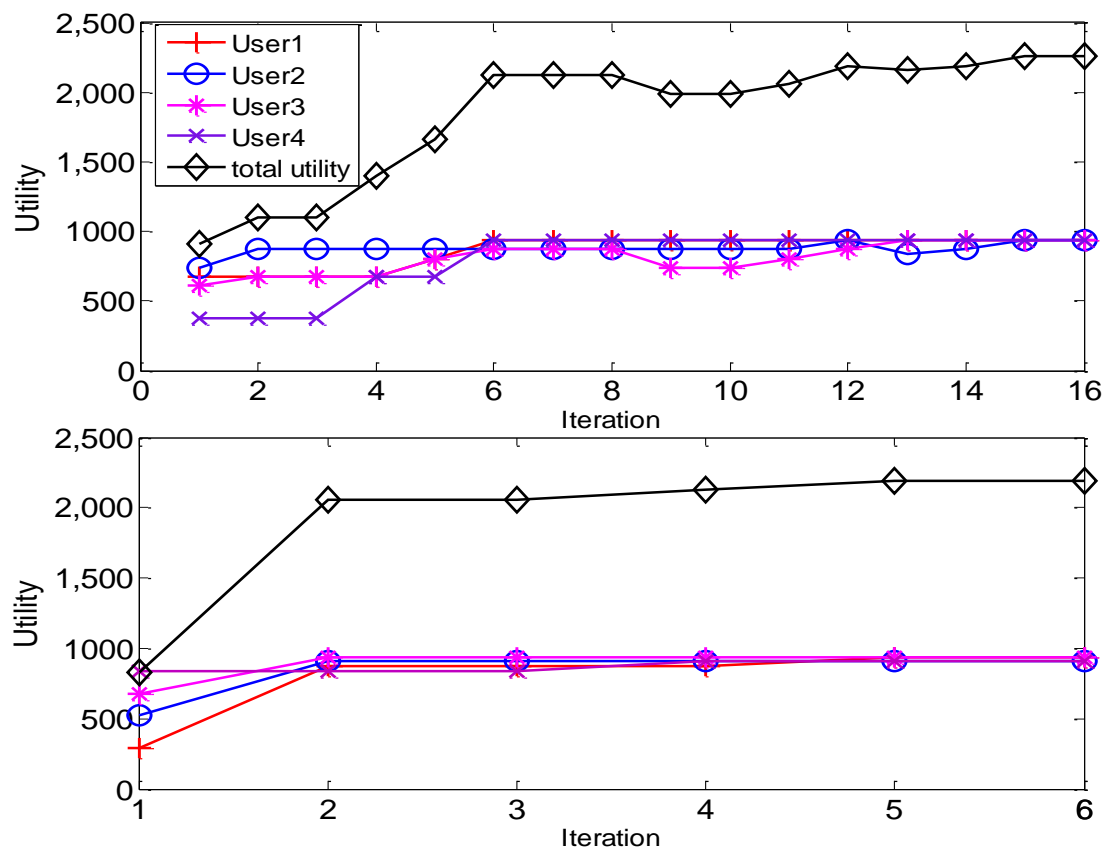


Figure 5-8 Utility analysis under a flat fading channel in direct link longest (upper) user direct link shortest (lower) scenarios

5.3.2 Snapshot Analysis under a Frequency Selective Fading Channel

We have introduced the frequency selective fading on UWB bands, and we show that the received power of a specific channel with central frequency f at any time instance t can be expressed by the equation 5.2

$$r(f, t) = p(f, t)PL(f, d, t)r_0(f, t) \quad 5.2$$

Chapter 5 Performance of Game Approach in UWB Multichannel Power Allocation Problem

In this section we will examine the performance of our proposed DCPA scheme under a frequency selective fading channel.

Figure 5.9 demonstrates the acquired data rate of 4 users under the frequency selective fading channel. Similar behaviour we have shown in Figure 5.3 can be seen in Figure 5.9. The four users with an uneven acquired data rate from first iteration gradually reach their target data rate at the final iteration. It suggests that our proposed DCPA scheme works well in both flat fading and frequency selective fading channels. It is however necessary for us to look at the power allocation pattern in order to better understand the effect of frequency selective fading channel on our game based power allocation scheme.

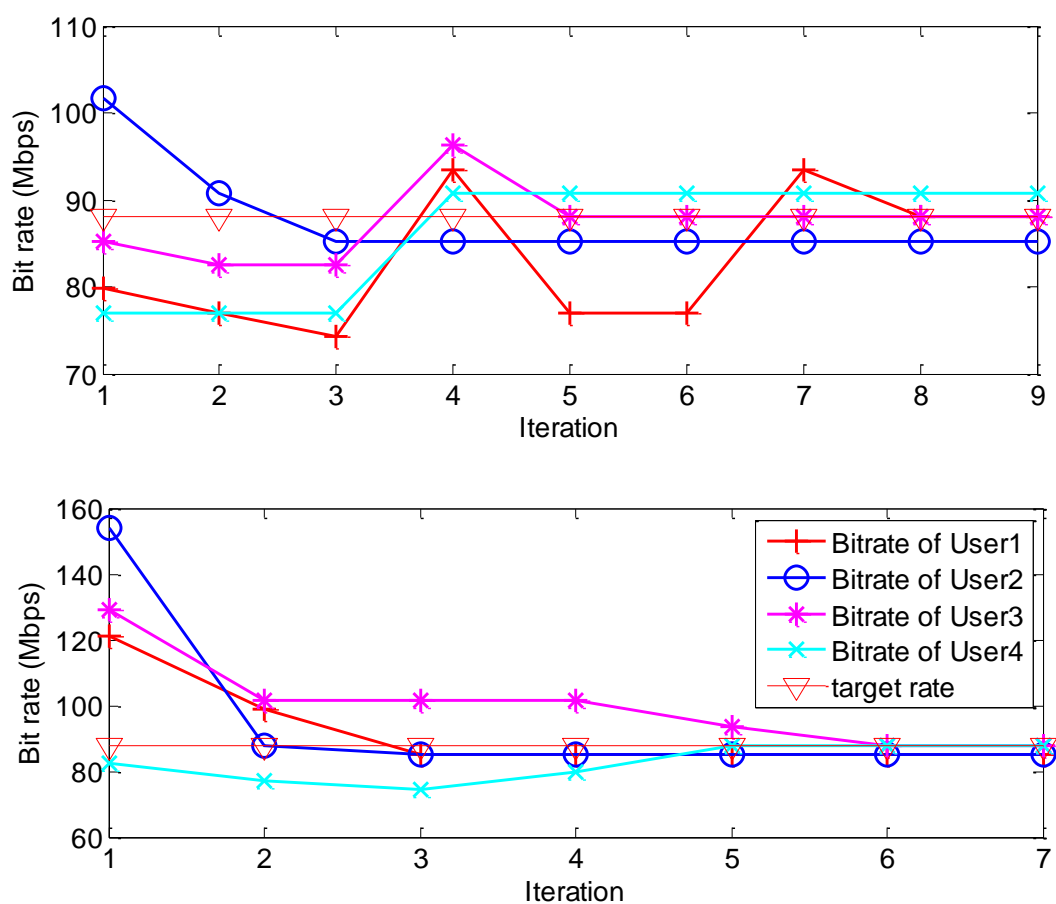


Figure 5-9 Acquired data rate analysis under a frequency selective fading channel in direct link longest (upper) user direct link shortest (lower) scenarios

Figure 5.10 shows the power allocation pattern for the first iteration. Compared with Figure 5.4, the power allocated pattern in frequency selective fading channel shows a discontinuous

Chapter 5 Performance of Game Approach in UWB Multichannel Power Allocation Problem

characteristic. In Figure 5.4 the users allocate power in a few consecutive channels. However, Figure 5.10 shows that the user 1 2 and 3 do not allocate their power on a few consecutive channels. Instead, there are some gaps in their channel assignment pattern. This is due to the frequency selective fading, and the gaps are likely the result of the deep fading presented on those channels. Figure 5.11 shows power allocation pattern at the final iteration. The blue line on the transmit power graph is the path gain of the direct link between transmitter and receiver of a specific user.

Chapter 5 Performance of Game Approach in UWB Multichannel Power Allocation Problem

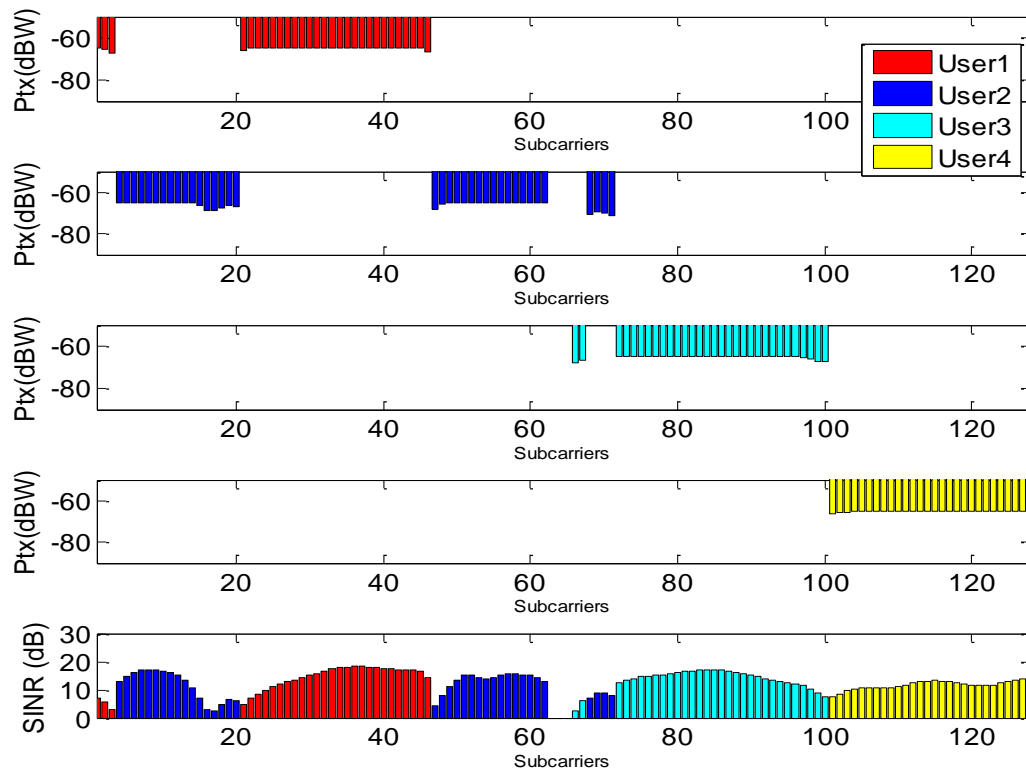


Figure 5-10 Power allocation pattern under a frequency selective fading channel at the first iteration (direct link longest)

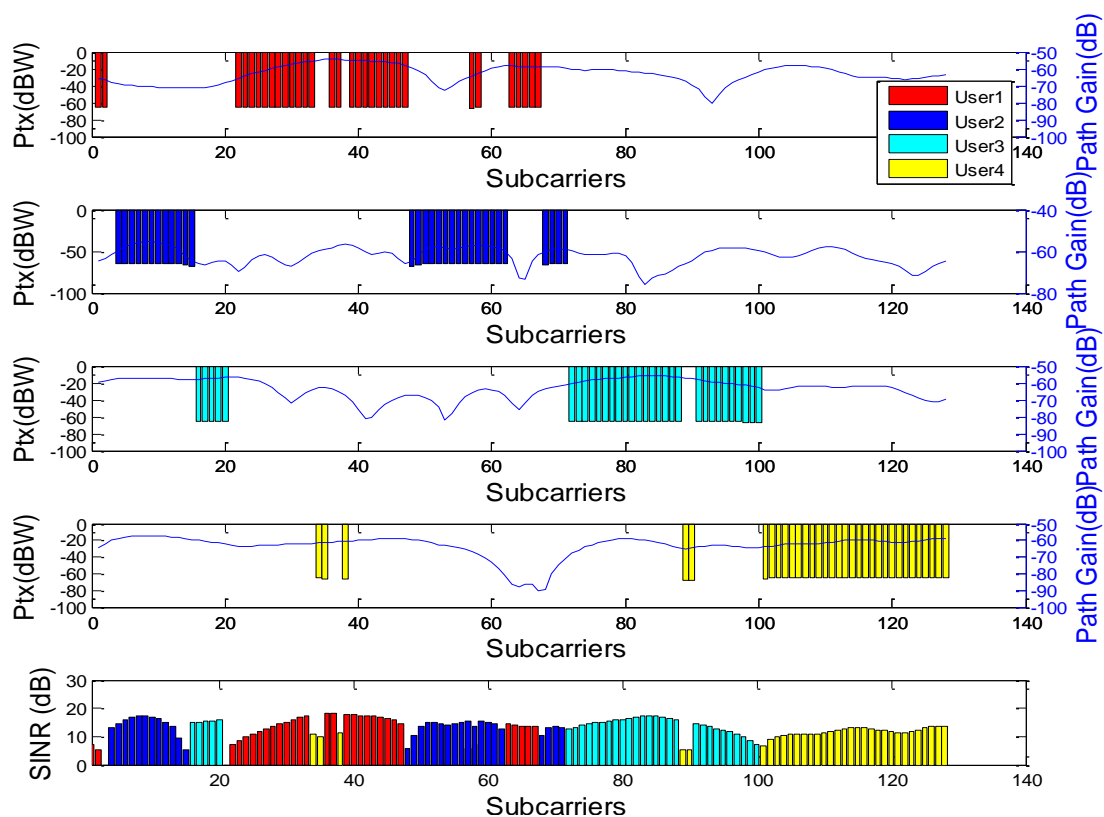


Figure 5-11 Power allocation pattern under a frequency selective fading channel at the final iteration (direct link longest)

Chapter 5 Performance of Game Approach in UWB Multichannel Power Allocation Problem

In Figure 5.11 we overlap the transmit power pattern with the channel path gain in order to better understand the effect of frequency selective fading on our proposed DCPA scheme. It should be noted that we did not show the channel frequency selective fading at the first iteration. It is because the power allocation at first iteration is dependent mostly on the immediate interference at receiver of the initial beaconing stage and the channel fading will only be fully reflected by power allocation pattern in the final iteration. The deep valleys on the path gain graph are path gains at frequencies under deep fading, and it is clear that some of the gaps in power allocation pattern are the direct results of deep fading. For example channel 46 – 55 shows deep fading on the path gain graph; and hence they are not used by user 1. Similar behaviour can be found on channel 63 to channel 67 for user 2, channel 22 to channel 70 for user 3 and channel 58 to channel 77 for user 4. On the other hand the power allocation pattern is still subject to our gradient power allocation scheme, and the final result shows that the whole bandwidth has been partitioned by 4 users.

Next we demonstrate the power allocation pattern in the direct link shortest scenario. The Figure 5.12 and Figure 5.13 show the power allocation pattern on the first and the last iteration respectively. Similar to the direct link longest scenario, the power allocated is not concentrated on a few consecutive channels as opposed to channel allocation pattern in the flat fading channel scenario. Especially, the user 3 and user 4 shown in Figure 5.12 allocate their power sparsely on the whole bandwidth. Also, we see that many channels have been reused by different users, which is due to the direct link shortest scenario that the interference from homogeneous UWB users is far less severe.

Frequency selective fading is one of the major factors that affect the behavior of the power allocation pattern due to the less severe interference from homogenous devices, which can be clearly viewed from Figure 5.13. In Figure 5.13, channel 27 – 33 are not used by user 1 because of the fading. Similarly, channel 62 – 64 was not been used by user 2, channel 121 – 124 was not been used by user 3, and channel 104 – 107 was used by user 4 because of the frequency selective fading. It is noted from the SINR graph that some channels, such as 104 – 107, have not been used by any of the four users. It is because that the user 1 and user 2 have fulfilled their target data rate without allocating power to channel 104 – 107 while user 3 and user 4 suffered deep fading on those channels and hence they are left unused. It is also noted

Chapter 5 Performance of Game Approach in UWB Multichannel Power Allocation Problem

that user 4 and user 2 share a lot channels on the final stage, which is due to both having less inter-user interference on the same channel and higher channel path gain.

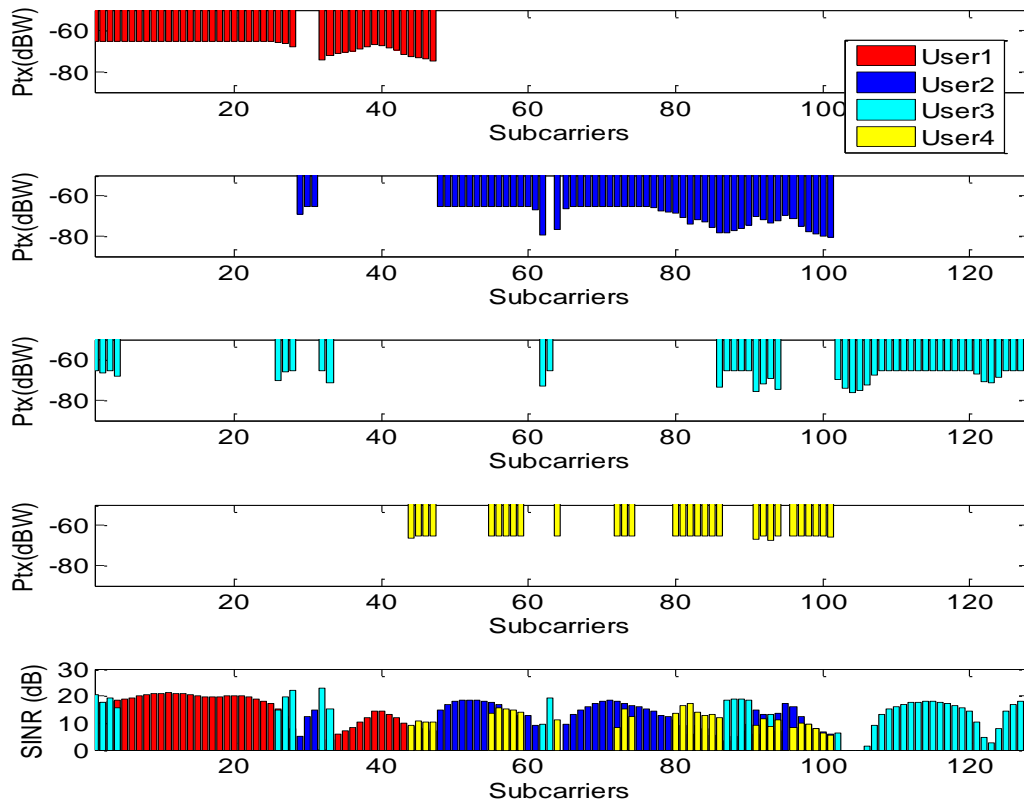


Figure 5-12 Power allocation pattern under a frequency selective fading channel at the first iteration (direct link shortest)

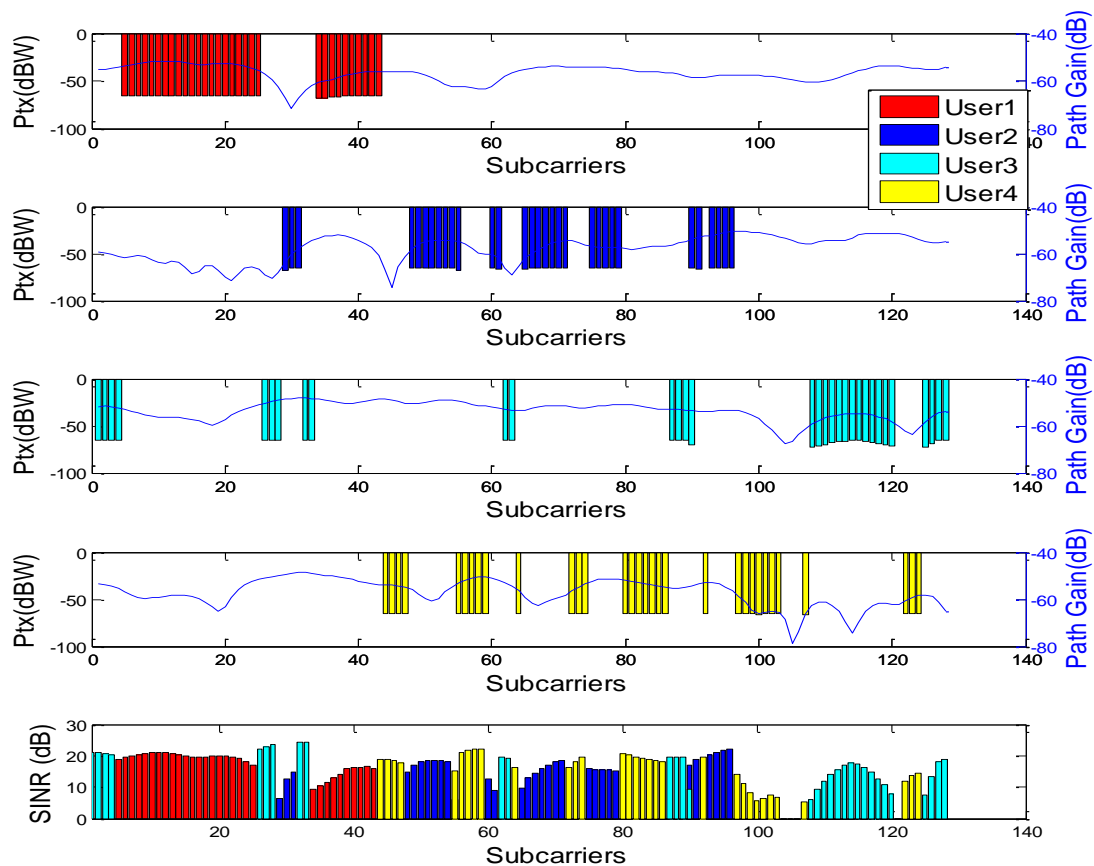


Figure 5-13 Power allocation pattern under a frequency selective fading channel at the final iteration (direct link shortest)

Lastly, we show the utility graph in Figure 5.14, and it shows that the overall utility increase though iterations and reach their maximum value in the final iteration for both direct link longest and direct link shortest scenarios. It is noted that the overall utility does not change dramatically in direct link shortest scenario, which is because of the characteristic that the utility function increases faster when the utility is close to the maximum point, while it increases slowly when it is farther away from maximum utility.

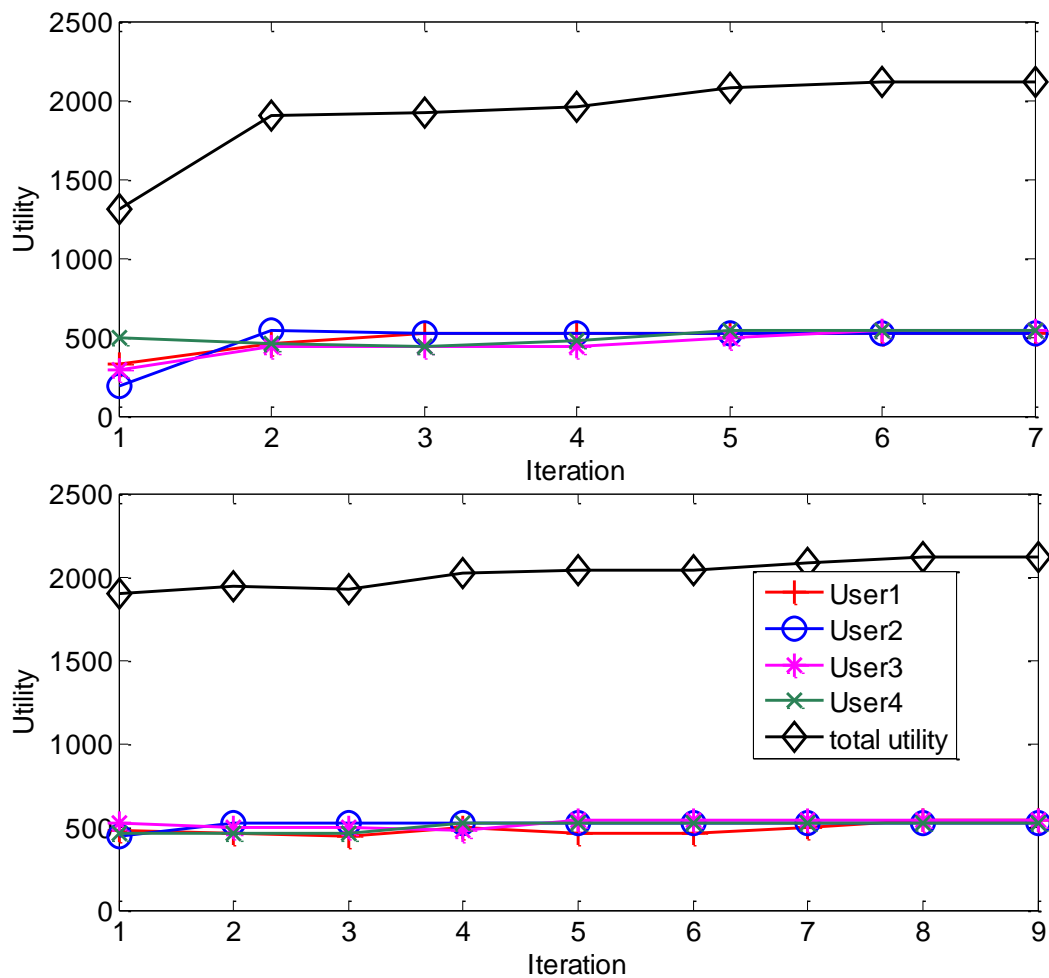


Figure 5-14 Utility analysis under a frequency selective fading channel in direct link longest (upper) user direct link shortest (lower) scenarios

5.4 General Performance under a Flat Fading Channel

To understand the system behaviour more generally, we generate 1000 different system layouts in a 30 cubic metre volume under direct link shortest and direct link longest condition respectively, and study the statistical performance of our proposed DCPA scheme through Monte Carlo simulations. First we examine the performance under a fixed target data rate of 88 Mbps, which is same with our previous snapshot simulation. Figure 5.15 shows the reliable convergence region for α , where α controls the power gradient and effectively decides the number of carriers that can be used by each system. 90 percent convergence can be guaranteed with α ranging from 0.4 to 1.8 dB in the direct link shortest scenario but must be reduced to the range between 0.5 to 1.4 dB in the direct link longest scenario. This is because the interference level in the direct link shortest scenario remains very low and users can easily

Chapter 5 Performance of Game Approach in UWB Multichannel Power Allocation Problem

achieve the target. The fact that convergence is subject to α is because α effects the SINR difference between carriers. If α is set too small, the SINR at each carrier cannot be sufficiently differentiated, and if α is set too big, the SINR will soon decrease below the threshold, which gives rise to an insufficient number of channels.

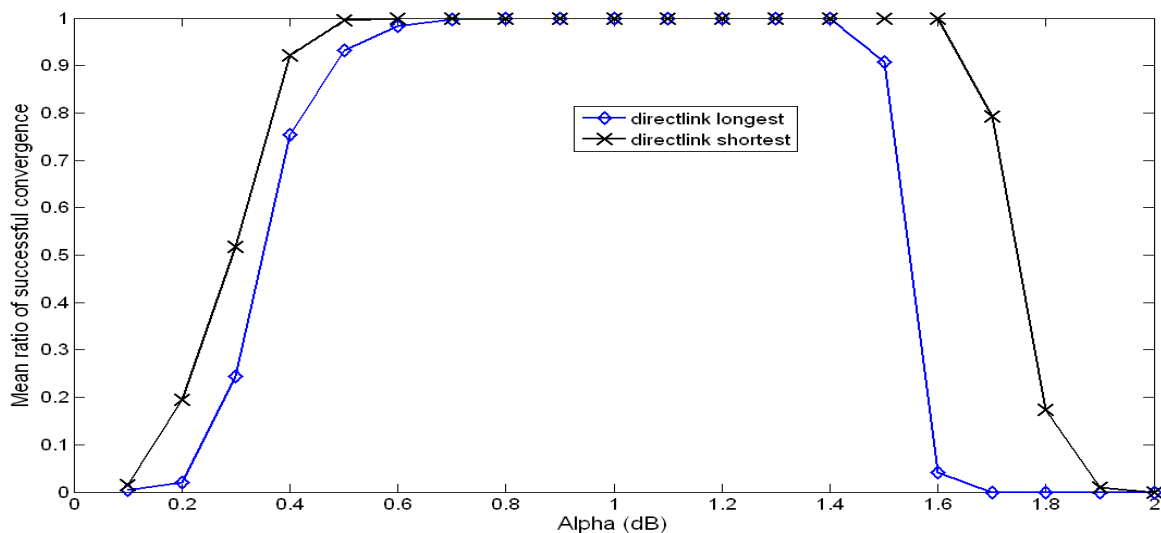


Figure 5-15 Mean degree of convergence under a flat fading channel

The convergence speed analysis in Figure 5.16 exhibits a similar trend where the convergence speed is a function of α . The best convergence speed occurs when α is set 0.8dB, and 0.9dB respectively. Once α is out of the reliable convergence region, the systems will either converge after many iterations or not converge at all.

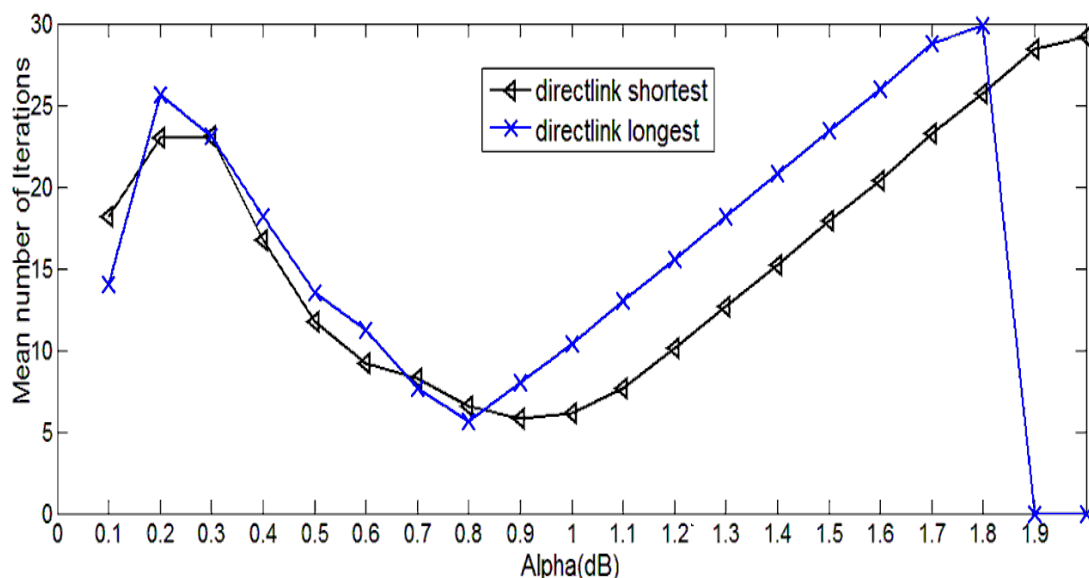


Figure 5-16 Convergence speed analysis under a flat fading channel

Furthermore, we examine the reliable convergence region for both α and the Target Data Rate. Figure 5.17 illustrate the direct link longest scenario and Figure 5.18 illustrate the direct link shortest scenario. It is noticed that the reliable convergence region is smaller under direct link longest condition than that of the direct link shortest. In the direct link shortest scenario however, the 90 percent convergence can be guaranteed with α ranging from 0.4 to 1.4 dB when the target data rate is between 20 Mbps and 50 Mbps. The 90 percent convergence can be guaranteed for a wider target range if the α is bounded between 0.5 to 1 dB. In the direct link longest scenario, due to the reduced degree of convergence, the 90 percent convergence can be guaranteed with the α bounded between 0.5 to 1 dB. Taking the two link length condition as a whole, a general suitable α that lies between 0.5 to 1 dB can meet most target data rate requirements. Take also the convergence speed into account, which we showed in Figure 5.16, the most suitable α should be between 0.8 and 0.9 as it offer both best convergence and convergence speed.

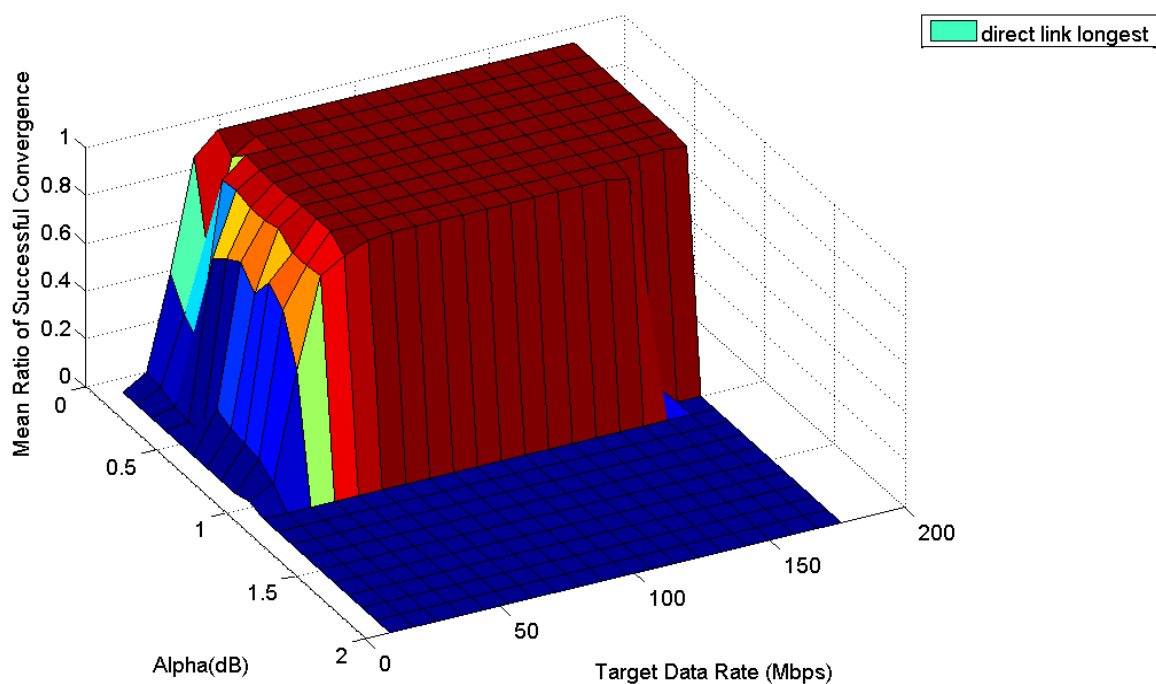


Figure 5-17 Mean degree of convergence under a flat fading channel (direct link longest)

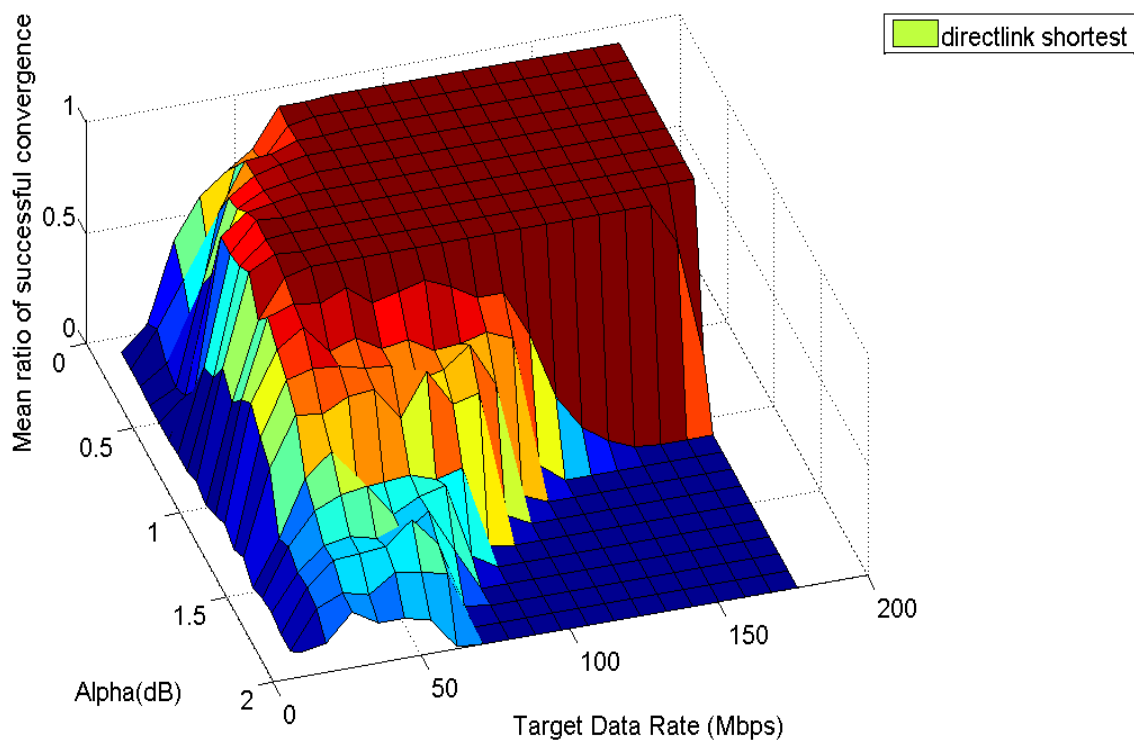


Figure 5-18 Mean degree of convergence under a flat fading channel (direct link shortest)

5.5 General Performance under a Frequency Selective Fading Channel

We have examined the performance of our proposed DCPA scheme under flat fading channel, and it reveals that there exists a suitable gradient value α range for reliable convergence. In order to guarantee a wide usability of our proposed DCPA scheme, it is necessary to check the reliable convergence condition on a frequency selective fading channel.

Figure 5.19 and Figure 5.20 show the direct link longest and direct link shortest scenario respectively. They show almost identical behaviours, except that the general convergence region is slight bigger for frequency selective fading channel under both direct link longest and direct link shortest conditions compared with that of flat fading channel. The 90 percentage convergence can be guaranteed for an α setting between 0.5 and 1 for most target data rate requirements, while it is extended to 0.4 to 1.4 under direct link shortest scenario. Therefore an α between 0.5 and 1 can guarantee an overall 90 percent convergence.

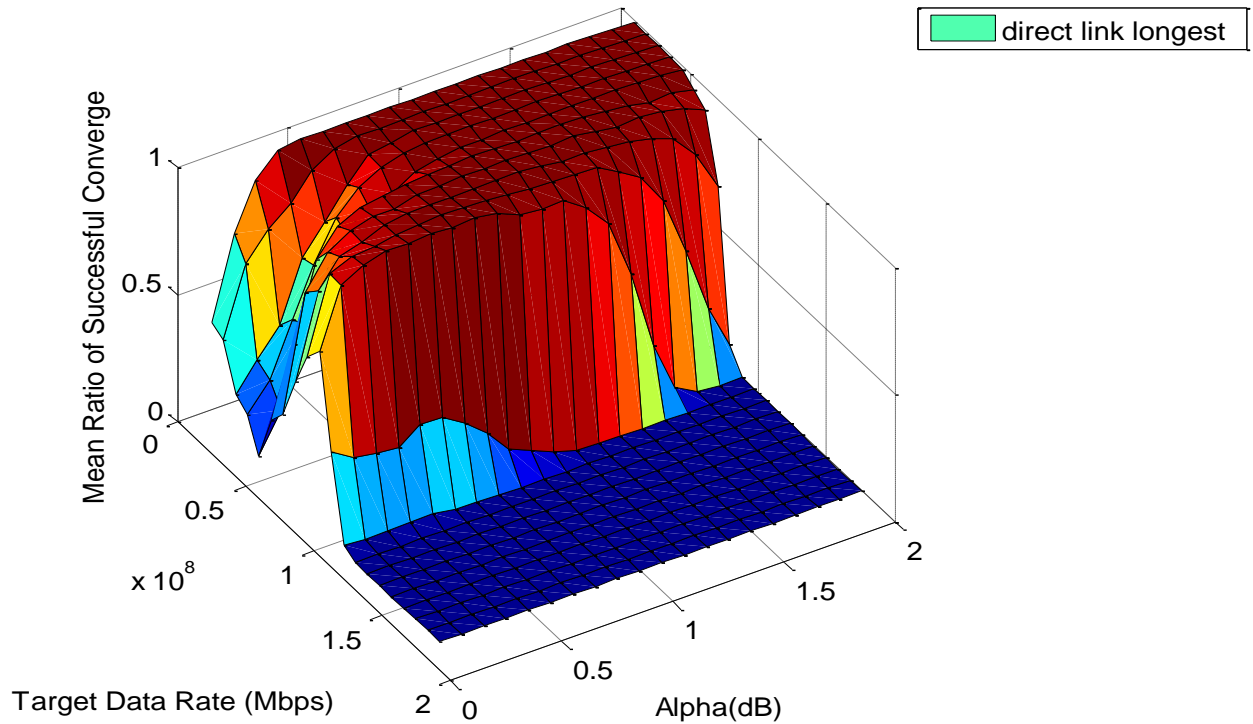


Figure 5-19 Mean degree of convergence under a frequency selective fading channel (direct link longest)

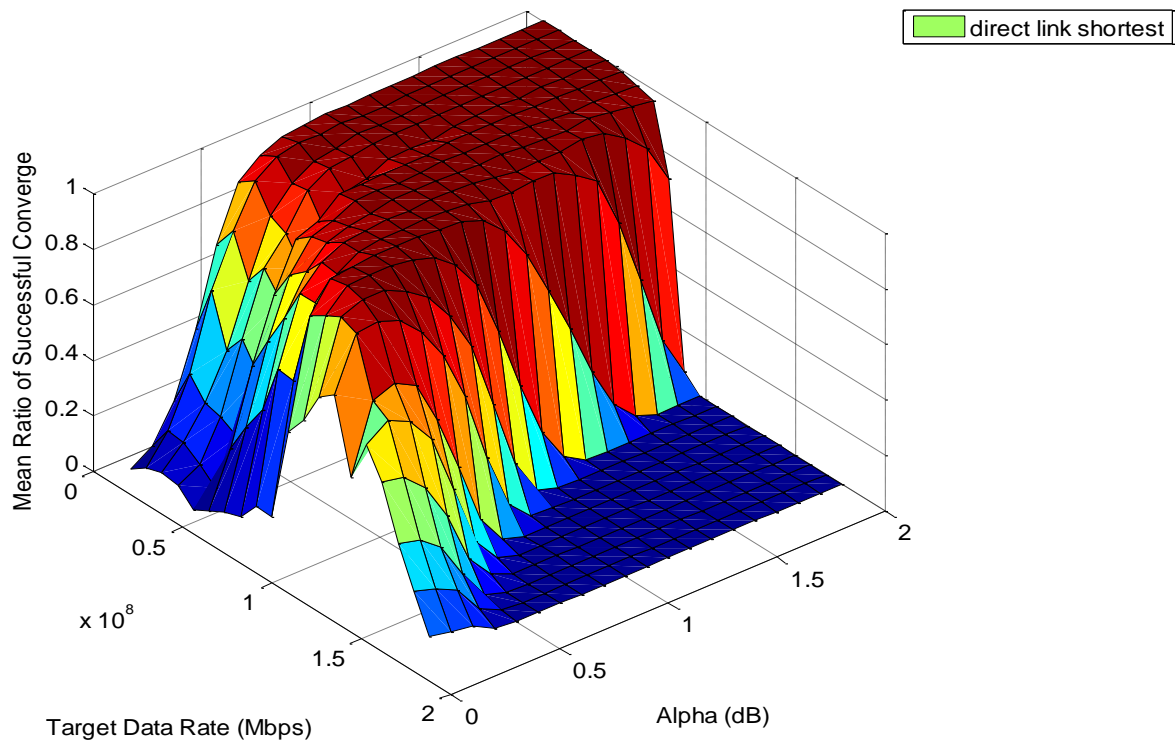


Figure 5-20 Mean degree of convergence under a frequency selective fading channel (direct link shortest)

Chapter 5 Performance of Game Approach in UWB Multichannel Power Allocation Problem

Further, Figure 2.21 and Figure 2.22 show the convergence speed in terms of gradient value α under direct link longest and direct link shortest respectively. The dark area means that the system converges faster, and the light area means that it takes more iteration to converge. Some similar behaviour can be seen from Figure 2.21 and Figure 2.22, where a bigger or smaller target data rates requires more iterations to converge, while the higher gradient value the faster it converges. However, as we already observed from Figure 2.19 and Figure 2.20, the α has to be set between 0.5 and 1 in order to guarantee an overall 90 percent convergence. Therefore we hold the previous conclusion we made from general performance under flat fading channel that the suitable α should be between 0.8 and 0.9 as it offer both best convergence and convergence speed.

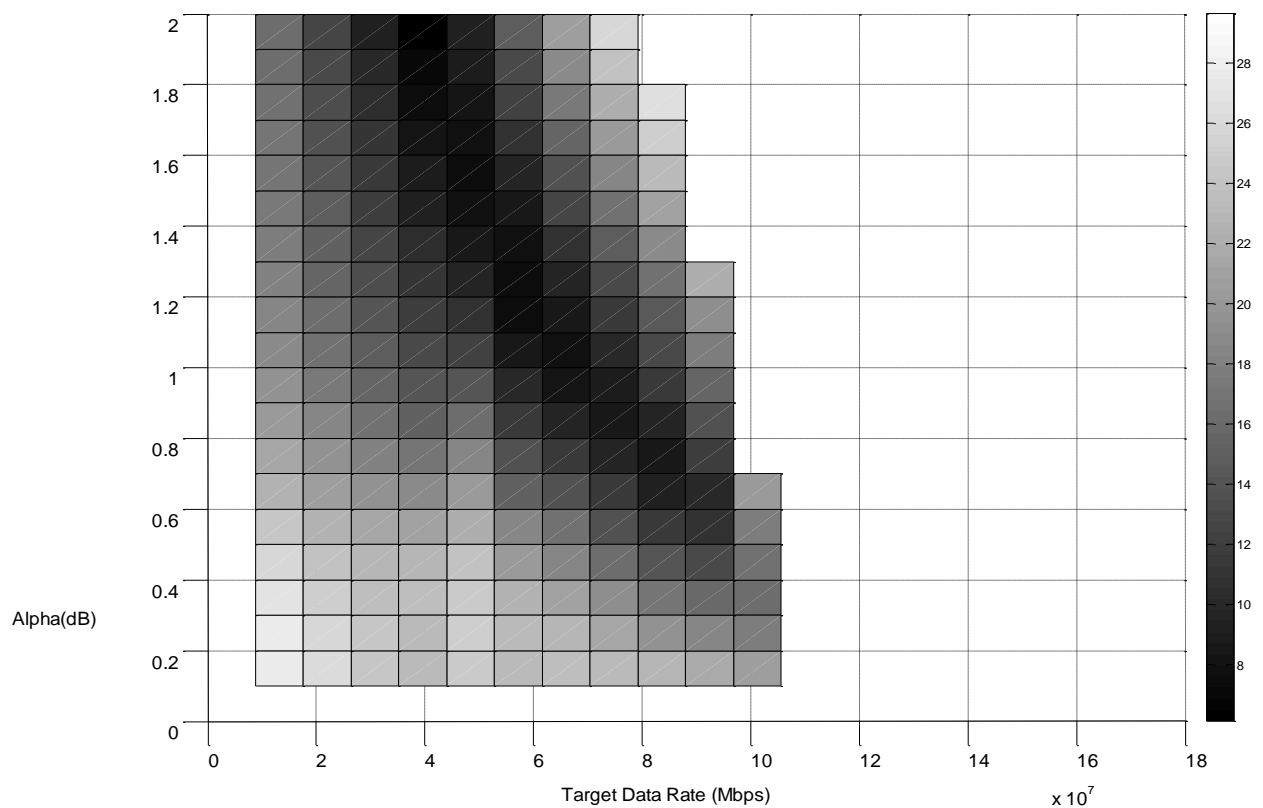


Figure 5-21 Mean convergence speed under a frequency selective fading channel (direct link longest)

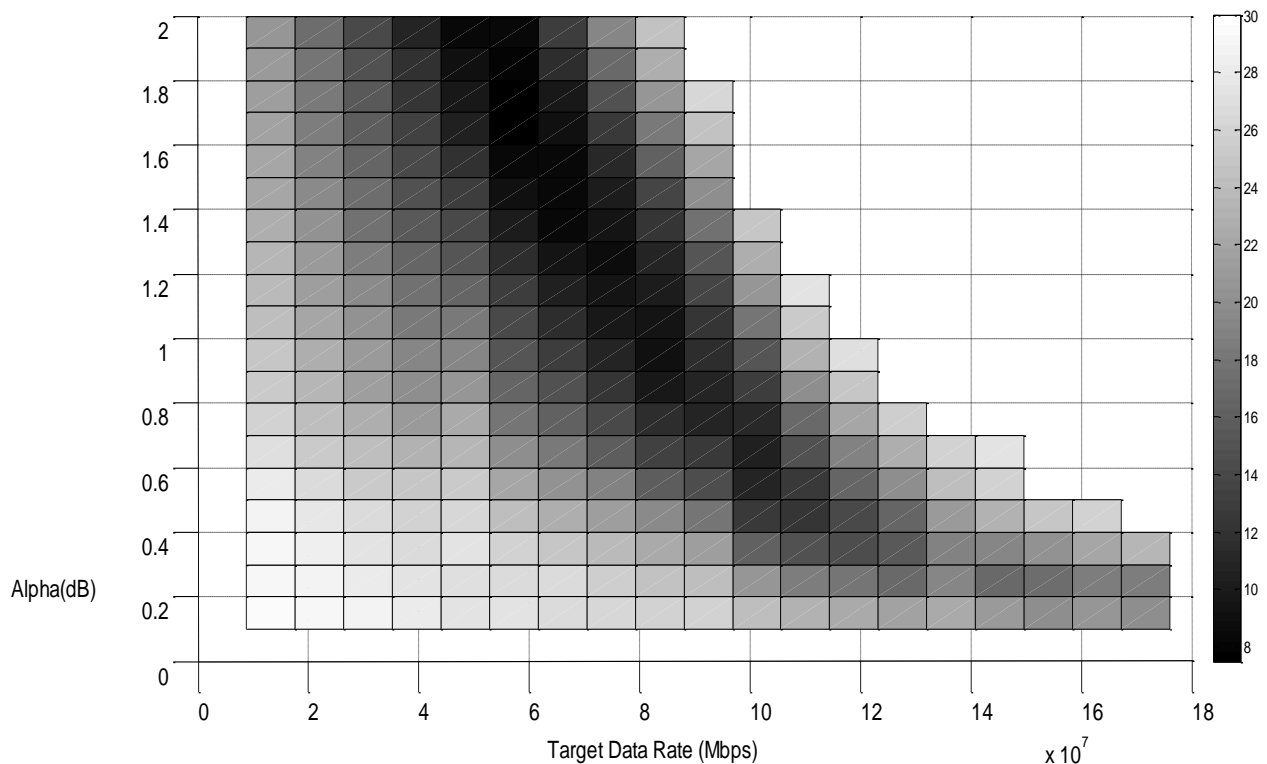


Figure 5-22 Mean convergence speed under a frequency selective fading channel (direct link shortest)

To sum up, the snap shot simulation results showed that a global utility maximum can be achieved given a proper α . The statistical simulation results illustrate that the convergence speed is affected by α , and there exists a best convergence speed for the given scenario and there exists a suitable gradient value α range for a general reliable convergence and a fast convergence.

5.6 Performance Comparison between Proposed Scheme and Iterative Water Filling Scheme

We have so far studied the snapshot performance, and general performance of our proposed DCPA scheme. However, it still remains to be seen whether our scheme achieves better performance compared with existing power allocation schemes. We found the Iterative Water Filling technique to be the most comparable scheme that can be applied to the UWB band power allocation problem. It is necessary though to give a detailed introduction to the Iterative Water Filling technique before we made the comparison.

5.6.1 Iterative Water Filling Technique

The Iterative Water Filling technique (IF) was originally designed for Asymmetric Digital Subscriber Line (ADSL) as a dynamic spectral management scheme. The work that has been done in [96] suggests that the Iterative Water Filling technique can also be a candidate for wireless UWB power allocation. Although Digital Subscriber Line (DSL) systems differ from wireless systems in many ways, it does however show significant similarity between DSL systems and short range ultra band wireless systems. First, the DSL environment is regarded as time invariant, as the copper cables that carry the high frequency DSL signals do not have significant change in status from loop to loop [96]. Second, fast fading and mobility are not considered in DSL power control problem. It is also not a problem for short range ultra wide band wireless systems. Third, the DSL loops according to [96] have severe frequency selective fading channels, while an ultra wide band wireless system that utilizes the frequency band over at least 500 MHz will have a frequency selective fading channel over the entire available bandwidth.

On the other hand, the DSL power control problem faces many difficulties, such as crosstalk interference and the near far problem [96]. The same difficulties are also presented in the short range wireless power control algorithms. Importantly, in [96] the Iterative Water Filling Algorithm is designed to be a distributed power control algorithm which do not require centralized control. It is, according to the authors, the major advantage over the old centralized schemes as it allows different service providers share the same binder [96] (binder here is referred to a bundle of digital subscriber lines which is bound together, and have electromagnetic interference between each other). All in all, it is reasonable to adapt the existing Iterative Water Filling technique to a wireless UWB power allocation problem.

The Iterative Water Filling can be expressed by the following flow chart. It should be noted that the flow chart only demonstrates a simplified two user scenario, and the Iterative Water Filling can be used in more complicated multiuser scenarios. Where P_i is the total power constraint for a specific user. T_i is the target data rate for a specific user. The whole process works in such a way that the target data rate of each user is achieved by iteratively adjusting the total power constraint and applying a Water Filling power allocation according to the new total power constraint in each of iterations.

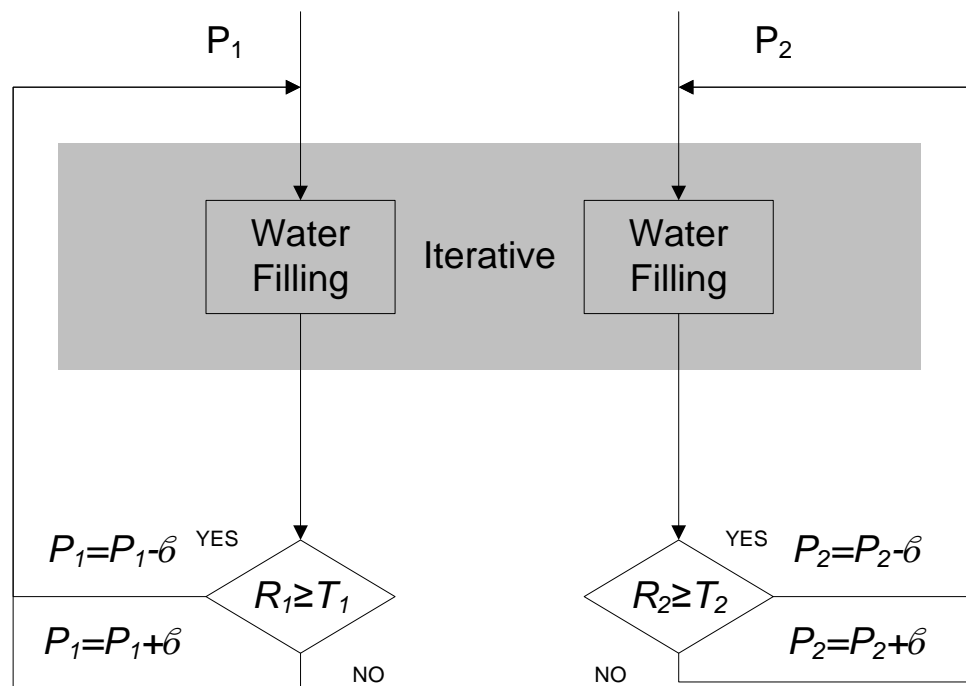


Figure 5-23 Flow chart of the iterative water filling technique

As can be seen from the flow chart, the Iterative Water Filling runs in two stages. The inner stage, shown in the shaded area, takes the total power constraint and the cross interference from homogenous systems as the input, and works out the Water Filling power allocation successively for each user, while the outer stage works out the total power constraint iteratively, according to whether the acquired data rate derived from the inner stage match the target data rate. The total power will be increased by predefined value δ if the acquired data rate is lower than the target data rate until the acquired data rate meets the target requirement, or the total power constraint will be reduced by the same amount if the acquired data rate is above the required target.

It may look similar to our proposed DCPA scheme at first glance. It is however different from our proposed DCPA scheme in three major areas. First and foremost, the Iterative Water Filling technique relies on Water Filling which is completely different from our proposed gradient power allocation scheme. Second, the outer stage that calculate the total transmit power has to begin with a very low initial power (-90dBW in our simulation) as a way to guarantee convergence, while ours begins with a fixed amount of total power that will reduced

Chapter 5 Performance of Game Approach in UWB Multichannel Power Allocation Problem

or increased according to the gap between acquired data rate and target data rate. Thirdly, the Iterative Water Filling Technique does not apply any cooperation strategy in the out stage, while our proposed DCPA scheme relied on a three staged strategy.

The advantage of the Iterative Water Filling technique is that it has better utilization of channel capacity as it uses water filling in the inner loop to acquire the data rate from the actual channel signal to noise plus interference ratio. The raw channel capacity is better utilized via this method. However, the disadvantage of this method is that it has to perform water filling in each of the iteration and it can be more complex if the power allocation requires many more iterations to converge. This is particularly significant in a UWB power allocation scenario or similar OFDM systems with many channels. One cause of this problem is considered to be the sensitivity to the actual SINR value of each channel. We will further explain it in detail in our simulation performance analysis.

5.6.2 Simulation Setup

Despite the relatively similar behaviour between a DSL environment and a short range wireless environment, there still needs some necessary changes and adaptations to be made in order to have the Iterative Water Filling Technique directly comparable to our proposed DCPA scheme.

In the previous simulation, we used the MB-OFDM PHY specification from [10], which has the data rate dependent equation expressed as equation 5.1.

This setup will constrain our performance analysis from comparing with other existing multicarrier channel assignment schemes. Especially, in the Iterative Water Filling, the data rate dependent equation is Shannon channel capacity equation. Therefore we find a Shannon truncated data rate expression a better way to calculate the acquired data rate in our simulation [84].

$$C = \begin{cases} 0, & \text{if } \text{SINR} \leq \text{SINR}_{\min} \\ \alpha \cdot Bw \cdot \log_2(1 + \text{SINR}), & \text{if } \text{SINR}_{\min} \leq \text{SINR} \leq \text{SINR}_{\max} \\ Bw \cdot C_{\max}, & \text{if } \text{SINR}_{\max} \geq \text{SINR} \end{cases} \quad 5.4$$

Only the channels with received signal to interference plus noise ratio between SINR_{\min} and SINR_{\max} will be calculated by means of the Shannon equation in 5.4. Where $\alpha \in [0,1]$ is an attenuation factor, and we set α as 1 in all our simulations. We set SINR_{\min} and SINR_{\max} as 1.8 dB and 21 dB respectively followed the parameter setup in [97]. B_w is the bandwidth of each channel which is 4.125 MHz. The channels with SINR less than 1.8 dB will be truncated. The channels with SINR more than 21 dB will not benefit from higher SINR and will only acquire a data rate that is equal to the data rate calculated at a 21 dB of SINR, which is C_{\max} that is equal to 19 Mbps.

On the other hand, some parameters need to be changed to accommodate the Iterative Water Filling in a UWB power allocation problem. First, we changed the parameter δ . In [96], the author claimed that the algorithm is found to work well with this value set to be 3dB, while in our simulation test, 3 dB will change the total transmit power too much, because the UWB device has very low transmit power at -14 dBm, while the DSL transmit power is much higher at 12.4 dBm [96]. Also we found that the Iterative Water Filling technique is very sensitive to the change of the total transmit power in UWB power allocation scenario, and hence, instead of an exponential increase or decrease in total power, we chose a linear power change in every iteration, and the value of power change is best set as -90 dBW .

The parameters can be seen from the following Table 5.3

Chapter 5 Performance of Game Approach in UWB Multichannel Power Allocation Problem

Iterative Water Filling Scheme	
Parameters	Value
$P_{initial}$ (dBW)	-90
δ (dBW)	-90
Proposed DCPA Scheme	
Parameters	Value
BW (MHz)	4.125
$P_{initial}$ (dBW)	-44
δ (dB)	1
α (dB)	0.8
μ (Mbps)	20
channels	128

Table 5-3 Parameters used in the simulations

The parameter for our proposed DCPA scheme is largely unchanged. It should be noted that the boundary μ of our proposed DCPA scheme is changed from 5 Mbps to 20 Mbps here. It is because the truncated Shannon Capacity is used in the new scheme instead of a modulation related value. Each channel can achieve a maximum throughput of C_{max} that is equal to 19Mbps. We set the boundary higher than C_{max} in order to improve convergence, so that the user can allocate power to one more channel or one less channel than that it is required for a specific target data rate, and the proposed DCPA scheme still achieves convergence. On the other hand gradient α is 0.8 dB due to the conclusion we drew from last section. Gradient α equal to 0.8 can provides both the fast convergence speed and a general reliable convergence.

5.6.3 Simulation Results

In this section, we compare the performance of our proposed DCPA scheme and the performance of Iterative Water Filling scheme in terms of their convergence speed, and power efficiency.

Similar to the general performance that we have studied in the previous section, We run our simulation for 1000 times with a random geographical setup (subject to the direct link

constraint), and each of the data point on our simulation graph is the mean value of the total realisations.

A. Convergence

First, we compare the convergence speed of our scheme against the Iterative Water Filling scheme. The number of iterations that are required for a power allocation scheme to converge is crucial, one it is because the faster a power allocation converges the less computation that is required. On the other hand, although the channel can be viewed as completely static for a wired copper loop, it is continuously varying for a wireless link. The faster the channel assignment pattern be established, the more robust the power allocation against the varying channel condition, as the power allocation scheme can simply adjust the channel assignment according to the changing channel condition in few iterations. However in our current simulation, we will assume the UWB channel remains static in a short range in door environment.

In Figure 5.22, we show the mean number of iterations versus target data rate. It should be noted that we set 1000 iterations as the maximum number of convergence; beyond this the Iterative Water Filling would be considered as unable to converge. We also set 30 as the maximum number of iterations for our proposed DCPA scheme. The maximum mutual target data rate is used to identify an available target data rate that can be acquired in both direct link shortest and direct link longest scenario, and any target data rate over this threshold would not converge in both extreme scenarios simultaneously. It is clear that our game based power allocation strategy converges much faster in both direct link longest scenario and direct link shortest scenario. Compared with iterative water filling, our scheme converges within 17 iterations in the direct link longest scenario, and 15 iterations in the direct link shortest scenario. Our proposed DCPA scheme converges faster in the direct link shortest than that in the direct link longest scenario because of the relative low interference level at receiver meaning that the target data rate can be easily achieved. A similar tendency can be seen from the Iterative Water Filling technique. It is also clear that our proposed scheme can achieve a much higher target data rate than the IW.

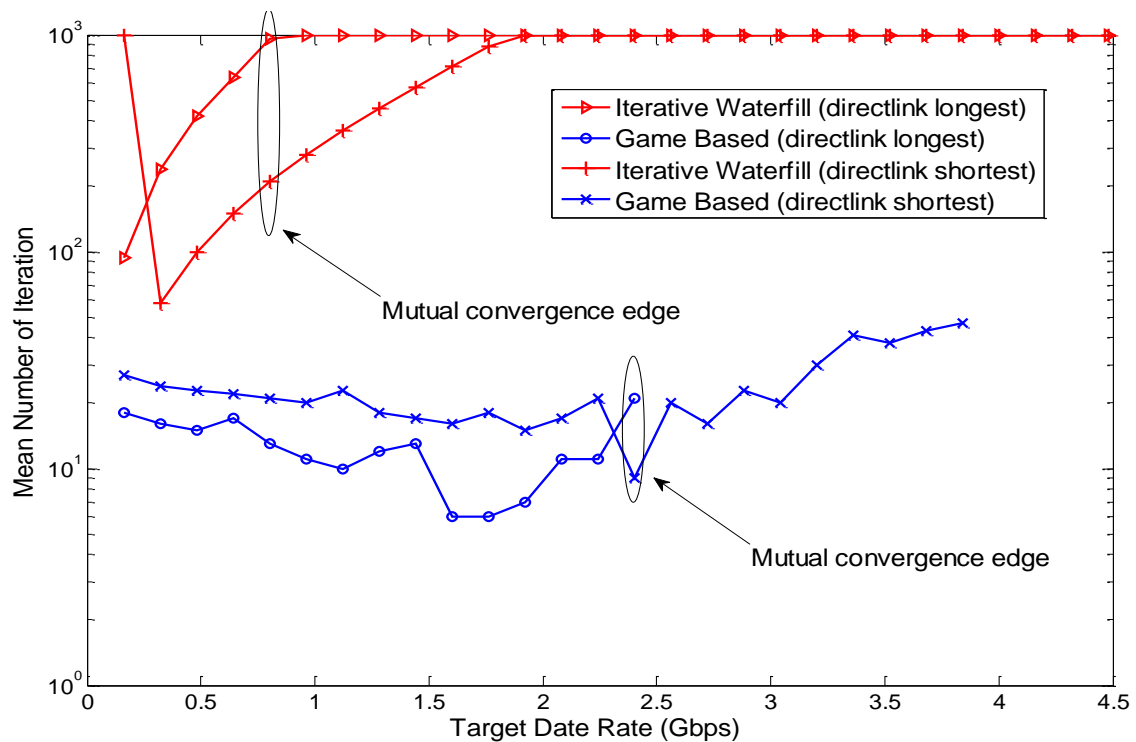


Figure 5-24 Mean number of iterations versus target data rate under a frequency selective fading channel

B. Signal to Interference Ratio

The previous simulation graph shows that our scheme converges faster, and achieves a higher target data rate in general. Now, we will explore the cause of this result.

On one hand, the Iterative Water Filling has to initiate the process from a zero power allocation, and adjust the total transmit power with a very small amount of power in each iteration, which restricts it from converging fast in a multiband wireless system that utilizes a large amount of channels. On the other hand, the Iterative Water Filling relies on the actual signal to interference plus noise ratio (SINR) to calculate the amount of power that allocated to the channel. The amount of changing interference or alternatively SINR value greatly influences the convergence. Our gradient power allocation does not rely on an exact SINR value to allocate the power, because it allocates the power to the channels according to the ranked SINR value and the gradient value α .

Chapter 5 Performance of Game Approach in UWB Multichannel Power Allocation Problem

The following graphs show the mean signal to interference ratio of different users in direct link longest scenario and direct link shortest scenario respectively. The mean SINR is a average SINR acquired from 1000 realisations.

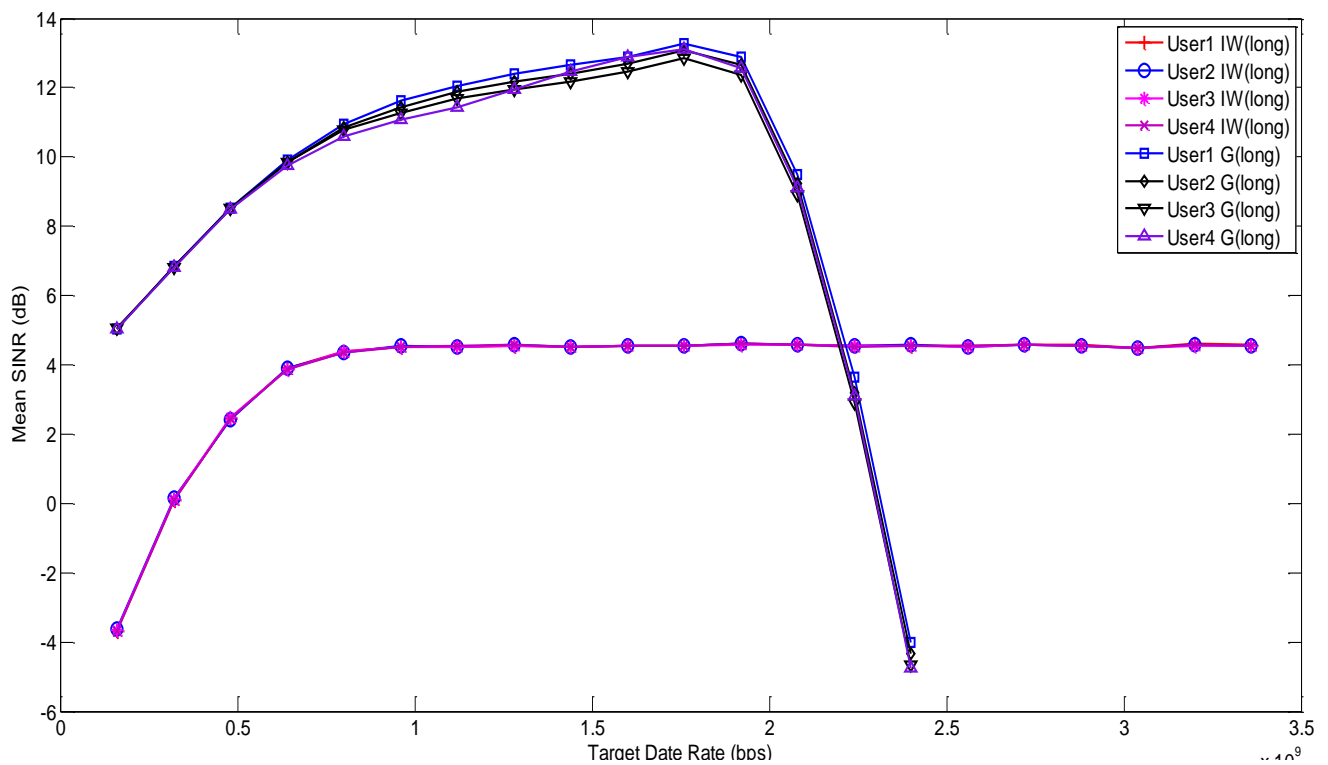


Figure 5-25 Mean SINR of 4 users under a frequency selective fading channel (direct link longest)

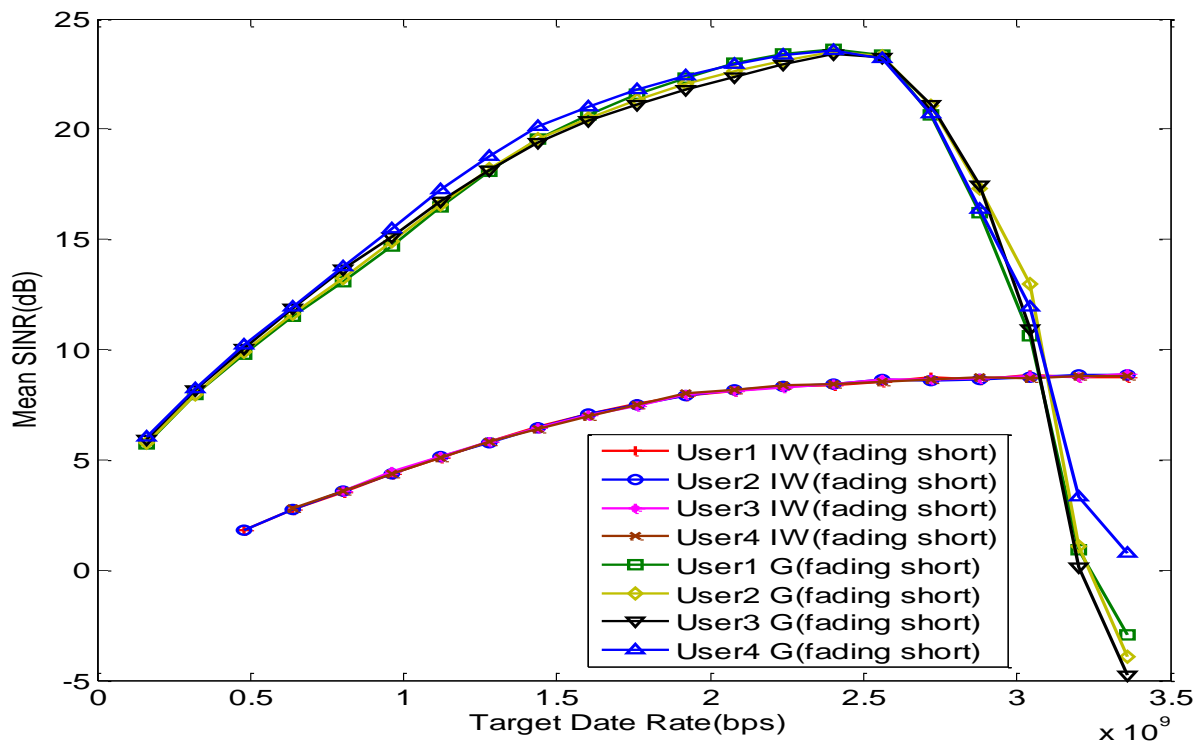


Figure 5-26 Mean SINR of 4 users under a frequency selective fading channel (direct link shortest).

Figure 5.23 shows the mean SINR value of 4 different users at different target data rate in direct link longest scenario. The IW is short for the Iterative Water Filling technique and the G represents our proposed game based DCPA scheme. First, we should note that the mean SINR value drops dramatically after the 2 Gbps target data rate point for our proposed DCPA scheme. We know that it is because the proposed scheme cannot achieve the target data rate higher than 2 Gbps point, and this behaviour can be viewed in Figure 5.22. The Iterative Water Filling approach, on the other hand, does not change its mean SINR value after 1 Gbps point, which is due to the fact we observed from graph 5.22 that IW ceases converging from 1Gbps target data rate point onwards. Therefore, the only relevant comparison part is before the 1 Gbps target data rate point.

It is clear that our scheme can achieve a higher mean SINR value. It is because our gradient power allocation scheme tends to partition the channel, while the Iterative Water Filling tends to utilize as many channels as possible if the channel has an interference plus noise ratio that is a constant defined by the total power constraint. Under very low transmit power and large number of channels conditions, some channels may be allocated a very small amount of power

and yield a low SINR value at the receiver end, and therefore it yields an overall lower signal to interference plus noise ratio.

Similar behaviour can be viewed in Figure 5.24 in a direct link shortest scenario. However, the overall mean SINR value is seen as an increase over the direct link longest scenario, which is due to the lower cross link interference and the higher direct link path gain. Consequently, a higher target data rate can be achieved with an overall higher SINR.

C. Power Efficiency

Power efficiency is a very popular topic in the wireless power allocation research [13,17,21]. A higher transmit power efficiency means lower power emission from wireless device, or a longer battery life for a mobile wireless device. We wish our power allocation scheme achieve the target rate with a high transmit power efficiency.

We investigate the power efficiency of both power allocation schemes in Figure 5.24. It shows that our proposed DCPA scheme outperforms the Iterative Water Filling technique in direct link longest scenario. It is only when the target data rate is over 700Mbps that our proposed DCPA scheme would have lower power efficiency than Iterative Water Filling in the direct link shortest scenario. On the other hand, the maximum mutual target data rate indicates the achievable data rate that can be acquired from two extreme scenarios. Given the mutual maximum target data rate that is located at 800Mbps for Iterative Water Filling technique, our proposed DCPA scheme that achieves a target data rate of 2400Mbps will offer a better performance overall.

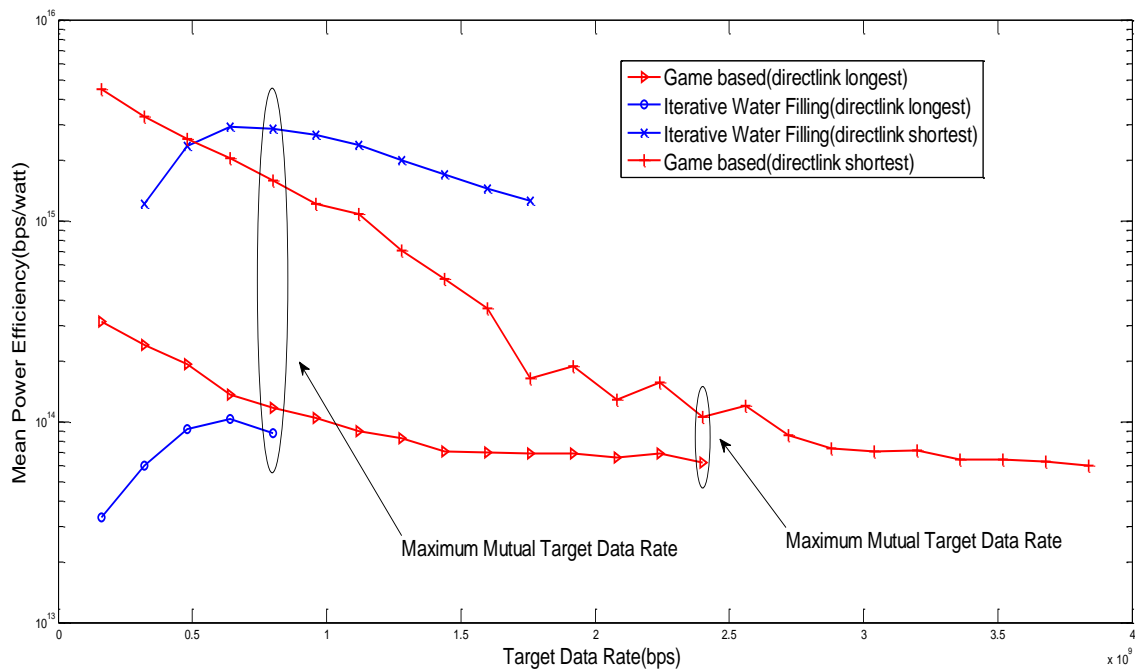


Figure 5-27 Mean power efficiency over the target data rate under a frequency selective fading channel

We should also agree that the inconsistency of the performance due to the two extreme link length scenarios is less significant for our game based power allocation scheme than that of the Iterative Water Filling.

5.7 Chapter Conclusion

The conclusion we draw in this chapter is that our proposed DCPA scheme works in both flat fading and frequency selective fading channels. The fact that the target data rate can be achieved in a very few iterations indicates a general fast convergence of our proposed DCPA scheme. Further, our proposed DCPA scheme performs better in terms of both convergence speed and power efficiency when compared with a modified Iterative Water Filling technique.

Chapter 6 Performance of Game Approach in Extended Range Scenario

Contents

6.1	Design of the Power Allocation Scheme for Longer Ranges.....	141
6.1.1	Link Budget Analysis and Power Threshold Design.....	141
6.1.2	Power Impact Factor	146
6.1.3	Estimation of Maximum Mutual Target Data Rate	147
6.2	Power Allocation Design and Simulation Setup.....	148
6.3	Snapshot Performance Analysis.....	154
6.3.1	Snapshot Analysis under Frequency Selective Fading Channel in Four User Coexistence Scenario	159
6.3.2	Snapshot Analysis in a Six User Coexistence Scenario.....	165
6.4	General Performance of Four Users Coexistence Scenario	170
6.5	General Performance of an Increased Number of Users Scenario.....	175
6.6	Chapter Conclusion	180

It has been shown in previous chapters that a Distributed Cognitive Power Allocation (DCPA) scheme can potentially reduce the interference from homogeneous devices located in close vicinity while maintaining a target data rate. However, it is not possible to achieve the same performance in a longer range scenario without increasing the transmit power due to the increased path loss associated with the range extension. Increasing transmit power beyond the FCC spectrum mask will inevitably cause excessive interference toward the existing wireless services. It is necessary that a DCPA scheme for longer ranges can guarantee a specific margin over the link budget while keeping the power emissions as low as possible.

In this chapter, we will introduce a modified power allocation scheme from our game based DCPA scheme where the highest transmit power threshold is determined by a link budget estimation algorithm. The performance is evaluated in terms of both degree of convergence and convergence speed. In addition, a new Power Impact Factor (PIF) is proposed to assess

the degree of excessive power emission caused by transmitting power over the FCC spectrum mask. The structure of the chapter is organized as follows. First, the design of the new power allocation scheme is introduced in section 6.1. This is followed by the simulation setup in section 6.2. Section 6.3 examines the performance of the new power allocation scheme in a single trial, while sections 6.4 and 6.5 provide some insight into the general performance of our proposed power allocation scheme by examining the statistical results. Finally, conclusions are drawn in section 6.5.

6.1 Design of the Power Allocation Scheme for Longer Ranges

In order to develop a feasible DCPA scheme for a longer range scenario, it is necessary to investigate a sensible transmit power decision mechanism that can guarantee a suitable link margin on an extended radio link, while ensuring relatively low interference towards the existing radio systems. Firstly, we begin our work by analysing the link budget of a UWB system, and then the design of power emission threshold will be given according to the link budget estimation. Lastly, we will consider the impact of such a power increase towards the existing radio services.

6.1.1 Link Budget Analysis and Power Threshold Design

According to the analysis we made in chapter 2, we have foreseen that the current FCC spectrum mask, an upper bound on the transmit power density, is not able to support a link length over 25 metres in outdoor environment. The specific link budget analysis can be seen as follows.

A link budget for a radio communication system can be expressed as

$$\text{Received Power} = \text{Transmitted Power} + \text{Gains (dB)} - \text{Losses (dB)} \quad 6.1$$

On the other hand, the link margin measures how much extra attenuation a particular radio link can tolerate subject to a minimal required signal to noise ratio (SNR). The receiver sensitivity can be expressed as equation, which assume 0 dB link margin.

$$\text{Receiver Sensitivity} = \text{SNR}_{\text{required}} + \text{Noise Power} \quad 6.2$$

Therefore the required transmit power can be expressed in terms of receiver sensitivity and path loss.

$$\text{Required Transmit Power} = \text{Receiver Sensitivity} + \text{Path Loss} \quad 6.3$$

In order to estimate the minimum required transmit power we consider the Truncated Shannon Capacity introduced in chapter 3. We assume that the channels with SINR less than 1.8 dB will be truncated. We make $\text{SNR}_{\text{required}}$ equal to 1.8 dB and the *Noise Power* equal to Gaussian white noise power density times bandwidth of a channel. Therefore the minimum required transmit power can be estimated according to equation 6.3 if path loss known.

As can be seen from the Figure 6.1, the required transmit power has to surpass the FCC spectrum mask at -65 dBW in order to transmit over 25 metres in an outdoor environment.

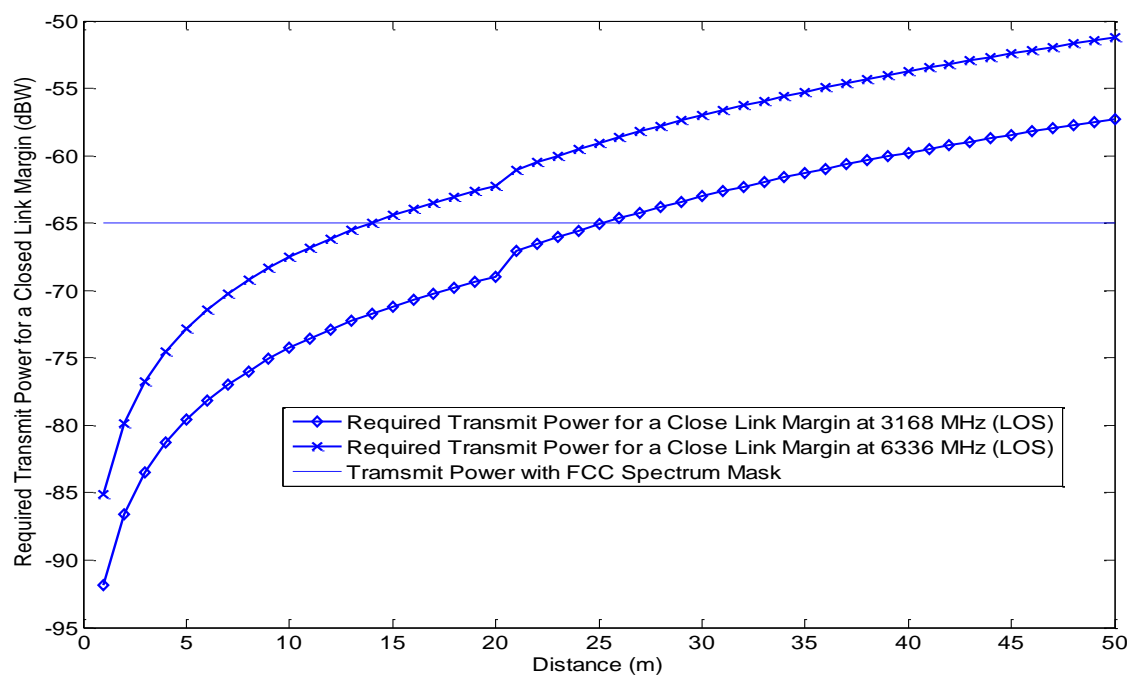


Figure 6-1 Required transmit power for a closed link margin in the outdoor environment

The minimum required transmit power can be calculated from equation 6.3. Although the minimum required transmit power is known, we have yet to find a maximum transmit power threshold in order to guarantee a specific target performance.

In order to find a proper maximum transmit power, we apply a gradient power profile to channels so that the maximum transmit can be determined according to total transmit power, estimated path loss, and an estimated required bandwidth. Such a power profile can be illustrated as Figure 6.2

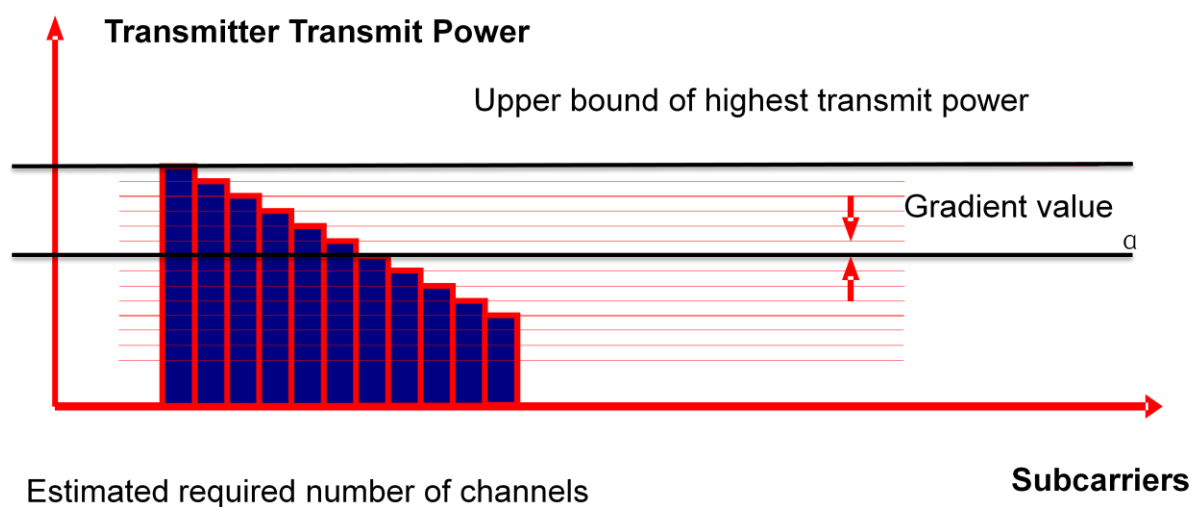


Figure 6-2 Illustration of a gradient power profile that used to determine the highest transmit power

The *upper bound of transmit power* can be expressed as equation 6.4

$$P_{max} = P_{floor} \alpha^{ERC} \quad 6.4$$

Where P_{floor} is the *estimated power floor*, and ERC is the estimated required number of channels. The *estimated power floor* is the minimum required transmit power calculated from Equation 6.5.

$$P_{floor} = SNR_{required} + Noise\ Power + Path\ Loss \quad 6.5$$

For a multicarrier system with LOS, an average path loss can be roughly estimated as the mean value of the difference between the transmit power from transmitter and received power at receiver [98].

$$Path\ Loss = mean(Received\ Power - Transmitted\ Power) \quad 6.6$$

The estimated required number of channels is the minimum number of channels that are required to exceed the power floor P_{floor} so that a target data rate can be guaranteed. It is associated with target data rate and the channel capacity of a single channel of multicarrier system. It can be calculated by equation 6.7

$$ERC = \frac{Target}{C_{max}} + C_{adjust} \quad 6.7$$

Where *Target* is the target data rate of the wireless system, and C_{max} is the maximum throughput of a single channel from truncated Shannon Capacity introduced in chapter 3. We assume that the channels with Signal to Interference plus Noise Ratio (SINR) of more than 21 dB will not benefit from the higher SINR and will only acquire a throughput that is equal to the throughput calculated at a 21 dB of SINR. Lastly, the C_{adjust} is an *adjustment factor* that is used to adjust the value of *ERC*. It is effectively an additional number of channels that can be added to *ERC* to assist in convergence.

By changing the C_{adjust} , the *ERC* will change accordingly. Therefore the peak transmit power P_{max} can be adjusted by setting C_{adjust} . A detailed analysis will be given later, since the peak transmit power is also a function of the *total transmit power*.

The *total transmit power* can be expressed in terms of *estimated power floor*, *gradient value α* and *estimated required number of channels*.

$$P_{total} = \sum_{n=1}^N P_{max} \alpha^{-(n-1)} \quad 6.8$$

or

$$P_{total} = \sum_{n=1}^N P_{floor} \alpha^{m-n+1} \quad 6.9$$

Where N is the number of all channels. α is an unknown gradient value, which can be determined by means of a lookup table.

We can think of the gradient power profile as a triangle, then the relationship between *total transmit power*, *estimated power floor*, *adjustment factor* and *upper bound of transmit power* can be illustrated as the following Figure 6.3. The shape A and shape B are identical triangles so that they have the same size of area, and the total transmit power can be represented by the area of the triangle. The horizontal axis represents the number of channels of the gradient power profile. The vertical axis represents the transmit power on each channel. The gradient of the triangle A represents the gradient factor α . Therefore, the peak power can be represented by the vertical edge of the triangle A, and it is measured as $d1$. The *estimated power floor* can be represented by d . The *estimated required number of channels* can be represented by length of the intersection part between *estimated power floor* and triangle A, and it is measured as $d3$. Keeping d and the size of area fixed, $d1$ will be reduced by $d4$ if $d3$ is increased by $d2$, and the new shape is triangle B. Here $d2$ can be thought of as adjustment factor, which changes the peak transmit power $d1$. Therefore we can draw the conclusion that the peak transmit power can be adjusted by changing the adjustment factor C_{adjust} given a fixed total transmit power P_{total} .

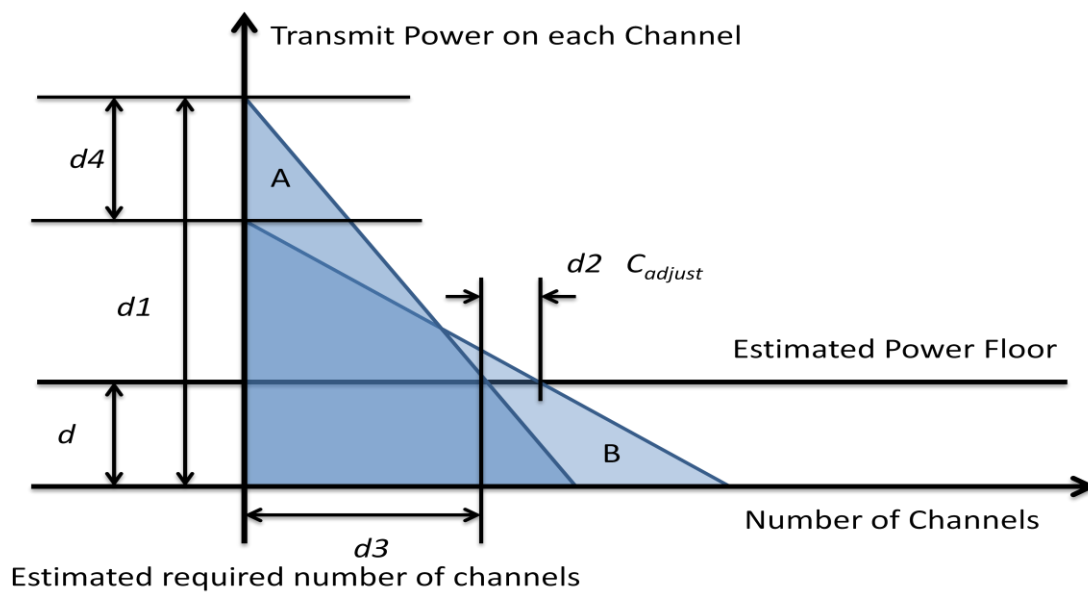


Figure 6-3 Illustration of a relationship between the total transmit power, estimated power floor, adjustment factor and the upper bound of transmit power.

The reasons why we use a gradient power profile to determine the maximum power threshold can be summarized into the following two points

1. The estimated power floor may be smaller than that is required due to the fading channel, and hence, it is necessary to have a margin over the estimated power floor.
2. It is also reasonable to use a gradient power profile, because the channels with higher channel path gain can be emphasised while the channel with lower path gain can still be explored and used if the collective interference is lower on those channels.
3. The peak transmit power can be changed flexibly by changing only *adjustment factor*.

6.1.2 Power Impact Factor

The original idea of UWB is that the UWB radio system will only transmit power at a very low power density so that the existing radio services will not be affected by the activities of the UWB systems. However, it is difficult to guarantee this when the UWB systems are deployed in a higher densities so that the collective interference will eventually become harmful to the existing systems in the close vicinity (relevant research can be found in [54] where the interference caused by UWB devices towards aviation system has been studied), let alone the long range UWB systems that are required to apply a higher power density to overcome the increased path loss at longer ranges. A local regulatory database that is constantly updated according to the local government policies can be used to regulate the frequency access policy of a cognitive ultra wide band device, thereby prevent it from accessing some crucial frequency bands. It is however necessary to invent a new measurement that is able to assess the excessive transmit power emission in order to prevent cognitive devices from creating too much interference to the available frequency bands.

For simplicity, the Power Impact Factor (PIF) is designed to be a single value that is able to assess the excessive power emission of a multicarrier radio system. However it is difficult to use a single value to assess the degree of harm caused by the power allocation activities of a cognitive multicarrier system. The debate here is whether transmitting at a relative higher power density on relative fewer channels is regarded as more harmful than transmitting a relative lower power density on more channels.

We express the PIF in the following form.

$$PIF = \sum_{l=1}^L \frac{P_l - P_{th}}{Bw_l} \quad 6.10$$

Where P_{th} is a maximum regulatory transmit power threshold on the licensed band from local regulatory bodies. It should be noted that some regulatory threshold is received interference threshold instead of transmit power threshold such as TV white band interference threshold [21]. P_l is the power allocation on channels that exceeds the maximum power threshold, and Bw_l is the bandwidth of the channels that have been allocated a power P_l .

The PIF can loosely represent the excessive power emission per Hz from a cognitive multicarrier radio system with a unit of W/Hz , if the Bw_l are equal. Therefore it measures an overall excessive power emission within the bandwidth of the multicarrier radio system. It should be noted that the PIF is not designed to assess the impact on individual channel.

Not only does the PIF function as an indication of the severity of the excessive power emission of cognitive devices, but it can also be used to guide the cognitive radio system with high PIF (the PIF can be measured locally by cognitive device itself) to choose a different frequency pool that it might has less interference, and hence reducing PIF of the cognitive radio device.

6.1.3 Estimation of Maximum Mutual Target Data Rate

Importantly, it should be noted that an upper bound of a mutual target data rate can be approximately estimated given the number of channels, the C_{max} and the number of users.

$$T_{max} = \frac{N \cdot C_{max}}{L} + \mu \quad 6.11$$

Where T_{max} is the maximum mutual target data rate, N is the total number of available channels, C_{max} is the maximum throughput that a single channel can acquire, L is the total

number of users, and μ is the boundary we applied to determine the state transition of the game strategy, which is 20Mbps. The reason that it is introduced in equation 6.11 is because user can acquire a higher data rate than target data rate by a maximum of μ . It should be noted that the maximum mutual target data rate estimation is only valid when all the users share the same target data rate and the channel is fully partitioned (the channel reuse will increase T_{max}).

6.2 Power Allocation Design and Simulation Setup

We have introduced the concepts of *Power Threshold Design* and Power Impact Factor. The new power allocation design is largely based on our previous game based power allocation scheme except that the initial procedure of the gradient power allocation is substituted by channel path gain estimation and power threshold setup. The three staged game strategy is unchanged.

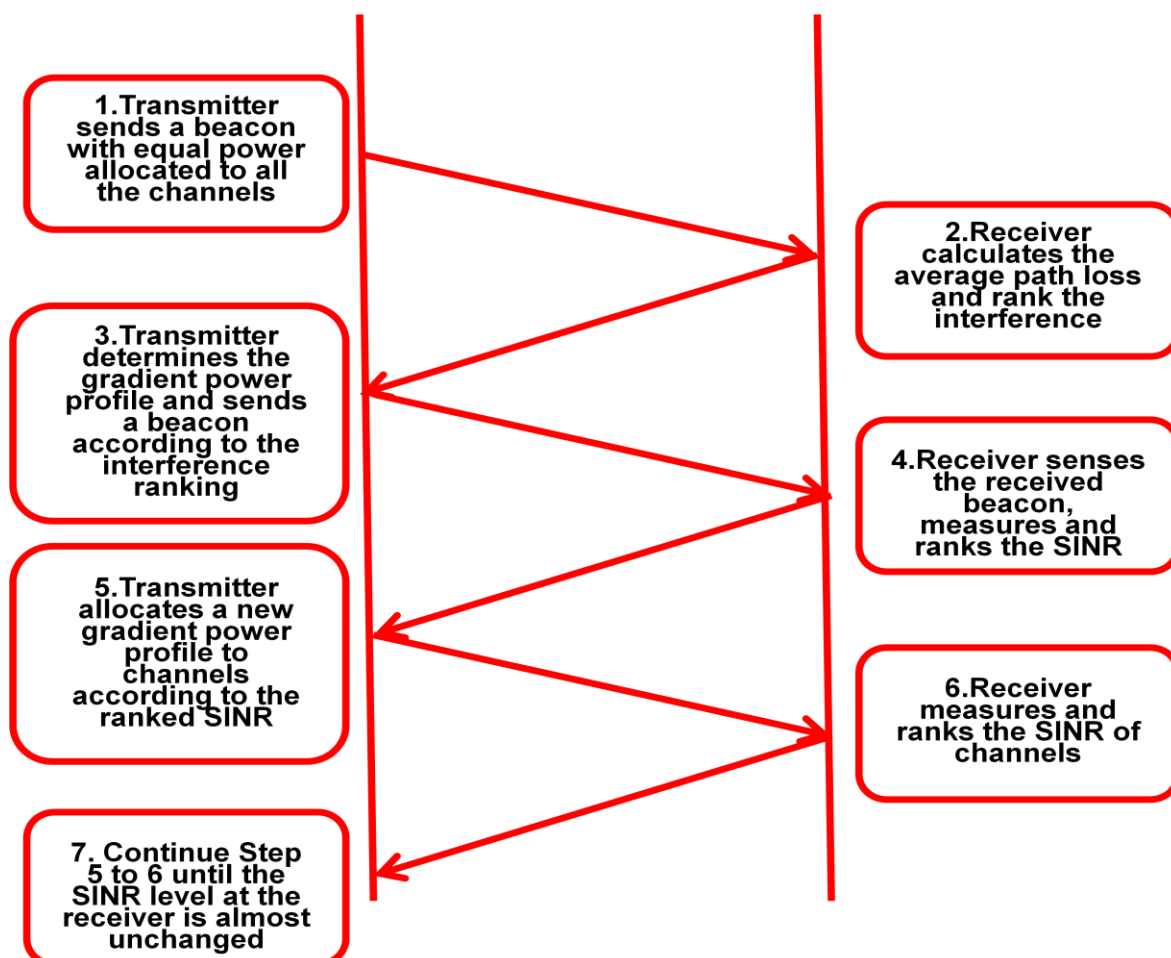


Figure 6-4 Flow chart of the new gradient power allocation process

Compared to the original gradient power allocation flow chart in chapter 4, the new gradient power allocation has to estimate an average channel path gain in step 1 and 2. In step 3, the transmitter has to calculate a gradient power profile according to the channel path gain and the estimated required bandwidth as we introduced in section 6.1.1. It is noted that the gradient value at the beaconing process at step 3 is different than the gradient value at step 5. The reason for this setup is because the different gradient values are used for different purpose. The gradient value calculated at step 3 is used to adjust the maximum power threshold while the fixed gradient value at step 5 is used to partition the channel among homogenous systems. The gradient value at step 3 is dynamically calculated according to the equation 6.7 from the measurement of average path gain and a lookup table, while the gradient value from step 5 onward is a fixed value that we used as the most efficient gradient value we found from last chapter.

The performance of our modified power allocation will be examined with the extended link length. For the channel path loss model, we use the 802.15.4a UWB outdoor channel model and Walfish-Ikegami model. The explanations can be found in chapter 2. As we discussed in chapter 2, for the channel path gain for a link length longer than 18 metre will be substituted by COST 231 Walfish-Ikegami model. The corresponding parameters can be found in the following tables 6.1 and 6.2.

	Outdoor	
	LOS	NLOS
n	1.76	2.5
PL_0 (dB)	45.6	73.0
K	0.12	0.13

Table 6-1 Parameters of the outdoor path loss model from 802.15.4a

LOS (Walfish-Ikegami)	
Parameters	Value
Mobile Height (m)	1 - 3
Distance (km)	0.02 - 5
Base Station Height (m)	4 - 50

Table 6-2 Walfish-Ikegami path loss model for the outdoor LOS

The path loss model for 802.15.4a is expressed as

$$PL(d, f) = \frac{1}{2} PL_0 \eta_{TX-ant}(f) \eta_{RX-ant}(f) \frac{(f / f_c)^{-2(\kappa+1)}}{(d / d_0)^n} \quad 6.12$$

The Walfish-Ikegami Pathloss Model is expressed as

$$L(d) = 42.6 + 26 \text{Log}_{10}(d) + 20 \text{Log}_{10} \text{Log}_{10}(f_c) \quad 6.13$$

Similar to chapter 5, the performance under a frequency selective fading channel will be examined. The received signal through a fading channel can be expressed as the following equation.

$$r(f, t) = p(f, t) PL(f, d, t) r_0(f, t) \quad 6.14$$

Further, we can simplify equation 6.13 by assuming the radio environment is static during the simulation period. The relevant analysis can be found in chapter 2.

$$r(f, t) = p(f, t) PL(f, d) H(f) \quad 6.15$$

It should be noted that the environment at an extended range scenario may less likely remain static and more likely to change from time to time as the movement of the moving object between transmitter and receiver. The DCPA in a none static environment will be our future research subject, it is however not covered in our current work.

It should also be noted that, we use the same impulse response generator in both short range scenario and long range scenario, so that the average fading depth will be equal in both

scenarios. The reason why we use this setup is due to the fact that the small scale fading is superimposed on to the large scale fading, and the path loss will be the dominant factor at longer range [48]. Using the same average fading depth will not greatly influence the performance estimation.

The performance of the proposed DCPA scheme in an increased user number scenario will be examined. It is reasonable that a short range system operate within 10 metres will have fewer homogenous devices deployed in close vicinity. However, it is likely that systems with increased range have more competitive homogenous devices located within their transmission range.

We generate random locations of the radio systems in a $100 \times 100 \times 100$ square metres volume according to a uniform distribution, which is similar to the geographical setup we introduced in chapter 4. The reason for the height being 100 metres is that the extended range simulation is scaled up from our previous short range geographical model.

Lastly, as we specified in the previous chapter, our simulation takes the relative distance between transmitters and receivers into consideration and generates the geographical locations of the UWB transmission pairs subject to a direct link longest and direct link shortest layouts in order to better understand the impact of different interference levels on the performance. However, when moving to the longer range, the relative geographical location of users will have less effect on the power allocation scheme as the major concern is to overcome the increased path loss at the longer ranges. On the other hand, the extreme geographical layouts we introduced in chapter 5 will be less likely to happen as more homogeneous systems will be involved as the transmission range is extended.

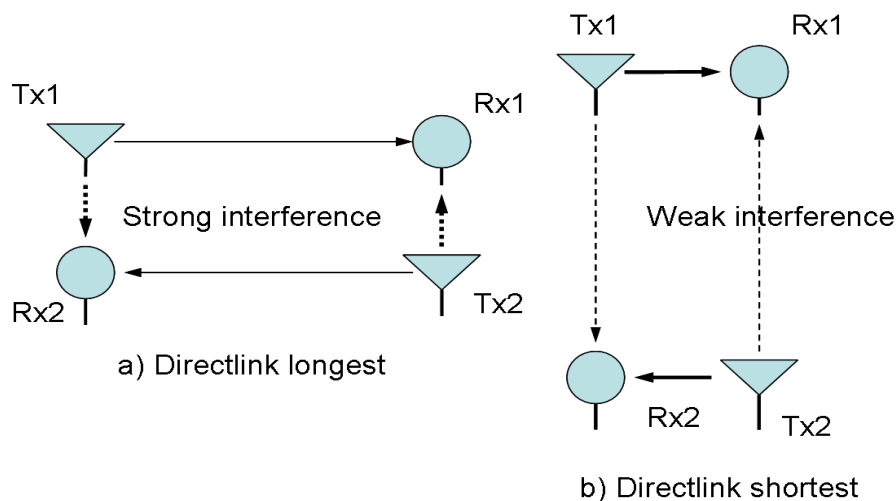


Figure 6-5 Geographical layouts of competing systems

Nevertheless, our simulation will still cover these two extreme geographical location setups, but they are only examined in a 4 user coexistence scenario.

Parameters wise, there are some necessary changes that have been made in order to ensure the power allocation scheme works properly.

Some of the other important parameters that are used in our simulations can be found in the following Table 6.3.

Parameters	Value
C1	352×10^6
C2	10^8
C3	e
$BW(\text{MHz})$	4.125
$P_{\max} \text{ (dBW)}$	- 30
$\delta \text{ (dB)}$	1
$\alpha \text{ (dB)}$	0.8
$\mu \text{ (Mbps)}$	20
channels	128
Target Data Rate (Mbps)	600

Table 6-3 Parameters used in the simulations

First of all, the change has been made to the total transmit power at first iteration. The total transmit power is now -30 dBW, 14 dB higher than the total transmit power we used in last chapter, due to the combination of the increased path loss at longer range and outdoor path loss model. In the following Figure 6.6, we present a comparison between the channel path gain at 64 metres of a UWB outdoor channel model and the channel path gain at 27 metres of a UWB indoor office channel model. It is noted that average fading depth for both short range indoor channel model and longer range outdoor channel model are equal due to using the same channel impulse response generator as we explained earlier. As can be seen from the figures, the channel path gain at 64 metres of a UWB outdoor channel model has an average channel path gain of -80dB while the channel path gain at 27 metres of a UWB indoor office model has an average channel path gain of -65 dB.

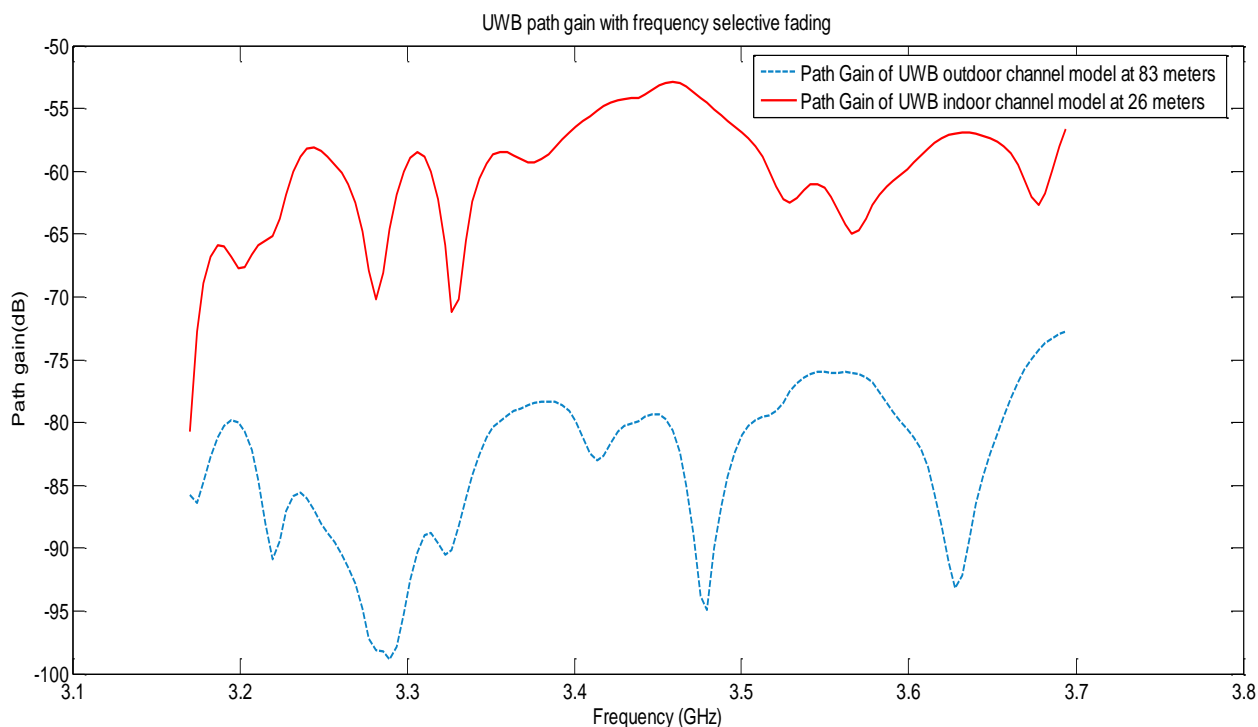


Figure 6-6 Example of channel path gains

The fixed gradient value α as we explained before is used to partition the channel, and it is set as the most efficient gradient value we found from the last chapter.

μ is the boundary we applied to determine the state transition of the game strategy, which can also be interpreted as max permitted target data rate variation. δ is the total power adjustment

factor between state transitions in our game strategy. The relevant introduction can be found in chapter 5. It is noted that the μ is changed from 5 Mbps to 20 Mbps here. It is because the truncated Shannon Capacity is used in the new scheme instead of a modulation related value. Each channel can achieve a maximum throughput of C_{\max} that is equal to 19Mbps. We set the boundary higher than C_{\max} in order to improve the degree of convergence, so that the user can allocate power to one more channel or one less channel than that it is required for a specific target data rate, and the proposed DCPA scheme can still achieve convergence.

6.3 Snapshot Performance Analysis

We begin by analysing the snapshot performance in which we show the performance of a four user coexistence scenario and a six user coexistence scenario with arbitrarily generated geographical locations subject to the previously given distance constraints.

6.3.1 Snapshot Analysis under Flat Fading Channel in four user coexistence scenario

Firstly, we examine the performance of our proposed DCPA scheme under a flat fading channel in a four user coexistence scenario, in which the direct link longest and direct link shortest geographical layouts are used.

Figure 6.7 shows similar behaviour we observed before in chapter 5. The users under the direct link longest setup all acquire their initial data rate at around 430 Mbps which is 170Mbps lower than their target data rate, while under direct link shortest setup, the user can acquired an initial data rate that is either much higher than or more close to the target data rate. For example user 2 and 3 acquired their initial data rate around 575Mbps which is only 25Mbps lower than target data rate, while user 4 acquired his initial data rate close 700 Mbps which is 100Mbps higher than target data rate. It suggests that the user under direct link longest setup has to gradually increase his total transmit power in order to meet the target data rate while, the user may have to decrease his transmit power in order to meet the target data rate under direct link shortest setup.

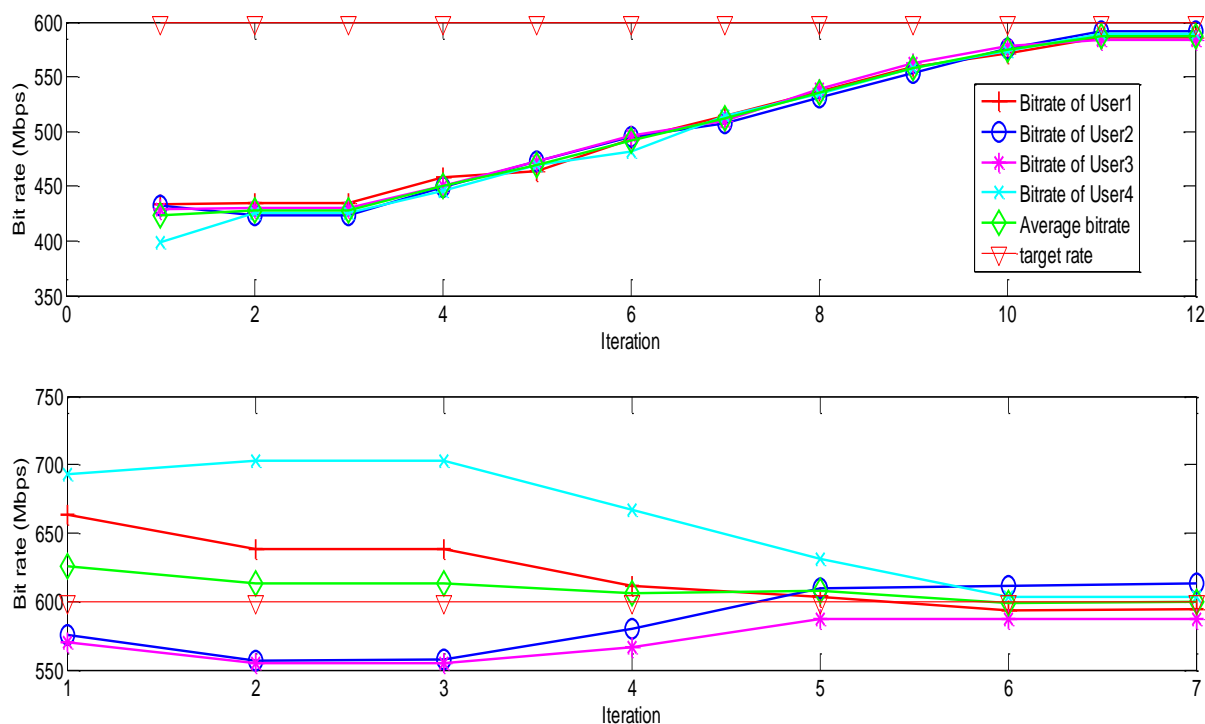


Figure 6-7 Acquired data rate analysis in direct link longest (upper) and direct link shortest (lower) scenarios

In order to further understand the behaviour of the new power allocation scheme, we should analyse the specific power allocation for each of users in the first iteration and final iteration.

Firstly, we analyse the power allocation pattern in direct link longest scenario. Figure 6.8 and 6.9 show the power allocation pattern of four users at first iteration and final iteration respectively. Apart from the similar behaviour that we described in chapter 5, the transmit power on each channel sees an increase. The peak transmit power in the first iteration is -47 dBW, and it is increased to -45 dBW at the final iteration, while the peak transmit power of users in chapter 5 is restricted by FCC spectrum mask, which is -65 dBW per channel.

Next we analyse the power allocation pattern in direct link shortest scenario. Figure 6.10 and 6.11 show that the power allocation patterns of four users only have minimal changes between the first iteration and the final iteration, which indicates that the user will keep its power allocation pattern unchanged when the acquired data rate is close to the target data rate.

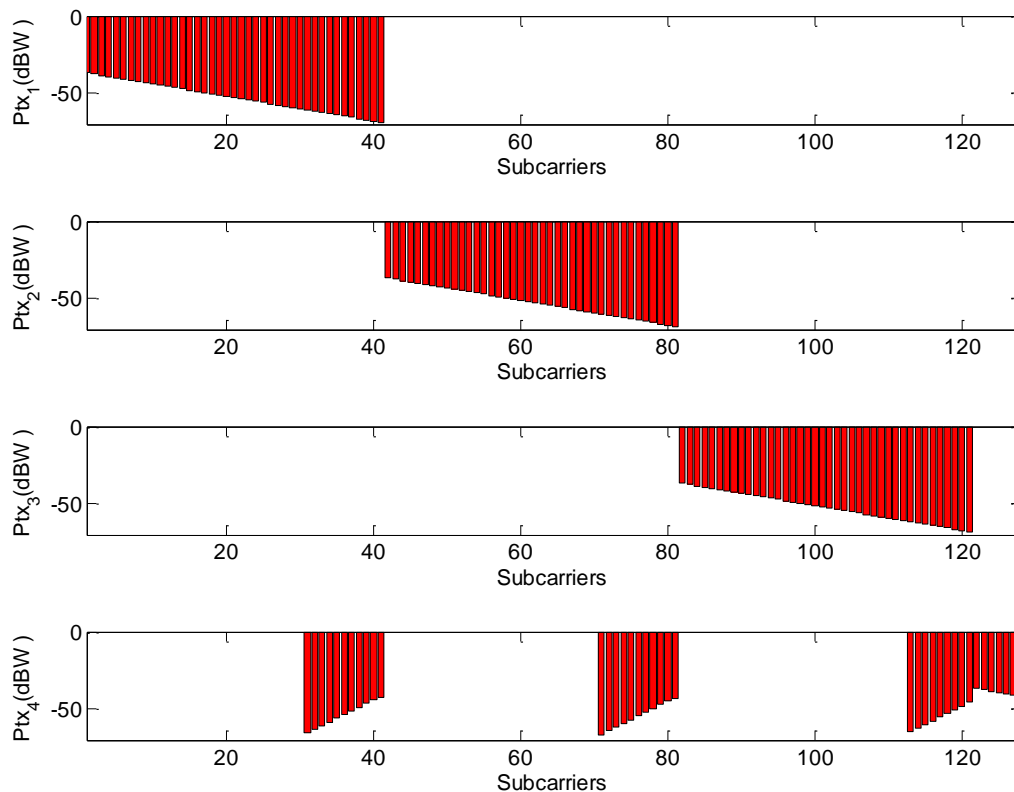


Figure 6-8 Power allocation pattern at the first iteration (Direct link longest)

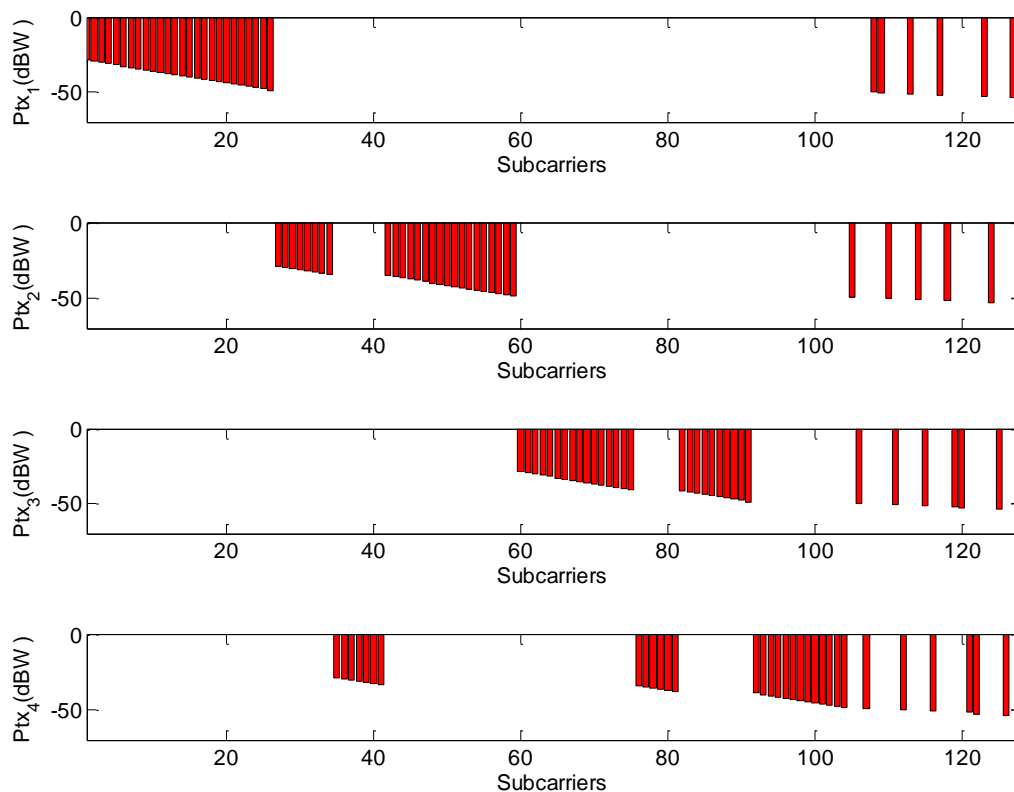


Figure 6-9 Power allocation pattern at the final iteration (Direct link longest)

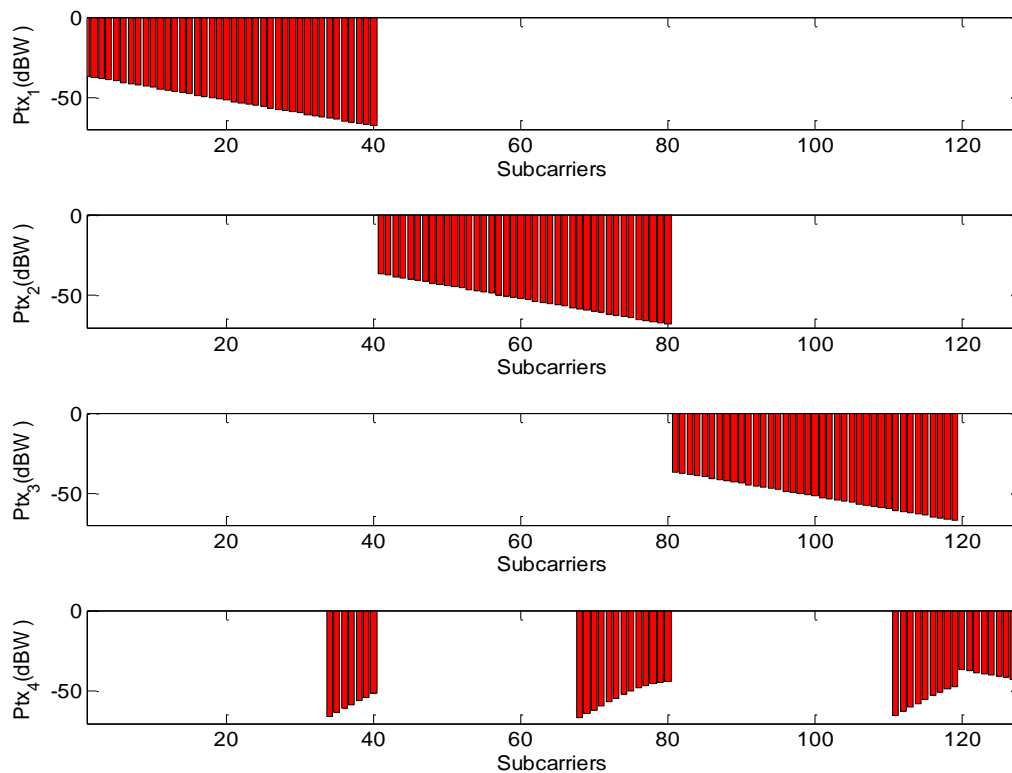


Figure 6-10 Power allocation pattern at the first iteration (Direct link shortest)

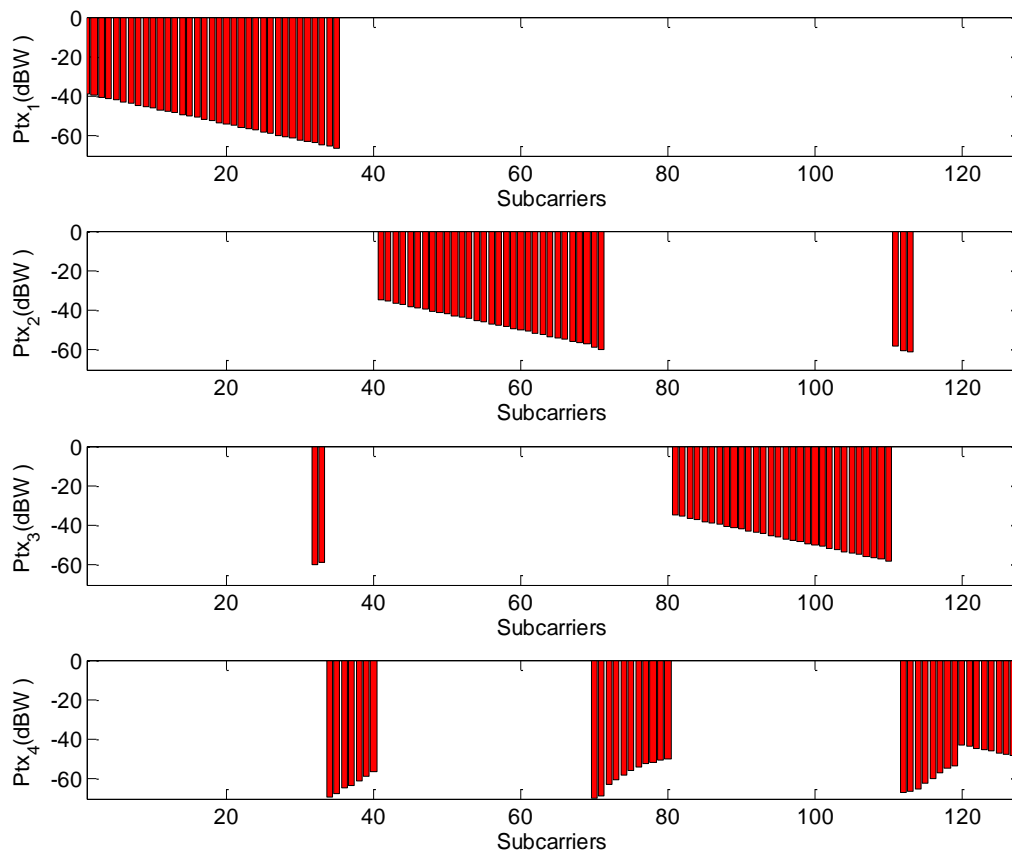


Figure 6-11 Power allocation pattern at the last iteration (Direct link shortest)

The utilities in Figure 6.12 show that the global utility increases to a maximum under both direct link longest and direct link shortest setups. However, the global utility increases faster under direct link longest scenario, which is probably due to the fact that the acquired data rate initially is far below than the target data rate in the initial iteration under direct link longest scenario.

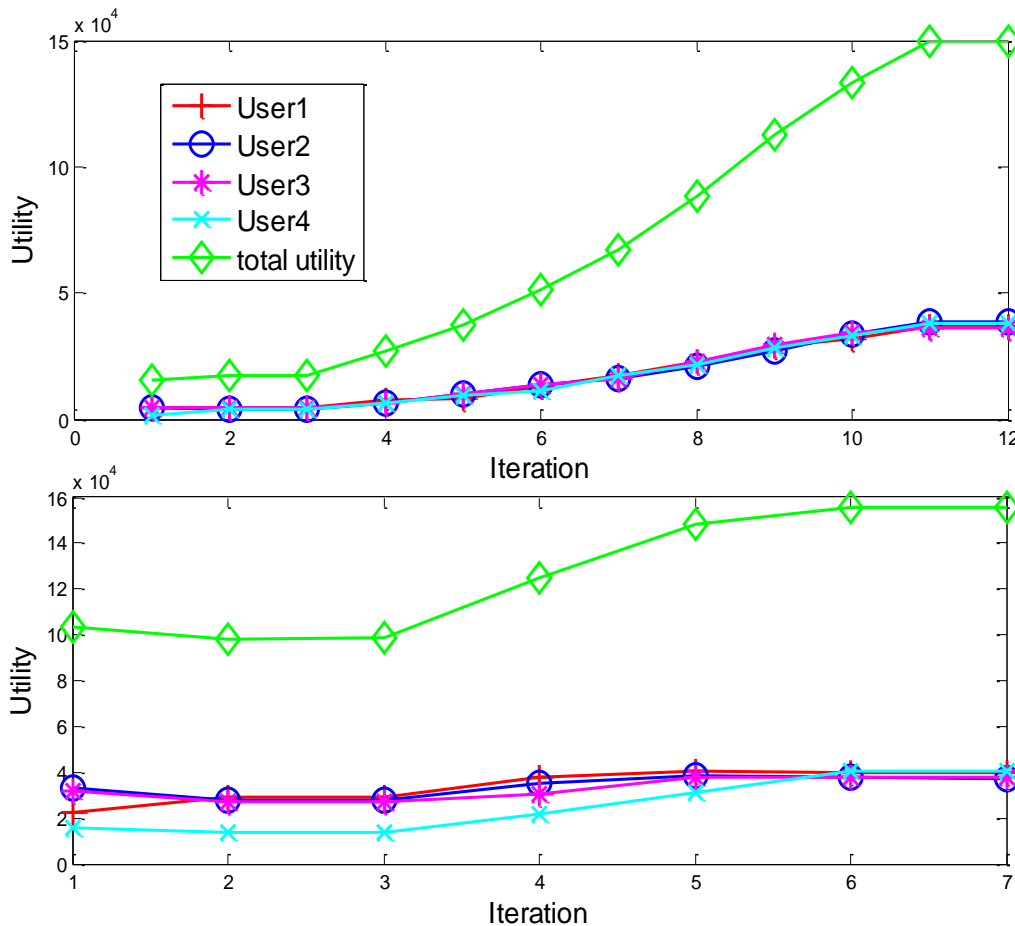


Figure 6-12 Utility analysis under a flat fading channel in direct link longest (upper) user direct link shortest (lower) scenarios

Lastly we will assess the amount of the excessive transmit power emission by looking at the Power Impact Factor (PIF). Table 6.4 shows the PIF of user at final iteration.

It shows that the PIF are the same for users under the direct link longest scenario, and it is overall much higher than that in direct link shortest scenario. It indicates that the user will not transmit an excessive amount of power in a low collective interference environment, while the higher collective interference environment force the user increase his transmit power. The

overall lower PIF in direct link shortest setup should also due to the average shorter link length between transmitter and receiver.

	User 1 PIF(W/MHz)	User 2 PIF(W/MHz)	User 3 PIF(W/MHz)	User 4 PIF(W/MHz)
Direct Link Longest	1.92×10^{-3}	1.92×10^{-3}	1.92×10^{-3}	1.92×10^{-3}
Direct Link Shortest	1.9×10^{-4}	4.81×10^{-4}	4.81×10^{-4}	7.43×10^{-5}

Table 6-4 Power impact factors analysis under a flat fading channel

6.3.1 Snapshot Analysis under a Frequency Selective Fading Channel in Four User Coexistence Scenario

In this section we examine the performance of our proposed DCPA scheme under a frequency selective fading channel. We keep the total number of users unchanged.

Figure 6.13 demonstrates the acquired data rate of 4 users under the frequency selective fading channel. Once again, we see the similar behaviour that we have seen in the flat fading channel scenario. It shows that the user can acquire an initial data rate much closer or higher than their target data rate under direct link shortest layout than that they can acquire under direct link longest layout. Nevertheless, it shows that the proposed DCPA scheme can achieve a target data rate in an extended link length in spite of the frequency selective fading on the channel.

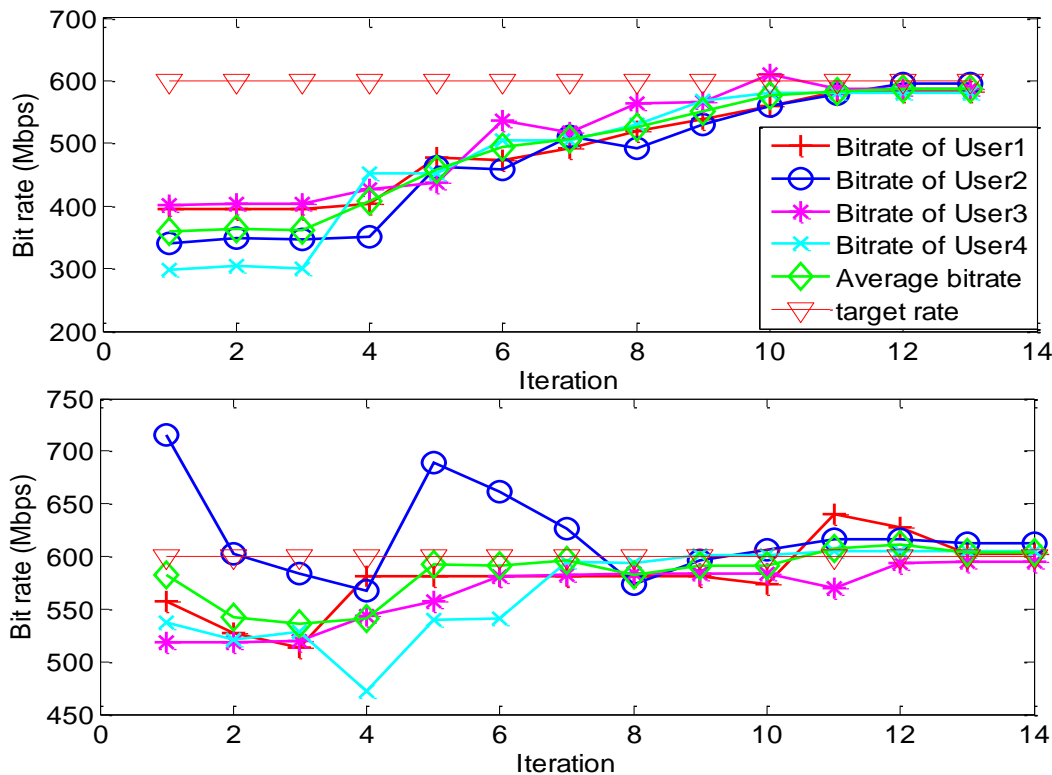


Figure 6-13 Acquired data rate analysis under a frequency selective fading channel in direct link longest (upper) user direct link shortest (lower) scenarios

Figures 6.14 and 6.16 show the power allocation pattern at the first iteration under direct link longest and direct link shortest layout respectively. Comparing Figures 6.8 and 6.10 the power allocated pattern in the frequency selective fading channel shows a discontinuous characteristic. In figures 6.8 and 6.10 the users allocate power in a few consecutive channels. However the Figures 6.14 and 6.16 show that there are gaps in power allocation pattern at first iteration. Similar behaviour has been seen in chapter 5.

In Figure 6.15 and 6.17 we overlap the transmit power pattern with the channel path gain in order to better understand the effect of frequency selective fading on our proposed DCPA scheme. It should be noted that we did not show the channel frequency selective fading at the first iteration. This is because the power allocation at first iteration is dependent mostly on the immediate interference at receiver of the initial beaconing stage and the channel fading will only be fully reflected by the power allocation pattern in the final iteration. The deep valleys on the path gain graph are path gains at frequencies under deep fading, and it is clear that

some of the gaps in power allocation pattern are the direct results of deep fading. Overall the power allocation patterns are very similar to the one we analyzed in short range scenario.

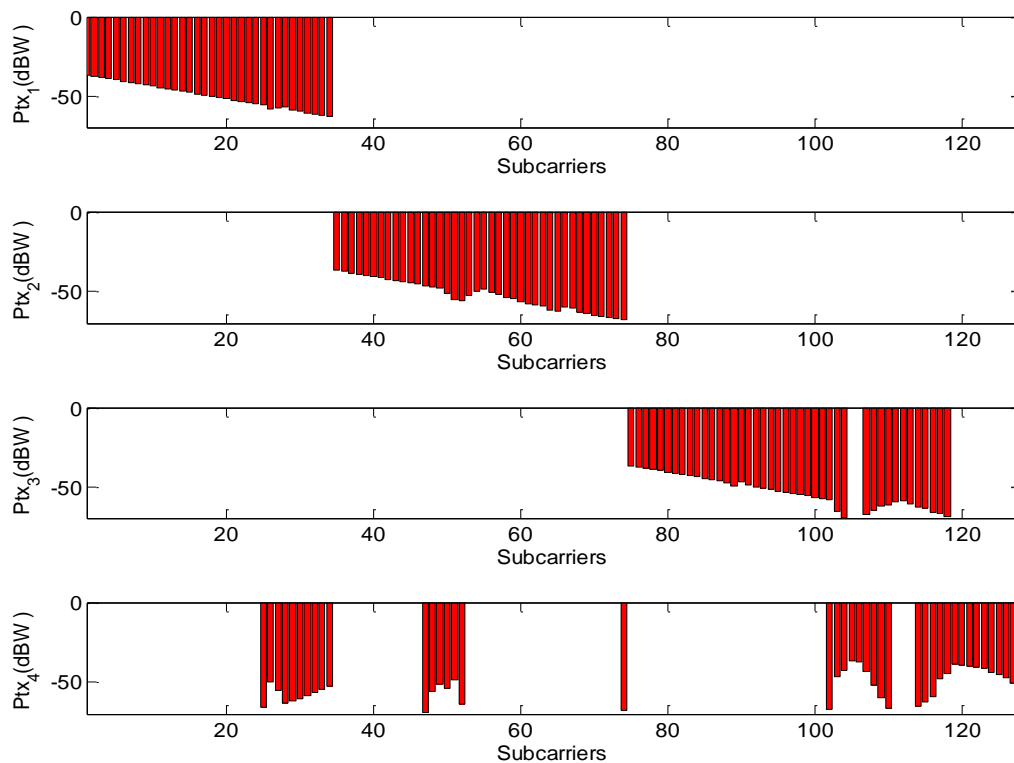


Figure 6-14 Power allocation pattern under a frequency selective fading channel at the first iteration (Direct link longest)

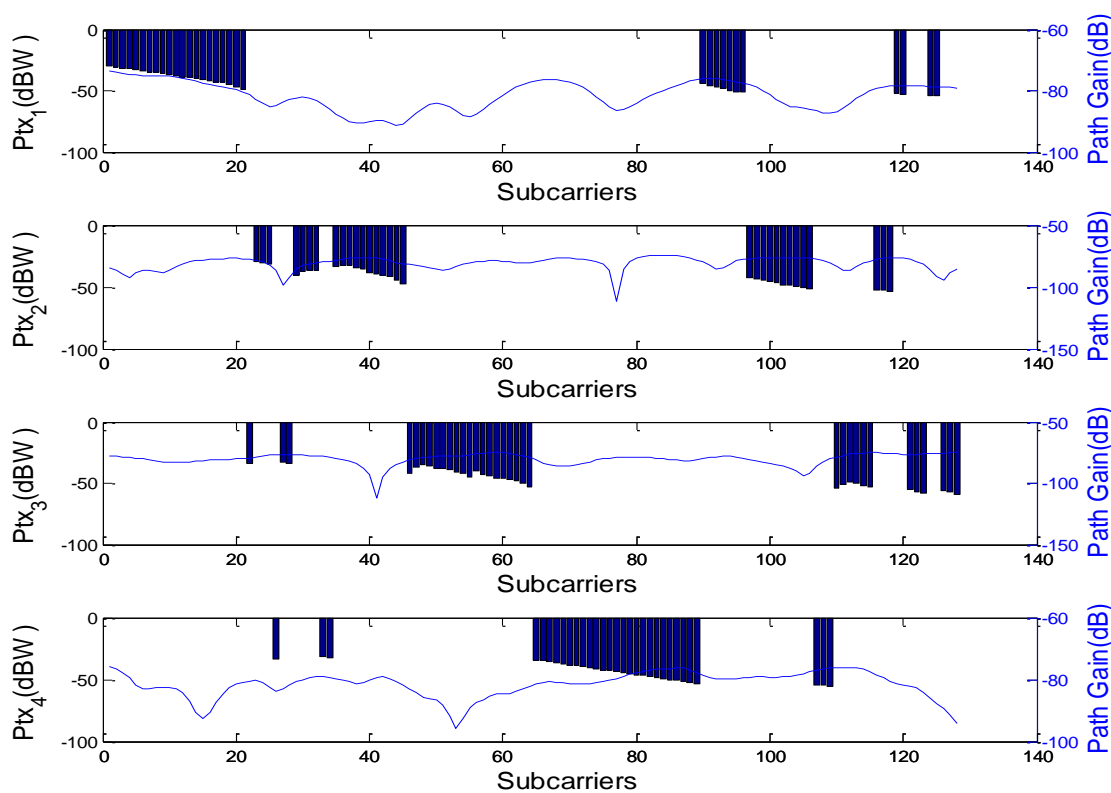


Figure 6-15 Power allocation pattern under a frequency selective fading channel at the final iteration (Direct link longest)

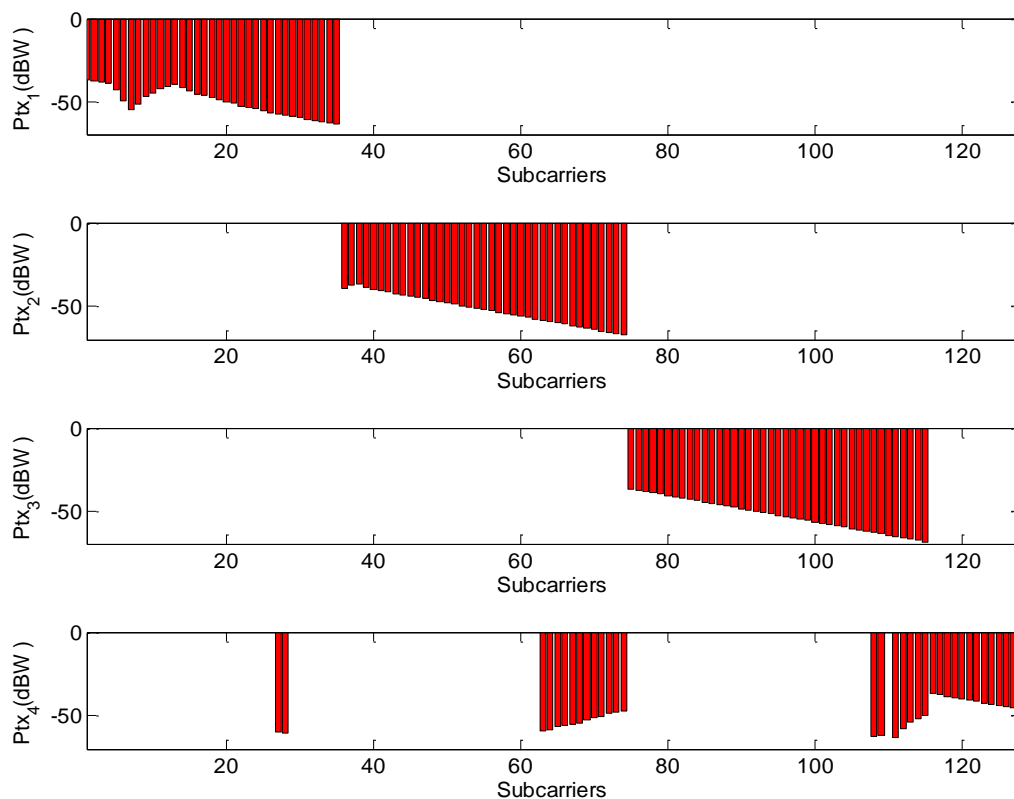


Figure 6-16 Power allocation pattern under a frequency selective fading channel at the first iteration (Direct link shortest)

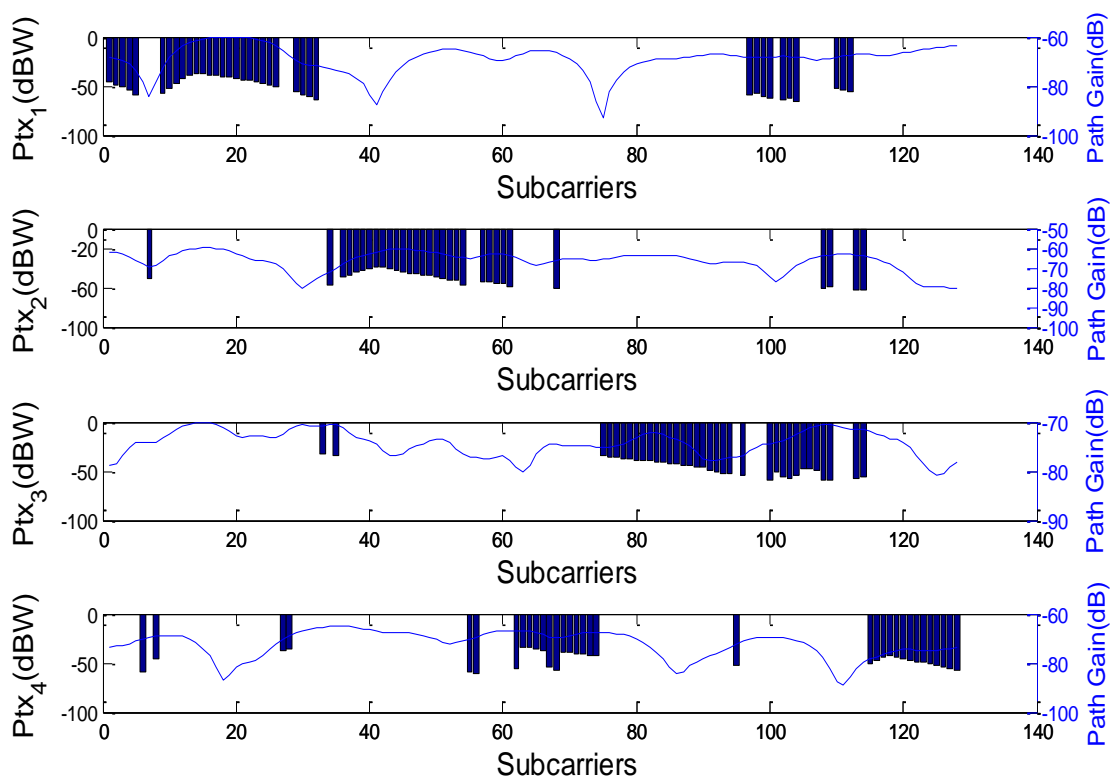


Figure 6-17 Power allocation pattern under a frequency selective fading channel at the final iteration (Direct link shortest)

In Figure 6.18, we show the utility graph, and it shows that the overall utility increases through the iterations and reach their maximum value in the final iteration for both direct link longest and direct link shortest scenarios. It is noted that the global utility reduces at iteration 11 in the direct link shortest scenario. It is because the boundary μ that is close to the target data rate, within which the user will not transfer to a different state even when the acquired data rate diverts from target that reduces its utility.

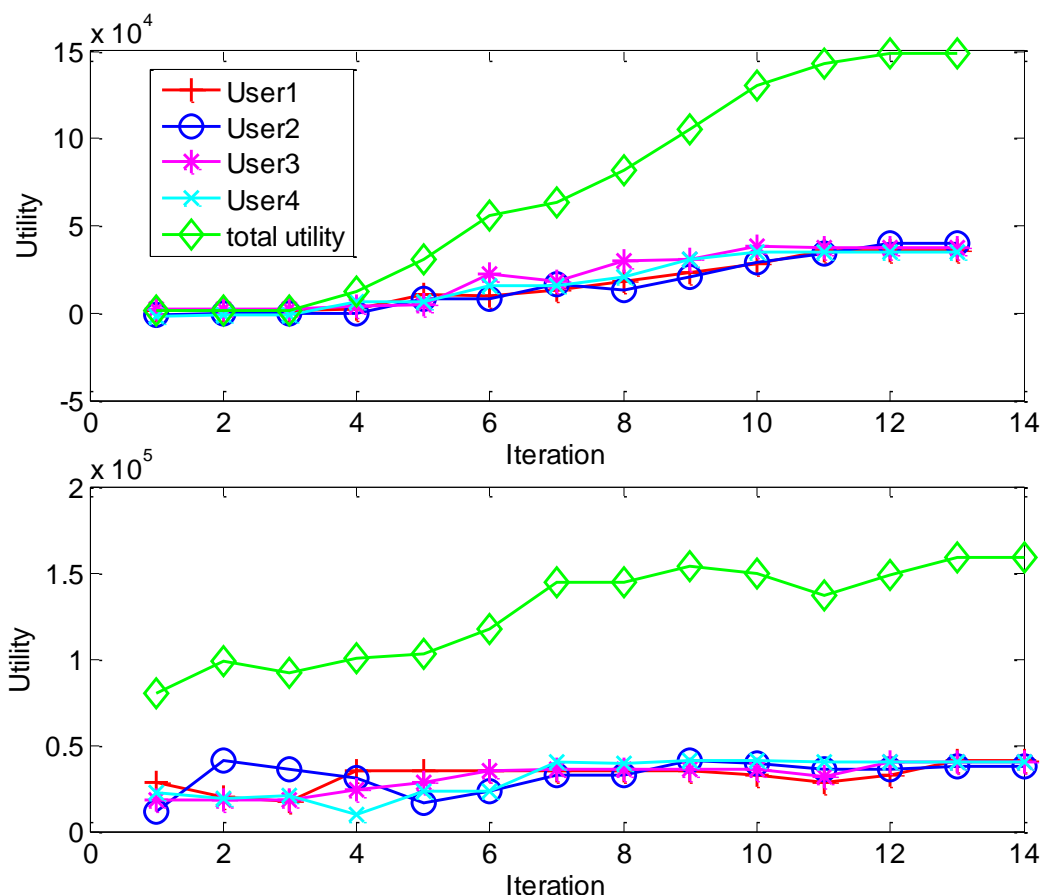


Figure 6-18 Utility analysis under a frequency selective fading channel in direct link longest (upper) user direct link shortest (lower) scenarios

Lastly, Table 6.5 shows the PIF under frequency selective fading channel. Compared with the PIF observed under flat fading channel, similar behaviour can be seen. The overall similar PIF suggests that PIF is not affected by channel fading conditions, but it is affected by geographical layout between systems.

	User 1 PIF(W/MHz)	User 2 PIF(W/MHz)	User 3 PIF(W/MHz)	User 4 PIF(W/MHz)
Direct Link Longest	1.53×10^{-3}	1.53×10^{-3}	7.64×10^{-4}	9.63×10^{-4}
Direct Link Shortest	3.02×10^{-4}	1.9×10^{-4}	7.64×10^{-4}	6.06×10^{-4}

Table 6-5 Power impact factors analysis under a frequency selective fading channel

6.3.2 Snapshot Analysis in a Six User Coexistence Scenario

In this section, we examine the performance of our proposed DCPA scheme in a scenario with an increased number of users. As we analysed before, the increased number of users is inevitable for an extended link length. The reason for choosing six transmitter and receiver pairs is because that it is difficult to illustrate clearly the performance and behaviour of each individual user for user number higher than 6.

Figure 6.19 demonstrates the acquired data rate of 6 users under the flat fading and the frequency selective fading channels. It should be noted that the direct link longest and direct link shortest geographical location layouts will not be examined in this section due to difficulty in generating more random locations than eight that are subject to the specific distance constraints. It is also noted that the target data rate has been dropped from 600Mbps to 400 Mbps due to the increased user number. It can be explained by calculating an estimated maximum mutual target data rate T_{max} in a 6 user scenario, which is 425.33 Mbps according to equation 6.11. Therefore, the target data rate for a 6 user scenario should at least no higher than 425Mbps.

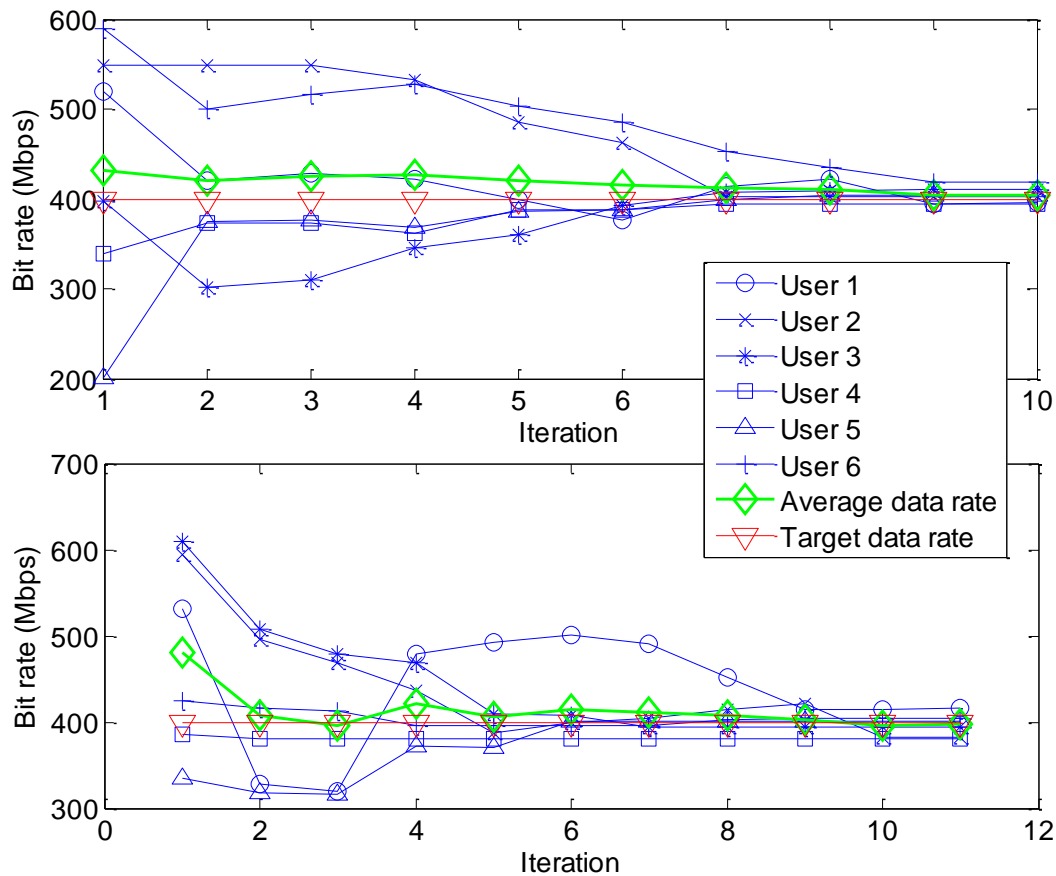


Figure 6-19 Acquired data rate analysis under flat fading (upper) frequency selective fading channel (lower) channels

Comparing the performance of flat fading and frequency selective fading channels, it shows that the proposed DCPA scheme is not restricted by the number of users, and performs similarly compared to a four user coexistence setup.

The power allocation pattern under a flat fading channel is examined in figures 6.20, and 6.21, and the power allocation pattern under a frequency selective fading channel is examined in figures 6.22 and 6.23. There is however no significant difference after changing the number of users. Similar analysis from the four user coexistence scenario is still valid in a six user coexistence scenario.

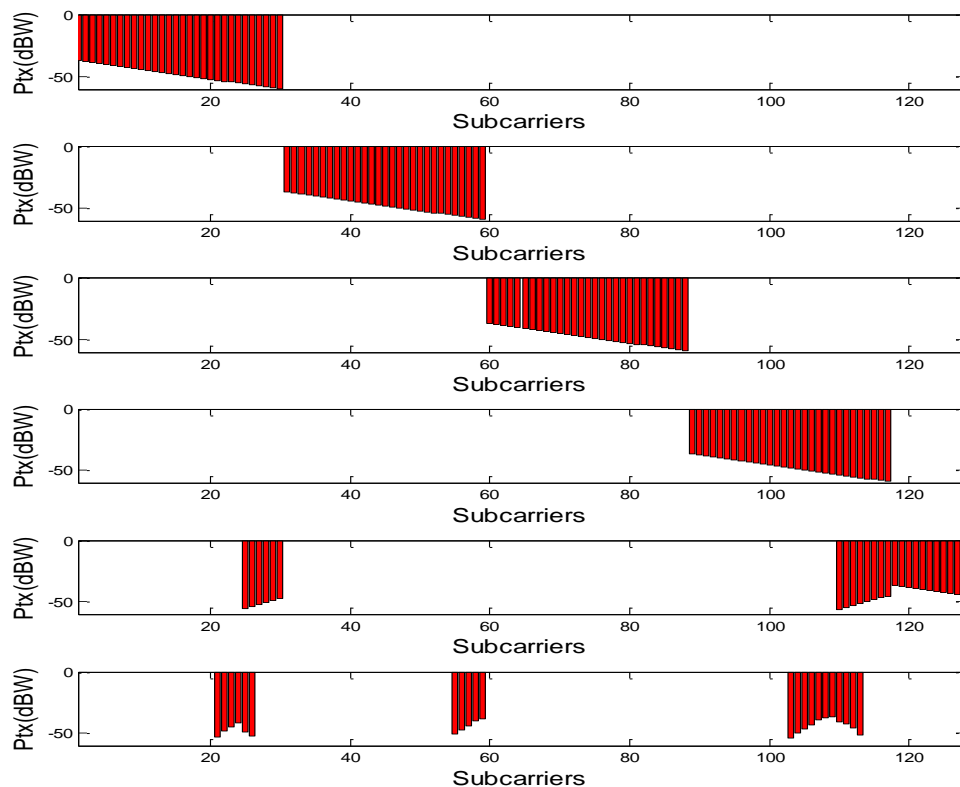


Figure 6-20 Power allocation pattern at the first iteration (flat fading channel)

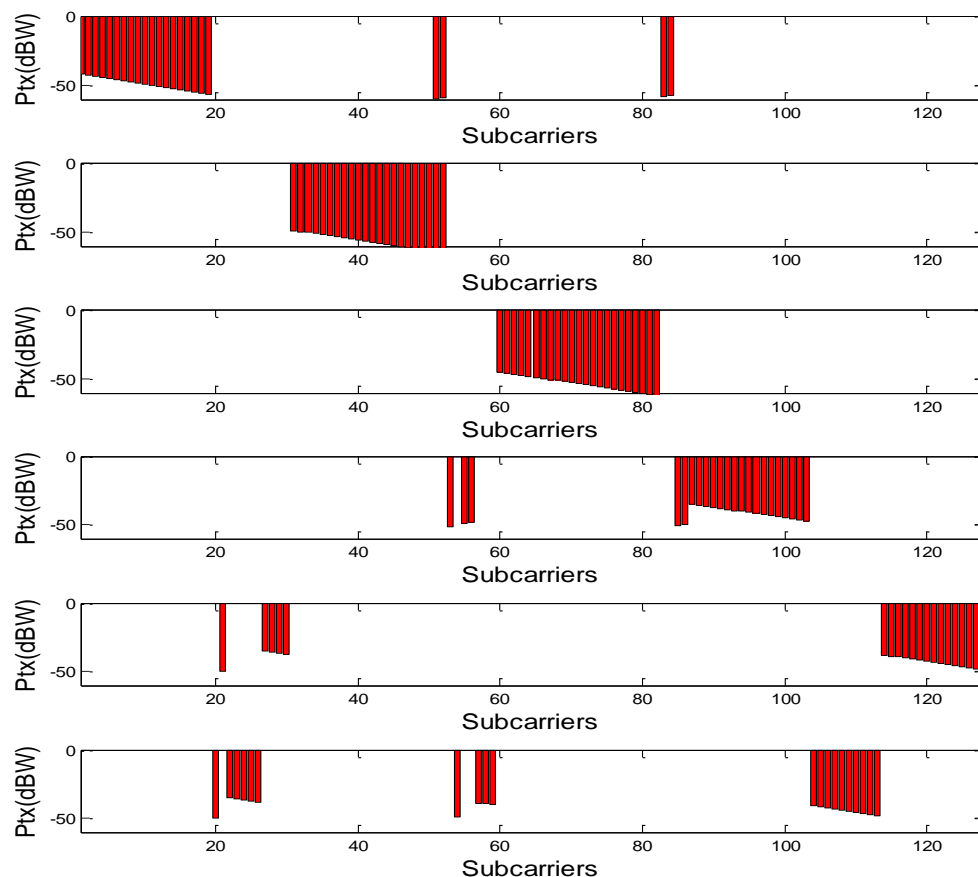


Figure 6-21 Power allocation pattern at last iteration (flat fading channel)

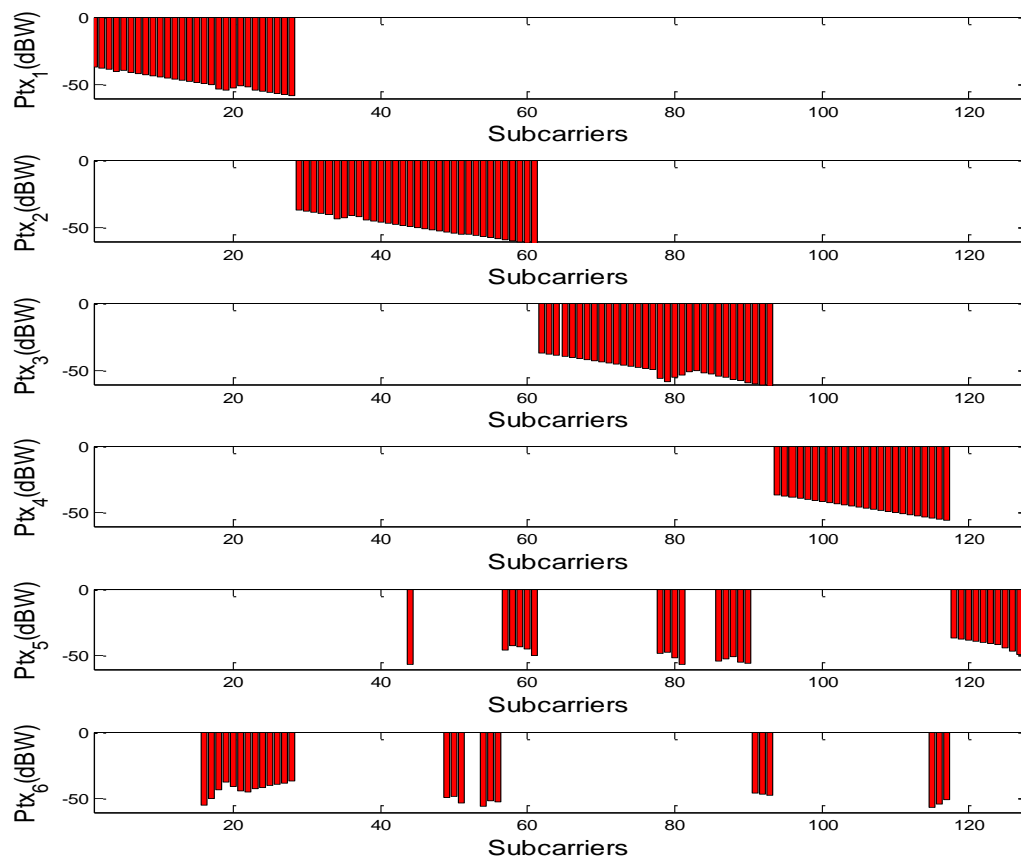


Figure 6-22 Power allocation pattern at first iteration (frequency selective fading channel)

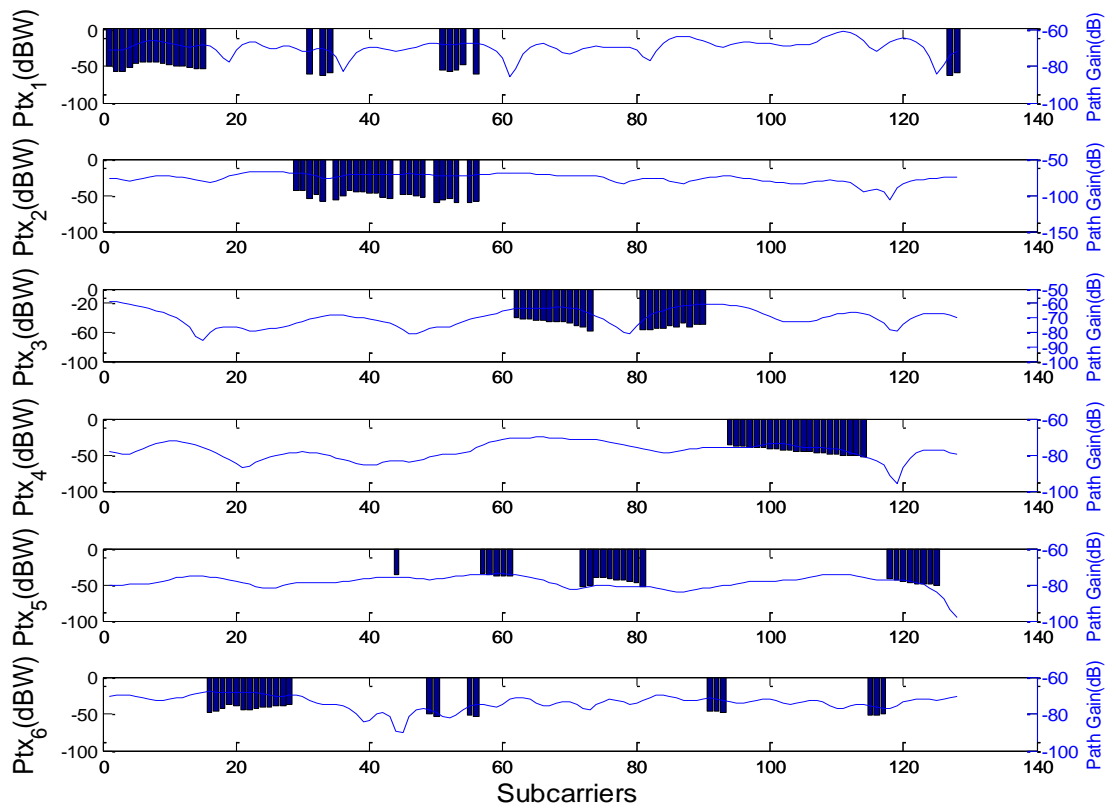


Figure 6-23 Power allocation pattern at the final iteration (frequency selective fading channel)

On the other hand, the total utilities reach their maximum despite the difference in channel conditions.

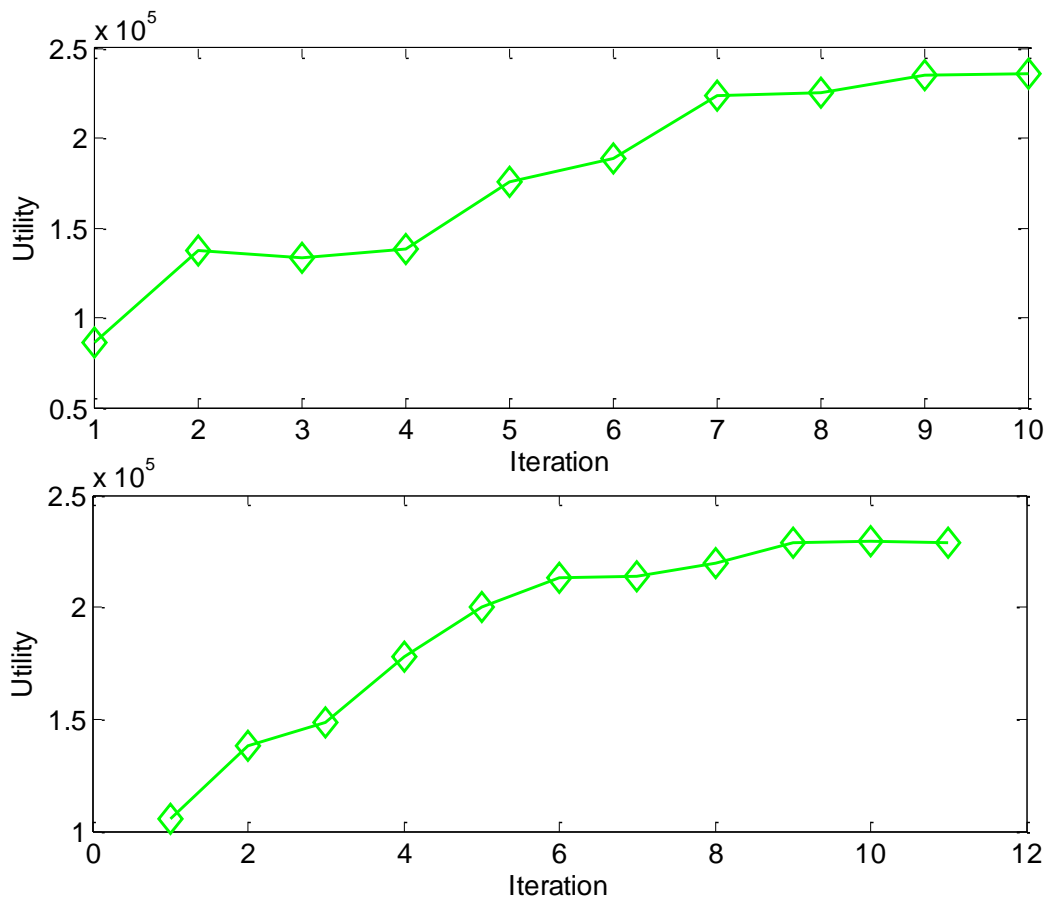


Figure 6-24 Total utility analysis under flat fading (upper) frequency selective fading (lower) channels

Lastly, we examine the PIF with the increased number of users. It can be seen from the Table 6.6 that the channel fading does not add excessive power emission in 6 user coexistence scenario. Compared to the PIF we observed from 4 user coexistence scenario, the average PIF is closer to the direct link shortest scenario than that of the direct link longest scenario, which suggests that the link length between transmitter and receiver may have greater impact on PIF than the number of users. However, the fact that the average PIF of 6 user coexistence scenario is close to the direct link shortest scenario of 4 user coexistence scenario suggests that the extreme geographical layouts (direct link longest and direct link shortest) of users is less likely to happen when the number of users is increased.

It is also noted in Table 6.6 that some of the users will have a PIF far higher than the others, such as user 5 which has the PIF that is much higher than the rest of users under frequency selective fading channel, which suggests that the channel may be better utilized with lower collective interference if the users with higher PIF are able to hop to another pool of frequency bands.

	User 1 PIF (W/MHz)	User 2 PIF (W/MHz)	User 3 PIF (W/MHz)	User 4 PIF (W/MHz)	User 5 PIF (W/MHz)	User 6 PIF (W/MHz)
Flat Fading	1.2 $\times 10^{-4}$	3.04 $\times 10^{-4}$	3.04 $\times 10^{-4}$	2.41 $\times 10^{-4}$	3.04 $\times 10^{-4}$	1.91 $\times 10^{-4}$
Frequency Selective Fading	7.52 $\times 10^{-5}$	3.82 $\times 10^{-4}$	2.41 $\times 10^{-4}$	3.04 $\times 10^{-4}$	4.82 $\times 10^{-4}$	3.03 $\times 10^{-4}$

Table 6-6 Power impact factor analysis under flat fading and frequency selective fading channels

6.4 General Performance of Four Users Coexistence Scenario

In order to understand the system behaviour more generally, we generate 1000 different system layouts in a 100 cubic metre volume according to a uniform distribution, and study the statistical performance of our proposed scheme through Monte Carlo simulation. The performance will be evaluated in terms degree of convergence, convergence speed and average PIF.

We have demonstrated that the peak power which is calculated from equation 6.6, and further controlled by the estimated power floor, estimated required number of channels and total transmit power.

Analysing Figure 6.3, we can draw the conclusion that the peak transmit power P_{max} can be adjusted by changing adjustment factor C_{adjust} given a fixed total transmit power P_{total} . The idea of adjusting factor C_{adjust} is to adjust the P_{max} in order to find a better power allocation

pattern under a given total transmit power constraint. Figure 6.25 shows the reliable convergence region given the adjustment factor and target data rate. It is necessary to note that the estimated bandwidth requirement will be equal to 0 when ERC calculated in equation 6.7 is equal to or smaller than 0. Therefore, the $P_{max} = P_{floor}$ when $m \leq 0$. The reliable convergence region is defined as the area that the proposed DCPA scheme achieves more than 99 percent convergence.

Figure 6.25 shows that the reliable convergence region is affected by both adjustment factor and target data rate. The reliable convergence of our proposed DCPA scheme can be guaranteed if an adjustment C_{adjust} is higher than 6 channels and a target data rate higher than 100Mbps. However, the target data rate cannot be higher than 740Mbps in four user coexistence scenario.

As we analyzed before, the maximum mutual target data rate can be approximately estimated by equation 6.11

The maximum mutual target data rate in a 4 user coexistence scenario is 628 Mbps, therefore the behaviour of Figure 6.25 can be explained. However, it is noted that the estimated target data rate is smaller than the 660Mbps, which means there exists channel reuse, and hence the actual achievable target data rate is higher than T_{max} .

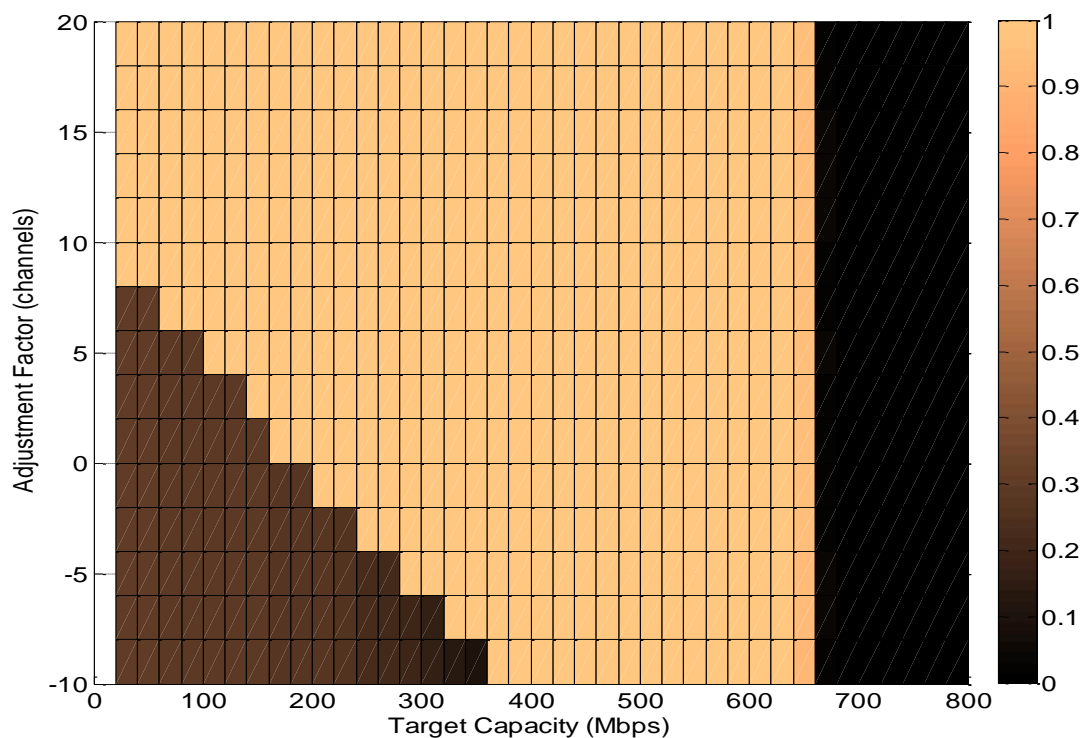


Figure 6-25 Degree of convergence under a flat fading channel

Figure 6.26 shows the degree of convergence under the frequency selective fading channel. Similar to the flat fading channel the adjustment factor will only affect the convergence at low target data rates. An adjustment factor that is equal to or higher than 6 channels can be used to guarantee convergence at low target data rate. On the other hand, the degree of convergence will drop from 100 percent to 90 percent in some specific combination of adjustment factor and target data rate.

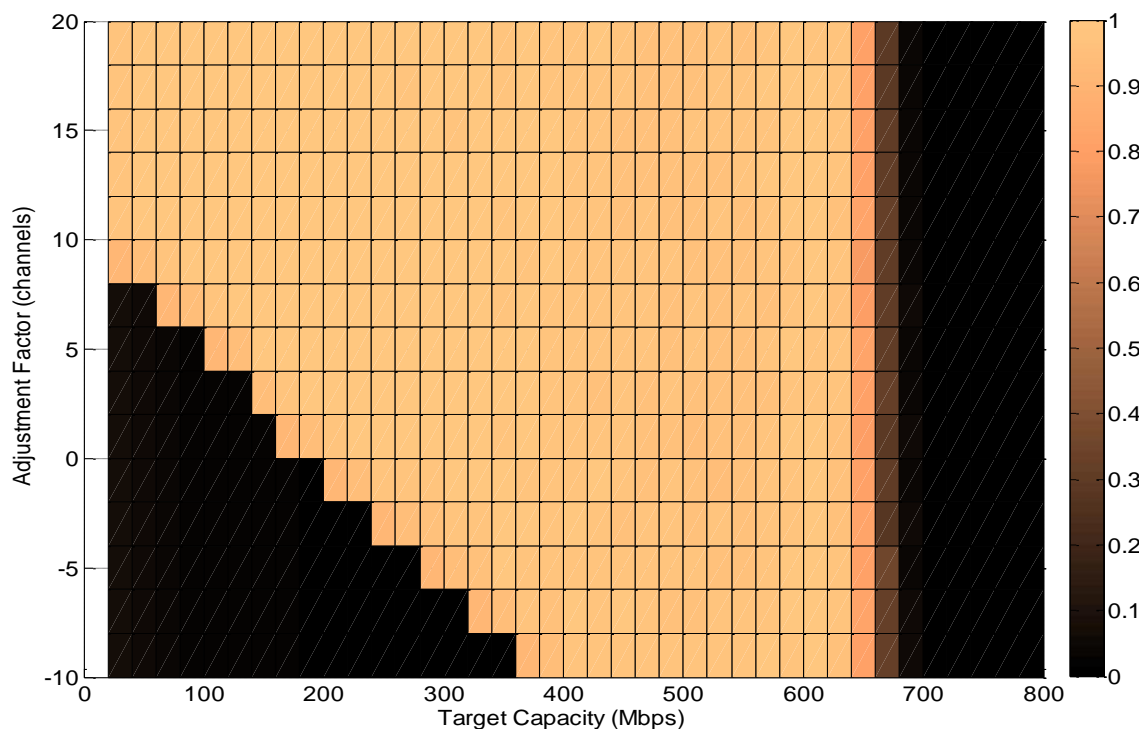


Figure 6-26 Degree of convergence under a frequency selective fading channel

Figures 6.27 and 6.28 show the convergence speed under a flat fading channel and a frequency selective fading channel respectively. It is noted that the convergence speed is unaffected by the adjustment factor, and only affected by the target data rate. Both flat fading channel and frequency selective fading channel show the ‘valley’ where the proposed DCPA scheme converges most rapidly. The ‘valley’ is located clearly at 500Mbps under flat fading condition, while it is located rough at 400 Mbps under frequency selective fading condition.

It should be noted that the convergence speed is blank for target data rate over 660Mbps under flat fading channel and 700 Mbps under frequency selective fading channel. It is because the power allocation scheme ceases converging over those specific target data rate.

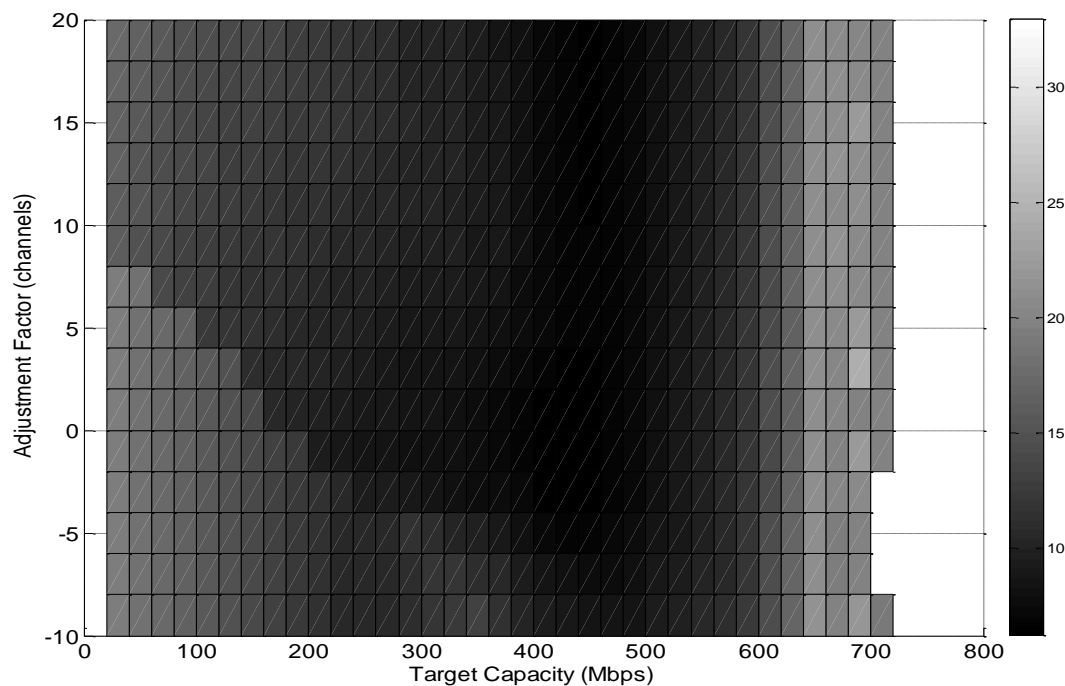


Figure 6-27 Convergence speed under a flat fading channel

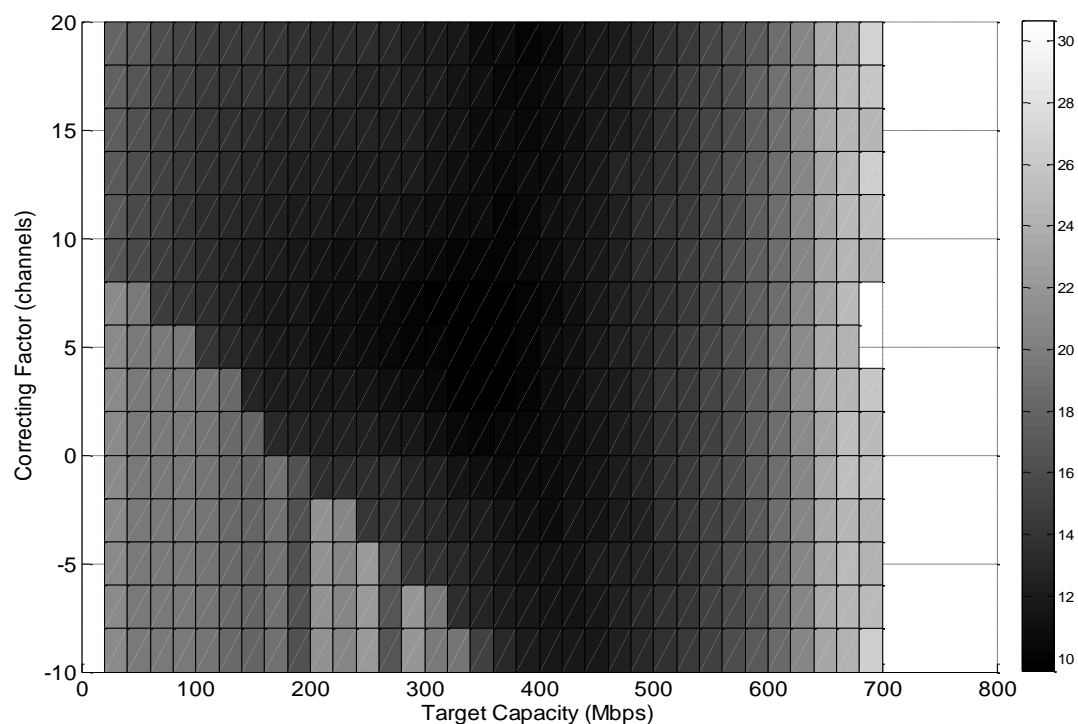


Figure 6-28 Convergence speed under a frequency selective fading channel

Next, we focus on the PIF. The PIF in this section is an average PIF. It reflects a general excessive power emission in relation to adjustment factor and target data rate. It is found from Figure 6.29 that the average PIF is not affected by changing adjustment factor, but it will

increase rapidly when the target data rate is close to the estimated maximum mutual target data rate. It suggests that the channels will not be fully partitioned by users at a lower target data rate, and the users will not increase their transmit power in order to acquire such a low target data rate. Therefore the low excessive power emission can be expected. When the target data rate is close to T_{max} , the channel will be fully partitioned and the further increase target data rate will be at the cost of increasing total transmit power, therefore the PIF will increase significantly when the target data rate is close to T_{max} .

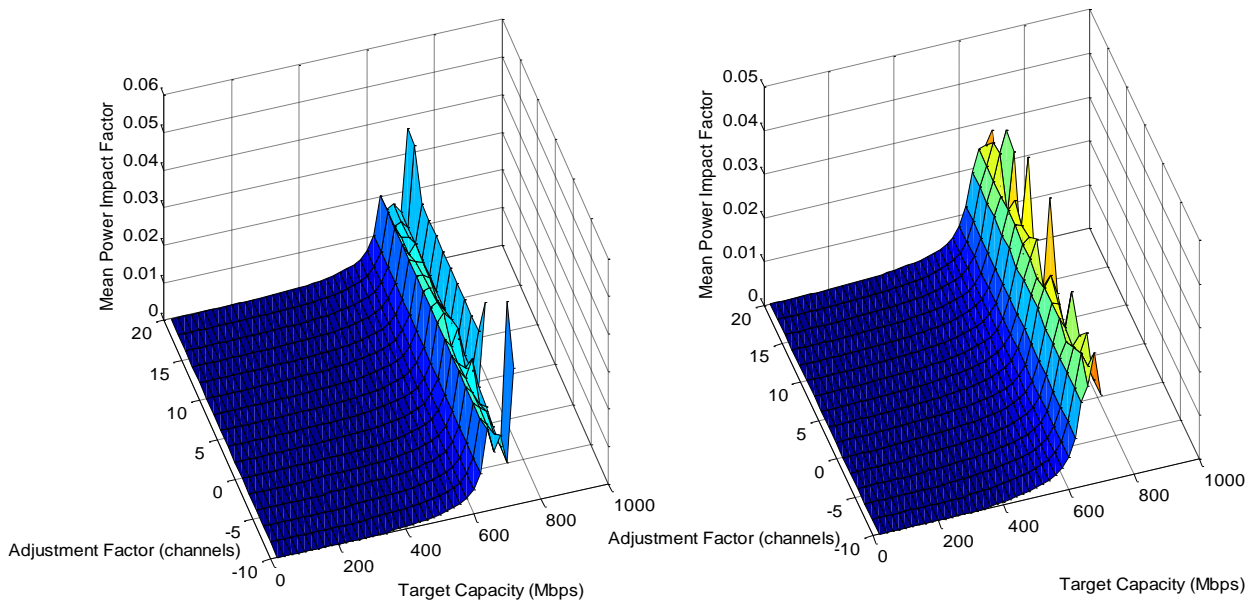


Figure 6-29 Power Impact Factor under flat fading (left) frequency selective fading (right) channels

6.5 General Performance of Various Number of Users Scenario

In previous snapshot analysis, we examined a 6 user coexistence scenario. In this section, we examine the performance of the proposed DCPA scheme with various number of users. The performance will be evaluated in terms of degree of convergence, convergence speed and PIF.

From the analysis in the last section, the adjustment factor C_{adjust} only affects the convergence once it is smaller than 6 channels, therefore, we set the C_{adjust} as 6 channels in the following simulations. Figure 6.30 illustrates the convergence of the proposed DCPA scheme when the various numbers of systems and different target data rate are considered. It shows that the more users share the same frequency pool, the less the achievable data rate can

each of them acquire. It is noted that the power allocation scheme cannot converge when there are more than 6 users that require a target data rate smaller than 100 Mbps. This is possibly due to the requirement of further total power reduction in order to have the user acquire a very low target data rate (power allocation process takes more than 30 iterations will be considered as failure).

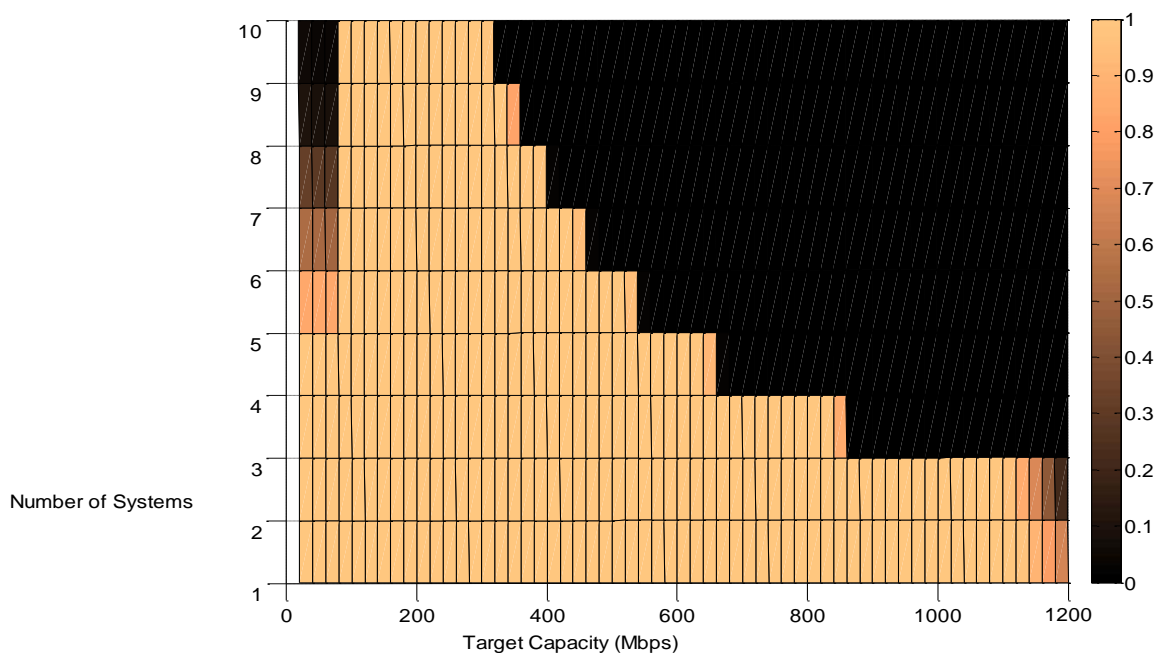


Figure 6-30 Degree of convergence under a flat fading channel

It should also be noted that we can estimate the maximum mutual target data rate by equation 6.15. It is possible to compare the actual achievable target data rate and the estimated maximum mutual target data rate. T_{actual} in Table 6.7 is the target data rate that a specific number of users can acquire with a minimum 99 percentage of convergence. It is illustrated in Table 6.7 that the T_{actual} is smaller than T_{max} when there are less than 3 users, while it becomes bigger than T_{max} when there are more than 3 users, but again it becomes smaller than T_{max} when there are 10 users sharing the same spectrum pool. It suggests that when the number of users is only 1 or 2, there is no channel reuse and the gradient factor α will restrict the user from allocating power to all available channels so that the actual available target data rate is lower than the estimated maximum mutual target data rate. As the number of users increasing, a few of channels will be reused by different users and the T_{actual} will be higher than the T_{max} . However, T_{actual} will eventually be very close or smaller to the T_{max} because

the available spectrum will be fully partitioned and the power allocation algorithm will be difficult to converge within a given number of iterations for a high number of users (power allocation process takes more than 30 iterations will be considered as failure), and it will be difficult to guarantee 99 percentage of convergence.

	1 user	2 users	3 users	4 users	5 users
T_{max} (Mbps)	2451	1235	829	627	505
T_{actual} (Mbps)	1100	1080	820	640	520
	6 users	7 users	8 users	9 users	10 users
T_{max} (Mbps)	424	366	323	289	262
T_{actual} (Mbps)	440	380	340	300	260

Table 6-7 Target data rates analysis under a flat fading channel

Figure 6.31 shows the degree of convergence of the proposed DCPA scheme under frequency selective fading channel. It shows the similar behavior that has been seen in Figure 6.30. However, the percentage of convergence will drop from 99 percent to 90 percent at some combination of user number and target data rate.

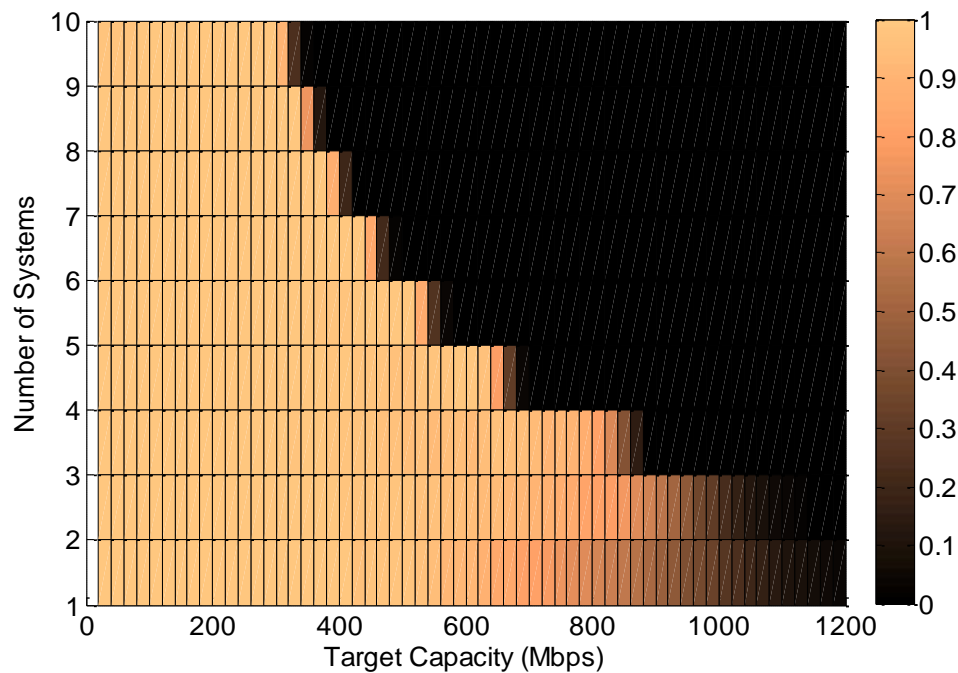


Figure 6-31 Degree of convergence under a frequency selective fading channel

Table 6.8 shows the comparison between T_{max} and T_{actual} under a frequency selective fading channel condition. It should be noted that the T_{actual} is the target data rate that a specific number of users can acquire with a minimum 90 percentage of convergence, which is reduced from 90 percentage of convergence due to the frequency selective fading channel. It can also be interpreted as the channel capacity being reduced as a result of the frequency selective fading channel. Compared with Table 6.7, the T_{actual} is smaller under a frequency selective fading channel condition given a specific number of users, but it shows the same behaviour as we analysed before.

	1 user	2 users	3 users	4 usres	5 users
T_{max} (Mbps)	2451	1235	829	627	505
T_{actual} (Mbps)	620	700	760	620	500
	6 users	7 users	8 users	9 users	10 users
T_{max} (Mbps)	424	366	323	289	262
T_{actual} (Mbps)	420	360	320	300	260

Table 6-8 Target data rates under a frequency selective fading channel

Figures 6.32 and 6.33 illustrate the convergence speed of the proposed DCPA scheme under flat fading channel and frequency selective fading channel respectively. It shows that our proposed DCPA scheme converges faster at a target data rate around 400Mbps under flat fading condition, while it converges faster at a target data rate around 300Mbps under frequency selective fading condition. Figure 6.32 and 6.33 also illustrate that the number of user will affect the convergence speed. The fewer users the faster the proposed DCPA scheme converges.

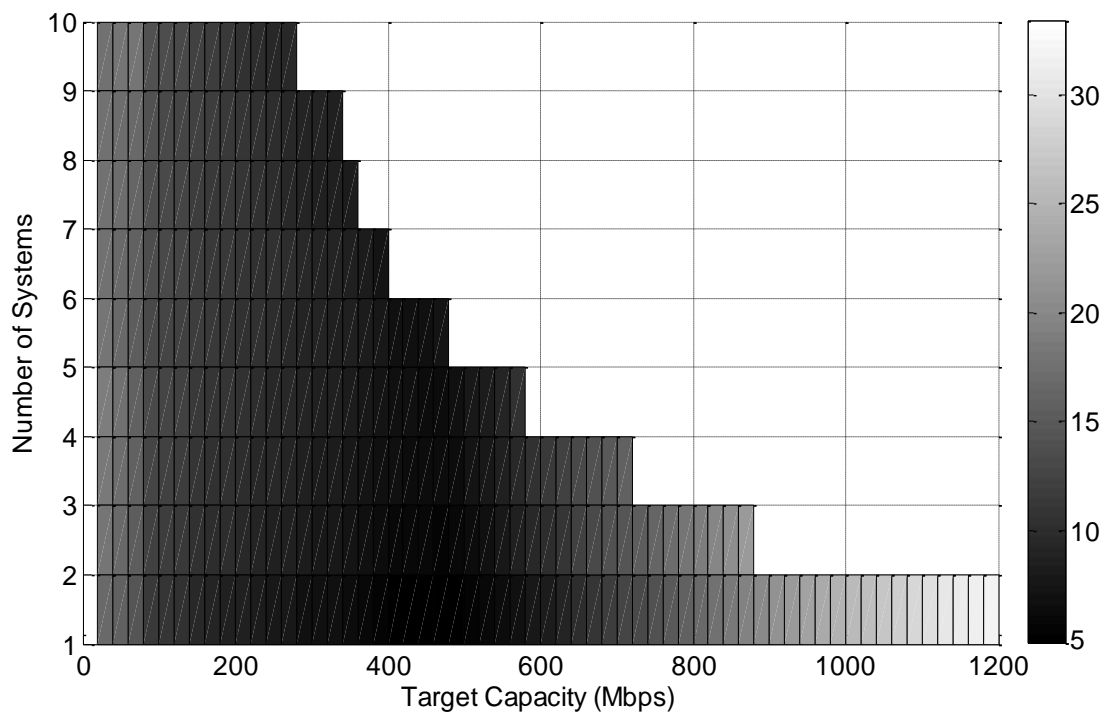


Figure 6-32 Convergence speed under a flat fading channel

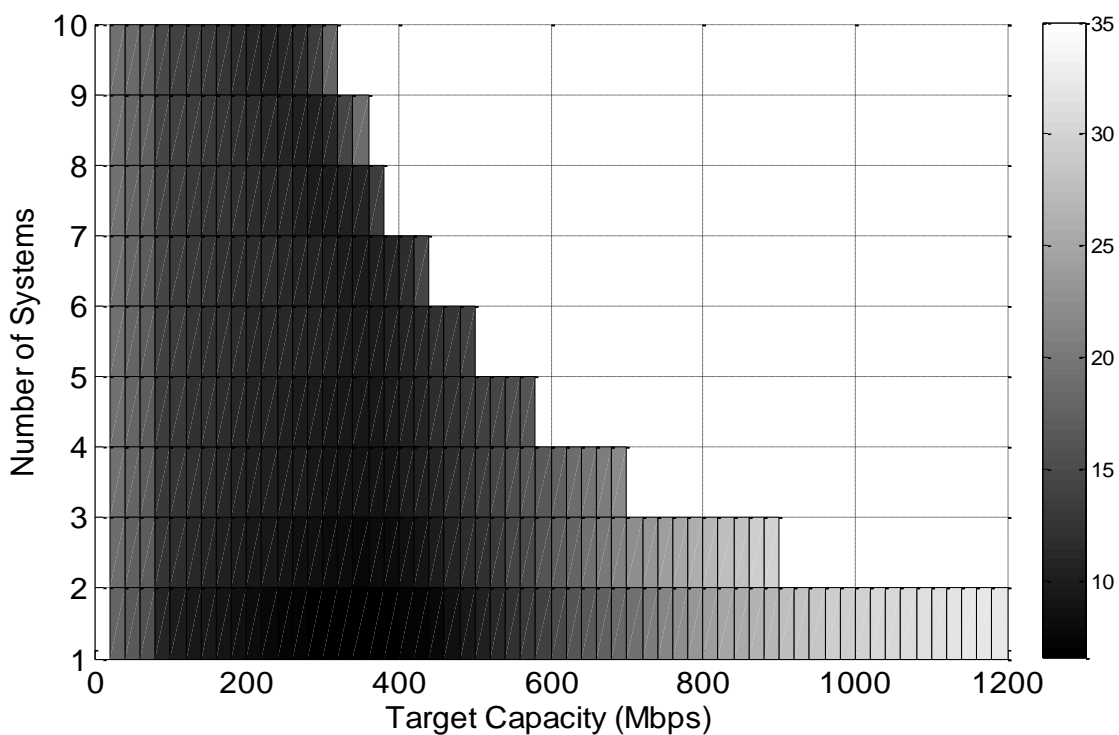


Figure 6-33 Convergence speed under a frequency selective fading channel

Lastly, we show the PIF of the increased number of users in Figure 6.34. It is found that the number of users will not greatly affect the PIF when the target data rate is low. However, the PIF will increase rapidly when there are more users. Especially, when the target data rate is close to T_{max} the PIF will increase dramatically. It suggests that the channel will not be fully partitioned by only a few users at a lower target data rate, and the user will not increase their transmit power in order to acquire such a small target data rate. Therefore the low excessive power emission can be expected. When the target data rate is close to T_{max} , the channel will be fully partitioned and the further increase in target data rate will be at the cost of increasing total transmit power, therefore the PIF will increase significantly when the target data rate is close to T_{max} . On the other hand, as more users sharing the same spectrum pool, the users will have to increase their total transmit power in order to achieve their target data rate.

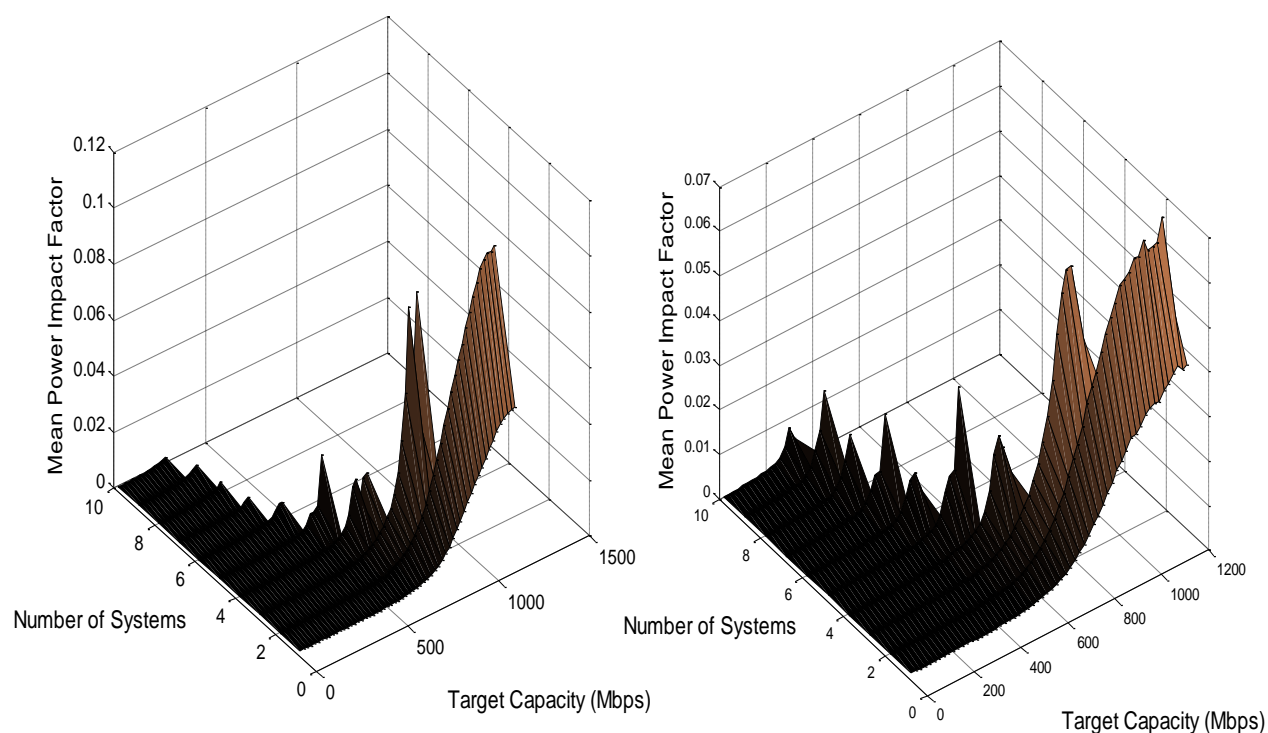


Figure 6-34 Power Impact factor under flat fading (left) frequency selective fading (right) channels

6.6 Chapter Conclusion

In this chapter, we proposed a new power allocation scheme based on previous DCPA scheme so that it can be applied to an extended range scenario. Simulation results show that the

proposed DCPA scheme can work under both flat fading and frequency selective fading channels. Importantly, the impact of increasing transmit power at longer range is emphasized and analyzed. A new Power Impact Factor (PIF) is designed to assess the excessive power emission. The simulation results show that the target data rate, and number of users are directly related to the PIF. By estimating the maximum achievable target data rate of a given number of channels, the relationship between PIF, number of users and target data rate is found and fully examined in this chapter. On the other hand, the simulation results show good scalability of the proposed DCPA scheme that the proposed DCPA scheme can work with various numbers of users under both flat fading and frequency selective fading channel conditions. It is however noted that the increased number of users is at the cost of the mutual target data rate.

Chapter 7 Future Work

Contents

7.1	Future Improvement based on Current Work	182
7.1.1	Dynamic Target Requirement with a Dynamic User Number.....	183
7.1.2	Primary User Recognition.....	183
7.2	Cognitive Power Allocation in Sensor Network and Cellular Network	186
7.3	Multi-agent Q-learning.....	186
7.4	Chapter Conclusion	187

We have shown in this thesis how the cognitive principles can be used to solve a distributed power allocation problem in a point-to-point OFDM based radio system context. In particular, we have investigated the application of a game theoretical approach in solving the OFDM based UWB power allocation problem. Convinced by the analytical research and simulation performance, we believe that our cognitive power allocation scheme is promising for the future multicarrier radio techniques. A number of improvements can be made to our existing power allocation schemes, and it is obvious that there are many more existing multicarrier radio applications can be benefit from cognitive power allocation. However, further work is needed in order to improve our current scheme and make it generally applicable to those existing multicarrier based applications.

Given the work that we have done so far, this chapter will provide suggestions and ideas for the future work.

7.1 Future Improvement based on Current Work

As introduced in chapter 4 and 5, we invent a new way of Distributed Cognitive Power Allocation (DCPA) scheme based on a game strategy, and we demonstrate our work with

Chapter 7 Future Work

both mathematical analysis and simulation results. There are still a number of improvements that can be made to our existing scheme, and also problems we have not yet tackled.

7.1.1 Dynamic Target Requirement with a Dynamic User Number

In chapter 4 and 5, we show that our game based approach can be used to acquire a specific target data rate in a distributed wireless environment where there are multiple homogenous systems coexisting in the close vicinity without direct information exchange. The work in this thesis focused on a static target requirement and a static number of users. This is reasonable for short range radio systems as most of the short range radio systems were employed in an indoor environment, and it is less likely that the wireless devices will have significant changes in number and location over a short time period. However, we should not rule out the possibility that the wireless devices were turned off either by people using them or shut down autonomously in order to save the battery power. Either way, there will be changes in number of systems. On the other hand, it is also possible that an adaptive wireless device, which is capable of utilizing the huge channel pool seen with UWB systems, as we introduced in chapter 2, will need occasionally to change the channel assignment and power allocation pattern in order to adapt to a wide range of applications from the relatively low data rate Voice over Internet Protocol (VOIP) to ultra high data rate high definition TV programs. It is presumed that the adaptive behaviour needs a dynamic power allocation scheme that is able to change the channel usage and power allocation pattern in the time domain as the requirement changes. Major work in the future needs to be centred on creating a new event driven system model with a dynamic number of systems generating mechanic along with a dynamic target requirement. Further, our existing scheme needs to be refined to cope with the new challenges posed by the dynamic behaviour. A new performance assessment also needs to be addressed.

7.1.2 Primary User Recognition

Spectrum sensing and reasoning are two of the most important tasks of cognitive radio. It is especially important in an *overlay* UWB power allocation problem, where the power can exceed the limitation of the FCC spectrum mask on some channels in order to overcome the increased path loss and fading seen in longer ranges. Currently, as we introduced in chapter

Chapter 7 Future Work

6, the protection of the existing agile service relies on information about the local band policy and an impacting factor that measures the excessive power emission over the FCC spectrum mask. Our work lacks a proper primary user sensing and spectrum reasoning mechanism. We consider the reinforcement learning as the proper candidate to realize the primary user recognition. Reinforcement learning is a process to learn a policy that can maximize a cumulative reward function, where the policy is a series of actions that control the sequential processes [99]. In wireless communications, reinforcement learning can be used to learn the channel pattern, where the past sensing knowledge will be measured as a collective reward, where the reward can be a value related to the heavily occupied primary user channel. The severely shadowed channels could also be identified and marked as less preferable channels from the spectrum pool. The successful transmission can also be weighted and learned by the radio agent and the sum up weighted successful transmission could be used as channel preference index to spot the primary user appearance and decide on further channel assignment. A system model in Figure 7.1 can illustrate the relationship between channel pattern recognition and dynamic power allocation.

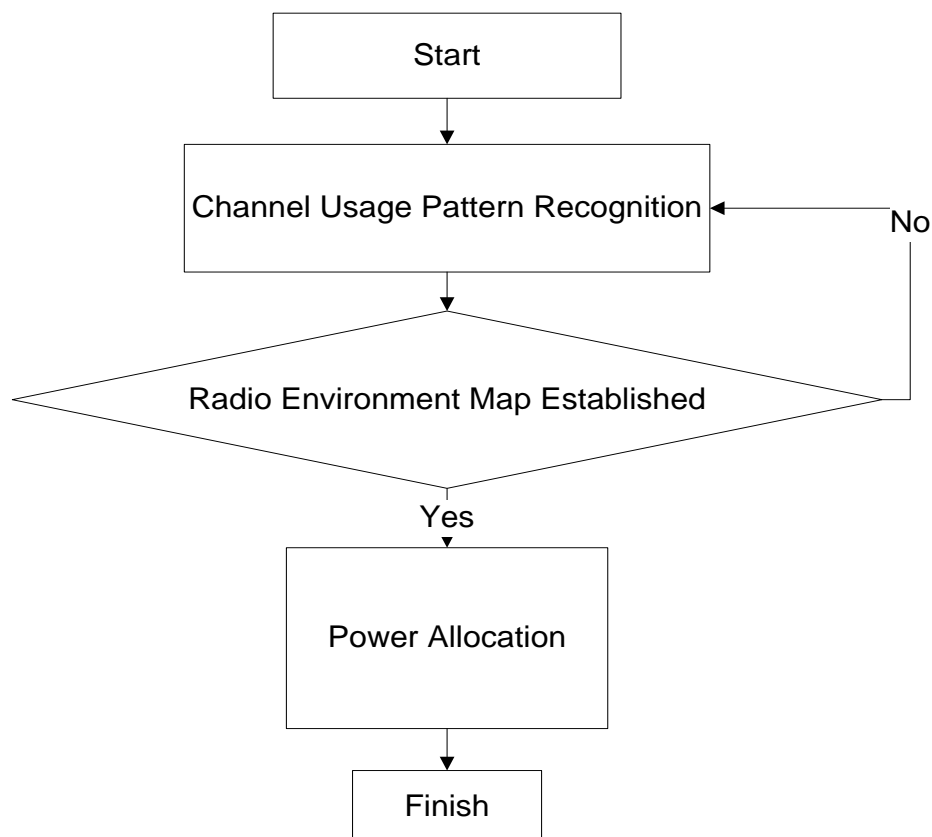


Figure 7-1 System model

Chapter 7 Future Work

As illustrated in Figure 7.1 the entire Cognitive Power Allocation works iteratively, which means the channel usage pattern is established first by a series of spectrum sensing and beacon transmissions, and the power allocation is thereafter built up upon the foundation of the established channel pattern. We assume that it can also work collectively, which means the channel pattern is obtained through the actions of a specific power allocation, as illustrated in Figure 7.2.

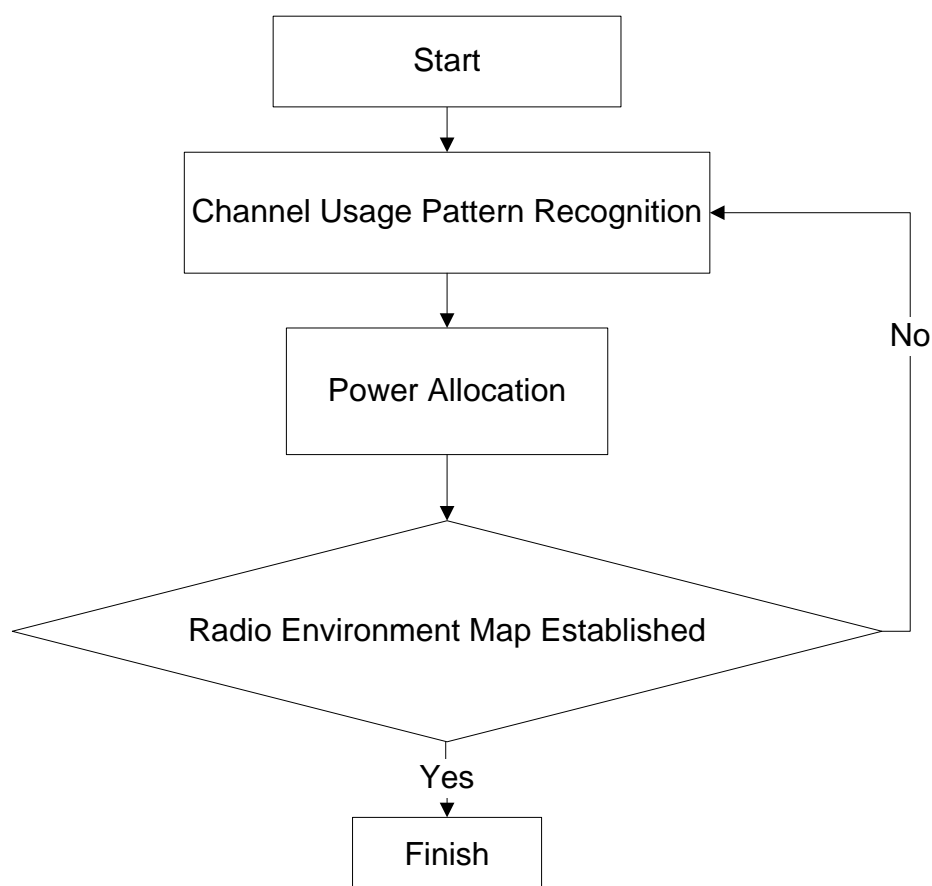


Figure 7-2 Alternative system model

The advantage of the system model shown in Figure 7.1 is the relative low risk of generating severe interference towards the agile primary service, as the channel pattern is fully recognised before the power allocation is applied; while the advantage of the system model shown in Figure 7.2 is the relative fast convergence speed of the entire process, as the power allocation is part of the learning process and channel pattern is established along the actions of power allocation. It is noted that the power allocation in the Figure 7.1 and Figure 7.2 is supposed to be our game based power allocation scheme.

Chapter 7 Future Work

7.2 *Cognitive Power Allocation in Sensor Network and Cellular Network*

The merits of our game based power allocation are many, and it has been investigated in a Multiband OFDM context. It is obvious that the work we have contributed is also valid to more existing multicarrier radio systems. Further work however is needed in order to make our work more generally applicable.

First, we can shed some light on cognitive power allocation in the context of the cellular based radio systems, where the point to point radio topology is replaced by the base station and multiple mobile station topologies. A dynamic multichannel power allocation scheme can be used to greatly reduce the co-channel interference from the *compact cells* (cells with minimum average distance between co-channel cells) [74]. On the other hand the coordinate ability offered by the central station can greatly reduce the overhead of the multi-agent learning.

Moreover, take wireless sensor networks as an example, a multicarrier based cognitive power allocation scheme can help the low power sensor nodes maintaining connection with a flexible power allocation to the available channels. Geographical location awareness should be taken into consideration in our future scheme, as well as a dynamic power constraint which is used to limit the channel accessing under the low battery life. The complexity of the power allocation algorithm also needs to be taken in to consideration.

7.3 *Multi-agent Q-learning*

As we introduced in chapter 2, there are many methodologies that can be used as an alternative approach in order to enable cognitive power allocation for multicarrier radio systems. Among these methodologies, we are particularly interested in Q-learning which is one type of Reinforcement learning. Different from the reinforcement learning we described in the previous section, the Q-learning based reinforcement learning is responsible for both channel pattern recognition and actual power allocation. The Q Table take record of channel usage pattern as well as the actions of the opponent behaviour, and the best power allocation police is chosen by the one that give the maximum estimated Q value. The motivation of a Q-

Chapter 7 Future Work

learning based scheme is on one hand the capability of multi-agent Q learning which has long been a research interest [100-102] and on the other hand, the learning by action style of learning can possibly lead a quick convergence upon best possible power allocation strategy.

7.4 Chapter Conclusion

In this chapter, we provided an overview of future work. In particular, our current research on distributed cognitive power allocation can be improved in two major aspects. On one hand, we can improve flexibility of our current scheme in terms of a dynamic user number and dynamic target requirement. On the other hand, a reinforcement learning based primary user identification is proposed for the future work. In addition to the possible improvement of our current work, the possible cognitive power allocations for cellular network and wireless sensor network are put up forward in this chapter. Lastly, we present an idea of the alternative method, a Q-learning based reinforcement learning in channel pattern recognition and cognitive power allocation.

Chapter 8 Conclusions

Contents

8.1	Summary of the Original Contributions.....	191
-----	--	-----

This thesis has studied the principles and techniques of Distributed Cognitive Power Allocation (DCPA) for multicarrier based Ultra Wide Band (UWB) wireless systems in a short range point-to-point configuration and a longer range point-to-point configuration. A game based approach has been investigated and implemented to solve the short range DCPA problem where the interference from homogeneous devices deployed in the close vicinity is the major concern; and a longer range DCPA problem where the channel path loss over longer ranges is the major concern. The theoretical analysis has shown that a DCPA problem can be modelled as a game competition with the goal of acquiring a certain target data rate, and such a game has been proven to have a Nash Equilibrium so that the specified game algorithm can achieve an operating point where no better performance can be gained by diverting from the present solution. A three staged game strategy has been proposed, and we demonstrated with Matlab simulation that the proposed game strategy performs well for both frequency selective fading and frequency non-selective fading channels in terms of general convergence and convergence speed.

Chapter 1 presented a general overview and outline of this thesis. Chapter 2 provided a detailed introduction to the related techniques. The general cognitive radio technique was discussed, followed by the UWB transmission technique, and UWB regulations. In particular, the UWB channel propagation model was introduced in detail. Three important factors of a UWB propagation model have been discussed, which are channel path loss for extended ranges, the UWB channel frequency selective fading behaviour and channel time variance respectively. Three approaches were mentioned, which are the possible methods that can be used to solve the specific distributed UWB power allocation problem. We introduced the game theory in wireless communications where we presented the initial idea of how a real

Chapter 8 Conclusions

world distributed power allocation can be modelled as a game competition. Reinforcement Learning was then introduced, which is capable of solving wireless power allocation problem. Specifically, Q-learning and multi-agent Q-learning were introduced along with its applications in wireless communications. Lastly, the optimisation process was introduced as well as its application in wireless communication, which is also called water filling technique.

In chapter 3, we introduced the simulation tool and the performance measures, along with the simulation techniques and simulation methodology. Matlab was chosen as our simulation tool throughout the work in this thesis. A Monte Carlo simulation technique was explored to predict a general performance of our proposed DCPA scheme. Also in this chapter an event driven simulation model was introduced. Regarding the channel modelling technique, a multicarrier based channel interference model was specified along with the mathematical expression of the UWB channel in frequency selective fading. In addition, the verification techniques were also introduced.

In chapter 4, we put forward a novel gradient power allocation scheme in order to partition the channel among several homogenous systems. An analysis of possible performance was given along with the simulation results, which showed that the proposed gradient power allocation scheme is capable of partition the channel and the portion of the channels that can be acquired is dependent on the total transmit power of each system. A game competition model was then built up upon this scheme. In particular, we analysed the possible utility function of a distributed power allocation and spectrum sharing game. A thorough mathematical analysis was given and we demonstrate that a Nash Equilibrium exists in our distributed power allocation game, which can alternatively be thought of as a proof of convergence of our proposed DCPA scheme.

Chapter 5 serves as the performance prediction and analysis of our proposed DCPA in short range scenarios by means of the Matlab simulations. We presented a geographical setup which takes into account both a interference dominated scenario due to the homogenous systems deployed in close vicinity, and a noise dominated scenario due to the sparsely deployment of homogenous systems, in order to better understand the possible performance of the low power emission systems. We then demonstrated the snapshot performance, which

Chapter 8 Conclusions

predicts the performance under a fixed geographical setup in terms of the interference or noise dominance. We showed that our proposed game-base DCPA scheme can help a distributed system acquire a target data rate in both frequency non-selective and frequency-selective fading channels. Later, the Monte Carlo simulation helped us predict the general performance of our proposed game based scheme, which also helped us determine the best possible ranges of critical parameters which are the gradient value α and the target data rate. The performance was then assessed by a comparison between our proposed DCPA scheme and a modified Iterative Water Filling technique. The results showed that our proposed scheme outperforms the Iterative Water Filling in terms of both convergence speed and the power efficiency.

In chapter 6 we adapted our DCPA scheme to an extended range scenario. A new power threshold estimation was proposed along with an analysis of the path loss for the extended link lengths. The new power threshold will determine the peak power and will be higher than the FCC spectrum mask in order to maintain a specific link budget over the longer ranges. The performance of our new DCPA scheme was analysed in both a single trial snapshot simulation and a Monte Carlo simulation. In order to assess the excessive power emission caused by transmit power over the FCC spectrum mask, a new performance measure was invented, Power Impact Factor (PIF), which takes into account both amount of excessive power emission and their bandwidth.

In chapter 7, we proposed some future work. The current work can be improved in several ways, including new dynamic target requirement model, which is able to simulate the dynamic requirement of the wireless agents; primary user recognition by means of reinforcement learning, which can learn the spectrum access behaviour of the primary users by reasoning the past and current sensing information. We could also broaden our current work to other multicarrier based wireless systems. Lastly, a possible alternative Q learning based methodology was discussed.

Chapter 8 Conclusions

8.1 Summary of the Original Contributions

This thesis has provided a study of DCPA from a game based approach. We evaluated the performance in terms of convergence and power efficiency. In this section, we will summarize the original contributions of our research.

1. Gradient Power Allocation Strategy

To date, many wireless multicarrier power allocation schemes were part of an optimising process where the power is allocated to channels in a way that maximum channel capacity can be acquired. The gradient power allocation scheme, we designed here does not perform an optimization process but rather it performs a channel partitioning process, and it performs in such way where power is only allocated to a portion of channels in order to acquire a target data rate. The idea of the gradient power allocation scheme is to find a way to differentiate the SINR levels on subcarriers so that a distributed wireless multicarrier system can gradually identify the best few channels that it can concentrate its transmit power on. We introduced a gradient value to differentiate the SINR by assigning this gradient power profile on channels according to their initial SINRs at receiver. Matlab simulation in chapter 4 showed that the gradient power allocation provides channel partitioning; while the portion of the channels that a distributed system can acquire is dependent on the total transmit power, interference and link length.

2. Power Threshold Estimation Scheme for Longer Range with Impacting Measurement

In order to maintain a specific link budget over an extended range, it is necessary to determine a transmit power threshold. A new power threshold estimation is proposed so that the transmit power will be determined in according to the specific link budget and path loss. The impact of the increased transmit power density is assessed by a new Power Impact Factor which is designed to provide an assessment of the excessive power emission of the cognitive multicarrier radio system. It should be noted that the impact to the primary users is measured in terms of interference level presented at receivers of the primary users as we introduced in chapter 6.

Chapter 8 Conclusions

3. A Target based Game Model and A Three Staged Game Strategy

There are many game models that can be used to describe the wireless power allocation such as the Cournot game model we introduced in chapter 2. Our game model design is different in two aspects: first, it does not rely on an existing game model that has been studied extensively in Economics. Second, it is build up on our unique gradient power allocation scheme and can be analytically expressed by a composite utility function. On the other hand, the proposed game model associates the gradient power allocation to a specific target requirement. Instead of competing for the maximum channel capacity, wireless systems in our proposed game model compete to acquire their target data rate so that the neither higher nor lower acquired data rate is preferable. Further, the proof of existence of Nash Equilibrium provides us a theoretical basis for the proposed DCPA scheme.

From the game strategy prospective, the strategy of achieving the best outcome in game competition differs depending on the game model and the real world problems. We presented a three stage game strategy that is modified from the existing game strategy designs in order to control the behaviour of the autonomous wireless devices. The three staged game strategy is comprised of competitive stage, cooperative stage and defecting stage. The simulation results show that the proposed game strategy used in our proposed DCPA scheme outperforms the Iterative water filling in terms of both convergence speed and power efficiency.

4. UWB Channel Propagation Model

Our work was carried out on the MB-OFDM standard of UWB wireless data communication technique. A new mathematical expression for UWB channel propagation model was presented, which takes frequency selective fading into consideration. The UWB channel propagation model is not new, and it has been studied and well documented in [40] and [41]. However, the mathematical expression of UWB path loss combined with frequency selective fading is new. The mathematical expression of path loss for longer ranges was also studied, however same average fading depth is assumed in our current work. While this has yet to be verified by experiment or other means, it provides a useful model for extended range analysis.

Publications

- Ruofan Jin, *Applying cognitive spectrum sharing to UWB*, URSI(International union for radio science) workshop 2009. Birmingham
- Ruofan Jin, David Grace, Paul Mitchell, *Cognitive Radio for UWB Spectrum Sharing and Power Allocation*, ISWCS 2010.
- Ruofan Jin, David Grace, Paul Mitchell, *Cognitive UWB Spectrum Sharing and PowerAllocation in a Multipath Fading Channel*, ISCIT 2011.

Reference

- [1] D. Cabric, M. S. Chen, D. A. Sobel, S. Wang, J. Yang, and R. W. Brodersen, "Novel Radio Architectures for UWB, 60 GHz, and Cognitive Wireless Systems," *EURASIP Journal on Wireless Communications and Networking*, vol. 2006, pp. 3-18, 2006.
- [2] T. A. Weiss and F. K. Jondral, "Spectrum pooling: an innovative strategy for the enhancement of spectrum efficiency," *Communications Magazine, IEEE*, vol. 42, pp. S8-14, 2004.
- [3] B. Fette, *Cognitive Radio Technology*, 1 ed.: Newnes, 2006.
- [4] G. R. Faulhaber, "Deploying Cognitive Radio: Economic, Legal and Policy Issues," *International Journal of Communication*, vol. 2, 11/2008 2008.
- [5] A. Goldsmith, S. A. Jafar, I. Maric, and S. Srinivasa, "Breaking Spectrum Gridlock With Cognitive Radios: An Information Theoretic Perspective," *Proceedings of the IEEE*, vol. 97, pp. 894-914, 2009.
- [6] J. Zhu and K. J. R. Liu, "Cognitive Radios For Dynamic Spectrum Access - Dynamic Spectrum Sharing: A Game Theoretical Overview," *Communications Magazine, IEEE*, vol. 45, pp. 88-94, 2007.
- [7] A. Shukla, A. Alptekin, J. Bradford, E. Burbidge, D. Chandler, M. Kennett, P. Levine, and S. Weiss, "Cognitive Radio Technology A Study for Ofcom," QinetiQ Proprietary 2006.
- [8] E. Skafidas, B. Jones, N. Kelly, and B. Eversole, "Cognitive Radio Technologies for Efficient Spectrum Utilization," National ICT Australia 2006.
- [9] S. Haykin, "Cognitive radio: brain-empowered wireless communications," *Selected Areas in Communications, IEEE Journal on*, vol. 23, pp. 201-220, 2005.
- [10] W. P. Siriwongpairat and K. J. R. Liu, *Ultra-Wideband Communications Systems Multiband OFDM Approach*: Wiley-IEEE Press, 2007.
- [11] J. Mitola. III, *COGNITIVE RADIO ARCHITECTURE The Engineering Foundations of Radio XML*: Wiley, 2006.
- [12] A. G. Burr, "Cognitive Channel and Power Allocation: Information Theoretic Bounds," presented at the Cognitive Radio Oriented Wireless Networks and Communications, 2009. CROWNCOM. 4th International Conference on, 2009.
- [13] S. Chen and A. M. Wyglinski, "Cognitive Radio-Enabled Distributed Cross-Layer Optimization Via Genetic Algorithms," presented at the IEEE Annual Communications Society, 2009.
- [14] R. Jin, D. Grace, and P. Mitchell, "Cognitive Radio for UWB Spectrum Sharing and Power Allocation," presented at the WUN COGCOM 2010 Workshop part of IEEE International Symposium on Wireless Communication Systems (ISWCS) 2010, York, UK, 2010.
- [15] H. Li, Y. Gai, Z. He, K. Niu, and W. Wu, "Optimal Power Control Game Algorithm for Cognitive Radio Networks with multiple interference temperature limits," presented at the Vehicular Technology Conference, 2008. VTC Spring 2008. IEEE, 2008.
- [16] A. Batra, S. Lingam, and J. Balakrishnan, "Multi-band OFDM: a cognitive radio for UWB," in *Circuits and Systems, 2006. ISCAS 2006. Proceedings. 2006 IEEE International Symposium on*, 2006, pp. 4 pp.-4097.

- [17] E. Bedeer, M. Marey, O. Dobre, and K. Baddour, "Adaptive bit allocation for OFDM cognitive radio systems with imperfect channel estimation," in *Radio and Wireless Symposium (RWS), 2012 IEEE*, 2012, pp. 359-362.
- [18] L. Giupponi, A. Galindo-Serrano, P. Blasco, and M. Dohler, "Cognitive networks: an emerging paradigm for dynamic spectrum management [Dynamic Spectrum Management]," *Wireless Communications, IEEE*, vol. 17, pp. 47-54, 2010.
- [19] R. V. Prasad, P. Pawelczak, J. A. Hoffmeyer, and H. S. Berger, "Cognitive functionality in next generation wireless networks: standardization efforts," *Communications Magazine, IEEE*, vol. 46, pp. 72-78, 2008.
- [20] J. Mitola. III, "Cognitive Radio: An integrated agent architecture for software defined radio," Doctor, Royal Institute of Technology, Stockholm, Sweden.
- [21] M. Fitch, M. Nekovee, S. Kawade, K. Briggs, and R. MacKenzie, "Wireless service provision in TV white space with cognitive radio technology: A telecom operator's perspective and experience," *Communications Magazine, IEEE*, vol. 49, pp. 64-73, 2011.
- [22] A. Ghasemi and E. S. Sousa, "Spectrum sensing in cognitive radio networks: requirements, challenges and design trade-offs," *Communications Magazine, IEEE*, vol. 46, pp. 32-39, 2008.
- [23] B. Fan, F.-j. Han, A.-m. Zhang, and F.-j. Han, "Spectrum sensing in MB-OFDM based cognitive UWB systems coexistence with WiMax," in *Communication Systems, 2008. ICCS 2008. 11th IEEE Singapore International Conference*, 2008, pp. 203-207.
- [24] I. F. Akyildiz, W.-Y. Lee, M. C. Vuran, and S. Mohanty, "NeXt generation/dynamic spectrum access/cognitive radio wireless networks: A survey," *JOURNAL OF COMMUNICATIONS AND NETWORKS*, vol. 50, pp. 2127-2159, 2006.
- [25] J. Xiangpeng, M. Siun-Chuon, D. Raychaudhuri, and R. Matyas, "Reactive cognitive radio algorithms for co-existence between IEEE 802.11b and 802.16a networks," in *Global Telecommunications Conference, 2005. GLOBECOM '05. IEEE*, 2005, pp. 5 pp.-2469.
- [26] J. Bard, V. J., and K. Jr., *Software Defined Radio: The Software Communications Architecture*, Wiley.
- [27] V. Surducun, M. Moudgill, G. Nacer, E. Surducun, P. Balzola, J. Glossner, S. Stanley, M. Yu, and D. Iancu, "The Sandblaster Software-Defined Radio Platform for Mobile 4G Wireless Communications," *International Journal of Digital Multimedia Broadcasting*, vol. 2009, p. 9, 2009.
- [28] D. Cabric, S. M. Mishra, and R. W. Brodersen, "Implementation issues in spectrum sensing for cognitive radios," in *Signals, Systems and Computers, 2004. Conference Record of the Thirty-Eighth Asilomar Conference*, 2004, pp. 772-776 Vol.1.
- [29] A. Tsertou and D. I. Laurenson, "Revisiting the Hidden Terminal Problem in a CSMA/CA Wireless Network," *Mobile Computing, IEEE Transactions on*, vol. 7, pp. 817-831, 2008.
- [30] Y. B. Reddy, "Spectrum Detection in Cognitive Networks by Minimizing Hidden Terminal Problem," in *Information Technology: New Generations (ITNG), 2012 Ninth International Conference*, 2012, pp. 77-82.
- [31] S. Filin, H. Harada, H. Murakami, and K. Ishizu, "International standardization of cognitive radio systems," *Communications Magazine, IEEE*, vol. 49, pp. 82-89, 2011.
- [32] C. M. Gómez and A. Flores, "A neurophysiological evaluation of a cognitive cycle in humans," *Neuroscience & Biobehavioral Reviews*, vol. 35, pp. 452-461, 2011.
- [33] *Commission's Rules Regarding Ultra-Wideband Transmission Systems* F. C. Commission, 2002.

- [34] K. Siwiak and D. McKeown, *Ultra-wideband radio technology*. Chichester/GB: John Wiley and Sons Ltd, 2004.
- [35] F. Nekoogar, *Ultra-Wideband Communications: Fundamentals and Applications*: Prentice Hall, 2005.
- [36] X. D. Lebing Liu, "WiMedia UWB Product Testing Report," Wireless and Networking Research Lab, University of Victoria 2008.
- [37] W. D. Prather, C. E. Baum, R. J. Torres, F. Sabath, and D. Nitsch, "Survey of worldwide high-power wideband capabilities," *Electromagnetic Compatibility, IEEE Transactions*, vol. 46, pp. 335-344, 2004.
- [38] M. Hämäläinen, "Analysis of Interference on DS-UWB System in AWGN Channel," presented at the 2005 IEEE International Conference on Ultra-Wideband, 2005.
- [39] M. P. Wylie-Green, P. A. Ranta, and J. Salokannel, "Multi-band OFDM UWB solution for IEEE 802.15.3a WPANs," in *Advances in Wired and Wireless Communication, 2005 IEEE/Sarnoff Symposium*, 2005, pp. 102-105.
- [40] A.F.Molisch, J. R. Foerster, and M. Pendergrass, "Channel models for ultrawideband personal area networks," *Wireless Communications, IEEE*, vol. 10, pp. 14-21, 2003.
- [41] A.F.Molisch, "IEEE 802.15.4a channel model - final report," 2005.
- [42] A.F.Molisch, "Ultrawideband propagation channels-theory, measurement, and modeling," *Vehicular Technology, IEEE Transactions*, vol. 54, pp. 1528-1545, 2005.
- [43] C. Chia-Chin, K. Youngeil, and L. Seong-Soo, "A modified S-V clustering channel model for the UWB indoor residential environment," in *Vehicular Technology Conference, 2005. VTC 2005-Spring. 2005 IEEE 61st*, 2005, pp. 58-62 Vol. 1.
- [44] M. Ghavami, L. Michael, and R. Kohno, *Ultra Wideband Signals and Systems in Communication Engineering* 2nd ed.: Wiley, 2007.
- [45] T. Schwengler and M. Gilbert, "Propagation models at 5.8 GHz-path loss and building penetration," in *Radio and Wireless Conference, 2000. RAWCON 2000. 2000 IEEE*, 2000, pp. 119-124.
- [46] A. Goldsmith, *Wireless Communications*: Cambridge University Press, 2005.
- [47] D. M. W. Leenaerts, "Transceiver Design for Multiband OFDM UWB," *EURASIP Journal on Wireless Communications and Networking*, vol. 2006, pp. 1-8, 2006.
- [48] B. Sklar, "Rayleigh Fading Channels in Mobile Digital Communication Systems .I. Characterization," *Communications Magazine, IEEE*, vol. 35, pp. 90-100, 1997.
- [49] S. Saunders and A. Aragón-Zavala, *Antennas and Propagation for Wireless Communication Systems*, 2 ed.: Wiley 2007.
- [50] A. A. El-Saleh, M. Ismail, O. B. A. Ghafoor, and A. H. Ibrahim, "Comparison between Overlay Cognitive Radio and Underlay Cognitive Ultra Wideband Radio for Wireless Communications," *2007 Waveform Diversity & Design*, pp. 69-73, 2007.
- [51] Y. Liu, H. Zhang, W. Gong, and D. Towsley, "On the interaction between overlay routing and underlay routing," in *INFOCOM 2005. 24th Annual Joint Conference of the IEEE Computer and Communications Societies. Proceedings IEEE*, 2005, pp. 2543-2553 vol. 4.
- [52] V. D. Chakravarthy, Z. Wu, A. Shaw, M. A. Temple, R. Kannan, and F. Garber, "A general overlay/underlay analytic expression representing cognitive radio waveform," in *Waveform Diversity and Design Conference, 2007. International*, 2007, pp. 69-73.
- [53] Z. Long, Z. Chenglin, and Z. Zheng, "Compatibility between devices using ultra-wideband technology and TD-SCDMA systems," in *Communications and Information Technology, 2004. ISCIT 2004. IEEE International Symposium*, 2004, pp. 1039-1043 vol.2.

- [54] J. J. Ely, W. L. Martin, G. L. Fuller, T. W. Shaver, J. Zimmerman, and W. E. Larsen, "UWB EMI to aircraft radios: field evaluation on operational commercial transport airplanes," in *Digital Avionics Systems Conference, 2004. DASC 04. The 23rd*, 2004, pp. 9.D.4-91-11 Vol.2.
- [55] F. Granelli and Z. Honggang, "Cognitive ultra wide band radio: a research vision and its open challenges," in *Networking with Ultra Wide Band and Workshop on Ultra Wide Band for Sensor Networks, 2005. Networking with UWB 2005. 2nd International Workshop*, 2005, pp. 55-59.
- [56] H. Arslan and M. E. Sahin, "Cognitive UWB-OFDM: Pushing Ultrawideband Beyond Its Limit via Opportunistic Spectrum Usage," *Journal of Communications AND Networks*, vol. 8, pp. 151-157, 2006.
- [57] J. Watson, *Strategy - an introduction to game theory* W. W. Norton & Company, 2002.
- [58] A. B. MacKenzie and L. A. DaSilva, *Game Theory for Wireless Engineers*: Morgan & Claypool, 2006.
- [59] J. F. Nash, "Equilibrium points in n-person games," *Proceedings of the National Academy of Sciences of the United States of America*, vol. 36, pp. 48-49, 1950.
- [60] S. Kapp. (2002) 802.11a More Bandwidth without the Wires. *Internet Computing, IEEE*. 75- 79.
- [61] A. B. MacKenzie and S. B. Wicker, "Game theory in communications: motivation, explanation, and application to power control," in *Global Telecommunications Conference, 2001. GLOBECOM '01. IEEE*, 2001, pp. 821-826 vol.2.
- [62] F. Meshkati, C. Mung, H. V. Poor, and S. C. Schwartz, "A Game-Theoretic Approach To Energy-Efficient Power Control in Sulticarrier CDMA Systems," *Selected Areas in Communications, IEEE Journal on*, vol. 24, pp. 1115-1129, 2006.
- [63] L. Berlemann, G. R. Hiertz, B. H. Walke, and S. Mangold, "Radio resource sharing games: enabling QoS support in unlicensed bands," *Network, IEEE*, vol. 19, pp. 59-65, 2005.
- [64] G. C. Wei Yu Ginis, J.M., "Distributed Multiuser Power Control for Digital Subscriber Lines," *Selected Areas in Communications, IEEE Journal on*, vol. 20, pp. 1105-1115, Jun 2002 2002.
- [65] A. B. W. MacKenzie, "Game Theory in Communications: Motivation, Explanation, and Application to Power Control," presented at the Global Telecommunications Conference, 2001. GLOBECOM '01. IEEE, San Antonio, TX, USA, 2001.
- [66] D. H. Niyato, "Competitive spectrum sharing in cognitive radio networks: a dynamic game approach," *Wireless Communications, IEEE Transactions*, vol. 7, pp. 2651 - 2660, July 2008 2008.
- [67] R. Etkin, A. Parekh, and D. Tse, "Spectrum sharing for unlicensed bands," *Selected Areas in Communications, IEEE Journal*, vol. 25, pp. 517-528, 2007.
- [68] D. Niyato and E. Hossain, "Competitive Spectrum Sharing in Cognitive Radio Networks: A Dynamic Game Approach," *Wireless Communications, IEEE Transactions on*, vol. 7, pp. 2651 - 2660, July 2008 2008.
- [69] H. N. Agiza, G.-I. Bischi, and M. Kopel, "Multistability in a dynamic Cournot game with three oligopolists," *Mathematics and Computers in Simulation*, vol. 51, pp. 63-90, 1999.
- [70] L. Busoniu, R. Babuska, and B. De Schutter, "A Comprehensive Survey of Multiagent Reinforcement Learning," *Systems, Man, and Cybernetics, Part C: Applications and Reviews, IEEE Transactions on*, vol. 38, pp. 156-172, 2008.

- [71] J. Hu and M. P. Wellman, "Nash q-learning for general-sum stochastic games," *The Journal of Machine Learning Research*, vol. 4, p. 30, 12/1/2003 2003.
- [72] T. M. Mitchell, *Machine Learning*, International ed.: McGRAW-HILL BOOK, 1997.
- [73] A. Schaerf, Y. Shoham, and M. Tennenholtz, "Adaptive Load Balancing: A Study in Multi-Agent Learning," *Journal of Artificial Intelligence Research*, vol. 2, p. 25, 04/1995 1995.
- [74] N. Junhong and S. Haykin, "A Q-learning-based dynamic channel assignment technique for mobile communication systems," *Vehicular Technology, IEEE Transactions on*, vol. 48, pp. 1676-1687, 1999.
- [75] J. B. Predd, S. B. Kulkarni, and H. V. Poor, "Distributed learning in wireless sensor networks," *Signal Processing Magazine, IEEE*, vol. 23, pp. 56-69, 2006.
- [76] H. Wymeersch, S. Marano, W. M. Gifford, and M. Z. Win, "A Machine Learning Approach to Ranging Error Mitigation for UWB Localization," *Communications, IEEE Transactions*, vol. 60, pp. 1719-1728, 2012.
- [77] H. Zhu, Z. Rong, and H. V. Poor, "Repeated Auctions with Bayesian Nonparametric Learning for Spectrum Access in Cognitive Radio Networks," *Wireless Communications, IEEE Transactions*, vol. 10, pp. 890-900, 2011.
- [78] E. Driouch, W. Ajib, and A. Ben Dhaou, "A greedy spectrum sharing algorithm for cognitive radio networks," in *Computing, Networking and Communications (ICNC), 2012 International Conference*, 2012, pp. 1010-1014.
- [79] S. Guocong and L. Ye, "Cross-layer optimization for OFDM wireless networks-part I: theoretical framework," *Wireless Communications, IEEE Transactions*, vol. 4, pp. 614-624, 2005.
- [80] S. Boyd and L. Vandenberghe, *Convex Optimization*: Cambridge university press, 2004.
- [81] Y. Wei, R. Wonjong, S. Boyd, and J. M. Cioffi, "Iterative water-filling for Gaussian vector multiple-access channels," *Information Theory, IEEE Transactions*, vol. 50, pp. 145-152, 2004.
- [82] J. S. Carson, "Introduction to modeling and simulation," in *WSC '04 Proceedings of the 36th conference on Winter simulation*, 2004, pp. 9-16.
- [83] R. Blahut, "Computation of channel capacity and rate-distortion functions," *Information Theory, IEEE Transactions on*, vol. 18, pp. 460-473, 1972.
- [84] A. Papadogiannis and A. G. Burr, "Multi-beam Assisted MIMO - A Novel Approach to Fixed Beamforming," in *Future Network and MobileSummit 2011*, 2011.
- [85] V. Shah, N. B. Mandayam, and D. J. Goodman, "Power Control for Wireless Data Based on Utility and Pricing," in *Personal, Indoor and Mobile Radio Communications, 1998. The Ninth IEEE International Symposium on*, 1998, pp. 1427-1432 vol.3.
- [86] S. Junyang, J. Tao, L. Siyang, and Z. Zhongshan, "Maximum channel throughput via cooperative spectrum sensing in cognitive radio networks," *Wireless Communications, IEEE Transactions*, vol. 8, pp. 5166-5175, 2009.
- [87] M. Filip and E. Vilar, "Optimum utilization of the channel capacity of a satellite link in the presence of amplitude scintillations and rain attenuation," *Communications, IEEE Transactions*, vol. 38, pp. 1958-1965, 1990.
- [88] J. Winters, "On the Capacity of Radio Communication Systems with Diversity in a Rayleigh Fading Environment," *Selected Areas in Communications, IEEE Journal*, vol. 5, pp. 871-878, 1987.
- [89] J. B. Rosen, "Existence and Uniqueness of Equilibrium Points for Concave N-Person Games," *Econometrica*, vol. 33, pp. 520-534, 1965.

- [90] A. Batra, J. Balakrishnan, G. R. Aiello, J. R. Foerster, and A. Dabak, "Design of a multiband OFDM system for realistic UWB channel environments," *Microwave Theory and Techniques, IEEE Transactions on*, vol. 52, pp. 2123-2138, 2004.
- [91] J. R. Hauser, "EXISTENCE AND UNIQUENESS OF PRICE EQUILIBRIA IN DEFENDER," 1987.
- [92] D. Manstretta, N. Laurenti, and R. Castello, "A Reconfigurable Narrow-Band MB-OFDM UWB Receiver Architecture," *Circuits and Systems II: Express Briefs, IEEE Transactions*, vol. 55, pp. 324-328, 2008.
- [93] L. E. L. Mahim Ranjan, "A Low-Cost and Low-Power CMOS Receiver Front-end for MB-OFDM Ultra-Wideband Systems," *IEEE JOURNAL OF SOLID-STATE CIRCUITS*, vol. 42, 2007.
- [94] N. Devroye, M. Vu, and V. Tarokh, "Achievable rates and scaling laws for cognitive radio channels," *EURASIP Journal on Wireless Communications and Networking* vol. 2008, 2008.
- [95] W. Wei, W. Wenbo, L. Qianxi, S. Kang, and P. Tao, "Geometry-based optimal power control of fading multiple access channels for maximum sum-rate in cognitive radio networks," *Wireless Communications, IEEE Transactions on*, vol. 9, pp. 1843-1848, 2010.
- [96] Y. Wei, G. Ginis, and J. M. Cioffi, "Distributed Multiuser Power Control for Digital Subscriber Lines," *Selected Areas in Communications, IEEE Journal*, vol. 20, pp. 1105-1115, 2002.
- [97] A. F. Molisch, K. Balakrishnan, C.-c. Chong, S. Emami, A. Fort, J. Karedal, J. Kunisch, H. Schantz, U. Schuster, and K. Siwiak, "IEEE 802.15.4a channel model - final report," 2004.
- [98] P. Supanakoon, S. Kaewsirisin, S. Promwong, S. Noppanakeepong, and J. i. Takada, "Ground Reflection Path Loss Based on Average Power Loss for Ultra Wideband Communications," in *Microwave Conference, 2007. APMC 2007. Asia-Pacific*, 2007, pp. 1-4.
- [99] D. Ma and J. Er Meng, "A survey of machine learning in Wireless Sensor networks From networking and application perspectives," in *Information, Communications & Signal Processing, 2007 6th International Conference*, 2007, pp. 1-5.
- [100] P. Y. Glorennec and L. Jouffe, "Fuzzy Q-learning," in *Fuzzy Systems, 1997., Proceedings of the Sixth IEEE International Conference on*, 1997, pp. 659-662 vol.2.
- [101] P. Y. Glorennec, "Fuzzy Q-learning and dynamical fuzzy Q-learning," in *Fuzzy Systems, 1994. IEEE World Congress on Computational Intelligence., Proceedings of the Third IEEE Conference*, 1994, pp. 474-479 vol.1.
- [102] Y. Nagayuki, S. Ishii, and K. Doya, "Multi-agent reinforcement learning: an approach based on the other agent's internal model," in *MultiAgent Systems, 2000. Proceedings. Fourth International Conference*, 2000, pp. 215-221.